The nonperturbative functional renormalization group: general formalism and applications to low-energy physics

N. Dupuis,[1] D. Mouhanna,[1] G. Tarjus,[1] M. Tissier,[1] B. Delamotte,[1] L. Canet,[2] and N. Wschebor[3]
[1] *Laboratoire de Physique Théorique de la Matière Condensée, CNRS UMR 7600, Université Pierre et Marie Curie, 4 Place Jussieu, 75252 Paris Cedex 05, France*
[2] *LPMMC, Universiteé Joseph Fourier Grenoble-Alpes, CNRS UMR 5493, 38042 Grenoble, France*
[3] *Instituto de Física, Facultad de Ingeniería, Universidad de la República, J.H.y Reissig 565, 11000 Montevideo, Uruguay*

(Dated: November 24, 2016)

CONTENTS

I. Introduction **(LPTMC)** 2
A. Wilson's RG 2
B. The nonperturbative RG 3
C. Scope of the review 3

II. The scale-dependent effective action Γ_k 4
A. Definition and basic properties 4
1. The regulator function $R_k(\mathbf{q})$ 5
2. The Legendre transform versus Γ_k 6
3. Effective potential and 1PI vertices 6
4. General properties of the effective action Γ_k 7
B. Exact flow equation 8
General properties of the flow equation 9

III. The derivative expansion 10
A. The local potential approximation (LPA) 11
1. Scaling form of the LPA flow equation 12
2. Fixed-point solutions and critical exponents 12
3. Upper and lower critical dimensions – Mermin-Wagner theorem 15
4. Spontaneous symmetry breaking and approach to the convex potential 15
B. Improving the LPA: the LPA' 15
1. Scaling form of the LPA' flow equations 16
2. Truncated LPA' 17
3. Critical behavior: the limits $d \to 4$, $d \to 2$ and $N \to \infty$ 18
4. The low-temperature phase 20
5. The two-dimensional O(2) model 22
C. Second order of the derivative expansion **(BD)** 23
1. Choice of the regulator function 23
2. Optimization 24
3. Critical exponents 24
D. Higher orders of the derivative expansion **(BD)** 24
E. Fixed points and scale invariance **(NW)** 24
F. First-order phase transitions 24

IV. The two-dimensional $O(2)$ model 24
A. Flow equations and optimized regulator 25
B. Kosterlitz-Thouless (KT) transition 27
1. Suppression of amplitude fluctuations 27
2. Low-temperature phase 27
3. High-temperature phase and essential scaling 28
4. Comparison with standard KT flow 28

V. The vertex expansion **(NW, ND)** 29
A. The Blaizot–Méndez-Galain–Wschebor approximation 29
1. $s = 0$: LPA 30
2. $s = 2$: full momentum dependence of $\Gamma_k^{(2)}(\mathbf{p}; \phi)$ 30
B. Critical behavior 32
1. Critical exponents 32
2. The 2-point vertex at and near criticality 33
C. Simplified BMW schemes 34

VI. The O(N) model in the large-N limit **(NW)** 34
A. Derivative expansion 34
B. BMW approximation 34

VII. Lattice NPRG 34
A. Lattice field theory 35
1. Standard NPRG scheme 35
2. Lattice NPRG scheme 36
3. The Ising model in the LPA 36
B. Classical spin models 38
1. Local potential approximation 39
2. Renormalization of the spectrum 39
3. LPA' 40
C. Comparison with HRT 41

VIII. Membranes **(DM)** 41

IX. Frustrated spins and matrix models **(DM)** 41

X. Disordered systems **(MT, GT, DM)** 41

XI. Out-of-equibrium systems: KPZ, reaction diffusion... **(LC, BD)** 41

XII. Quantum O(N) model 41
A. Quantum phase transitions 42
B. RG flows 43
1. Quantum critical regime 45
2. Quantum disordered regime 45

3. Renormalized classical regime 45
C. Universal thermodynamics 47
D. "Higgs" amplitude mode 49

XIII. Interacting bosons 51
A. Superfluidity in a dilute Bose gas 51
1. Breakdown of Bogoliubov's theory 51
2. NPRG approach 51
3. Superfluid transition of a dilute Bose gas 56
B. Superfluid–Mott-insulator transition 58
1. The Bose-Hubbard model 58
2. NPRG approach 59

XIV. Interacting fermions 65
A. Wilsonian fermionic RG 65
B. 1PI formalism 66
C. Beyond perturbative RG 67

Acknowledgments 68

A. Fourier transforms 68

B. The effective action formalism 68
1. Effective action 69
2. 1PI vertices 69
3. Loop expansion 70

C. Threshold functions for the classical O(N) model 71
1. Definitions 71
2. Large-w behavior 72
3. Universal values 72
4. Theta regulator 72

D. Anomalous dimension in the LPA' 72

E. Derivative expansion to second order 73

F. Flow equations in the BMW approximation 74

G. Numerical methods **(BD, NW)** 76

H. Symmetries **(BD, NW)** 76

I. Connection with perturbation theory **(NW)** 76

References 76

I. INTRODUCTION (LPTMC)

An important goal in many areas of physics, from condensed matter to high-energy physics, is to understand the behavior of systems with a large number of degrees of freedom. Theoretical studies of such systems meet with two major difficulties. Often there is no small parameter that would allow for a systematic perturbative expansion. Even if such a parameter exists, perturbation theory may break down, especially in low dimensions, when the correlation length is large (i.e. significantly larger than the distance between microscopic objects) and collective effects important.

When the correlation length ξ is small, perturbation theory (or mean-field methods) allows us to relate the physical properties of the system to those of a simpler system, e.g. the noninteracting system or a small subsystem. This is no longer true when ξ is large. In this case, the large number of degrees of freedom plays an essential role. The system usually exhibits very distinct behavior on different energy (or length) scales. The low-energy behavior is dominated by collective effects for which details of the microscopic interactions are often irrelevant: collective behavior primarily depends on general properties of the system (space dimension, nature of the degrees of freedom that are correlated over large distances, etc.). A prime example is given by systems near a second-order phase transition where cooperative behavior is responsible for scaling and universality.

The Wilson renormalization group (RG) has proven to be an efficient method to understand systems with many degrees of freedom (Fisher, 1998; Kadanoff, 1966; Wilson, 1971a,b, 1975, 1983; Wilson and Kogut, 1974). On the one hand, the RG provides us with an explanation of cooperative behavior and universality. On the other hand, it constitutes a practical tool to (approximately) solve models where correlations and fluctuations play an important role.

Most applications of the Wilson RG rely on the existence of a small parameter allowing us to obtain RG equations using perturbation theory. The aim of this review is to describe an approach, the nonperturbative RG (NPRG),[1] which does not suffer from this limitation. It is based on an exact functional RG equation satisfied by a scale-dependent "effective action" (or Gibbs free energy in the terminology of statistical mechanics). While this approach is conceptually equivalent to the usual formulation of Wilson's RG, as a practical computation tool it presents many advantages and allows for genuinely nonperturbative approximations.

A. Wilson's RG

To illustrate the basic idea of Wilson's RG, let us consider a system whose partition function

$$Z = \int \mathcal{D}[\varphi] e^{-S[\varphi]} \tag{1}$$

can be written as a functional integral over a field $\varphi(\mathbf{r})$ with action $S[\varphi]$ (the Hamiltonian $H[\varphi]$ multiplied by $\beta = 1/k_B T$ in statistical mechanics). We assume a ultraviolet momentum cutoff Λ (the Fourier transformed field $\varphi(\mathbf{p})$ is defined only for $|\mathbf{p}| \leq \Lambda$). In Wilson's RG approach, instead of considering all degrees of freedom on the same footing, one first integrates out short-distance (high-energy) degrees of freedom. This leads to an effective action for the long-distance (low-energy) degrees of

[1] In the literature the NPRG is also called the functional RG or the exact RG, even though in practice it is never (except in trivial models) exact and not necessary functional.

freedom. In practice, this is achieved by splitting the field $\varphi = \varphi_> + \varphi_<$ into fast and slow modes. The fast modes $\varphi_>$ have Fourier components in the range $k \leq |\mathbf{p}| \leq \Lambda$ and the slow modes in $0 \leq |\mathbf{p}| \leq k$. Integrating out the fast modes, one obtains an effective action $S_k[\varphi_<]$ for the slow modes,

$$e^{-S_k[\varphi_<]} = \int \mathcal{D}[\varphi_>] e^{-S[\varphi_> + \varphi_<]}. \tag{2}$$

$S_k[\varphi_<]$ depends on renormalized coupling constants $r_{0,k}$ and $u_{0,k}$ and contains additional coupling constants (not present in the original action) that are generated by the integration of the fast modes. Thus, the set of all possible coupling constants $\{g_{i,k}\} = \{r_{0,k}, u_{0,k}, \cdots\}$ defines a trajectory in the parameter space of the action. One generally finds that the trajectories flow into fixed points: $\lim_{k\to 0} g_{i,k} = g_i^*$.[2] The RG flow near a fixed-point governs the long-distance behavior of the system and explains universality and scaling in the vicinity of a second-order phase transition.

A RG calculation usually amounts to calculating $\{g_{i,k}\}$ in a restricted space $\mathcal{G} = \{g_1, \cdots, g_M\}$ of coupling constants. Moreover, this calculation is often performed within a perturbation expansion assuming that the coupling constants are small: the beta functions $\beta_i(\{g_{j,k}\}) = k dg_{i,k}/dk$ are obtained to a finite order in the $g_{j,k}$'s. For this reason, Wilson's RG is often restricted to weakly interacting systems. In the study of second-order phase transitions, the perturbative approach has been particularly useful for systems near the upper critical dimension[3] (the ϵ-expansion with $\epsilon = 4 - d$ for the O(N) model) (Wilson and Fisher, 1972). Beyond leading order in ϵ, the standard perturbative field theory has nevertheless proven to be more efficient than the Wilson approach (Wilson, 1972; Zinn-Justin, 1996).

There is however no fundamental reason for Wilson's RG to be perturbative. Nor is it necessary to restrict the action to a finite number of coupling constants. The action $S_k[\varphi]$ satisfies an exact RG equation known as the Wilson-Polchinski or Wegner-Houghton equation depending on whether a soft or hard momentum cutoff between slow and fast modes is used (Bagnuls and Bervillier, 2001; Polchinski, 1984; Wegner and Houghton, 1973; Wilson and Kogut, 1974). Due to its complexity, the integro-differential functional equation $\partial_k S_k[\varphi]$ cannot be solved exactly and calls for approximations. The most common one is the derivative expansion where the action $S_k[\varphi]$ is expanded to finite order in derivatives of the field. While this type of approximations yields a reasonable estimate of the correlation-length exponent ν for a second-order phase transition, the anomalous dimension η turns out to be strongly dependent on the choice of the momentum cutoff between fast and slow modes. This shortcoming seriously limits the use of the Wilson-Polchinski and Wegner-Houghton equations.

B. The nonperturbative RG

Statistical mechanics (and field theory) is often based on the Helmholtz free energy $F[h] = -k_B T \ln Z[h]$ where $Z[h]$ is the partition function in the presence of an external field $h(\mathbf{r})$ (the "magnetic" field). The free energy at equilibrium, in the absence of external field, is simply $F[h = 0]$ whereas correlation function $\langle \varphi(\mathbf{r}_1) \cdots \varphi(\mathbf{r}_n) \rangle$ are obtained from the functional derivatives of $F[h]$ (see Appendix B).

Alternatively, statistical mechanics (and field theory) can be formulated using the Gibbs free energy $\Gamma[\phi]$ (the "effective action" in the field theory terminology) defined as the Legendre transform of $F[h]$, where $\phi(\mathbf{r}) = \langle \varphi(\mathbf{r}) \rangle = \delta F[h]/\delta h(\mathbf{r})$ is the average value of the field $\varphi(\mathbf{r})$ (the "magnetization"). The effective action contains the same information as the Helmholtz free energy. In particular, $\Gamma[\phi]$ is the generating functional of the one-particle irreducible vertices $\Gamma^{(n)}[\mathbf{r}_1 \cdots \mathbf{r}_n; \phi]$ (the nth-order functional derivative of $\Gamma[\phi]$), from which we can deduce the correlation functions (see Appendix B).

The key quantity in the NPRG approach is the scale-dependent effective action $\Gamma_k[\phi]$ defined as a (slightly modified) Legendre transform of the free energy $F_k[h]$ of the fast modes. $\Gamma_k[\phi]$ interpolates between the microscopic action $\Gamma_\Lambda[\phi] = S[\phi]$ with no fluctuations taken into account (as in Landau's mean-field theory) and the effective action $\Gamma_{k=0}[\phi] \equiv \Gamma[\phi]$ where all fluctuations are included. It satisfies an exact RG equation which can be seen as the counterpart of the Wilson-Polchinski and Wegner-Houghton equations.[4] In general, the flow equation satisfied by $\Gamma_k[\phi]$ cannot be solved exactly. We shall show in the review that there are reliable (and numerically tractable) approximation schemes that are genuinely nonperturbative and allow us to study many physical systems.

C. Scope of the review

This aim of this review is twofold.[5] On the one hand, we present the NPRG with sufficient detail so that read-

[2] *Stricto sensu* this is true only for properly defined (dimensionless) coupling constants $\tilde{g}_{i,k}$.

[3] The upper critical dimension d_c^+ is defined as the dimension below which the mean-field predictions for the critical exponents are wrong.

[4] The Wilson-Polchinski equation can also be seen as an exact RG equation for the Helmholtz free energy $F_k[h]$.

[5] For previous reviews on the NPRG, see (Berges *et al.*, 2002; Delamotte, 2012; Kopietz *et al.*, 2010).

ers with little or no prior knowledge of Wilson's RG can understand the method and use it for their own subject of interest. After defining the scale-dependent effective action Γ_k and deriving its exact flow equation (Sec. II), with the d-dimensional O(N) model as an example, we discuss two approximation schemes: i) the derivative expansion, based on an ansatz for $\Gamma_k[\phi]$ involving a finite number of derivatives in the field (Sec. III). This leads to coupled differential equations for functions which can be solved numerically. We show that this approach, even to lowest order (and sometimes with additional simplifying assumptions, see Secs. III.A and III.B) yields a qualitatively correct picture of the O(N) model for all space dimensions $d \geq 2$ and all values of N. When pushed to order 4 or 6, the derivative expansion gives estimates of the critical exponents that compare well with the best results obtained from Monte Carlo simulations or resummed perturbative field theory. In Sec. IV, we show that the derivative expansion captures most features of the Kosterlitz-Thouless transition in the two-dimensional O(2) model. ii) the Blaizot–Méndez-Galain–Wschebor approximation which enables to close the infinite hierarchy of flow equations satisfied by the vertices $\Gamma_k^{(n)}[\phi]$ and thus obtain the low-order ones including their full momentum dependence (Sec. V). In Sec. VI, we study the large-N limit of the O(N) model in the framework of the NPRG. In Sec. VII, we discuss a version of the NPRG which applies to lattice models and takes into account both local (onsite) and critical fluctuations and thus allows us to compute not only universal quantities (e.g. critical exponents) but also nonuniversal quantities such as transition temperatures and the amplitude of the order parameter.

On the other hand, we review various applications of the NPRG, restricting ourselves to low-energy physics. More specifically, we cover the following subjects: physics of membranes, disordered systems (random-field Ising models, etc.), out-of-equilibrium systems (Kardar-Parisi-Zhang equation, reaction diffusion models, etc.), quantum O(N) model, interacting bosons and the Bose-Hubbard model. While this review mostly deals with classical or quantum bosonic systems, we briefly discuss application of RG techniques to fermions in Sec. XIV, emphasizing conceptual and technical difficulties originating from the Fermi-Dirac statistics.

Throughout the paper we use units where $\hbar = k_B = 1$. Conventions for Fourier transforms used in Secs. II-VII are given in Appendix A. In other sections, different conventions may be used in order to follow standard notations in the literature.

II. THE SCALE-DEPENDENT EFFECTIVE ACTION Γ_k

The strategy of the NPRG is to build a family of models indexed by a momentum scale k such that fluctuations are smoothly taken into account as k is lowered from a microscopic scale Λ (e.g. an inverse lattice spacing) down to zero. The central quantity in this approach is the scale-dependent effective action Γ_k (Wetterich, 1993a,c), which is a generalization of the effective action Γ (the Gibbs free energy in statiscal mechanics) (see Appendix B). In the following, we give the definition of Γ_k, discuss its basic properties and derive the exact flow equation it satisfies. Section II is self-contained; nevertheless a more detailed discussion of the effective action formalism can be found in Appendix B.

While we wish to stress the general concepts of the NPRG rather than its application to a particular model, for definiteness we shall base our discussion on the O(N) model defined by the "microscopic" action

$$S[\boldsymbol{\varphi}] = \int_{\mathbf{r}} \left\{ \frac{1}{2}(\boldsymbol{\nabla}\boldsymbol{\varphi})^2 + \frac{r_0}{2}\boldsymbol{\varphi}^2 + \frac{u_0}{4!}(\boldsymbol{\varphi}^2)^2 \right\}, \qquad (3)$$

where $\boldsymbol{\varphi}$ is a N-component real field and $\mathbf{r}$ a d-dimensional coordinate. The model is regularized by a ultraviolet momentum cutoff Λ. $r_0 = \bar{r}_0(T - T_0)$ is assumed to vary linearly with $T - T_0$ (T_0 denotes the mean-field temperature) whereas u_0 is temperature independent.

A. Definition and basic properties

There are many possible ways to suppress fluctuations in a strongly correlated system below a given (momentum) scale k. We choose here to add to the microscopic action S of the system a quadratic term ΔS_k defined by

$$\begin{aligned} \Delta S_k[\boldsymbol{\varphi}] &= \frac{1}{2}\int_{\mathbf{r},\mathbf{r}'} \varphi_i(\mathbf{r}) R_{k,ij}(\mathbf{r}-\mathbf{r}')\varphi_j(\mathbf{r}') \\ &= \frac{1}{2}\sum_{\mathbf{p}} \varphi_i(-\mathbf{p}) R_{k,ij}(\mathbf{p})\varphi_j(\mathbf{p}) \end{aligned} \qquad (4)$$

with an implicit sum over repeated discrete indices $i, j = 1 \cdots N$ (see Appendix A for conventions on Fourier transforms). For simplicity, since it is compatible with the $O(N)$ symmetry, we choose the matrix R_k diagonal: $R_{k,ij}(\mathbf{p}) = \delta_{i,j} R_k(\mathbf{p})$. The typical shape of the regulator function $R_k(\mathbf{p})$ is given in Fig. 1; it is exponentially small for $|\mathbf{p}| \gg k$ and of order k^2 for $|\mathbf{p}| \ll k$. To understand the rationale behind this choice, let us imagine that the model defined by action (3) is close to criticality. At the mean field level, this implies that r_0 is very small; beyond the mean field level, this means that r_0 is fine-tuned to be close to a critical value r_{0c}. Changing S to $S + \Delta S_k$ changes r_0 to $r_0 + R_k(\mathbf{p})$ and the modified system is no longer close to criticality (for $k > 0$). More precisely, Fourier modes with momentum $|\mathbf{p}| \lesssim k$ are no longer critical while those with $|\mathbf{p}| \gtrsim k$ remain very close to criticality since $R_k(|\mathbf{p}| \gg k) \simeq 0$. In the language of high energy physics, the quadratic term in S is called the mass term and r_0 is the (bare) square

mass.[6] The regulator function $R_k(\mathbf{p})$ can therefore be interpreted as a momentum-dependent mass-like term that, loosely speaking, gives a mass to the slow modes ($|\mathbf{p}| \lesssim k$) and leaves unchanged the fast modes ($|\mathbf{p}| \gtrsim k$). At $r_0 = r_{0c}$, criticality is recovered for $k \to 0$ since in this limit $R_k(\mathbf{p}) \to 0$ for all $\mathbf{p}$, see Fig. 1. We discuss below in more detail the specifications the regulator function $R_k(\mathbf{p})$ must satisfy to achieve this goal.

The partition function of the modified model with action $S + \Delta S_k$ reads

$$\mathcal{Z}_k[\mathbf{h}] = \int \mathcal{D}[\boldsymbol{\varphi}] \exp\Big\{-S[\boldsymbol{\varphi}] - \Delta S_k[\boldsymbol{\varphi}] + \int_{\mathbf{r}} \mathbf{h}\cdot\boldsymbol{\varphi}\Big\}. \quad (5)$$

Here $\mathbf{h}(\mathbf{r})$ denotes an external "source" (e.g. a magnetic field for a ferromagnetic system). In statistical mechanics $W_k[\mathbf{h}] = \ln \mathcal{Z}_k[\mathbf{h}]$ is simply related to the Helmoltz free energy $-T \ln \mathcal{Z}_k[\mathbf{h}]$ (Appendix B). Its first-order functional derivative wrt to $\mathbf{h}$ gives the mean-value of the field,

$$\phi_{i,k}[\mathbf{r};\mathbf{h}] = \langle\varphi_i(\mathbf{r})\rangle = \frac{\delta W_k[\mathbf{h}]}{\delta h_i(\mathbf{r})}. \quad (6)$$

For a vanishing external source ($\mathbf{h} = 0$), $\boldsymbol{\phi}_k(\mathbf{r}) \equiv \boldsymbol{\phi}_k[\mathbf{r};\mathbf{h} = 0]$ is nothing but the order parameter. It vanishes in the high-temperature (disordered) phase and takes a finite value in the low-temperature (ordered) phase where the $O(N)$ symmetry is spontaneously broken.

More generally, $W_k[\mathbf{h}]$ is the generating functional of connected Green functions: its nth-order functional derivative yields the n-point connected Green function[7]

$$G^{(n)}_{k,i_1\cdots i_n}[\mathbf{r}_1\cdots\mathbf{r}_n;\mathbf{h}] = \frac{\delta^n W_k[\mathbf{h}]}{\delta h_{i_1}(\mathbf{r}_1)\cdots\delta h_{i_n}(\mathbf{r}_n)} = \langle\varphi_{i_1}(\mathbf{r}_1)\cdots\varphi_{i_n}(\mathbf{r}_n)\rangle_c, \quad (7)$$

where the notation $\langle\cdots\rangle_c$ denotes the connected part: $\langle\varphi_i(\mathbf{r})\varphi_j(\mathbf{r}')\rangle_c = \langle\varphi_i(\mathbf{r})\varphi_j(\mathbf{r}')\rangle - \langle\varphi_i(\mathbf{r})\rangle\langle\varphi_j(\mathbf{r}')\rangle$, etc. Note that $G^{(n)}_k$ is a functional of the external source $\mathbf{h}(\mathbf{r})$.

The scale-dependent effective action[8]

$$\Gamma_k[\boldsymbol{\phi}] = -W_k[\mathbf{h}] + \int_{\mathbf{r}} \mathbf{h}\cdot\boldsymbol{\phi} - \Delta S_k[\boldsymbol{\phi}] \quad (8)$$

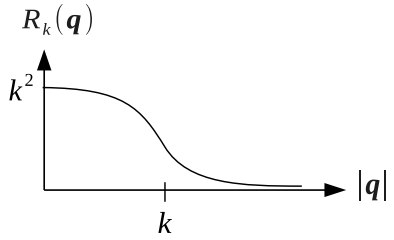

FIG. 1 Typical shape of the regulator function $R_k(\mathbf{q})$.

is defined as a (slightly modified) Legendre transform which includes the explicit subtraction of $\Delta S_k[\boldsymbol{\phi}]$. Note that in Eq. (8) $\boldsymbol{\phi}$ is taken as the independent variable so that $\mathbf{h}$, which is now obtained by inverting (6), becomes a k-dependent functional of $\boldsymbol{\phi}$: $\mathbf{h} \equiv \mathbf{h}_k[\boldsymbol{\phi}]$. From Eqs. (8) and (6), we find that $\Gamma_k[\boldsymbol{\phi}]$ satisfies the equation of state

$$\frac{\delta\Gamma_k[\boldsymbol{\phi}]}{\delta\phi_i(\mathbf{r})} = h_i(\mathbf{r}) - \int_{\mathbf{r}'} R_k(\mathbf{r}-\mathbf{r}')\phi_i(\mathbf{r}'). \quad (9)$$

The last term in (9) comes from the $\Delta S_k[\boldsymbol{\phi}]$ term in the definition of $\Gamma_k[\boldsymbol{\phi}]$. An important property of the effective action $\Gamma_k[\boldsymbol{\phi}]$, which will be used below, is that it inherits the $O(N)$ symmetry of the microscopic action S provided that $\Delta S_k[\boldsymbol{\varphi}]$ is $O(N)$ invariant. More generally, all symmetries of the microscopic action are also symmetries of the effective action $\Gamma_{k=0}[\phi]$ and it is important, for a proper implementation of the NPRG approach, to ensure that the regulator term ΔS_k does satisfy these symmetries.

1. The regulator function $R_k(\mathbf{q})$

The regulator function $R_k(\mathbf{q})$ is chosen such that the effective action Γ_k smoothly interpolates between the microscopic action S for $k = \Lambda$ and the effective action of the original model for $k = 0$. It must therefore satisfy the following properties:

- At $k = \Lambda$, $R_\Lambda(\mathbf{q}) = \infty$. All fluctuations are then frozen since the system is infinitely far from criticality and the saddle-point approximation for the partition function $\mathcal{Z}_{k=\Lambda}[\mathbf{h}]$ becomes exact. It follows that the effective action reduces to the microscopic action as in Landau's (mean-field) theory:

$$\Gamma_\Lambda[\boldsymbol{\phi}] = S[\boldsymbol{\phi}]. \quad (10)$$

  The subtraction of ΔS_k in the definition of Γ_k is crucial to obtain Eq. (10); we would otherwise find $\Gamma_\Lambda[\boldsymbol{\phi}] = S[\boldsymbol{\phi}] + \Delta S_\Lambda[\boldsymbol{\phi}]$. Equation (10) can be proven rigorously by using the function integral representation of the effective action (see Sec. B.1).

- At $k = 0$, $R_{k=0}(\mathbf{q}) = 0$, $\forall\ \mathbf{q}$. Since $\Delta S_{k=0}$ vanishes, all fluctuations are included, and the effective ac-

[6] In relativistic quantum field theory the mass defines a scale called the Compton wave length: $L_{\text{Compt.}} = \hbar/mc$ which gives the range of the interaction mediated by the field φ. The analogue of $L_{\text{Compt.}}$ in statistical mechanics is the correlation length. In the following, we will sometimes follow the high-energy physics terminology and use the term "mass" in place of the inverse of the correlation length.

[7] We denote the connected correlation functions merely by $G^{(n)}$ and not by $G^{(n)}_c$ as in Appendix B.

[8] Historically, the scale-dependent effective action (or a close version of it) was first termed the effective average action (Wetterich, 1993a,c).

tion

$$\Gamma_{k=0}[\boldsymbol{\phi}] = \Gamma[\boldsymbol{\phi}] \tag{11}$$

coincides with the effective action of the model we are interested in [Eq. (3)].

- for $0 < k < \Lambda$, $R_k(\mathbf{q})$ must suppress fluctuations with momenta below the scale k while leaving unchanged those with momenta larger than k. In general we choose a soft regulator[9] (as opposed to the sharp regulator commonly used in the weak-coupling momentum-shell RG) satisfying

$$R_k(\mathbf{q}) \simeq \begin{cases} 0 & \text{if } |\mathbf{q}| \gg k, \\ k^2 & \text{if } |\mathbf{q}| \ll k, \end{cases} \tag{12}$$

as illustrated in Fig. 1.

A possible (and common) choice for the regulator function is given by the exponential form

$$R_k(\mathbf{q}) = \alpha \frac{\mathbf{q}^2}{\exp(\mathbf{q}^2/k^2) - 1}. \tag{13}$$

where α is a number of order one. This form does not satisfy $R_\Lambda(\mathbf{q}) = \infty$. Below we argue that in general this does not matter for continuum models (see item (1) page 7); lattice models are discussed in Sec. VII. Note that when a field renormalization is considered, e.g. for the calculation of the anomalous dimension at a critical point, it is necessary to include in R_k the field renormalization factor (see Secs. III.B and III.C).

Another popular choice is the theta regulator (Litim, 2001)

$$R_k(\mathbf{q}) = \alpha(k^2 - \mathbf{q}^2)\Theta(k^2 - \mathbf{q}^2), \tag{14}$$

where $\Theta(x)$ is the step function. This form allows us to perform some momentum integrations analytically. However it is not well suited to a study of the derivative expansion beyond the second order (Sec. III).

The sharp momentum regulator $R_k(|\mathbf{p}| < k) = \infty$ and $R_k(|\mathbf{p}| > k) = 0$ has also been used in the past. It leads to severe nonanalytical behavior when the derivative expansion is used beyond its lowest order (the local potential approximation, see Sec. III.A) and will not be further discussed in this review.

Unless specified otherwise, we shall take $\alpha = 1$ in Eqs. (13) and (14).

[9] With a sharp (or hard) regulator, contrary to a soft one, all modes with momentum $|\mathbf{q}| > k$ are fully integrated out in the partition function $\mathcal{Z}_k[\mathbf{h}]$ while modes with $|\mathbf{q}| < k$ do not contribute at all. Note that some authors refer to this type of regulators as "ultrasharp".

2. The Legendre transform versus Γ_k

Why do we consider the functional $\Gamma_k[\boldsymbol{\phi}]$ rather than the true Legendre transform of W_k: $\Gamma_k^{\rm LT}[\boldsymbol{\phi}] = \Gamma_k[\boldsymbol{\phi}] + \Delta S_k[\boldsymbol{\phi}]$? The reason is that the modified model described by the action $S(\boldsymbol{\varphi}) + \Delta S_k(\boldsymbol{\varphi})$ may be very different from the original model described by $S(\boldsymbol{\varphi})$, in particular when $k \simeq \Lambda$ since $\Delta S_{k=\Lambda}(\boldsymbol{\varphi})$ is very large. When considering Γ_k, we partially compensate the effect of the $\Delta S_k(\boldsymbol{\varphi})$ term in the action by subtracting $\Delta S_k[\boldsymbol{\phi}]$ to the Legendre transform $\Gamma_k^{\rm LT}[\boldsymbol{\phi}]$ [Eq. (8)]. This compensation is exact only at the mean-field level where the fluctuations of the $\boldsymbol{\varphi}$ field are ignored and the effective action reduces to the action. Thus, $\Gamma_k[\boldsymbol{\phi}]$ is the quantity that represents best the effective action of the model where only the fluctuations of the rapid modes have been integrated over while the slow modes are taken into account only at the mean field level. Therefore, $\Gamma_k[\boldsymbol{\phi}]$, and not $\Gamma_k^{\rm LT}[\boldsymbol{\phi}]$, has the physical meaning of a coarse-grained free energy at scale $\sim k^{-1}$ that, *in fine*, converges to the free energy $\Gamma_{k=0}$ we are interested in.[10]

3. Effective potential and 1PI vertices

Most of the physically relevant information encoded in Γ_k can be obtained either from the effective potential or the 1PI vertices.

The effective potential is nothing but Γ_k evaluated in a constant (i.e. uniform) field configuration $\boldsymbol{\phi}(\mathbf{r}) = \boldsymbol{\phi}$,

$$U_k(\rho) = \frac{1}{V}\Gamma_k[\boldsymbol{\phi}]\Big|_{\boldsymbol{\phi}\ \text{const}}, \tag{15}$$

where V denotes the volume of the system. Because of the $O(N)$ symmetry of $\Gamma_k[\boldsymbol{\phi}]$, U_k is a function of the $O(N)$ invariant[11]

$$\rho = \frac{1}{2}\boldsymbol{\phi}^2. \tag{16}$$

For $k = 0$, the effective potential reduces to the free energy per unit volume $F/V = TU_{k=0}(\rho)$ and the equation of state takes the form

$$\frac{\partial U_{k=0}(\rho)}{\partial \boldsymbol{\phi}} = \mathbf{h} \tag{17}$$

in the presence of a uniform external field $\mathbf{h}$.

[10] Nothing prevents us to work with $\Gamma_k^{\rm LT}$ rather than Γ_k. However, since it is Γ_k that carries the physical meaning of a coarse-grained free energy, approximations such as the derivative expansion (see below) are naturally implemented on this quantity (and not on $\Gamma_k^{\rm LT}$).

[11] When there are more than one invariant, the effective potential is a multidimensional function.

The functional $\Gamma_k^{\rm LT}[\boldsymbol{\phi}] = \Gamma_k[\boldsymbol{\phi}] + \Delta S_k[\boldsymbol{\phi}]$ is the Legendre transform of $W_k[\mathbf{h}]$ and therefore a convex function of $\boldsymbol{\phi}$. For a constant field, this implies that the function $U_k(\rho) + \rho R_k(0)$ is convex. The matrix

$$\begin{aligned}\frac{\partial^2}{\partial\phi_i\partial\phi_j}&[U_k(\rho)+\rho R_k(0)]\\ &= \left(\delta_{i,j} - \frac{\phi_i\phi_j}{2\rho}\right)[U_k'(\rho)+R_k(0)]\\ &\quad + \frac{\phi_i\phi_j}{2\rho}[U_k'(\rho)+2\rho U_k''(\rho)+R_k(0)] \end{aligned} \tag{18}$$

of second derivatives must therefore be positive semi-definite, which implies

$$\begin{aligned} U_k'(\rho)+R_k(0) &\geq 0,\\ U_k'(\rho)+2\rho U_k''(\rho)+R_k(0) &\geq 0. \end{aligned} \tag{19}$$

On the other hand, $\Gamma_k[\boldsymbol{\phi}]$ needs not be convex for $k > 0$ since it is not a Legendre transform. In particular, the effective potential $U_k(\rho)$ may exhibit a minimum at $\rho_{0,k} > 0$ for all $k > 0$. Spontaneous symmetry breaking of the $O(N)$ symmetry is characterized by a nonvanishing expectation value of the field, that is, $\lim_{k\to 0}\rho_{0,k} = \rho_0 > 0$. In this case, the effective potential $U_{k=0}(\rho)$ is constant (and minimum) for $0 \leq \rho \leq \rho_0$. When $\rho_{0,k}$ vanishes at a finite value k_0, the latter is naturally identified with the inverse of the correlation length: $k_0 \sim \xi^{-1}$. Following the location of the minimum of the effective potential will therefore be of particular importance.[12]

The 1PI vertices[13] $\Gamma_k^{(n)}$ evaluated in a constant field configuration $\boldsymbol{\phi}(\mathbf{r}) = \boldsymbol{\phi}$,

$$\Gamma^{(n)}_{k,i_1\cdots i_n}(\{\mathbf{r}_i\};\boldsymbol{\phi}) = \left.\frac{\delta^n\Gamma_k[\boldsymbol{\phi}]}{\delta\phi_{i_1}(\mathbf{r}_1)\cdots\delta\phi_{i_n}(\mathbf{r}_n)}\right|_{\boldsymbol{\phi}\ \text{const}}, \tag{20}$$

are simply related to the correlation functions $G_k^{(n)}$ (see Appendix B). In particular, the two-point vertex $\Gamma_k^{(2)}$ directly determines the (connected) correlation function $G_k \equiv G_k^{(2)}$. Taking the functional derivative $\delta/\delta h_j(\mathbf{r}')$ of Eq. (9), we obtain

$$\begin{aligned}\int_{\mathbf{r}''}&\left[\Gamma^{(2)}_{k,il}[\mathbf{r},\mathbf{r}'';\boldsymbol{\phi}] + \delta_{i,l}R_k(\mathbf{r}-\mathbf{r}'')\right]\\ &\times G_{k,lj}[\mathbf{r}'',\mathbf{r}';\boldsymbol{\phi}] = \delta_{i,j}\delta(\mathbf{r}-\mathbf{r}')\end{aligned} \tag{21}$$

or, in matrix form,

$$G_k[\boldsymbol{\phi}] = \left(\Gamma_k^{(2)}[\boldsymbol{\phi}] + R_k\right)^{-1}. \tag{22}$$

Note that by using the equation of state (9) to relate the external source $\mathbf{h}$ to the order parameter $\boldsymbol{\phi}$, we can consider $G_k[\boldsymbol{\phi}]$ as a functional of $\boldsymbol{\phi}$ (rather than $\mathbf{h}$). Because of the $O(N)$ symmetry,

$$\Gamma^{(2)}_{k,ij}(\mathbf{p};\boldsymbol{\phi}) \equiv \Gamma^{(2)}_{k,ij}(\mathbf{p},-\mathbf{p};\boldsymbol{\phi}) = \left.\frac{\delta^2\Gamma_k[\boldsymbol{\phi}]}{\delta\phi_i(-\mathbf{p})\delta\phi_j(\mathbf{p})}\right|_{\boldsymbol{\phi}\ \text{const}} \tag{23}$$

can be expressed in terms of its longitudinal and transverse parts,

$$\Gamma^{(2)}_{k,ij}(\mathbf{p};\boldsymbol{\phi}) = \frac{\phi_i\phi_j}{2\rho}\Gamma^{(2)}_{k,\mathrm{L}}(\mathbf{p};\rho) + \left(\delta_{i,j} - \frac{\phi_i\phi_j}{2\rho}\right)\Gamma^{(2)}_{k,\mathrm{T}}(\mathbf{p};\rho), \tag{24}$$

where $\Gamma^{(2)}_{k,\mathrm{L}}(\mathbf{p};\rho)$ and $\Gamma^{(2)}_{k,\mathrm{T}}(\mathbf{p};\rho)$ are functions of the $O(N)$ invariant ρ. A similar expression holds for the two-point Green function $G_{k,ij}(\mathbf{p};\boldsymbol{\phi})$, with

$$\begin{aligned} G_{k,\mathrm{L}}(\mathbf{p};\rho) &= [\Gamma^{(2)}_{k,\mathrm{L}}(\mathbf{p};\rho) + R_k(\mathbf{p})]^{-1},\\ G_{k,\mathrm{T}}(\mathbf{p};\rho) &= [\Gamma^{(2)}_{k,\mathrm{T}}(\mathbf{p};\rho) + R_k(\mathbf{p})]^{-1}. \end{aligned} \tag{25}$$

4. General properties of the effective action Γ_k

Let us mention some important properties of the effective action Γ_k:

1) In a model with a UV momentum cutoff Λ, in principle one should ensure that $R_\Lambda = \infty$ so that $\Gamma_\Lambda = S$. In some cases however, in particular when one is interested in universal quantities, the property $\Gamma_\Lambda = S$ is not essential as the microscopic physics can be directly parametrized by Γ_Λ (with no need to specify the microscopic action S). In continuum models, where the UV cutoff Λ has usually no precise physical meaning (except, maybe, as the remnant of an inverse lattice spacing), we shall not in general impose the condition $R_\Lambda = \infty$.[14] In other cases, for example in lattice models, it is important to treat the initial condition carefully if one wants to compute (non-universal) quantities as a function of the microscopic parameters of the model (see Sec. VII).

2) Since k acts as an infrared regulator, somewhat similar to a box of finite size $\sim k^{-1}$, the critical fluctuations are cut off by the R_k term and the effective action Γ_k is analytic for $k > 0$, at least if $\boldsymbol{\phi}$ is the order parameter. The singularities associated with critical behavior can therefore arise only for $k = 0$.[15] This implies in

[12] It is often said, somewhat inappropriately, that the system with action $S + \Delta S_k$ is in the broken-symmetry phase whenever $\rho_{0,k} > 0$ although the "true" effective potential $U_k(\rho) + \rho R_k(0)$ associated to $\Gamma_k^{\rm LT}[\boldsymbol{\phi}]$, being convex, has a single minimum at $\rho = 0$ for $k > 0$.

[13] The reason for this terminology is given in Appendix B.

[14] The easiest way to satisfy the condition $\Gamma_{\Lambda_{\rm in}}[\boldsymbol{\phi}] = S[\boldsymbol{\phi}]$ in a continuum model with a UV momentum cutoff Λ is to take an initial value $\Lambda_{\rm in}$ of k which differs from Λ. In the limit where $\Lambda_{\rm in}$ is much larger than Λ as well as all characteristic momentum scales, all fluctuations are effectively frozen by the regulator function $R_{\Lambda_{\rm in}}(\mathbf{q}) \sim \Lambda_{\rm in}^2$ and the relation $\Gamma_{\Lambda_{\rm in}}[\boldsymbol{\phi}] = S[\boldsymbol{\phi}]$ holds.

[15] Singularities can occur in the flow at finite k if critical fluctuations show up in higher-order correlation functions, the or-

particular that the vertices $\Gamma^{(n)}_{k,i_1\cdots i_n}(\mathbf{p}_1,\cdots,\mathbf{p}_n;\boldsymbol{\phi})$ are smooth functions of the momenta and can be expanded in powers of $\mathbf{p}_i^2/k^2$ or $\mathbf{p}_i^2/m^2$, whichever is the smallest, where m is the smallest mass of the problem. For the same reason, the effective action $\Gamma_k[\boldsymbol{\phi}]$ itself can be expanded in derivatives if one is interested only in the physics at length scales larger than either k^{-1} or the correlation length. This property of the effective action and the n-point vertices is crucial as it underlies both the derivative expansion (Sec. III) and the Blaizot–Méndez-Galain–Wschebor approximation (Sec. V).

3) All symmetries of the model that are respected by the infrared regulator ΔS_k are automatically symmetries of Γ_k. As a consequence, Γ_k can be expanded in terms of invariants of these symmetries (see Eqs. (15) and (24)).

4) There are important conceptual differences between the effective action $\Gamma_k[\boldsymbol{\phi}]$ and the Wilsonian effective action $S_k^{\mathrm{W}}[\boldsymbol{\varphi}]$. In the Wilson approach k plays the role of a UV cutoff for the slow modes. $S_k^{\mathrm{W}}[\boldsymbol{\varphi}]$ describes a set of different actions, parametrized by k, for the same model. The correlation functions are independent of k and have to be computed from $S_k^{\mathrm{W}}[\boldsymbol{\varphi}]$ by further functional integration. Information about correlation functions with momenta above k is lost. In contrast k acts as an infrared regulator for the fast modes in the effective action method. Moreover, Γ_k is the effective action for a set of different models. The n-point correlation functions depend on k and can be obtained from the n-point vertices $\Gamma_k^{(n)}$. The latter can be obtained for any value of external momenta.

B. Exact flow equation

We now derive the flow equation satisfied by the effective action Γ_k as the momentum scale k varies. Taking the k-derivative of Eq. (5), we obtain

$$\partial_t \mathcal{Z}_k[\mathbf{h}] = -\frac{1}{2}\int_{\mathbf{r},\mathbf{r}'} \dot{R}_k(\mathbf{r}-\mathbf{r}')\frac{\delta^2 \mathcal{Z}_k[\mathbf{h}]}{\delta h_i(\mathbf{r})h_i(\mathbf{r}')} \tag{26}$$

and therefore[16]

$$\begin{aligned}\partial_t W_k[\mathbf{h}] = &-\frac{1}{2}\int_{\mathbf{r},\mathbf{r}'} \dot{R}_k(\mathbf{r}-\mathbf{r}') \\ &\times\left(\frac{\delta^2 W_k[\mathbf{h}]}{\delta h_i(\mathbf{r})h_i(\mathbf{r}')}+\frac{\delta W_k[\mathbf{h}]}{\delta h_i(\mathbf{r})}\frac{\delta W_k[\mathbf{h}]}{\delta h_i(\mathbf{r}')}\right).\end{aligned} \tag{27}$$

der parameter being then defined by a composite field, e.g. $\langle\varphi_i(\mathbf{r})\varphi_j(\mathbf{r})\rangle$. A proper treatment of critical fluctuations would require a regulator term of higher order in the field, e.g. a quartic regulator ΔS_k. It is also possible that nonanalyticities be not directly related to criticality. This the case, for instance, in the random field Ising model where a cusp in an effective potential shows up at a finite scale related to the Larkin length (Sec. X).

[16] Equation (27) is closely related to the Wilson-Polchinski equation.

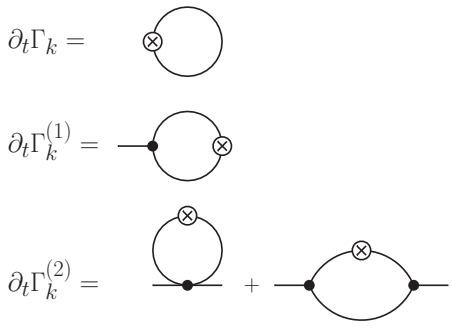

FIG. 2 Diagrammatic representation of Eqs. (30), (35) and (36). The solid line stands for the propagator G_k, the cross for $\dot{R}_k$ and the dot with n legs for $\Gamma_k^{(n)}$. Signs and symmetry factors are not shown explicitly.

Here and in the following we use the (negative) RG "time" $t=\ln(k/\Lambda)$:

$$k=\Lambda e^t, \quad \partial_t = k\partial_k, \quad \dot{R}_k = \partial_t R_k. \tag{28}$$

The derivative ∂_t in (27) is taken at fixed external source $\mathbf{h}$. To obtain the flow equation of the effective action $\Gamma_k[\boldsymbol{\phi}]$ at fixed $\boldsymbol{\phi}$, we must consider $\mathbf{h}\equiv\mathbf{h}_k[\boldsymbol{\phi}]$ as a k-dependent functional of $\boldsymbol{\phi}$ defined by (6) or (9). Using

$$\begin{aligned}\partial_t W_k[\mathbf{h}]\Big|_{\boldsymbol{\phi}} &= \partial_t W_k[\mathbf{h}]\Big|_{\mathbf{h}} + \int_{\mathbf{r}} \frac{\delta W_k[\mathbf{h}]}{\delta h_i(\mathbf{r})}\partial_t h_i(\mathbf{r})\Big|_{\boldsymbol{\phi}} \\ &= \partial_t W_k[\mathbf{h}]\Big|_{\mathbf{h}} + \int_{\mathbf{r}} \phi_i(\mathbf{r})\partial_t h_i(\mathbf{r})\Big|_{\boldsymbol{\phi}},\end{aligned} \tag{29}$$

we find (Wetterich, 1993b)

$$\begin{aligned}\partial_t\Gamma_k[\boldsymbol{\phi}] &= \frac{1}{2}\int_{\mathbf{r},\mathbf{r}'} \dot{R}_k(\mathbf{r}-\mathbf{r}')\frac{\delta^2 W_k[\mathbf{h}]}{\delta h_i(\mathbf{r})h_i(\mathbf{r}')} \\ &= \frac{1}{2}\mathrm{Tr}\left[\dot{R}_k G_k[\mathbf{h}]\right] \\ &= \frac{1}{2}\mathrm{Tr}\left[\dot{R}_k\big(\Gamma_k^{(2)}[\boldsymbol{\phi}]+R_k\big)^{-1}\right].\end{aligned} \tag{30}$$

where Tr denotes a trace wrt space as well as the internal index of the field and (22) has been used to obtain the last equation.[17]

It is sometimes convenient to write the flow equation as

$$\partial_t\Gamma_k[\boldsymbol{\phi}] = \frac{1}{2}\tilde{\partial}_t \mathrm{Tr}\ln\big(\Gamma_k^{(2)}[\boldsymbol{\phi}]+R_k\big), \tag{31}$$

where $\tilde{\partial}_t$ acts only on the k dependence of R_k and not on $\Gamma_k^{(2)}$,

$$\tilde{\partial}_t = \dot{R}_k\frac{\partial}{\partial R_k}. \tag{32}$$

[17] Eq. (30) is sometimes referred to as Wetterich's equation (Wetterich, 1993b).

Equation (30) is shown diagrammatically in Fig. 2.

By taking successive functional derivatives of (30) wrt $\phi_i(\mathbf{r})$, one obtains an infinite hierarchy of equations for the vertices where $\partial_t \Gamma_k^{(n)}$ involves $\Gamma_k^{(n+1)}$ and $\Gamma_k^{(n+2)}$. For instance,

$$\partial_t \Gamma_{k,i}^{(1)}[\mathbf{r};\boldsymbol{\phi}] = \partial_t \frac{\delta \Gamma_k[\boldsymbol{\phi}]}{\delta \phi_i(\mathbf{r})} = \frac{1}{2}\tilde{\partial}_t \mathrm{Tr}\left[G_k[\boldsymbol{\phi}] \frac{\delta \Gamma_k^{(2)}[\boldsymbol{\phi}]}{\delta \phi_i(\mathbf{r})}\right] \quad (33)$$

and

$$\partial_t \Gamma_{k,ij}^{(2)}[\mathbf{r},\mathbf{r}';\boldsymbol{\phi}] = \frac{1}{2}\tilde{\partial}_t \mathrm{Tr}\Big[G_k[\boldsymbol{\phi}] \frac{\delta^2 \Gamma_k^{(2)}[\boldsymbol{\phi}]}{\delta \phi_i(\mathbf{r}) \delta \phi_j(\mathbf{r}')} - G_k[\boldsymbol{\phi}] \frac{\delta \Gamma_k^{(2)}[\boldsymbol{\phi}]}{\delta \phi_i(\mathbf{r})} G_k[\boldsymbol{\phi}] \frac{\delta \Gamma_k^{(2)}[\boldsymbol{\phi}]}{\delta \phi_j(\mathbf{r}')}\Big]. \quad (34)$$

For a constant field $\boldsymbol{\phi}$, this gives

$$\partial_t \Gamma_{k,i}^{(1)}(\mathbf{p};\boldsymbol{\phi}) = \frac{\delta_{\mathbf{p},0}}{2} \sum_{\mathbf{q}} \tilde{\partial}_t G_{k,i_1 i_2}(\mathbf{q};\boldsymbol{\phi}) \times \Gamma_{k,i i_2 i_1}^{(3)}(0,\mathbf{q},-\mathbf{q};\boldsymbol{\phi}) \quad (35)$$

and

$$\partial_t \Gamma_{k,ij}^{(2)}(\mathbf{p};\boldsymbol{\phi}) = \sum_{\mathbf{q}} \tilde{\partial}_t G_{k,i_1 i_2}(\mathbf{q};\boldsymbol{\phi}) \times \Big[\frac{1}{2}\Gamma_{k,ij i_2 i_1}^{(4)}(\mathbf{p},-\mathbf{p},\mathbf{q},-\mathbf{q};\boldsymbol{\phi}) - \Gamma_{k,i i_2 i_3}^{(3)}(\mathbf{p},\mathbf{q},-\mathbf{p}-\mathbf{q};\boldsymbol{\phi}) \times G_{k,i_3 i_4}(\mathbf{p}+\mathbf{q};\boldsymbol{\phi}) \Gamma_{k,j i_4 i_1}^{(3)}(-\mathbf{p},\mathbf{p}+\mathbf{q},-\mathbf{q};\boldsymbol{\phi})\Big], \quad (36)$$

where

$$\tilde{\partial}_t G_{k,i_1 i_2}(\mathbf{q};\boldsymbol{\phi}) = -\dot{R}_k(\mathbf{q}) G_{k,i_1 i_3}(\mathbf{q};\boldsymbol{\phi}) G_{k,i_3 i_2}(\mathbf{q};\boldsymbol{\phi}). \quad (37)$$

Equations (35) and (36) are represented diagrammatically in Fig. 2.

General properties of the flow equation

Let us mention some important properties of the flow equation $\partial_t \Gamma_k[\boldsymbol{\phi}]$:

1) The standard perturbative expansion about the Gaussian model can be retrieved from the flow equation (30) (Appendix I).

2) The flow equations (30), (35) and (36) look very much like one-loop equations. The one-loop expression for Γ_k reads

$$\Gamma_k[\boldsymbol{\phi}] = S[\boldsymbol{\phi}] + \frac{1}{2}\mathrm{Tr}\ln\big(S^{(2)}[\boldsymbol{\phi}] + R_k\big), \quad (38)$$

where $S^{(2)}[\boldsymbol{\phi}]$ denotes the second functional derivative of the action $S[\boldsymbol{\phi}]$ [Eq. (B23)]. Taking a k derivative leads to a flow equation,

$$\partial_t \Gamma_k[\boldsymbol{\phi}] = \frac{1}{2}\mathrm{Tr}\left[\dot{R}_k\big(S^{(2)}[\boldsymbol{\phi}] + R_k\big)^{-1}\right], \quad (39)$$

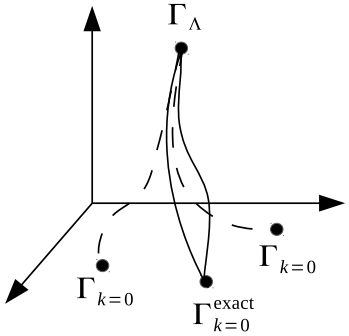

FIG. 3 RG flow in the parameter space of the effective action. The solid lines show the exact RG flows obtained with two different regulator functions R_k. The dashed lines show the RG flows obtained by solving approximately the RG equation with two different regulator functions.

very similar to Eq. (30). Substitution of $S^{(2)}[\boldsymbol{\phi}]$ by $\Gamma_k^{(2)}[\boldsymbol{\phi}]$ turns the one-loop flow equation into an exact flow equation. This one-loop structure is important in practice as it implies that a single (d-dimensional) momentum integration has to be carried out. This is very different from perturbation theory where l-loop diagrams require l momentum integrals.

3) Any sensible approximation, which does not spoil the one-loop structure, is one-loop exact (in the sense that it encompasses the one-loop result when expanded in the coupling constant). This implies that all results obtained from a one-loop approximation must be recovered from the nonperturbative flow equation. This includes the computation of the critical exponents to $\mathcal{O}(\epsilon)$ in the $\epsilon = 4 - d$ expansion of the $O(N)$ model, and to leading order in the large-N limit. We shall see that the $\epsilon = d - 2$ expansion obtained from the nonlinear sigma model is also reproduced from the nonperturbative flow equation in the (linear) $O(N)$ model (Sec. III.C).

4) The presence of $\dot{R}_k$ in the trace of Eq. (30) implies that only momenta of order k or less contribute to the flow at scale k (provided that $R_k(\mathbf{p})$ decays sufficiently fast for $|\mathbf{p}| \gg k$), which implements Wilson's idea of momentum shell integration of fluctuations (with a soft separation between fast and slow modes). This, in particular, ensures that the momentum integration is UV finite. Furthermore, the R_k term appearing in the propagator $G_k = (\Gamma_k^{(2)} + R_k)^{-1}$ acts as an infrared regulator and ensures that the momentum integration in (30) is free of infrared divergences. This makes the formulation well-suited to deal with theories that are plagued with infrared problems in perturbation theory, e.g. in the vicinity of a second order phase transition. In particular, the flow equation can be used in phases with spontaneously broken continuous symmetries despite the presence of (gapless) Goldstone modes.

5) Different choices of the regulator function R_k correspond to different trajectories in the space of effective

actions. If no approximation were made on the flow equation, the final point $\Gamma_{k=0}$ would be the same for all trajectories. However, once approximations are made, $\Gamma_{k=0}$ acquires a dependence on the precise shape of R_k (Fig. 3). This dependence can be used to study the robustness of the approximations (see, for example, Sec. III) either by changing the analytical form of R_k or by varying a parameter in a given family of regulators such as the prefactor α in Eqs. (13) and (14). Note that the choice $\alpha = 1$ commonly made in the literature for this family of regulators is only one particular choice among infinitely many others (see, e.g., Sec. III.C).

The dependence of the renormalization trajectories upon the choice of regulator function is very reminiscent of the dependence of the perturbative β-function on the choice of renormalization prescription.[18]

6) The regulator R_k must be such that the effective action Γ_Λ can be computed (possibly numerically) to reasonable accuracy from the microscopic action $S+\Delta S_\Lambda$.[19] Γ_Λ is then used as the initial condition of the exact flow equation (30) (which, in general, will be solved approximately). In the standard implementation of the NPRG that we have discussed so far, the regulator function is chosen such that the mean-field solution is exact at scale Λ, leading to $\Gamma_\Lambda = S$. This is however not the only possible choice. For lattice models, it can be advantageous to choose a regulator function such that $S + \Delta S_\Lambda$ corresponds to a system of decoupled sites. The flow equation then implements an expansion about the single-site limit (see Sec. VII).

7) The flow equation (30) is a complicated functional integro-differential equation, which cannot (except in trivial cases) be solved exactly. Two main types of approximations have been designed: the derivative expansion, which is based on an ansatz for Γ_k involving a finite number of derivatives of the field, and the vertex expansion, which is based on a truncation of the infinite hierarchy of equations satisfied by the $\Gamma_k^{(n)}$'s. Both types of approximation are discussed in the following sections.

[18] In general, the coefficients of a perturbative β-function are not universal and only the first nontrivial one is (or the first two, depending on the model). Two different ways of defining the renormalized coupling constant lead therefore to two different β-functions and any truncation of the perturbative series at a finite order yields a dependence of the physical quantities upon this choice. Resummations of the perturbative β-functions such as Padé approximants do not remove this problem. Although they can lead to accurate results they, in fact, introduce a supplementary level of arbitrariness since there are infinitely many ways of resumming perturbative series. (Mettre ce commentaire plutôt dans Sec. sur la DE?)

[19] As pointed out above, this requirement can be released if one is interested only in universal quantities and not in the solution of a particular model, the microscopic physics being then parametrized directly by Γ_Λ.

III. THE DERIVATIVE EXPANSION

The derivative expansion is based on an ansatz for the scale-dependent effective action Γ_k involving a finite number of derivatives in the field. To second order,

$$\Gamma_k[\phi] = \int_{\mathbf{r}} \left\{ \frac{1}{2} Z_k(\rho)(\boldsymbol{\nabla}\boldsymbol{\phi})^2 + \frac{1}{4} Y_k(\rho)(\boldsymbol{\nabla}\rho)^2 + U_k(\rho) \right\} \tag{40}$$

is parameterized by three functions of the O(N) invariant ρ, with U_k the effective potential introduced in the previous section. There are two $\mathcal{O}(\boldsymbol{\nabla}^2)$ terms, reflecting the fact that longitudinal and transverse fluctuations (wrt the local order parameter $\boldsymbol{\phi}(\mathbf{r})$) have different stiffness. For $N = 1$, the term $Y_k(\rho)(\boldsymbol{\nabla}\rho)^2$ should be omitted since it can be put in the form $Z_k(\rho)(\boldsymbol{\nabla}\boldsymbol{\phi})^2$. Within the ansatz (40), the flow equation $\partial_t \Gamma_k[\boldsymbol{\phi}]$ reduces to three coupled partial differential equations for the functions $U_k(\rho)$, $Z_k(\rho)$ and $Y_k(\rho)$. The derivative expansion can be systematically improved by considering higher-order terms in derivatives (Sec. III.D).

The possibility of a derivative expansion is a consequence of the regulator term ΔS_k in the action. The latter ensures that all vertices $\Gamma_k^{(n)}(\mathbf{p}_1 \cdots \mathbf{p}_n; \boldsymbol{\phi})$ are smooth functions of momenta and can be expanded in powers of $\mathbf{p}_i^2/k^2$ when $|\mathbf{p}_i| \ll k$, even in the critical case.[20] Thus the derivative expansion of the effective action is justified as long as we are interested only in the long-wavelength physics (corresponding to length scales larger than k^{-1} or the correlation length of the theory). Moreover, the $\dot{R}_k$ term in the flow equation (30) implies that the integral over the loop momentum $\mathbf{q}$ is dominated by $|\mathbf{q}| \lesssim k$. This allows us to use the derivative expansion of Γ_k in the rhs of the flow equation.

While the derivative expansion seems perfectly fine to obtain the effective potential $U_{k=0}(\rho)$, it is restricted to the computation of the n-point vertices $\Gamma_{k=0}^{(n)}(\mathbf{p}_1 \cdots \mathbf{p}_n; \boldsymbol{\phi})$ at vanishing momenta. Although this is true *stricto sensu*, we shall see that some properties of the vertices at finite momenta can nevertheless be obtained. The most striking example is the anomalous dimension η which can be deduced from the derivative expansion even though the momentum dependence of the 2-point vertex is singular, i.e. $\Gamma_k^{(2)}(\mathbf{p}) \sim |\mathbf{p}|^{2-\eta}$, only for $k \ll |\mathbf{p}| \ll \xi_G^{-1}$ (with ξ_G the Ginzburg length) but remains regular for $k \gg |\mathbf{p}|$ (Sec. III.C).

Before discussing the derivative expansion in detail (Secs. III.C and III.D), we consider a further approximation, the local potential approximation (Secs. III.A and III.B).

[20] Following Eq. (20) we denote by $\Gamma_k^{(n)}(\mathbf{p}_1 \cdots \mathbf{p}_n; \boldsymbol{\phi})$ the vertices evaluated in a constant field configuration $\boldsymbol{\phi}(\mathbf{r}) = \boldsymbol{\phi}$, not to be confused with the vertices $\Gamma_k^{(n)}[\mathbf{p}_1 \cdots \mathbf{p}_n; \boldsymbol{\phi}]$ defined in an arbitrary field configuration [Eq. (B11)].

A. The local potential approximation (LPA)

In the LPA, one sets $Z_k(\rho)=1$ and $Y_k(\rho)=0$ in (40). The effective action

$$\Gamma_k[\phi]=\int_{\mathbf{r}}\left\{\frac{1}{2}(\boldsymbol{\nabla}\boldsymbol{\phi})^2+U_k(\rho)\right\} \tag{41}$$

is then entirely determined by the effective potential $U_k(\rho)$. The corresponding 2-point vertex in a constant field is given by

$$\Gamma^{(2)}_{k,ij}(\mathbf{p};\boldsymbol{\phi})=\delta_{i,j}[\mathbf{p}^2+U_k'(\rho)]+\phi_i\phi_j U_k''(\rho) \tag{42}$$

or, equivalently,

$$\begin{aligned}\Gamma^{(2)}_{k,\mathrm{L}}(\mathbf{p};\rho)&=\mathbf{p}^2+U_k'(\rho)+2\rho U_k''(\rho),\\ \Gamma^{(2)}_{k,\mathrm{T}}(\mathbf{p};\rho)&=\mathbf{p}^2+U_k'(\rho).\end{aligned} \tag{43}$$

Higher-order vertices are momentum independent in the LPA since[21]

$$\Gamma^{(n)}_{k,i_1\cdots i_n}(\{\mathbf{p}_i\};\boldsymbol{\phi})=\delta_{\sum_i \mathbf{p}_i,0}V^{1-\frac{n}{2}}\frac{\partial^n U_k(\rho)}{\partial\phi_{i_1}\cdots\partial\phi_{i_n}} \tag{44}$$

for $n\geq 3$. From the point of view of perturbation theory, the LPA is a highly nontrivial approximation as it includes the zero-momentum contribution of all n-point vertices.

The flow equation of the effective potential follows directly from its definition (15),

$$\begin{aligned}\partial_t U_k(\rho)&=\frac{1}{V}\partial_t\Gamma_k[\phi]\Big|_{\boldsymbol{\phi}\text{ const}}\\ &=\frac{1}{2}\int_{\mathbf{q}}\dot{R}_k(\mathbf{q})G_{k,ii}(\mathbf{q};\boldsymbol{\phi})\Big|_{\boldsymbol{\phi}\text{ const}}.\end{aligned} \tag{45}$$

We deduce

$$\partial_t U_k(\rho)=\frac{1}{2}\int_{\mathbf{q}}\dot{R}_k(\mathbf{q})[G_{k,\mathrm{L}}(\mathbf{q};\rho)+(N-1)G_{k,\mathrm{T}}(\mathbf{q};\rho)], \tag{46}$$

where the longitudinal and transverse parts of the propagator are defined by (25). Note that the contribution of transverse fluctuations appears with a factor $N-1$.

From Eqs. (43,46), we find for the flow of U_k

$$\begin{aligned}\partial_t U_k=&-2v_d k^d\int_0^\infty dy\, y^{\frac{d}{2}+1}r'\left[\frac{N-1}{y(r+1)+k^{-2}U_k'}\right.\\ &\left.+\frac{1}{y(r+1)+k^{-2}\left(U_k'+2\rho U_k''\right)}\right].\end{aligned} \tag{47}$$

[21] Recall that our conventions for Fourier transforms imply $\phi_i(\mathbf{p})=\delta_{\mathbf{p},0}\sqrt{V}\phi_i$ in a constant field $\boldsymbol{\phi}(\mathbf{r})=\boldsymbol{\phi}$.

Here we use the dimensionless quantity $y=q^2/k^2$ and the function $r\equiv r(y)$ (with $r'=dr/dy$) defined by

$$R_k(\mathbf{q})=\mathbf{q}^2 r(y), \tag{48}$$

and write the momentum integral as

$$\int\frac{d^dq}{(2\pi)^d}=2v_d k^d\int_0^\infty dy\, y^{d/2-1}, \tag{49}$$

where $v_d^{-1}=2^{d+1}\pi^{d/2}\Gamma(d/2)$ ($S_d=4(2\pi)^d v_d$ is the surface of the unit sphere in a d-dimensional space). The exponential and the theta regulators (13,14) correspond to $r=1/(e^y-1)$ and $r=((1-y)/y)\Theta(1-y)$, respectively.

For the theta regulator, using

$$r'=-\frac{1}{y^2}\Theta(1-y)-\left(\frac{1}{y}-1\right)\delta(1-y) \tag{50}$$

and noting that $y(r+1)=1$ for $y\leq 1$, the momentum integral in (47) can be done analytically. This leads to a particularly simple form of the flow equation,

$$\partial_t U_k=4\frac{v_d}{d}k^{d+2}\left[\frac{1}{k^2+U_k'+2\rho U_k''}+\frac{N-1}{k^2+U_k'}\right]. \tag{51}$$

We can now integrate this flow starting with various initial conditions at scale Λ.

We choose to consider the simplest class of nontrivial initial conditions exhibiting an $O(N)$ symmetry,

$$U_\Lambda(\rho)=r_0\rho+\frac{u_0}{6}\rho^2 \tag{52}$$

(this corresponds to $\Gamma_\Lambda[\boldsymbol{\phi}]=S[\boldsymbol{\phi}]$ with S the action (3) of the $O(N)$ model). Its minimum is given by

$$\rho_{0,\Lambda}=\begin{cases}0 & \text{if } r_0\geq 0,\\ -3\,\dfrac{r_0}{u_0} & \text{if } r_0\leq 0.\end{cases} \tag{53}$$

Thermal fluctuations tend to disorder the system so that the minimum $\rho_{0,k}$ of U_k decreases with k. As discussed above, the phase of the system depends on the value of $\rho_0=\lim_{k\to 0}\rho_{0,k}$. If $\rho_0=0$ the system is in its symmetric phase whereas if $\rho_0>0$ it is in its symmetry-broken phase. In between these two situations, the system is at criticality; this occurs when the initial condition is fine tuned in such a way that $\rho_{0,k}$ remains positive for all $k>0$ and vanishes only at $k=0$. Therefore, at fixed u_0, there exists a critical value $r_{0c}<0$ such that: (i) for $r_0>r_{0c}$ the system is in the high-temperature phase ($\rho_0=0$); (ii) for $r_0<r_{0c}$ the system is in the low-temperature phase and ρ_0 is, in the magnetic language, (half of the square of) the spontaneous magnetization.[22] These two cases

[22] For $N>2$ and $d=2$, Mermin-Wagner theorem implies that the system is always in its high temperature phase and thus, $\rho_0=0$, $\forall r_0$. The LPA is not sufficient to retrieve this result but a variant, the LPA', discussed below, is. Vraiment? Discuter plus tard

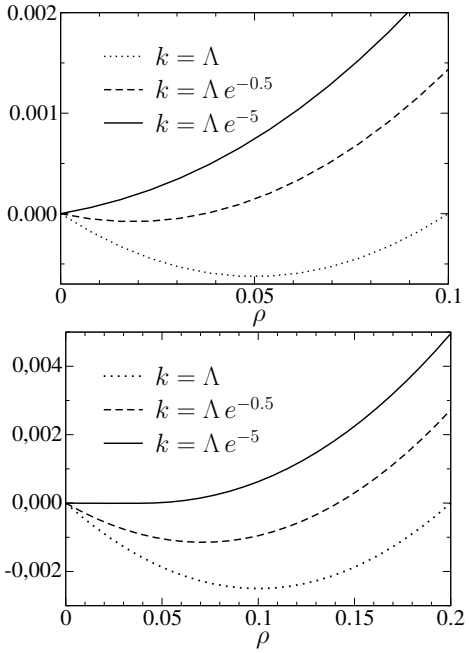

FIG. 4 Effective potential $U_k(\rho) - U_k(0)$ obtained from the flow equation (47) and the initial condition (52) with $u_0 = 1.5$, $N = 3$ and $d = 3$. Top panel: disordered phase, $\rho_{0,\Lambda} = 0.05$ and $\rho_0 = 0$. Bottom panel: ordered phase, $\rho_{0,\Lambda} = 0.1$ and $\rho_0 \simeq 0.05$. Note that the potential becomes (almost) flat for $\rho \in [0, \rho_0]$ as $k \to 0$, showing the approach to the convex effective potential (Sec. III.A.4). (Because we are using the variable ρ (rather than $\boldsymbol{\phi}$), the usual picture of the Mexican-hat shape potential when $\rho_{0,k} > 0$ is partially lost (in particular because $U_k'(\rho = 0) \neq 0$).)

are shown in Fig. 4. In the low-temperature phase, U_k becomes convex when $k \to 0$ with a flat inner part for $\rho \leq \rho_0$. Furthermore the mass at $\rho = \rho_0$ in the transverse 2-point vertex $\Gamma^{(2)}_{k=0,\mathrm{T}}$ vanishes,

$$\Gamma^{(2)}_{k=0,\mathrm{T}}(\mathbf{p} = 0; \rho_0) = U'_{k=0}(\rho_0) + R_{k=0}(\mathbf{p} = 0) = 0, \quad (54)$$

in agreement with Goldstone's theorem.

1. Scaling form of the LPA flow equation

For $r_0 = r_{0c}$, the system is critical. In this case, the minimum $\rho_{0,k}$ of the effective potential remains nonzero for all $k > 0$ and vanishes only when $k = 0$. Since at criticality the only relevant scale at large distances is k^{-1}, we expect that the running (i.e k-dependent) potential will not depend on k (for k small enough) if we measure all quantities in units of k. Technically, this means that any explicit dependence on k can be removed from the flow equation by using properly defined dimensionless quantities. At criticality, the running dimensionless potential (almost) stops evolving when $k \to 0$: it reaches a fixed point.[23]

We thus define the following dimensionless quantities:

$$\begin{aligned} \tilde{\mathbf{r}} &= k\mathbf{r}, \\ \tilde{\boldsymbol{\phi}}(\tilde{\mathbf{r}}) &= k^{-(d-2)/2}\boldsymbol{\phi}(\mathbf{r}), \\ \tilde{U}_k\big(\tilde{\rho}(\tilde{\mathbf{r}})\big) &= k^{-d} U_k\big(\rho(\mathbf{r})\big), \end{aligned} \quad (55)$$

in terms of which the effective action in the LPA writes

$$\Gamma_k[\boldsymbol{\phi}] = \int_{\tilde{\mathbf{r}}} \left\{ \frac{1}{2}\big(\boldsymbol{\nabla}_{\tilde{\mathbf{r}}}\tilde{\boldsymbol{\phi}}\big)^2 + \tilde{U}_k(\tilde{\rho}) \right\}. \quad (56)$$

The flow equation

$$\begin{aligned} \partial_t \tilde{U}_k = &- d\tilde{U}_k + (d-2)\tilde{\rho}\tilde{U}'_k + 2v_d\big[l_0^d(\tilde{U}'_k + 2\tilde{\rho}\tilde{U}''_k) \\ &+ (N-1)l_0^d(\tilde{U}'_k)\big] \end{aligned} \quad (57)$$

of the dimensionless effective potential follows from Eqs. (47,55) once the derivative wrt t in Eq. (47) has been changed for a derivative wrt t at fixed $\tilde{\rho}$:

$$\partial_t\big|_{\tilde{\rho}} = \partial_t\big|_{\rho} + \partial_t\rho\big|_{\tilde{\rho}}\, \frac{\partial}{\partial\rho}. \quad (58)$$

In Eq. (57) we have introduced the "threshold" function (see Appendix C)

$$l_0^d(w) = -\int_0^\infty dy\, y^{d/2+1} \frac{r'}{y(1+r)+w}. \quad (59)$$

With the theta regulator (14), the threshold function $l_0^d(w)$ can be calculated analytically (Appendix C).

2. Fixed-point solutions and critical exponents

In the plot of $\tilde{U}_k(\tilde{\rho})$, using dimensionless instead of dimensionful quantities amounts to stretching the $\tilde{\rho}$ and $\tilde{U}$ axes by k-dependent factors [Eqs. (55)]. At criticality and for systems undergoing a second order phase transition this stretching compensates exactly the shrinking of the "Mexican-hat" shape of U_k coming from the integration over the fluctuations of the rapid modes: $\tilde{U}_k$ reaches a limit $\tilde{U}^*$ at large (negative) RG time t, called the fixed-point potential. It is a solution of $\partial_t \tilde{U}^* = 0$, i.e.

$$\begin{aligned} 0 = &- d\tilde{U}^* + (d-2)\tilde{\rho}\tilde{U}^{*\prime} + 2v_d\big[l_0^d(\tilde{U}^{*\prime} + 2\tilde{\rho}\tilde{U}^{*\prime\prime}) \\ &+ (N-1)l_0^d(\tilde{U}^{*\prime})\big]. \end{aligned} \quad (60)$$

In the following we discuss how we can determine $\tilde{U}^*$ and compute the critical exponents.

[23] Note that using dimensionless quantities is equivalent to the usual momenta and fields rescaling step in the standard formulation of the Wilsonian RG.

a. Gaussian fixed point. Equation (60) admits the trivial solution

$$\tilde{U}^*(\tilde{\rho}) = 2\frac{v_d}{d} N l_0^d(0) \tag{61}$$

corresponding to the (noninteracting) Gaussian fixed point with all n-point vertices $\Gamma^{(n)}$ ($n \geq 3$) vanishing while $\Gamma^{(2)}(\mathbf{p}) = \mathbf{p}^2$. For simplicity we now consider the case $N = 1$ and the theta regulator for which $l_0^d(w) = (2/d)(1+w)^{-1}$ (Appendix C). To obtain the critical exponents associated with the Gaussian fixed point, we must linearize the flow equation about $\tilde{U}^*(\tilde{\rho}) = 4v_d/d^2$. To lowest order in $g_k = \tilde{U}_k - \tilde{U}^*$,

$$\partial_t g_k = -d g_k + (d-2)\tilde{\rho} g_k' - 4\frac{v_d}{d}(g_k' + 2\tilde{\rho} g_k''). \tag{62}$$

This equation can be put in a more convenient form by using the variable x defined by $\tilde{\rho} = x^2/2$ and noting that $\partial_x^2 g_k = \partial_{\tilde{\rho}} g_k + 2\tilde{\rho}\partial_{\tilde{\rho}}^2 g_k$. The rescaling $x \to \sqrt{\alpha} x$ and $g_k \to \alpha g_k$ with $\alpha = 4v_d/d$ yields the following equation

$$\partial_t g_k = -d g_k + \left(\frac{d}{2} - 1\right) x g_k' - g_k''. \tag{63}$$

Finally, to get rid of the field independent part of g_k, it is convenient to consider the function $f_k = g_k'$.

To solve the equation[24]

$$\partial_t f_k = -\left(\frac{d}{2} + 1\right) f_k + \left(\frac{d}{2} - 1\right) x f_k' - f_k'', \tag{64}$$

we write

$$f_k(x) = h(\beta x) e^{-\lambda t}, \tag{65}$$

where $\beta = \sqrt{d-2}/2$ (we assume $d > 2$), which leads to

$$h''(y) - 2y h'(y) + \frac{2}{d-2}(2 + d - 2\lambda) h(y) = 0 \tag{66}$$

with $y = \beta x$. This equation is known to have polynomial solutions,[25] given by the Hermite polynomials $h(y) = \hat{H}_{2k-1}(y) = 2^{k-1/2} H_{2k-1}(y)$ of degree $2k-1$, only for the set of discrete values of λ satisfying

$$2k - 1 = \frac{d + 2 - 2\lambda_k}{d-2} \quad \text{i.e.} \quad \lambda_k = d - k(d-2), \tag{67}$$

where $k = 1, 2, 3...$ Even degree Hermite's polynomials are not allowed since the function $f_k(x)$ is odd ($g_k(x)$ is even). Note that the λ_k's coincide with the scaling dimension $[v_{2k}]$ of the vertex $v_{2k} \int_{\mathbf{r}} \varphi^{2k}$ at the Gaussian fixed point.

When $d > 4$, all eigenvalues λ_k are negative except $\lambda_1 = 2$, which determines the correlation-length critical exponent $\nu = 1/\lambda_1 = 1/2$ (Wilson and Kogut, 1974). The corresponding relevant eigenvector is given by $\hat{H}_1(y) \propto y$ (which corresponds to a ϕ^2 term in U_k). The less negative eigenvalue $\lambda_2 = 4 - d$ determines the correction-to-scaling exponent $\omega = -\lambda_2 = d - 4$, i.e. the speed at which $\tilde{U}_k$ approaches the fixed-point solution $\tilde{U}^*$ when the system is critical. For $d < 4$, λ_2 becomes relevant[26] and we expect the phase transition to be described by a nontrivial fixed point with a single relevant field. For the φ^4 theory, we shall see below that this fixed point is the Wilson-Fisher fixed point (Wilson and Fisher, 1972).

b. Nontrivial fixed points. Nontrivial fixed points cannot be found analytically and one must solve (60) numerically. Since Eq. (60) is a second-order differential equation, a solution is *a priori* parameterized by two arbitrary constants. However, if we require $\tilde{U}^*(\tilde{\rho})$ to be regular at the origin, setting $\tilde{\rho} = 0$ in (60) we obtain

$$-d\tilde{U}^*(0) + 2v_d N l_0^d(\tilde{U}^{*\prime}(0)) = 0. \tag{68}$$

Moreover, if $\tilde{U}^*(\tilde{\rho})$ is not a constant, it must behaved as[27]

$$\tilde{U}^*(\tilde{\rho}) \sim \tilde{\rho}^{d/(d-2)} \quad \text{for} \quad \tilde{\rho} \to \infty. \tag{69}$$

We now have a second-order differential equation with two boundary equations [Eqs. (68,69)]. Most solutions are found to be singular at some $\tilde{\rho}_c$ and should be discarded (Morris, 1994a,b). We thus end up with a finite set of acceptable solutions. In practice, the fixed-point solution can be determined by fine tuning $\tilde{U}^*(0)$ and $\tilde{U}^{*\prime}(0)$ with the constraint (68) until a regular solution is obtained (shooting method) (Bagnuls and Bervillier, 2001).

For $d \geq 4$ only the Gaussian fixed point is found. For $3 \leq d < 4$, a nontrivial fixed point (the Wilson-Fisher fixed point) is found. A new nontrivial fixed point emanates from the Gaussian fixed point each time that one of the eigenvalues λ_k [Eq. (67)] becomes negative, which occurs at the dimensional thresholds $d_k = 2k/(k-1)$ ($k \geq 2$).

[24] The same linearized equation is obtained from the Wilson-Polchinski equation (Polchinski, 1984) in the LPA. This result follows from an exact map between the Wilson-Polchinski and NPRG equations in the LPA when the theta regulator is used (Morris, 2005).

[25] Nonpolynomial solutions imply a continuum of eigenvalues and can be discarded on physical ground (Bagnuls and Bervillier, 2001).

[26] To see whether the field associated to the eigenvalue $\lambda_2 = 4 - d$ is relevant or irrelevant in four dimensions, one must go beyond the linear approximation (64). We do not discuss the case $d = 4$ here.

[27] The large-$\tilde{\rho}$ behavior of $\tilde{U}^*(\tilde{\rho})$ is obtained by noting that the threshold functions give subleading terms in the limit $\tilde{\rho} \to \infty$.

Once a fixed point is identified, one can determine the critical exponents by linearizing the flow about $\tilde{U}^*$. Setting

$$\tilde{U}_k(\tilde{\rho}) = \tilde{U}^*(\tilde{\rho}) + e^{-\lambda t} g(\tilde{\rho}), \tag{70}$$

we find

$$0 = (\lambda - d)g + (d-2)\tilde{\rho}g' + 2v_d[(N-1)g' l_0^{d\prime}(\tilde{U}^{*\prime}) + (g' + 2\tilde{\rho}g'')l_0^{d\prime}(\tilde{U}^{*\prime} + 2\tilde{\rho}U^{*\prime\prime})]. \tag{71}$$

Again we expect solutions of this second-order differential equation to be labeled by two parameters. However, one can choose $g(0) = 1$ (arbitrary normalization) while $g(0)$ and $g'(0)$ are not independent if $g(\tilde{\rho})$ is regular at the origin: $(d-\lambda)g(0) = 2Nv_d g'(0) l_0^{d\prime}(\tilde{U}^{*\prime}(0))$. The solution is then unique for a given λ. Regular solutions are obtained only for a countable set of λ's and behave as $g(\tilde{\rho}) \sim \tilde{\rho}^{(d-\lambda)/(d-2)}$ for $\tilde{\rho} \to \infty$. They can be determined by the shooting method. For $3 \leq d < 4$, the Wilson-Fisher fixed point possesses only one positive eigenvalue $\lambda_1 = 1/\nu$. For $d = 3$ and $N = 3$, the LPA with the exponential regulator (13) gives (Refs.)

$$\nu \simeq 0.6496, \quad \omega \simeq 0.6557, \tag{72}$$

to be compared with Monte Carlo estimates $\nu = 0.7112(5)$ and $\omega = 0.773$ (Campostrini *et al.*, 2002).[28] Since $\eta = 0$ in the LPA, other critical exponents (α, β, γ and δ) follow from the usual scaling laws. For a more detailed discussion of the shooting method we refer to (Bagnuls and Bervillier, 2001; Ball *et al.*, 1995; Comellas, 1998; Morris, 1994a,b; Morris and Turner, 1998; Zumbach, 1994).

The shooting method suffers from some drawbacks. Beyond the LPA, there are other functions to be considered in addition to the effective potential, e.g. $Z_k(\rho)$ and $Y_k(\rho)$ in the derivative expansion to second order (Sec. III.C). When there are more than one invariant, the effective potential is a multidimensional function and its determination is difficult even within the LPA.

As an alternative to the shooting method, one can numerically solve the flow equation for a system near criticality.[29] Let us assume that the initial dimensionless effective potential $\tilde{U}_\Lambda$ is parameterized by $\tilde{r}_0$ and $\tilde{u}_0$ [Eq. (52)]. The critical point can be reached by fine tuning $\tilde{r}_0$ (with $\tilde{u}_0$ fixed). When $\tilde{r}_0$ is near the critical value $\tilde{r}_{0c}$, the solution takes the form

$$\tilde{U}_k(\tilde{\rho}) = \tilde{U}^*(\tilde{\rho}) + g_1(\tilde{\rho}) e^{\omega t} + g_2(\tilde{\rho}) e^{-t/\nu} \tag{73}$$

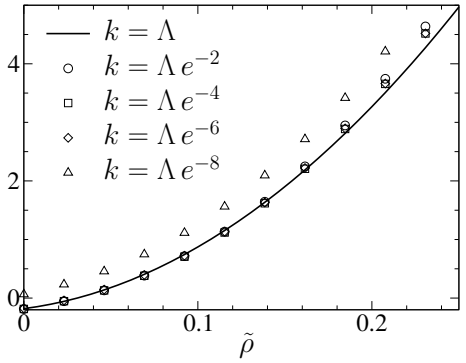

FIG. 5 Flow of the derivative $\tilde{U}_k'(\tilde{\rho})$ of the effective potential ($d = 3$, $N = 1$ and $\Lambda = 1$). The initial condition $\tilde{U}_\Lambda'(\tilde{\rho}) = -0.1806 + 3.8156\tilde{\rho} + 67.137\tilde{\rho}^2$ (with $\Lambda = 1$) is very close to the critical solution $\tilde{U}^{*\prime}(\tilde{\rho})$ as can be seen from the very slow flow when $\Lambda\, e^{-7} \lesssim k \leq \Lambda$.

for large $|t|$. For $\tilde{r}_0 = \tilde{r}_{0c}$, g_2 vanishes and the approach to the critical point is controlled by the correction-to-scaling exponent ω.[30] For $\tilde{r}_0$ slightly detuned from $\tilde{r}_{0c}$, $\tilde{U}_k$ first moves closer to $\tilde{U}^*$, remains nearly equal to $\tilde{U}^*$ for a long time, before eventually running away with a rate $1/\nu$ given by the inverse of the correlation-length exponent. This allows us to determine both $\tilde{U}^*(\tilde{\rho})$ and the critical exponents ν and ω. The fixed-point solution $\tilde{U}^{*\prime}(\tilde{\rho})$ obtained with this method is shown in Fig. 5 for $d = 3$ and $N = 1$. By considering $\tilde{U}^{*\prime}$ rather than $\tilde{U}^*$ one eliminates the field-independent part of the potential which diverges for $k \to 0$. Note that the vanishing of $\tilde{U}^{*\prime}$ at some nonzero $\tilde{\rho}_0^*$ (corresponding to the minimum of $\tilde{U}^*$) is not in contradiction with the system being critical. Going back to dimensional variables, one finds that $U_k(\rho)$ has a minimum at $\rho_{0,k} = k^{d-2}\tilde{\rho}_0^*$ which vanishes for $k \to 0$.

The (approximate) fixed-point potential $\tilde{U}^*$ found from the numerical solution of the flow equation can also be used as an initial guess of the solution of Eq. (60). Discretizing the $\tilde{\rho}$ variable, i.e. $\tilde{\rho}_i = i\Delta\tilde{\rho}$ ($i = 0, \cdots, M-1$), one is then left with a system of M equations for the M variables $\tilde{U}^*(\tilde{\rho}_i)$, which can be solved with standard numerical algorithms. The initial guess, being close to the exact solution, ensures convergence to the physical solution, the accuracy being limited by the finite number M of $\tilde{\rho}_i$ variables and the maximum value $\tilde{\rho}_{M-1}$. To compute the correlation-length exponent ν, one writes $\tilde{U}_k(\tilde{\rho}_i) = \tilde{U}_k^*(\tilde{\rho}_i) + e^{-\lambda t} g(\tilde{\rho}_i)$ [Eq. (70)] and linearize the flow equation $\partial_t \tilde{U}_k$ about $\tilde{U}^*$. Possible λ's are determined

[28] Estimates (72) are obtained with the "best" value of the prefactor α in Eq. (13) determined using the principle of minimum sensitivity (see Sec. III.C). OK ???

[29] This method, as well as the following ones, can be used not only for the LPA but also for the derivative expansion discussed in Secs III.C and III.D.

[30] In practice, the critical point is determined by fine tuning $\tilde{r}_{0c}$ so that $\tilde{U}_k'(0)$ (one could also choose $\tilde{\rho}_{0,k}$, etc.) reaches a plateau for large $|t|$. Since the condition $\tilde{r}_0 = \tilde{r}_{0c}$ cannot be fulfilled exactly in a numerical calculation, $\tilde{U}_k'(0)$ always runs away from its plateau value for sufficiently large $|t|$.

by the eigenvalues of the stability matrix

$$L_{ij} = \left.\frac{\delta \partial_t \tilde{U}_k(\tilde{\rho}_i)}{\delta \tilde{U}_k(\tilde{\rho}_j)}\right|_{\tilde{U}_k = \tilde{U}_k^*}. \tag{74}$$

The largest eigenvalue (the only positive one) determines $1/\nu$. The absolute value of the less negative eigenvalue gives the correction-to-scaling exponent ω.

Finally it is possible to determine the critical exponents directly from physical quantities computed at $k = 0$. For instance, in the disordered phase, $G_{k=0,ii}(\mathbf{p}; \phi = 0) = (\mathbf{p}^2 + U'_{k=0}(0))^{-1}$ and the correlation length ξ is given by $[U'_{k=0}(0)]^{-1/2}$. This allows us to obtain ν using

$$U'_{k=0}(0) \sim (r_0 - r_{0c})^{2\nu} \quad \text{for} \quad r_0 \to r_{0c}^+. \tag{75}$$

Similarly, in the ordered phase, one can compute the magnitude of the order parameter

$$|\boldsymbol{\phi}| = \lim_{k\to 0} \sqrt{2\rho_{0,k}} \sim (r_{0c} - r_0)^{\beta} \quad \text{for} \quad r_0 \to r_{0c}^- \tag{76}$$

to obtain the exponent β.

3. Upper and lower critical dimensions – Mermin-Wagner theorem

The LPA recovers the well-known result that the upper critical dimension is $d_c^+ = 4$ for the O(N) model: for $d \geq d_c^+$, the fixed point controlling the transition is the (trivial) Gaussian fixed point and the critical exponents take their mean-field values $\nu = 1/2$, $\eta = 0$, etc. For $d \leq 2$ no fixed point is obtained, the RG flow always drives the system to the disordered phase. For $N \geq 2$ this agrees with the Mermin-Wagner theorem (Mermin and Wagner, 1966). The latter is a consequence of the term $\dot{R}_k(\mathbf{q})(N-1)G_{k,\mathrm{T}}(\mathbf{q}, \rho)$ in the rhs of the flow equation (46). A nonzero $\rho_{0,k}$ is defined by $U'_k(\rho_{0,k}) = 0$. Differentiating this equation wrt t we find (see Eq. (96))

$$\partial_t \rho_{0,k} = -\frac{1}{U''_k(\rho_{0,k})} \partial_t U'_k(\rho = \rho_{0,k}). \tag{77}$$

Considering the theta regulator for simplicity,

$$\partial_t U'_k = -4\frac{v_d}{d} k^{d+2} \left[\frac{3U''_k + 2\rho U'''_k}{(k^2 + U'_k + 2\rho U''_k)^2} + \frac{(N-1)U''_k}{(k^2 + U'_k)^2} \right] \tag{78}$$

(see Eq. (51)). Thus $\partial_t U'_k(\rho_{0,k}) \sim -k^{d-2}$ for $k \to 0$ and $U'_k(\rho_{0,k})$ diverges if $d \leq 2$, which is incompatible with $\rho_{0,k}$ being finite. Therefore $\rho_{0,k}$ must vanish at a nonzero momentum scale k.

However the LPA fails in two dimensions when $N = 2$ and $N = 1$ due to the absence of field renormalization factor. The LPA', the simplest improvement over the LPA which includes a field renormalization factor (Sec. III.B), does describe the transition in the two-dimensional $N = 1$ model (Ising universality class). A good description of the Kosterlitz-Thouless transition in the two-dimensional O(2) model requires the derivative expansion to second order (Sec. IV) although some features are captured by the LPA' (Sec. III.B.5).

4. Spontaneous symmetry breaking and approach to the convex potential

Stability of the flow equations requires

$$\begin{aligned} &\mathbf{q}^2 + R_k(\mathbf{q}^2) + U'_k(\rho) \geq 0, \\ &\mathbf{q}^2 + R_k(\mathbf{q}^2) + U'_k(\rho) + 2\rho U''_k(\rho) \geq 0. \end{aligned} \tag{79}$$

If conditions (79) are not fulfilled, a pole appears in the propagators and the threshold functions become singular. In the broken-symmetry phase, $U'_k(\rho)$ is negative for $0 \leq \rho \leq \rho_{0,k}$ and there is no guarantee that Eqs. (79) are satisfied. In the LPA, and for some regulators, the singularity of the threshold functions is approached but never reached. This is the case for the theta regulator (14) or the exponential regulator (13) with $\alpha > 2$ (Berges *et al.*, 2002; Peláez and Wschebor, 2015; Tetradis and Litim, 1996; Tetradis and Wetterich, 1992). A detailed analysis shows that for these regulators the potential behaves as $U'_k(\rho) \sim -k^2$ in the internal region $0 \leq \rho \lesssim \rho_{0,k}$. This implies that the convexity of the free energy $U_{k=0}(\rho)$ is preserved, with a flat part $U_{k=0}(\rho) = \text{const}$ for $0 \leq \rho \leq \rho_0 = \lim_{k\to 0} \rho_{0,k}$, as shown in Fig. 4. It should be emphasized that, in contrast to most perturbative approaches, the convexity of the thermodynamic potential is not obtained here from the Maxwell construction but is a genuine property of the NPRG flow equation in the LPA.

From a practical point of view, the approach to convexity of the potential makes its numerical determination difficult. Indeed, a tiny numerical error can lead to negative values of $\mathbf{q}^2 + R_k(\mathbf{q}^2) + U'_k(\rho)$, even in cases where we know that conditions (79) should remain fulfilled, thus making the threshold functions ill-defined. This difficulty is more pronounced for $N = 1$, mainly because the longitudinal susceptibility $G_{k,\mathrm{L}}(\mathbf{q} = 0, \rho)$ becomes a discontinuous function of ρ for $k \to 0$. Nevertheless, analytical solutions of the potential in the internal region can be exploited to set up efficient algorithms for the broken-symmetry phase (Caillol, 2012b; Peláez and Wschebor, 2015).[31]

B. Improving the LPA: the LPA'

An important shortcoming of the LPA is the absence of anomalous dimension at criticality. The anomalous di-

[31] We refer to (Peláez and Wschebor, 2015) for a discussion of the approach to convexity in the derivative expansion beyond the LPA.

mension is small in three dimensions and can be neglected in first approximation but is crucial in two dimensions. In this section we discuss a simple improvement of the LPA where the effective action

$$\Gamma_k[\boldsymbol{\phi}] = \int_{\mathbf{r}} \left\{ \frac{Z_k}{2} (\boldsymbol{\nabla}\boldsymbol{\phi})^2 + U_k(\rho) \right\} \tag{80}$$

includes a field renormalization factor Z_k (Refs.). This improvement allows us to qualitatively describe the critical behavior of the O(N) model for $2 \leq d \leq 4$ and $1 \leq N$ in a single framework with modest numerical effort (Sec. III.B.3). The matching with known (perturbative) results obtained around $d = 2$ and $d = 4$ is a very important feature of the NPRG approach as it allows us to interpolate smoothly between two and four dimensions in a unified framework. Furthermore, it suggests that it is possible to reliably explore the behavior of the system in any dimension d and in particular in $d = 3$ (see Secs. III.C and III.D).

The expression (80), which is referred to as the LPA', can be seen as an approximation of the lowest-order derivative expansion (40) where the function $Z_k(\rho)$ is approximated by a constant Z_k and the $(\boldsymbol{\nabla}\rho)^2$ term neglected. Z_k must therefore be understood as the first term in the expansion of the function $Z_k(\rho)$ about a particular point. One usually expands about the minimum of the effective potential $U_k(\rho)$,[32]

$$Z_k(\rho) = Z_k + Z_k^{(1)}(\rho - \rho_{0,k}) + \frac{Z_k^{(2)}}{2}(\rho - \rho_{0,k})^2 + \cdots \tag{81}$$

At the critical point, we expect the following behavior for the 2-point vertex,

$$\Gamma_k^{(2)}(\mathbf{p}) \sim \begin{cases} Z_k \mathbf{p}^2 & \text{if} \quad |\mathbf{p}| \ll k, \\ p_G^{\eta} |\mathbf{p}|^{2-\eta} & \text{if} \quad k \ll |\mathbf{p}| \ll p_G, \end{cases} \tag{82}$$

where $p_G \sim \xi_G^{-1}$ is the Ginzburg momentum scale. For reasons previously discussed, only the limiting behavior for $|\mathbf{p}| \ll k$ is accessible in the derivative expansion. However, by continuity at $|\mathbf{p}| \sim k$, we expect Z_k to vary as $k^{-\eta}$.[33] This allows us to compute η from the derivative expansion,

$$\eta = \lim_{k \to 0} \eta_k, \qquad \eta_k = -\partial_t \ln Z_k. \tag{83}$$

The equivalence between the two determinations of η, from Z_k or the momentum dependence of the 2-point vertex, will be shown in Sec. V.

[32] Another natural choice, the expansion about $\rho = 0$, yields rather poor estimates of the critical exponents (Aoki *et al.*, 1998).

[33] Thus, if we assume that $\Gamma^{(2)}_{k=0}(\mathbf{p}) \simeq \Gamma^{(2)}_{k\sim|\mathbf{p}|}(\mathbf{p})$ (arguing that the momentum $\mathbf{p}$ acts as an effective infrared cutoff) and use the derivative expansion result $\Gamma_k(\mathbf{p}) = Z_k \mathbf{p}^2$ to compute $\Gamma^{(2)}_{k\sim|\mathbf{p}|}(\mathbf{p})$, we obtain $\Gamma^{(2)}_{k=0}(\mathbf{p}) \sim |\mathbf{p}|^{2-\eta}$.

The flow equation for the effective potential $U_k(\rho)$ is similar to that obtained within the LPA [Eq. (46)]. The only difference is that the 2-point vertex

$$\begin{aligned} \Gamma^{(2)}_{k,\mathrm{L}}(\mathbf{p};\rho) &= Z_k \mathbf{p}^2 + U_k'(\rho) + 2\rho U_k''(\rho), \\ \Gamma^{(2)}_{k,\mathrm{T}}(\mathbf{p};\rho) &= Z_k \mathbf{p}^2 + U_k'(\rho), \end{aligned} \tag{84}$$

now includes the field renormalization factor Z_k. The equation $\partial_t Z_k$ is obtained from

$$Z_k = \lim_{\mathbf{p} \to 0} \frac{\partial}{\partial \mathbf{p}^2} \Gamma^{(2)}_{k,\mathrm{T}}(\mathbf{p}; \rho_{0,k}). \tag{85}$$

We define Z_k from the transverse 2-point vertex (and not the longitudinal one). The reason is that $\Gamma^{(2)}_{k,\mathrm{L}}(\mathbf{p};\rho)$ includes a term $Y_k \mathbf{p}^2$ in the full derivative expansion to order $\mathcal{O}(\partial^2)$ [Eq. (40) and Sec. III.C]. Although this term is neglected in the LPA', the equation $\partial_t \Gamma^{(2)}_{k,\mathrm{L}}$ yields contributions to both $\partial_t Z_k$ and $\partial_t Y_k$, whereas $\partial_t \Gamma^{(2)}_{k,\mathrm{T}}$ contributes only to $\partial_t Z_k$. Equation (85) gives

$$\begin{aligned} \partial_t Z_k = 16 \frac{v_d}{d} \rho_{0,k} U_k''(\rho_{0,k})^2 \tilde{\partial}_t \int_0^\infty d|\mathbf{p}|\, |\mathbf{p}|^{d+1} \\ \times G'_{k,\mathrm{L}}(\mathbf{p};\rho_{0,k}) G'_{k,\mathrm{T}}(\mathbf{p};\rho_{0,k}) \end{aligned} \tag{86}$$

where $G_k'(\mathbf{p};\rho) = \partial_{\mathbf{p}^2} G_k(\mathbf{p};\rho)$ denotes a derivative wrt $\mathbf{p}^2$, and $\tilde{\partial}_t$ is defined in (32). Equation (86) is derived in Appendix D.

1. Scaling form of the LPA' flow equations

To cast the effective action (80) in the dimensionless form (56), we must define the dimensionless field

$$\tilde{\boldsymbol{\phi}}(\tilde{\mathbf{r}}) = \sqrt{Z_k} k^{-(d-2)/2} \boldsymbol{\phi}(\mathbf{r}) \tag{87}$$

with a factor $\sqrt{Z_k}$. We also include the field renormalization factor Z_k in the definition of the regulator function,

$$R_k(\mathbf{p}) = Z_k \mathbf{p}^2 r(y) \tag{88}$$

($y = \mathbf{p}^2/k^2$). This is necessary for eliminating Z_k from dimensionless quantities. Proceeding as in the LPA, we then obtain

$$\begin{aligned} \partial_t \tilde{U}_k = -d\tilde{U}_k + (d - 2 + \eta_k)\tilde{\rho}\tilde{U}_k' \\ + 2v_d[(N-1) l_0^d(\tilde{U}_k', \eta_k) + l_0^d(\tilde{U}_k' + 2\tilde{\rho}\tilde{U}_k'', \eta_k)], \end{aligned} \tag{89}$$

where the threshold function

$$l_0^d(w,\eta) = -\frac{1}{2} \int_0^\infty dy\, y^{d/2} \frac{\eta r + 2y r'}{y(1+r) + w}, \tag{90}$$

generalizes the definition (59) to the case where η is nonzero.

Similarly, we can rewrite Eq. (86) in terms of dimensionless variables (see Appendix D) (Wetterich, 1993a),

$$\eta_k = 16\frac{v_d}{d}\tilde{\rho}_{0,k}\tilde{U}''_{0,k}{}^2 m_{22}^d(2\tilde{\rho}_{0,k}\tilde{U}''_{0,k},\eta_k), \tag{91}$$

where we use the notation $\tilde{U}''_{0,k} = \tilde{U}''_k(\tilde{\rho}_{0,k})$. We have introduced the threshold function

$$m_{22}^d(w,\eta) = -\frac{1}{2}\tilde{\partial}_t\int_0^\infty dy\,\frac{y^{d/2}(1+r+yr')^2}{[y(1+r)+w]^2[y(1+r)]^2}. \tag{92}$$

With the theta regulator (14), the threshold function $m_{22}^d(w,\eta) = 1/(1+w)^2$ can be computed exactly (see Appendix C), which leads to a simple expression for the "running" anomalous dimension (Adams *et al.*, 1995; Tetradis and Wetterich, 1994),

$$\eta_k = 16\frac{v_d}{d}\frac{\tilde{\rho}_{0,k}\tilde{U}''_{0,k}{}^2}{(1+2\tilde{\rho}_{0,k}\tilde{U}''_{0,k})^2}. \tag{93}$$

At the critical point, $\tilde{\rho}_{0,k}\to\tilde{\rho}_0^*$ and $\tilde{U}''_{0,k}\to\tilde{U}_0^{*\prime\prime}$ when $k\to 0$. The anomalous dimension $\eta = \lim_{k\to 0}\eta_k$ is nonzero only if the fixed point is interacting, i.e. $\tilde{U}_0^{*\prime\prime}\neq 0$.[34]

To find the fixed-point solution $\tilde{U}^*$ and the critical exponents, we can use the same methods as in the LPA. When the fixed point is reached by fine tuning r_0, the anomalous dimension can be estimated from the value of η_k (see Sec. III.C for a more detailed discussion). With the exponential regulator (13) and $\alpha = 2$,[35] one finds

$$\nu \simeq 0.738, \quad \eta = 0.037 \tag{94}$$

for $d = 3$ and $N = 3$, to be compared with Monte Carlo estimates $\nu = 0.7112(5)$ and $\eta = 0.375(5)$ (Campostrini *et al.*, 2002). The surprisingly accurate value of η is accidental and in fact deteriorates if one considers the full derivative expansion to second order. We shall discuss the convergence of the derivative expansion in Sec. III.D.

Dire que Ising 2D OK avec LPA'?

2. Truncated LPA'

It is possible to simplify the LPA' by expanding the effective potential $U_k(\rho)$ about $\rho_{0,k}$. To lowest (nontrivial) order,

$$U_k(\rho) = \begin{cases} U_{0,k} + \dfrac{\lambda_k}{2}(\rho-\rho_{0,k})^2 & \text{if } \rho_{0,k}\geq 0, \\ U_{0,k} + \delta_k\rho + \dfrac{\lambda_k}{2}\rho^2 & \text{if } \rho_{0,k} = 0. \end{cases} \tag{95}$$

The effective action is now parameterized by a small number of coupling constants, $U_{0,k}$, $\rho_{0,k}$ or δ_k, λ_k and Z_k, which makes the numerical solution of the flow equation particularly easy. In spite of its simplicity, the truncated LPA' turns out to be highly nontrivial and goes much beyond the perturbative RG approach as we will see in the following.

In order to determine the flow equations of the coupling constants, we must relate the latter to the effective potential. When $\rho_{0,k}$ is nonzero, it is defined by $U'_k(\rho_{0,k}) = 0$, so that

$$0 = \frac{d}{dt}U_k(\rho_{0,k}) = \partial_t U_k(\rho_{0,k}) + U''_k(\rho_{0,k})\partial_t\rho_{0,k}, \tag{96}$$

where d/dt is a total derivative while $\partial_t U_k(\rho_{0,k})$ is computed at fixed $\rho_{0,k}$. This leads to

$$\partial_t\rho_{0,k} = -\frac{1}{\lambda_k}\partial_t U'_k(\rho_{0,k}), \tag{97}$$

where $\lambda_k = U''_k(\rho_{0,k})$. When $\rho_{0,k} = 0$, $\delta_k = U'_k(0)$ satisfies the flow equation

$$\partial_t\delta_k = \partial_t U'_k(0). \tag{98}$$

The equation $\partial_t\lambda_k$ follows from

$$\partial_t\lambda_k = \partial_t U''_k(\rho_{0,k}) + U'''_k(\rho_{0,k})\partial_t\rho_{0,k} = \partial_t U''_k(\rho_{0,k}) \tag{99}$$

since $U'''_k(\rho)$ vanishes with the truncation (95). The flow equations $\partial_t U'_k(\rho)$ and $\partial_t U''_k(\rho)$ are directly deduced from $\partial_t U_k(\rho)$ by taking ρ-derivatives.

In order to write the flow equations in dimensionless form, we introduce the dimensionless variables

$$\begin{aligned} \tilde{U}_{0,k} &= k^{-d}U_{0,k}, \quad \tilde{\rho}_{0,k} = Z_k k^{2-d}\rho_{0,k}, \\ \tilde{\delta}_k &= (Z_k k^2)^{-1}\delta_k, \quad \tilde{\lambda}_k = Z_k^{-2}k^{d-4}\lambda_k, \end{aligned} \tag{100}$$

and deduce $\partial_t\tilde{U}'_k(\rho)$ and $\partial_t\tilde{U}''_k(\rho)$ from (89). Using

$$\frac{\partial}{\partial w}l_n^d(w,\eta) = -(n+\delta_{n,0})l_{n+1}^d(w,\eta), \tag{101}$$

where

$$l_n^d(w,\eta) = -\frac{n+\delta_{n,0}}{2}\int_0^\infty dy\,\frac{y^{d/2}(\eta r+2yr')}{[y(1+r)+w]^{n+1}} \tag{102}$$

is a generalization of the threshold function (90) to any positive value of n, we eventually obtain

$$\begin{aligned} \partial_t\tilde{U}_{0,k} &= -d\tilde{U}_{0,k} + 2v_d\big[l_0^d(2\tilde{\lambda}_k\tilde{\rho}_{0,k}+\tilde{\delta}_k,\eta_k) \\ &\quad + (N-1)l_0^d(\tilde{\delta}_k,\eta_k)\big], \\ \partial_t\tilde{\rho}_{0,k} &= (2-d-\eta_k)\tilde{\rho}_{0,k} + 2v_d\big[3l_1^d(2\tilde{\lambda}_k\tilde{\rho}_{0,k},\eta_k) \\ &\quad + (N-1)l_1^d(0,\eta_k)\big], \\ \partial_t\tilde{\delta}_k &= (\eta_k-2)\tilde{\delta}_k - 2v_d(N+2)\tilde{\lambda}_k l_1^d(\tilde{\delta}_k,\eta_k), \\ \partial_t\tilde{\lambda}_k &= (d-4+2\eta_k)\tilde{\lambda}_k + 2v_d\tilde{\lambda}_k^2\big[9l_2^d(2\tilde{\lambda}_k\tilde{\rho}_{0,k}+\tilde{\delta}_k,\eta_k) \end{aligned} \tag{103}$$

[34] A nonzero $\tilde{U}''_{0,k}$ implies that the fixed point is not Gaussian.

[35] $\alpha = 2$ is the "best" value of α following the principle of minimum sensitivity (Sec. III.C). This principle cannot be satisfied for the computation of ν in the LPA'. OK ???

$$+ (N-1) l_2^d(\tilde{\delta}_k, \eta_k)\big],$$

while the (running) anomalous dimension η_k is given by (91). Even though we started from a quartic truncation of the effective action [Eqs. (80,95)], the flow equations are still nonperturbative since they are of infinite order in the coupling constant λ_k (the threshold functions are nonpolynomial functions of their arguments).[36] This makes the truncated LPA' fundamentally different from a perturbative RG approach based on a loop expansion.

3. Critical behavior: the limits $d \to 4$, $d \to 2$ and $N \to \infty$

Figure 6 shows typical solutions of the flow equations (103) for a nearly critical system ($d = 3$ and $N = 3$). One clearly observes a critical regime where $\tilde{\rho}_{0,k}$, $\tilde{\lambda}_k$ and η_k are nearly equal to their fixed point values $\tilde{\rho}_0^*$, λ^* and η. The critical regime starts when $k \sim p_G \sim \xi_G^{-1}$, where ξ_G is the Ginzburg length. It ends when $k \sim \xi^{-1}$ (disordered phase) or $k \sim \xi_J^{-1}$ (ordered phase), where ξ and ξ_J are the correlation length and the Josephson length, respectively.

With the theta regulator (14), the truncated LPA' gives $\nu = 0.699$ and $\eta = 0.051$ for $N = 3$ and $d = 3$ (Delamotte *et al.*, 2004) OK ???, which is in rough agreement with QMC estimates $\nu = 0.7112(5)$ and $\omega = 0.773$ (Campostrini *et al.*, 2002). Although the truncated LPA' is not reliable for an accurate estimate of the critical exponents, equations (103) provide a rather complete picture of the long-distance physics at and near criticality regardless of the values of N and $d \geq 2$ (the case $d = 2$ and $N = 2$ is discussed in Secs. III.B.5 and IV). Below we show that they yield the correct results in the limiting cases $d \to 4$, $d \to 2$ and $N \to \infty$,[37] and also enable us to study the ordered phase when $N \geq 2$ despite the presence of (gapless) Goldstone modes (Sec. III.B.4).

a. Limit $d \to 4$ Near four dimensions, we anticipate that the fixed-point value $\tilde{\lambda}^*$ is of order $\epsilon = 4 - d$, while $\tilde{\rho}_0^*$ is $\mathcal{O}(\epsilon^0)$. To obtain the flow equations in the limit $\epsilon \to 0$, we expand wrt the (square) "mass" $2\tilde{\lambda}_k \tilde{\rho}_{0,k} = \mathcal{O}(\epsilon)$ of the longitudinal mode. We use

$$l_n^d(w, \eta) = l_n^d(0, \eta) - (n + \delta_{n,0}) l_{n+1}^d(0, \eta) w + \mathcal{O}(w^2) \quad (104)$$

[36] *Stricto sensu* this is true only if $\tilde{\rho}_{0,k}$ is nonzero (hence the importance of expanding the effective potential about its minimum). When $\tilde{\rho}_{0,k} = 0$, Eqs. (103) reproduce the perturbative one-loop RG equations. Note that for a system in the disordered phase, the condition $\tilde{\rho}_{0,k} > 0$ is fulfilled as long as k is larger than (roughly) the inverse of the correlation length ξ.

[37] This follows from Eqs. (103) being one-loop exact (see remark 3 page 9), while to leading (nontrivial) order in $\epsilon = 4 - d$, $\epsilon = d - 2$ or $1/N$, the one-loop approximation becomes exact.

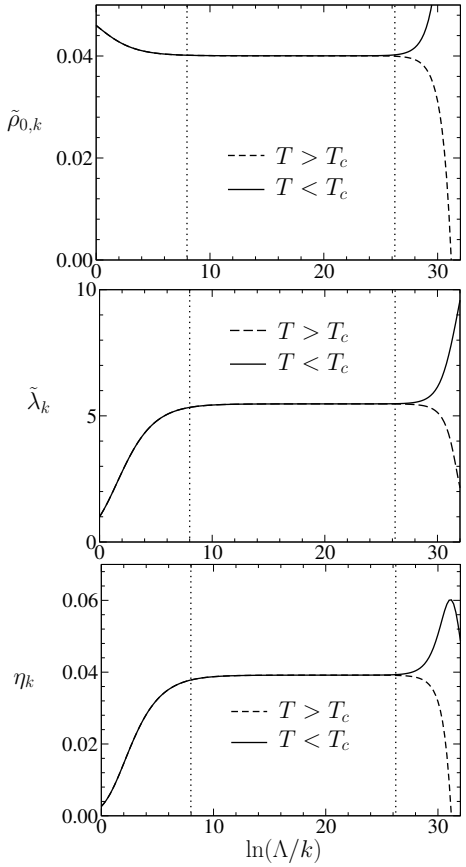

FIG. 6 $\tilde{\rho}_{0,k}$, $\tilde{\lambda}_k$ and η_k vs $\ln(\Lambda/k) = -t$ near criticality for $d = 3$ and $N = 3$ ($\tilde{\rho}_{\Lambda,0} \simeq 0.046$, $\tilde{\lambda}_\Lambda = 1$, $\Lambda = 1$) as obtained from (103) with the theta regulator. The vertical dotted lines show the Ginzburg scale $\ln(\Lambda \xi_G) = -t_G$ and the correlation length scale $t_\xi = -\ln(\Lambda\xi)$ ($T > T_c$) or the Josephson scale $\ln(\Lambda \xi_J) = -t_J$ ($T < T_c$).

(see Eq. (101)) and $\eta = \lim_{k\to 0} \eta_k = \mathcal{O}(\epsilon^2)$ at the fixed point. This gives

$$\begin{aligned} \partial_t \tilde{\rho}_{0,k} &= (\epsilon - 2)\tilde{\rho}_{0,k} + 2v_d(N+2) l_1^d(0,0) \\ &\quad - 12 v_d \tilde{\lambda}_k \tilde{\rho}_{0,k} l_2^4(0,0) + \mathcal{O}(\epsilon^2), \\ \partial_t \tilde{\lambda}_k &= -\epsilon \tilde{\lambda}_k + 2v_4(N+8)\tilde{\lambda}_k^2 l_2^4(0,0) + \mathcal{O}(\epsilon^3), \end{aligned} \quad (105)$$

where $v_4 = 1/32\pi^2$ and $l_2^4(0,0) = 1$ (Appendix C). In addition to the noninteracting (Gaussian) fixed point

$$\tilde{\rho}_0^* = (N+2)\frac{l_1^4(0,0)}{32\pi^2} + \mathcal{O}(\epsilon), \qquad \tilde{\lambda}^* = 0, \quad (106)$$

equations (105) admit the nontrivial (Wilson-Fisher) fixed point

$$\begin{aligned} \tilde{\rho}_0^* &= (N+2)\frac{l_1^4(0,0)}{32\pi^2} + \mathcal{O}(\epsilon), \\ \tilde{\lambda}^* &= \epsilon \frac{16\pi^2}{N+8} + \mathcal{O}(\epsilon^2). \end{aligned} \quad (107)$$

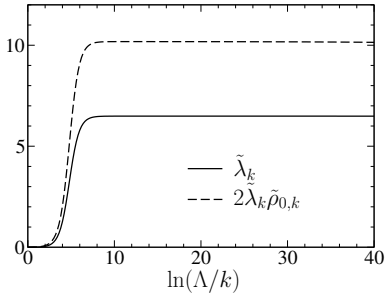

FIG. 7 Flow of $\tilde\lambda_k$ and $2\tilde\lambda_k\rho_{0,k}$ vs $\ln(\Lambda/k)$ near two dimensions for a critical system as obtained from (103) ($d = 2.1$, $N = 3$, $\tilde\lambda_\Lambda = 10^{-3}$, $\tilde\rho_{0,\Lambda} \simeq 1.147$ and $\Lambda = 1$).

Linearizing the flow equations about the Wilson-Fisher fixed point,

$$\begin{pmatrix} \partial_t\delta\tilde\rho_{0,k} \\ \partial_t\delta\tilde\lambda_k \end{pmatrix} = \begin{pmatrix} -2+\frac{N+2}{N+8}\epsilon & -12v_d\tilde\rho_0^* \\ 0 & \epsilon \end{pmatrix} \begin{pmatrix} \delta\tilde\rho_{0,k} \\ \delta\tilde\lambda_k \end{pmatrix}, \tag{108}$$

we find that the stability matrix has eigenvalues $-y_1 = -2+\epsilon(N+2)/(N+8)$ and $-y_2 = \epsilon$ to order ϵ.[38] These eigenvalues are independent of the choice of the regulator function R_k. Since the largest one $y_1 = 1/\nu$ determines the correlation-length exponent, we deduce

$$\nu = \frac{1}{2} + \frac{N+2}{N+4}\frac{\epsilon}{4} + \mathcal{O}(\epsilon^2) \tag{109}$$

in agreement with the known result from the one-loop perturbative RG (Ma, 2000; Zinn-Justin, 1996). The second eigenvalue y_2 is negative for $d < 4$ and determines the correction-to-scaling exponent $\omega = -y_2 = \epsilon$.

b. Limit $d \to 2$ We anticipate that near two dimensions, $\tilde\rho_0^* = \mathcal{O}(\epsilon^{-1})$ and $\tilde\lambda^* = \mathcal{O}(\epsilon^0)$ so that $2\tilde\lambda^*\tilde\rho^* = \mathcal{O}(\epsilon^{-1})$ where $\epsilon = d-2$. In the critical regime $\xi^{-1}, \xi_J^{-1} \ll k \ll \xi_G^{-1}$, the longitudinal mode has a large (square) mass $2\tilde\lambda_k\tilde\rho_{0,k} \sim 2\tilde\lambda^*\tilde\rho_0^* \sim 1/\epsilon \gg 1$ (Fig. 7). Since the threshold functions decrease as power laws for large arguments [Eq. (C10)], the contribution of the longitudinal mode (proportional to $l_n^d(2\tilde\lambda^*\tilde\rho_0^*, \eta)$) is subdominant compared to the contribution of the transverse modes (proportional to $l_n^d(0,\eta)$). We thus recover the fact that near two dimensions the critical behavior is determined by the Goldstone modes only. To leading order in ϵ, the flow equations read

$$\begin{aligned} \partial_t\tilde\rho_{0,k} &= (-\epsilon-\eta_k)\tilde\rho_{0,k} + 2v_d(N-1)l_1^d(0,\eta_k), \\ \partial_t\tilde\lambda_k &= (-2+\epsilon+2\eta_k)\tilde\lambda_k + 2v_d(N-1)\tilde\lambda_k^2 l_2^d(0,\eta_k), \end{aligned} \tag{110}$$

[38] We denote by $-y_1$ and $-y_2$ the eigenvalues of the stability matrix in agreement with the fact that the RG "time" $t = \ln(k/\Lambda)$ is negative. A positive (negative) y_i then corresponds to a relevant (irrelevant) direction.

Using $m_{22}^{d=2}(w,0) = w^{-2} + \mathcal{O}(w^{-3})$ (Appendix C) and equation (91) with $v_2 = 1/8\pi$, we deduce

$$\eta_k = \frac{1}{4\pi\tilde\rho_{0,k}} + \mathcal{O}(\epsilon^2). \tag{111}$$

Since $l_1^2(0,0) = 1$ (Appendix C), we finally obtain

$$\begin{aligned} \partial_t\tilde\rho_{0,k} &= -\epsilon\tilde\rho_{0,k} + \frac{N-2}{4\pi} + \mathcal{O}(\epsilon), \\ \partial_t\tilde\lambda_k &= -2\tilde\lambda_k + \frac{N-1}{4\pi}l_2^2(0,0)\tilde\lambda_k^2 + \mathcal{O}(\epsilon). \end{aligned} \tag{112}$$

The anomalous dimension is crucial to obtain the factor $N-2$ in the first equation (and therefore a vanishing beta function $\partial_t\tilde\rho_{0,k}$ for $d = 2$ and $N = 2$). The beta function for $\partial_t\tilde\rho_{0,k}$ is universal, depending only on the large-w behavior of $m_{22}^{d=2}(w,0)$ which is independent of the regulator function R_k (Appendix C).

Linearizing near the fixed point

$$\begin{aligned} \tilde\rho_0^* &= \frac{N-2}{4\pi\epsilon} + \mathcal{O}(\epsilon^0), \\ \tilde\lambda^* &= \frac{8\pi}{(N-1)l_2^2(0,0)} + \mathcal{O}(\epsilon), \end{aligned} \tag{113}$$

we find the eigenvalues $-y_1 = -\epsilon$ and $-y_2 = 2$. We deduce the correlation-length exponent

$$\nu = \frac{1}{d-2} + \mathcal{O}(\epsilon^0) \tag{114}$$

and the anomalous dimension

$$\eta = \frac{1}{4\pi\tilde\rho_0^*} + \mathcal{O}(\epsilon^2) = \frac{\epsilon}{N-2} + \mathcal{O}(\epsilon^2), \tag{115}$$

in agreement with the results obtained from the nonlinear sigma model near two dimensions (Zinn-Justin, 1996).

The agreement with the nonlinear sigma model is not surprising since to obtain (114) and (115) we have considered only the Goldstone modes. To make the origin of this agreement more apparent (Delamotte *et al.*, 2004), let us consider the (Wilsonian) action of the dimensionless field $\tilde{\boldsymbol\varphi}$ (defined in the same way as $\tilde{\boldsymbol\phi}$ in Eq. (87)),

$$S[\tilde{\boldsymbol\varphi}] = \int_{\tilde{\mathbf r}} \left\{ \frac{1}{2}(\boldsymbol\nabla\tilde{\boldsymbol\varphi})^2 + \frac{\tilde\lambda}{2}(\tilde\rho-\tilde\rho_0)^2 \right\}, \tag{116}$$

where $\tilde\rho = \tilde{\boldsymbol\varphi}^2/2$. Rescaling the field, $\tilde{\boldsymbol\varphi} \to \sqrt{2\tilde\rho_0}\tilde{\boldsymbol\varphi}$, we obtain

$$S[\tilde{\boldsymbol\varphi}] = \tilde\rho_0 \int_{\tilde{\mathbf r}} \left\{ (\boldsymbol\nabla\tilde{\boldsymbol\varphi})^2 + \frac{\tilde\lambda\tilde\rho_0}{2}(\tilde{\boldsymbol\varphi}^2-1)^2 \right\}. \tag{117}$$

In the limit $\tilde\lambda\tilde\rho_0 \to \infty$, the last term in (117) imposes the constraint $\tilde{\boldsymbol\varphi}^2 = 1$, and we obtain a nonlinear sigma model

$$S[\tilde{\boldsymbol\varphi}] = \frac{1}{2\tilde g}\int_{\tilde{\mathbf r}} (\boldsymbol\nabla\tilde{\boldsymbol\varphi})^2, \qquad (\tilde{\boldsymbol\varphi}^2 = 1) \tag{118}$$

with (dimensionless) coupling constant $\tilde{g} = 1/2\tilde{\rho}_0$. From (112), we deduce that $\tilde{g}_k = 1/2\tilde{\rho}_{0,k}$ satisfies the equation

$$\partial_t \tilde{g}_k = \epsilon \tilde{g}_k - \frac{N-2}{2\pi}\tilde{g}_k^2 + \mathcal{O}(\epsilon^3), \tag{119}$$

which is identical, to order ϵ^2, to the flow equation obtained from the nonlinear sigma model to one-loop order (Nelson and Pelcovits, 1977; Polyakov, 1975; Zinn-Justin, 1996).

There is nevertheless an important difference between the usual perturbative RG approach to the nonlinear sigma model [Eq. (119)] and the NPRG approach to the linear O(N) model [Eqs. (103)] near two dimensions. While in the former case the RG equation is not valid anymore when the coupling constant g_k becomes of order one, in the latter case there is no difficulty to continue the flow in the strong-coupling regime and describe the disordered phase with a finite correlation length.

c. Limit $N \to \infty$ In the large-N limit, the leading contribution comes from the Goldstone modes, whose contribution to the flow equations appears with a factor N. Anticipating that the anomalous dimension η_k is of order $1/N$, we obtain

$$\begin{aligned} \partial_t \tilde{\rho}_{0,k} &= (2-d)\tilde{\rho}_{0,k} + 2v_d N l_1^d(0,0), \\ \partial_t \tilde{\lambda}_k &= (d-4)\tilde{\lambda}_k + 2v_d N \tilde{\lambda}_k^2 l_2^d(0,0), \end{aligned} \tag{120}$$

to leading order. These equations admit the interacting (Wilson-Fisher) fixed point

$$\tilde{\rho}_0^* = N\frac{2v_d l_1^d(0,0)}{d-2}, \qquad \tilde{\lambda}^* = \frac{1}{N}\frac{4-d}{2v_d l_2^d(0,0)}, \tag{121}$$

when $d < 4$. From (91) we check that η is $\mathcal{O}(1/N)$. Linearizing the flow equations (120) about the fixed point (121), we obtain the eigenvalues $-y_1 = 2-d$ and $-y_2 = 4-d$, i.e. a correlation-length exponent

$$\nu = \frac{1}{d-2} + \mathcal{O}(N^{-1}), \tag{122}$$

in agreement with the known result in the large-N limit (Ma, 2000; Zinn-Justin, 1996). When $d > 4$, the eigenvalue y_2 becomes positive and the phase transition is governed by the Gaussian fixed point ($\tilde{\lambda}^* = 0$).

4. The low-temperature phase

The physics of the O($N \geq 2$) model remains nontrivial in the whole low-temperature phase because of the Goldstone modes associated to the spontaneously broken O(N) symmetry. In the ordered phase, a Gaussian fluctuation theory about the mean-field solution predicts (Ma, 2000)

$$G_{\rm T}(\mathbf{p}) = \frac{1}{\mathbf{p}^2}, \quad G_{\rm L}(\mathbf{p}) = \frac{1}{\mathbf{p}^2 + 2|r_0|} \tag{123}$$

(see also Eqs. (B22)). The transverse propagator is gapless, in agreement with Goldstone's theorem, while longitudinal fluctuations have a finite correlation length $\xi = (2|r_0|)^{-1/2}$. The last result is an artifact of the Gaussian approximation (Dupuis, 2011; Patasinskij and Pokrovskij, 1973). In the low-energy limit, below the momentum scale $k_c \sim 2|r_0|$, the good hydrodynamic variables are the amplitude and direction of the vector field $\boldsymbol{\varphi}$. Direction fluctuations are described by a nonlinear sigma model. Amplitude fluctuations are essentially frozen so that transverse and longitudinal fluctuations $\delta\boldsymbol{\varphi}_\parallel, \delta\boldsymbol{\varphi}_\perp$ become strongly coupled: $\boldsymbol{\varphi}^2 = (\boldsymbol{\varphi}_0 + \delta\boldsymbol{\varphi}_\parallel)^2 + \delta\boldsymbol{\varphi}_\perp^2 \simeq \boldsymbol{\varphi}_0^2$ with $\boldsymbol{\varphi}_0$ the mean value of $\boldsymbol{\varphi}$. As a result, in the long-distance limit the longitudinal propagator is dominated by transverse fluctuations: $G_{\rm L}(\mathbf{r}) \sim (N-1)G_{\rm T}^2(\mathbf{r}) \sim 1/|\mathbf{r}|^{2d-4}$. In Fourier space, we thus obtain

$$G_{\rm L}(\mathbf{p}) \sim \frac{1}{|\mathbf{p}|^{4-d}} \tag{124}$$

for $d < 4$, while $G_{\rm L}(\mathbf{p})$ diverges logarithmically for $d = 4$. The presence of a singularity in the longitudinal channel, driven by transverse fluctuations, is a general phenomenon in systems with a continuous broken symmetry (Patasinskij and Pokrovskij, 1973).[39]

In perturbation theory, the divergence of the longitudinal propagator manifests itself by infrared divergences. Equations (123) correspond to zero-loop-order self-energies $\Sigma_{11}^{(0)}(\mathbf{p}) = -3r_0$ and $\Sigma_{ii}^{(0)}(\mathbf{p}) = -r_0$ for $i \neq 1$, assuming the order parameter along the first direction: $\langle\varphi_i\rangle = |\boldsymbol{\varphi}_0|\delta_{i,1}$. The one-loop correction is shown diagrammatically in Fig. 8. While the first diagram is finite, the second one gives a diverging contribution for $d \leq 4$ in the limit $\mathbf{p} \to 0$ (arising when both internal lines correspond to transverse fluctuations)

$$\Sigma_{11}^{(1)}(\mathbf{p}) \simeq -\frac{N-1}{18}u_0^2\varphi_0^2 \int_{\mathbf{q}} \frac{1}{\mathbf{q}^2(\mathbf{p}+\mathbf{q})^2}, \tag{125}$$

where $\varphi_0 = |\boldsymbol{\varphi}_0| = (-6r_0/u_0)^{1/2}$ denotes the order parameter in the mean-field approximation. By comparing the one-loop correction to the zero-loop result, i.e. $|\Sigma_{11}^{(1)}(\mathbf{p})| \sim |\Sigma_{11}^{(0)}(\mathbf{p})|$, one can define a characteristic momentum scale, the Ginzburg momentum scale $k_G \sim u_0^{1/(4-d)}$ ($k_G \sim \Lambda e^{-\text{const}/u_0}$ for $d = 4$), below which the Gaussian approximation (123) breaks down (Dupuis, 2011).

In this section, we show how the main properties of the low-temperature phase of the O(N) model follow from the NPRG analysis in the LPA'. In the ordered phase

[39] Historically, the divergence of the longitudinal propagator was encountered (although not recognized as such) early on in superfluid boson systems; see Sec. XIII.

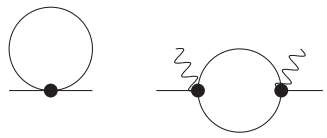

FIG. 8 One-loop correction $\Sigma^{(1)}$ to the self-energy. The dots represent the bare interaction, the zigzag lines the order parameter φ_0, and the solid lines the connected propagator $G^{(0)}$.

for $d > 2$, the (square) mass $2\tilde{\lambda}_k\tilde{\rho}_{0,k}$ of the longitudinal mode eventually becomes much larger than unity since $\tilde{\rho}_{0,k} \sim k^{2-d}\rho_0$ and $\tilde{\lambda}_k \sim \tilde{\lambda}^*$ for $k \to 0$ (see below). We can therefore introduce an hydrodynamic scale k_c defined by

$$2\tilde{\lambda}_{k_c}\tilde{\rho}_{0,k_c} \sim 1. \tag{126}$$

If $\tilde{\lambda}_{k_c} \ll 1$, we can ignore any renormalization when k decreases from Λ to k_c: $Z_{k_c} \simeq 1$, $\lambda_{k_c} \simeq \lambda_\Lambda = u_0/3$, and $\rho_{0,k_c} \simeq \rho_{0,\Lambda} = -3r_0/u_0$ ($\tilde{\lambda}_{k_c} \ll 1$ then translates into the weak-coupling condition $u_0\Lambda^{d-4} \ll 1$). We then find

$$k_c \simeq \sqrt{2|r_0|} \qquad \text{and} \qquad \tilde{\lambda}_{k_c} \sim \frac{u_0}{|r_0|^{\epsilon/2}}, \tag{127}$$

where $\epsilon = 4 - d$. For $k \ll k_c$, $2\tilde{\lambda}_k\tilde{\rho}_{0,k}$ becomes much larger than unity and one can ignore the contribution of the longitudinal mode to the flow equations. This leads to

$$\begin{aligned} \partial_t\tilde{\rho}_{0,k} &= (2 - d - \eta_k)\tilde{\rho}_{0,k} + 2v_d(N-1)l_1^d(0,0), \\ \partial_t\tilde{\lambda}_k &= (d-4)\tilde{\lambda}_k + 2v_d(N-1)\tilde{\lambda}_k^2 l_2^d(0,0), \end{aligned} \tag{128}$$

where $\eta_k \simeq 4v_d/(d\tilde{\rho}_{0,k})$ [Eqs. (91,C10)]. We have set $\eta_k = 0$ everywhere except in the term $\eta_k\tilde{\rho}_{0,k}$. For $d = 2$, $\eta\tilde{\rho}_{0,k} = 2v_2 l_1^d(0,0)$ and $N - 1$ in the first equation (128) is replaced by $N - 2$ (Sec. III.B.3.b). Although, on general grounds, we expect $N - 2$ to appear in the equation $\partial_t\tilde{\rho}_{0,k}$ in any dimension, so that we recover the one-loop RG equation of the nonlinear sigma model (with coupling constant $\tilde{g}_k = 1/2\tilde{\rho}_{0,k}$) describing the direction fluctuations of the $\boldsymbol{\varphi}$ field, the relation $\eta\tilde{\rho}_{0,k} = 2v_2 l_1^d(0,0)$ is not satisfied for a generic regulator (it is for the theta cutoff). This is clearly a failure of the LPA'. In the regime where (128) is valid, the $\mathcal{O}(\tilde{g}_k^2)$ term is however small and the LPA' remains a good approximation to the flow of $\tilde{g}_k = 1/2\tilde{\rho}_{0,k}$. For $k \to 0$, it describes Goldstone bosons with a vanishing interaction.

In the following we use the theta regulator (14) so that $l_2^d(0,0) = 4/d$. Solving the second equation (128) with the boundary condition $\tilde{\lambda}_k \simeq \tilde{\lambda}_{k_c}$ for $k = k_c$, we find

$$\begin{aligned} \tilde{\lambda}_k &= \frac{\epsilon\tilde{\lambda}_{k_c}k_c^\epsilon}{\epsilon k^\epsilon + 8\frac{v_d}{d}(N-1)\tilde{\lambda}_{k_c}(k_c^\epsilon - k^\epsilon)} \\ &\simeq \frac{\epsilon\tilde{\lambda}_{k_c}k_c^\epsilon}{\epsilon k^\epsilon + 8\frac{v_d}{d}(N-1)\tilde{\lambda}_{k_c}k_c^\epsilon} \end{aligned} \tag{129}$$

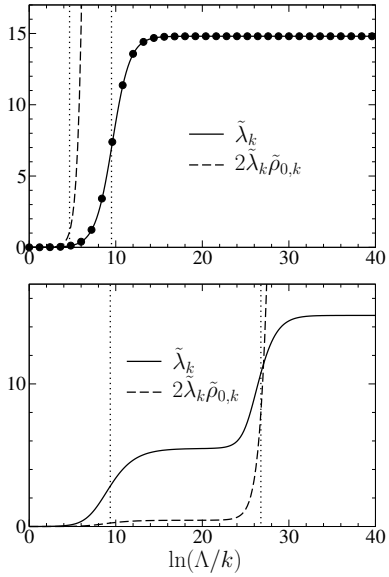

FIG. 9 $\tilde{\lambda}_k$ and $2\tilde{\lambda}_k\rho_{0,k}$ vs $\ln(\Lambda/k)$ for $d = 3$ and $N = 3$ as obtained from Eqs. (103) ($\tilde{\lambda}_\Lambda = 10^{-3}$ and $\Lambda = 1$). A very small value of the initial coupling constant λ_Λ is chosen to have $k_G \ll \Lambda$. Top panel: deep in the ordered phase $T_c - T_G \ll T_c - T$ ($\tilde{\rho}_{0,\Lambda} = 0.1$). The dots correspond to the analytical result (130). The dotted vertical lines show the hydrodynamic (k_c) and Ginzburg (k_G) scales. Bottom panel: critical regime $T_c - T \ll T_c - T_G$ ($\tilde{\rho}_{0,\Lambda} \simeq 0.0506$). The dotted vertical lines show the Ginzburg (k_G) and Josephson (k_J) scales. The first plateau, $\tilde{\lambda}_k \sim \tilde{\lambda}^*_{\rm crit}$, corresponds to the critical regime and the second one, $\tilde{\lambda}_k \sim \tilde{\lambda}^*$ ($\ln(\Lambda/k) \gtrsim 30$), to the low-temperature fixed point.

for $k \ll k_c$ (and $\epsilon > 0$). The last expression can be rewritten in the more insightful form

$$\tilde{\lambda}_k = \frac{\tilde{\lambda}^*}{1 + (k/k_G)^\epsilon}, \tag{130}$$

where

$$\tilde{\lambda}^* = \lim_{k\to 0}\tilde{\lambda}_k = \frac{\epsilon d}{8v_d(N-1)} \tag{131}$$

and

$$k_G = \left[(N-1)\frac{8v_d k_c^\epsilon \tilde{\lambda}_{k_c}}{d\epsilon}\right]^{1/\epsilon} \simeq \left[(N-1)\frac{8v_d u_0}{3d\epsilon}\right]^{1/\epsilon} \tag{132}$$

is the Ginzburg scale. Equation (130) is in remarkable agreement with the numerical solution of the flow equations (103) (Fig. 9, top panel). $\tilde{\lambda}^*$ is the fixed-point value of $\tilde{\lambda}_k$ in the ordered phase; it should not be confused with the fixed-point value $\tilde{\lambda}^*_{\rm crit}$ at the critical point as discussed in section III.B.3.

The dimensionless coupling constant at the Ginzburg scale,

$$\tilde{\lambda}_{k_G} \sim \lambda_{k_G} k_G^{-\epsilon}, \tag{133}$$

is of order one (Eq. (132) and Fig. 9). We can therefore identify a perturbative regime $k \gg k_G$ where the Gaussian approximation or perturbative approach is justified ($\tilde{\lambda}_k \ll 1$) and a nonperturbative regime $k \ll k_G$ where $\tilde{\lambda}_k \sim \tilde{\lambda}^* \gtrsim 1$.

Deep in the ordered phase, the hydrodynamic scale is reached before the Ginzburg scale in the RG flow ($k_c \gg k_G$) (Fig. 9, top panel). The ratio k_G/k_c increases with temperature and becomes of order one at the Ginzburg temperature $T_G < T_c$. For $T_c - T \ll T_c - T_G$ the system is in the critical regime of the ordered phase: as k decreases, the condition $\tilde{\lambda}_k \sim 1$ (i.e. $k \sim k_G$) is reached while $2\tilde{\lambda}_k \tilde{\rho}_{0,k} \ll 1$, so that the hydrodynamic scale k_c is not defined anymore. The condition $2\tilde{\lambda}_k \tilde{\rho}_{0,k} \sim 1$ defines a new momentum scale, the Josephson scale $k_J \ll k_G$. The latter separates the critical regime $k_J \ll k \ll k_G$, where $\tilde{\rho}_{0,k} \sim \tilde{\rho}^*_{0,\mathrm{crit}}$ and $\tilde{\lambda}_k \sim \tilde{\lambda}^*_{\mathrm{crit}}$, from the Goldstone regime $k \ll k_J$ where $\tilde{\rho}_{0,k} \sim k^{2-d}$ and $\tilde{\lambda}_k \sim \tilde{\lambda}^*$ (Figs. 9 (bottom panel) and 6). As discussed in section III.B.3, the limit $d \to 2^+$ is very peculiar. For $\epsilon = d - 2 \ll 1$ the hydrodynamic scale k_c remains defined in the critical regime $T_c - T \ll T_c - T_G$ since $2\tilde{\lambda}^*_{\mathrm{crit}} \tilde{\rho}^*_{0,\mathrm{crit}} \gg 1$: the critical behavior is then controlled by the Goldstone modes.

Thus the low-temperature phase is described by an interacting fixed point ($\tilde{\lambda}^* > 0$); this is the price to pay for using the $\boldsymbol{\varphi}$ field rather than the amplitude and direction variables. Nevertheless the anomalous dimension vanishes, $\eta = \lim_{k\to 0} \eta_k = 0$, in agreement with the fact that the transverse 2-point vertex $\Gamma^{(2)}_{k=0,\mathrm{T}}(\mathbf{p}; \rho_0)$ is expected to vanish as $\mathbf{p}^2$. In the NPRG analysis the vanishing of η_k when $k \to 0$, in spite of the fixed point being interacting, is ensured by the vanishing of the threshold function $m^d_{22}(2\tilde{\lambda}_k \tilde{\rho}_{0,k}, \eta_k)$ in the limit $2\tilde{\lambda}_k \tilde{\rho}_{0,k} \to \infty$ (see Eqs. (91) and (C10)).

The nonzero value of $\tilde{\lambda}^*$ is crucial to understand the divergence of the longitudinal propagator in the ordered phase. Since $\lambda_k \sim \tilde{\lambda}^* k^{4-d}$ for $k \to 0$, the square mass $2\lambda_k \rho_{0,k}$ of the longitudinal mode vanishes for $k \to 0$ and $G_{k,\mathrm{L}}(\mathbf{p} = 0; \rho_{0,k}) = 1/2\lambda_k \rho_{0,k} \sim 1/k^{4-d}$ diverges for $k \to 0$. If we approximate $G_{k=0,\mathrm{L}}(\mathbf{p}; \rho_0)$ by $G_{k\sim|\mathbf{p}|,\mathrm{L}}(\mathbf{p} = 0; \rho_0)$ (arguing that $\mathbf{p}$ acts as an infrared cutoff), one finds $G_{k=0,\mathrm{L}}(\mathbf{p}; \rho_0) \sim 1/|\mathbf{p}|^{4-d}$ for $|\mathbf{p}| \to 0$ and $d < 4$ (the divergence is logarithmic for $d = 4$).

The behavior of the longitudinal propagator can be summarized as follows (Dupuis, 2011). In the non-critical regime $T_c - T_G \ll T_c - T$, there are two characteristic momentum scales (k_G and k_c) and two regimes for the behavior of $G_{\sigma\sigma}(\mathbf{p})$: i) a Goldstone regime ($|\mathbf{p}| \ll k_G$) characterized by a diverging longitudinal propagator $G_{\sigma\sigma}(\mathbf{p}) \sim 1/|\mathbf{p}|^{4-d}$, ii) a Gaussian (perturbative) regime ($|\mathbf{p}| \gg k_G$) where $G_{\sigma\sigma}(\mathbf{p}) \simeq 1/(\mathbf{p}^2 + k_c^2)$. The critical regime $T_c - T \ll T_c - T_G$ is characterized by two momentum scales (k_J and k_G) and three regimes for the behavior of $G_{\sigma\sigma}(\mathbf{p})$: i) a Goldstone regime ($|\mathbf{p}| \ll k_J$) with a diverging longitudinal propagator, ii) a critical regime ($k_J \ll |\mathbf{p}| \ll k_G$) where $G_{\sigma\sigma}(\mathbf{p}) \sim 1/|\mathbf{p}|^{2-\eta}$, iii) a Gaussian regime ($k_G \ll |\mathbf{p}|$) where $G_{\sigma\sigma}(\mathbf{p}) \simeq 1/\mathbf{p}^2$. The momentum dependence of the longitudinal propagator can be more rigorously obtained from the BMW approximation (Sec. V).

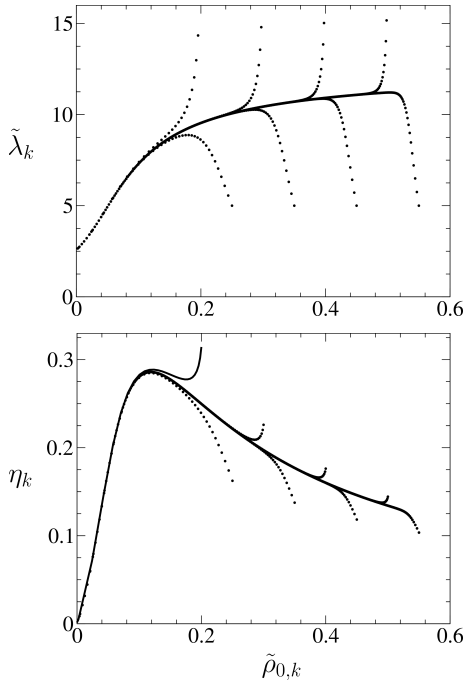

FIG. 10 RG trajectories in the planes $(\tilde{\rho}_0, \tilde{\lambda})$ and $(\tilde{\rho}_0, \eta)$, obtained from various initial conditions $\tilde{\rho}_{0,\Lambda}$, $\tilde{\lambda}_\Lambda$, showing the approximate line of fixed points. (The points correspond to equal steps in $t = \ln(k/\Lambda)$.) (Gräter and Wetterich, 1995)

5. The two-dimensional O(2) model

We expect the two-dimensional O(2) model to undergo a Kosterlitz-Thouless (KT) phase transition between a high-temperature (disordered) phase and a low-temperature phase with algebraic order. While we shall discuss in detail the two-dimensional O(2) model and the KT transition in Sec. IV, here we briefly discuss the results obtained from the truncated LPA' equations in the case $d = 2$ and $N = 2$ (103) (Gräter and Wetterich, 1995).

In Sec. III.B.3.b, we have shown that to leading order in $\tilde{g}_k = 1/2\tilde{\rho}_{0,k}$ the LPA' yields the one-loop beta function of the nonlinear sigma model with coupling constant $\tilde{g}_k$. We expect the nonlinear sigma model to be the correct low-energy description in the low-temperature phase. For $N = 2$, this model is trivial, since Goldstone bosons are noninteracting in that (abelian) case, and the perturbative beta function $\partial_t \tilde{g}_k$ vanishes. The linear O(2) model is of course much richer than the nonlinear sigma model. In particular, it allows for topological defects

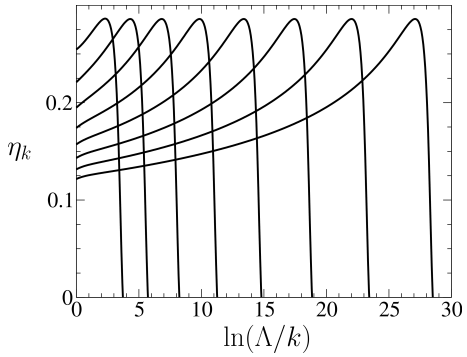

FIG. 11 Scale-dependent anomalous dimension η_k for various initial conditions ($\tilde{\rho}_{0,\Lambda}$ increases from left to right). (Gräter and Wetterich, 1995)

(vortices) which are responsible for a phase transition to a high-temperature phase with exponentially decaying correlations.

Figure 10 shows the RG flow in the planes $(\tilde{\rho}_0, \tilde{\lambda})$ and $(\tilde{\rho}_0, \eta)$ obtained from the numerical solution of the truncated LPA' equations (103). When $\tilde{\rho}_{0,\Lambda}$ is sufficiently large (for a given $\tilde{\lambda}_\Lambda$), the RG trajectories rapidly hit an approximate line of fixed points where the running of the superfluid stiffness $\tilde{\rho}_{0,k}$ becomes very slow.[40] This implies a very large correlation length ξ. For very long RG time $-t$ (such that $k \sim \xi^{-1}$), the RG flow eventually crosses over to the disordered regime. On the approximate line of fixed points, the scale-dependent anomalous dimension η_k varies slowly as a function of $\tilde{\rho}_{0,k}$. It reaches its maximum value $\eta_c \simeq 0.29$ (to be compared with the exact value $\eta_c = 1/4$ at the KT transition) before rapidly dropping to zero once $k \sim \xi^{-1}$ (Fig. 11). When $\tilde{\rho}_{0,\Lambda}$ is small, the RG trajectories do not reach the approximate line of fixed points.

Thus, although the LPA' does not yield a low-temperature phase with an infinite correlation length, we can nevertheless define a KT "transition" temperature $T_{\rm KT}$ below which the correlation length is very large(Gräter and Wetterich, 1995). A reasonable estimate of the KT transition temperature in the two-dimensional XY model has been obtained from the LPA' and the lattice NPRG (Sec. VII) (Machado and Dupuis, 2010). The LPA' has also been used to determine $T_{\rm KT}$ in a two-dimensional Bose gas (Rançon and Dupuis, 2012c), in very good agreement with Monte Carlo simulations (Prokof'ev *et al.*, 2001; Prokof'ev and Svistunov, 2002), and in the quantum O(2) model near the $T = 0$ quantum phase transition (Rançon *et al.*, 2013).

[40] The equivalence between $\tilde{\rho}_{0,k}$ and the superfluid stiffness in the two-dimensional case is shown in Sec. IV.

FIG. 12 ν and η vs α in the three-dimensional O(1) model obtained with the exponential regulator function (13).

C. Second order of the derivative expansion (BD)

In this section, we discuss the derivative expansion to second order, where the effective action is approximated by (40). The corresponding 2-point vertex is given by

$$\Gamma^{(2)}_{k,\mathrm{L}}(\mathbf{p};\rho) = [Z_k(\rho) + \rho Y_k(\rho)]\mathbf{p}^2 + U'_k(\rho) + 2\rho U''_k(\rho),$$
$$\Gamma^{(2)}_{k,\mathrm{T}}(\mathbf{p};\rho) = Z_k(\rho)\mathbf{p}^2 + U'_k(\rho), \tag{134}$$

in a constant field. RG equations for $Z_k(\rho)$ and $Y_k(\rho)$ are derived from

$$Z_k(\rho) = \lim_{\mathbf{p}\to 0} \frac{\partial}{\partial \mathbf{p}^2} \Gamma^{(2)}_{k,\mathrm{T}}(\mathbf{p};\rho),$$
$$Z_k(\rho) + \rho Y_k(\rho) = \lim_{\mathbf{p}\to 0} \frac{\partial}{\partial \mathbf{p}^2} \Gamma^{(2)}_{k,\mathrm{L}}(\mathbf{p};\rho) \tag{135}$$

and the exact RG equation (30), while $\partial_t U_k(\rho)$ is obtained as previously by noting that $\Gamma_k[\boldsymbol{\phi}] = V U_k(\rho)$ in a constant field. The regulator function $R_k(\mathbf{q}) = Z_k r(\mathbf{q}^2/k^2)$ is chosen as in the LPA', where the field renormalization factor Z_k is defined below.

To solve numerically the flow equations and look for possible fixed points, we define the dimensionless quantities

$$\tilde{U}_k(\tilde{\rho}) = v_d^{-1} k^{-d} U_k(\rho), \quad \tilde{Z}_k(\tilde{\rho}) = Z_k^{-1} Z_k(\rho),$$
$$\tilde{Y}_k(\tilde{\rho}) = v_d Z_k^{-2} k^{d-2} Y_k(\rho), \tag{136}$$

where $\tilde{\rho} = v_d^{-1} Z_k k^{2-d} \rho$. The factor $v_d^{-1} = 2^{d+1}\pi^{d/2}\Gamma(d/2)$ is introduced for convenience (see Appendix E). The field renormalization factor Z_k is defined by imposing the condition $\tilde{Z}_k(\tilde{\rho}_{\mathrm{r}}) = 1$, where $\tilde{\rho}_{\mathrm{r}}$ is an arbitrary renormalization point. The (running) anomalous dimension is defined as before: $\eta_k = -\partial_t \ln Z_k$. The flow equations are given in Appendix E.

1. Choice of the regulator function

The choice of the regulator function is crucial when looking for accurate estimates of critical exponents. The flow equations involve derivatives of $R_k(\mathbf{q})$, e.g. $\partial_{\mathbf{q}^2} R_k(\mathbf{q})$ and $\partial^2_{\mathbf{q}^2} R_k(\mathbf{q})$ to second order of the derivative expansion. The regulator function need not be analytic but should be sufficiently differentiable to preserve the analyticity of the vertex $\Gamma^{(n)}_k(\mathbf{p}_1 \cdots \mathbf{p}_n)$ in the variables $\mathbf{p}_i$, which is the basic assumption underlying the derivative expansion. For instance, the theta regulator function (14) can be used to second order, but not to higher orders of the derivative expansion.

In the high- and low-temperature phases of the O(1) model it is known that the low-momentum expansion of

TABLE I Critical exponent ν in the O(N) model obtained from the derivative expansion (DE) for $d = 3$ (left) and $d = 2$ (right). Also shown are the results obtained from field theory (FT) and Monte Carlo (MC) simulations.

N	DE	FT	MC
1			
2			
3			
4			
10			
100			

N	DE	FT	MC
1			
2			
3			
4			
10			
100			

TABLE II Same as Table I but for the anomalous dimension η.

N	DE	FT	MC
1			
2			
3			
4			
10			
100			

N	DE	FT	MC
1			
2			
3			
4			
10			
100			

$\Gamma^{(2)}_{k=0}(\mathbf{p})$ wrt $|\mathbf{p}|/m$ (with $\xi = m^{-1}$ the correlation length) has a finite radius of convergence equal to 3 and 2, respectively (Ref???). For the critical theory of the O(N) model, it is therefore plausible that $\Gamma^{(2)}_k(\mathbf{p})$ has a finite radius of convergence in $|\mathbf{p}|/k$, since k typically plays the role of a mass. By analogy with the massive case, we expect the radius of convergence to be of order 1. This suggests that vertices $\Gamma^{(n)}_k$ differ significantly from their derivative-expansion approximation at momenta larger than typically a few k. It is therefore crucial to suppress the contribution of this momentum region in the integrals appearing in the flow equations. Since the large-momentum region is cut off by the $\partial_t R_k(\mathbf{q})$ term, it is important to use a regulator function $R_k(\mathbf{q})$ which decays rapidly for $|\mathbf{p}| \gtrsim k$. This issue is particularly important beyond the second order of the derivative expansion.

2. Optimization

If the flow equation of the effective action were solved exactly, the results wold be independent of the regulator function R_k (Fig. 3). This is not the case when the effective action is expanded in a derivative expansion. In particular, with the regulator function (13) or (14), critical exponents depend on the parameter α. We determine what we consider as the optimal value of α from the principle of minimal sensitivity (PMS), that is by demanding that locally critical exponents be independent of α (e.g., for the correlation length exponent ν, $d\nu/d\alpha = 0$ for $\alpha = \alpha_{\rm opt}$). The renormalization point is taken fixed (for numerical convenience) and, provided the fixed point exists, a change in $\tilde{\rho}_{\rm r}$ is equivalent to a change in α so that the critical exponents are independent of $\tilde{\rho}_{\rm r}$ (Canet *et al.*, 2015). The optimal value $\alpha_{\rm opt}$ can be different for different critical exponents (ν, η, etc.). Note that the k-dependent renormalization point $\tilde{\rho}_{0,k}$ (the choice usually made in the LPA', see Sec. III.B), which becomes k-independent at small k since $\tilde{\rho}_{0,k} \to \tilde{\rho}^*_0$ at criticality, is equivalent to any other choice $\tilde{\rho}_{\rm r} = $ const. The PMS can be used with any family of regulators, possibly depending on more than one parameter.

To illustrate the PMS, we show in Fig. 12 the critical exponents ν and η in the three-dimensional O(1) model as a function of the parameter α computed with the exponential regulator function (13).

3. Critical exponents

The critical exponents of the three- and two-dimensional O(N) models obtained in the derivative expansion are shown in Tables I-II and compared to those of resummed perturbation theory (referred to as field theory) and Monte Carlo simulations.

D. Higher orders of the derivative expansion (BD)

E. Fixed points and scale invariance (NW)

F. First-order phase transitions

IV. THE TWO-DIMENSIONAL $O(2)$ MODEL

In this section we discuss the two-dimensional linear O(2) model and show that the derivative expan-

sion captures the main characteristics of the Kosterlitz-Thouless (KT) transition.[41] The KT transition differs from more conventional finite-temperature phase transitions in a number of aspects (Berezinskii, 1971; Kosterlitz and Thouless, 1973, 1974). It is not characterized by spontaneous symmetry breaking and the low-temperature phase exhibits algebraic order (rather than true long-range order). Nevertheless, the system shows a nonzero "stiffness" $\rho_s(T)$ for all temperatures $T < T_{\rm KT}$. Above the transition temperature $T_{\rm KT}$, one observes a standard disordered phase with exponentially decaying correlation functions. However, the correlation length ξ does not diverge as a power law of $\tau = T - T_{\rm KT}$ but shows an essential singularity $\xi \sim \exp(c/\sqrt{\tau})$. The transition is also characterized by a jump of the stiffness which vanishes for $T > T_{\rm KT}$ and takes the universal value $2/\pi$ for $T \to T_{\rm KT}^-$ (Minnhagen and Warren, 1981; Nelson and Kosterlitz, 1977).

The key role of topological defects (vortices) was recognized by Kosterlitz and Thouless who formulated the KT transition as a vortex/anti-vortex pair unbinding transition (Ambegaokar *et al.*, 1980; Chaikin and Lubensky, 1995; José *et al.*, 1977; Kosterlitz and Thouless, 1973, 1974; Minnhagen, 1987). Standard studies of the KT transition explicitly introduce the vortices in the analysis and use a mapping to the Coulomb gas or Sine-Gordon models. A perturbative renormalization-group approach is then sufficient to derive the universal features of the KT transition.

The KT transition in the two-dimensional linear O(2) model provides an important benchmark for the NPRG. A distinctive feature of the NPRG approach is that the vortices are not introduced explicitly and thus the RG equations are the standard ones of the d-dimensional O(N) model with $N = 2$ and $d = 2$. The first NPRG approach of the KT transition is due to Gräter *et al.* (Gersdorff and Wetterich, 2001; Gräter and Wetterich, 1995). This work was later on re-examined by Jakubczyk *et al.* who emphasize the importance of a proper choice of the infrared regulator (Jakubczyk *et al.*, 2014).

Our discussion of the KT transition is based on the flow equations obtained from the derivative expansion to second order (Sec. III.C). The scale-dependent effective action Γ_k is then parameterized by three functions of the O(N) invariant $\rho = \boldsymbol{\phi}^2/2$: $U_k(\rho)$, $Z_k(\rho)$ and $Y_k(\rho)$ [Eq. (40)].

The effective potential $U_k(\rho)$, and the location of its minimum $\rho_{0,k}$, provide information about the phase of the system. In the high-temperature phase ($T > T_{\rm KT}$), we expect $\rho_{0,k}$ to vanish for a value of k of the order of the inverse of the correlation length ξ. In the low-temperature phase ($T_{\rm KT}$), characterized by algebraic order and an infinite correlation length, we expect $\rho_{0,k}$ to vanish as a power law of k (a nonzero value of $\lim_{k\to 0}\rho_{0,k}$ would imply spontaneous symmetry breaking and is forbidden by the Mermin-Wagner theorem).

Additional information can be obtained from the transverse part of the propagator in the equilibrium field configuration,

$$G_{k,\rm T}(\mathbf{p};\rho_{0,k}) = \frac{2\rho_{0,k}}{\rho_{s,k}\mathbf{p}^2}, \tag{137}$$

where $2\rho_{0,k} = \langle\boldsymbol{\varphi}(\mathbf{r})\rangle^2$ is the square of the order parameter at scale k. Equation (137) defines the running stiffness $\rho_{s,k}$. Note that the momentum dependence of $G_{k,\rm T}$ in Eq. (137) follows from the derivative expansion and is therefore valid only for $|\mathbf{p}| \ll k$. Alternatively, $\rho_{s,k}$ can be defined from the change $\Delta\Gamma_k$ of the effective action when the direction of the order parameter $\boldsymbol{\phi}(\mathbf{r}) = \sqrt{2\rho_{0,k}}(\cos\theta(\mathbf{r}), \sin\theta(\mathbf{r}))$ at scale k varies slowly in space,

$$\Delta\Gamma_k[\boldsymbol{\phi}] = \frac{1}{2}\rho_{s,k}\int d^dr\,(\boldsymbol{\nabla}\theta)^2. \tag{138}$$

Equations (137) and (138) lead to the same expression

$$\rho_{s,k} = 2Z_k(\rho_{0,k})\rho_{0,k} \tag{139}$$

of the stiffness. The physical stiffness is defined as $\rho_s(T) = \lim_{k\to 0}\rho_{s,k}(T)$.

We define the anomalous dimension $\eta_k = -\partial_t \ln Z_k$ as in Sec. III, by writing $Z_k(\rho) = Z_k\tilde{Z}_k(\tilde{\rho})$ and imposing the condition $\tilde{Z}_k(\tilde{\rho}_{\rm r}) = 1$ where $\tilde{\rho}_{\rm r}$ is an arbitrary renormalization point. The (true) anomalous dimension is simply $\eta(T) = \lim_{k\to 0}\eta_k$. Both the stiffness $\rho_{s,k}$ and the anomalous dimension η_k are crucial to understand the long-distance physics of the two-dimensional O(2) model. In the high-temperature phase both $\rho_{s,k}$ and $\rho_{0,k}$ vanish for a nonzero value of k of the order of the inverse of the correlation length ξ. Z_k reaches a finite limit for $k \to 0$ since the anomalous dimension $\eta = \lim_{k\to 0}\eta_k$ vanishes. In the low-temperature phase, we expect η_k and $\rho_{s,k}$ to take a finite value in the limit $k \to 0$ (this implies $Z_k \sim k^{-\eta}$ for $k \to 0$). This is possible only if $\rho_{0,k} \sim k^\eta$ when $k \to 0$, which is consistent with $\tilde{\rho}_{0,k} = Z_k\rho_{0,k}$ taking a finite limit (as expected for a critical system with an infinite correlation length). The result $\rho_{0,k} \sim k^\eta$ is in agreement with both the absence of long-range order ($\lim_{k\to 0}\rho_{0,k} = 0$) and an infinite correlation length ($\rho_{0,k} > 0$ for any $k > 0$).

A. Flow equations and optimized regulator

We consider the exponential regulator function (13) with an arbitrary parameter α. We numerically integrate the flow equations of $\tilde{U}_k', \tilde{Z}_k, \tilde{Y}_k$ starting at scale

[41] The KT transition has also been studied using the NPRG in the framework of the Sine-Gordon model: see (Bacsó *et al.*, 2015; Nagy *et al.*, 2009; Nandori, 2011; Pangon, 2012).

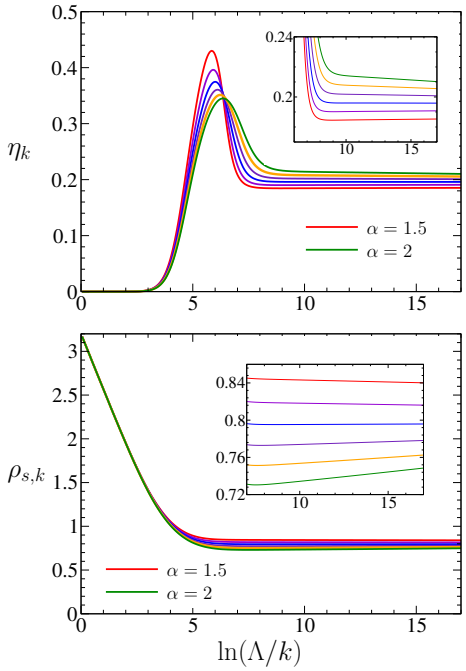

FIG. 13 (Color online) η_k and $\rho_{s,k}$ in the low-temperature phase for $\alpha = 1.5, 1.6, 1.7, 1.8, 1.9, 2$ (from bottom to top in the inset of the top figure and the reverse in the bottom inset) and a fixed temperature $T < T_{\rm KT}$ ($\Lambda = 1$ and $u_0 = 0.003$) (Jakubczyk *et al.*, 2014).

$k = \Lambda$ with the bare action (3) and for various values of $r_0 \propto T - T_0$ (we take $u_0 = 0.003$ and $\Lambda = 1$). From the behavior of the RG flow in the $k \to 0$ limit, we can clearly identify a high-temperature and a low-temperature phase. The high-temperature phase is characterized by the vanishing of $\rho_{s,k}$ and η_k at a nonzero value of k. In the low-temperature phase, both $\rho_{s,k}$ and η_k remain finite for $k \to 0$ while $\rho_{0,k}$ vanishes as a power law as anticipated. The transition temperature $T_{\rm KT}$ is defined from the critical value r_{0c} separating the two phases.

In the low-temperature phase and at fixed $\tilde\rho_{\rm r}$, the long-distance behavior of the RG flow depends on the infrared regulator (i.e. the parameter α in (13)) in a crucial way. We expect the RG trajectory to flow into a fixed point as in the standard KT theory. η_k and $\rho_{s,k}$ (and more generally the functions $\tilde U_k(\tilde\rho)$, $\tilde Z_k(\tilde\rho)$ and $\tilde Y_k(\tilde\rho)$) should then become k independent for sufficiently small k. Figure 13 shows that for an arbitrary value of α, in general we do not reach a fixed point, and $\rho_{s,k}$ and η_k exhibit only quasi-plateaus at small k with slopes that are either positive or negative depending on α. Thus, for each temperature $T < T_{KT}$ (but not too small, see below), it is possible to fine tune α such that we obtain a true plateau. We view this particular value $\alpha_{\rm opt} \equiv \alpha_{\rm opt}(T)$ as the optimal choice of the regulator. We find $\alpha_{\rm opt}(T_{\rm KT}) = 2.0$ and $\alpha_{\rm opt}(T) < 2$ for $T < T_{\rm KT}$. In the high-temperature phase, we take $\alpha_{\rm opt} = 2$. In the following, we shall always consider the optimal regulators. The fact that $\alpha_{\rm opt}$ changes with T is a limitation of the derivative expansion used to solve the flow equation (30). In the exact solution, we expect the RG flow to reach a fixed point in the low-temperature phase regardless of the choice of the regulator. It should be noted however that a nonoptimal choice ($\alpha \neq \alpha_{\rm opt}$) leads to essentially the same long-distance physics even though there is no fixed point. In particular, the system exhibits algebraic order (except perhaps at extremely large length scales). The ultimate fate of $\rho_{s,k}$ and η_k as $k \to 0$ (which depends on the sign of the slope of the quasi-plateau) is clearly irrelevant at macroscopic length scales of interest.[42]

The optimal value $\alpha_{\rm opt} \equiv \alpha_{\rm opt}(\tilde\rho_{\rm r})$ depends on $\tilde\rho_{\rm r}$ but the universal features of the KT transition are independent of the choice of $(\tilde\rho_{\rm r}, \alpha_{\rm opt}(\tilde\rho_{\rm r}))$. In the low-temperature phase, when $\tilde\rho_{\rm r}$ is too large the propagator $G_k = (\Gamma_k^{(2)} + R_k)^{-1}$ does not remain positive definite due to the appearance of a pole at finite k, and the RG flow cannot be continued to lower k.[43] The lower the temperature, the smaller the renormalization point should be. We find that $\tilde\rho_{\rm r}$ must always be smaller than the minimum $\tilde\rho_{0,k}$ of the effective potential because, otherwise, a pole in the propagator appears at finite RG time t. Thus, contrary to the three-dimensional case, it is never possible to choose $\tilde\rho_{\rm r} = \tilde\rho_{0,k}$. Below a certain temperature, even with $\tilde\rho_{\rm r} = 0$, it is not possible to avoid the appearance of a pole in the propagator. The lowest temperature that can be reached corresponds to an anomalous dimension $\eta(T) \simeq 0.17$ (obtained with $\alpha = 1.45$). It should be noted however that the low-temperature regime $T \ll T_{\rm KT}$, which is dominated by spinwave excitations, becomes trivial when one works with the Goldstone boson (i.e. the phase of the complex field $\varphi_1 + i\varphi_2$) and there is no need to use the NPRG.

Figure 14 shows $\rho_{s,k}$ and η_k for various temperatures below the KT transition temperature, obtained with the optimal parameter $\alpha_{\rm opt}$. The renormalized stiffness $\rho_s(T) = \lim_{k\to 0} \rho_{s,k}$ and the anomalous dimension $\eta(T) = \lim_{k\to 0} \eta_k$ are obtained from the plateau values of $\rho_{s,k}$ and η_k. The highest temperature for which we find a phase with a nonzero stiffness $\rho_s(T)$ provides an estimate $r_{0c} \simeq -0.0015831$ of the KT transition temperature $T_{\rm KT}$. We shall discuss other determinations of $T_{\rm KT}$ in the following.

[42] If we take a microscopic cutoff Λ of the order of 0.1 $\mathring{A}^{-1}$, $k = \Lambda e^{-20}$ then corresponds to a length scale of the order of 0.5 meter.

[43] A nonpositive propagator means that the Legendre transform of the free energy $-\ln Z[\mathbf{J}]$ is not convex.

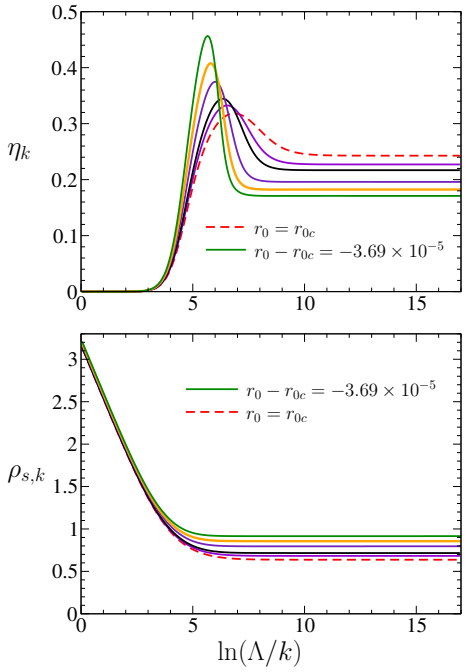

FIG. 14 (Color online) Anomalous dimension η_k and stiffness $\rho_{s,k}$ vs $\ln(\Lambda/k)$ for $\alpha = \alpha_{\rm opt}$ and various values of r_0 from $r_{0c} \simeq -0.0015831$ to $r_{0c} - 3.69 \times 10^{-5}$ (Jakubczyk *et al.*, 2014).

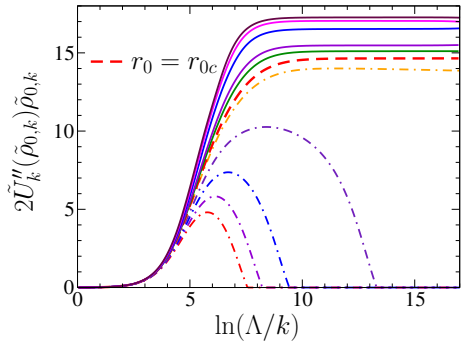

FIG. 15 (Color online) Longitudinal square mass $2\tilde{U}_k''(\tilde{\rho}_{0,k})\tilde{\rho}_{0,k}$ vs $\ln(\Lambda/k)$ for various values of $r_0 - r_{0c}$ in the low-T (solid lines) and high-T (dot-dashed lines) phases (Jakubczyk *et al.*, 2014).

B. Kosterlitz-Thouless (KT) transition

1. Suppression of amplitude fluctuations

Our results show that in the low-temperature phase as well as in the high-temperature phase in the vicinity of the KT transition, the dimensionless square "mass" $2\tilde{\rho}_{0,k}\tilde{U}_k''(\tilde{\rho}_{0,k})$ of the longitudinal propagator $G_{k,\rm L}$ becomes much larger than unity (Fig. 15). For k smaller than the characteristic momentum scale k_c defined by $2\tilde{\rho}_{0,k_c}\tilde{U}_{k_c}''(\tilde{\rho}_{0,k_c}) \sim 1$, amplitude fluctuations of the two-component vector field $\boldsymbol{\varphi}$ are strongly suppressed and the

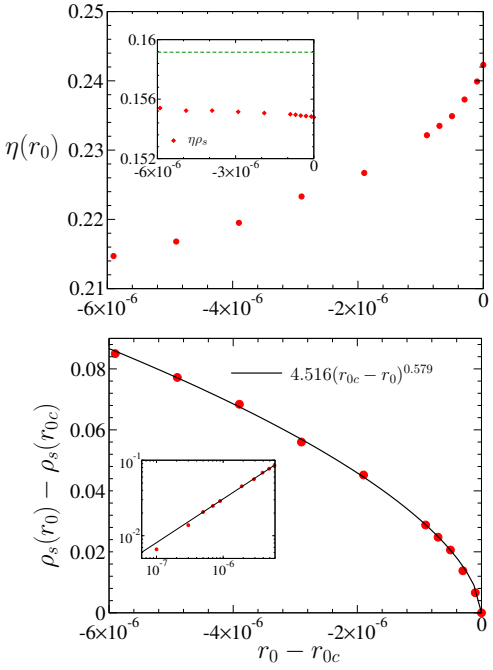

FIG. 16 (Color online) Top: anomalous dimension η vs $r_0 - r_{0c}$ in the low-temperature phase for $\alpha = \alpha_{\rm opt}$. The inset shows the product $\eta\rho_s$ together with $1/2\pi$ (dashed line). Bottom: stiffness ρ_s vs $r_0 - r_{0c}$ in the low-temperature phase for $\alpha = \alpha_{\rm opt}$. The straight line in the inset shows the best power-law fit (with an exponent 0.579) in a logarithmic plot (Jakubczyk *et al.*, 2014).

flow is primarily controlled by direction fluctuations.[44] In this long-distance regime, we expect the physics of the linear O(2) model to be similar to that of the XY model, i.e. dominated by spinwaves and vortex excitations. Note that we do not expect amplitude fluctuations to be completely frozen as this would prevent the formation of vortices since in our continuum model the field vanishes at the center of the vortex.

2. Low-temperature phase

In this section we discuss the results in the low-temperature phase $T \leq T_{\rm KT}$. From the numerical results obtained for $r_0 \to r_{0c} \simeq -0.0015831$ (Fig. 14), we deduce

$$\rho_s(T_{\rm KT}^-) \simeq 0.64, \qquad \eta(T_{\rm KT}^-) \simeq 0.24, \tag{140}$$

in very good agreement with the exact result $\rho_s(T_{\rm KT}^-) = 2/\pi \simeq 0.6366$ and $\eta(T_{\rm KT}^-) = 1/4$. By changing the initial value of u_0 or including a $(\boldsymbol{\varphi}^2)^3$ term in the action (3), we have verified that these results are independent of the initial conditions.

[44] The characteristic length scale k_c^{-1} is analog to the healing length of a superfluid.

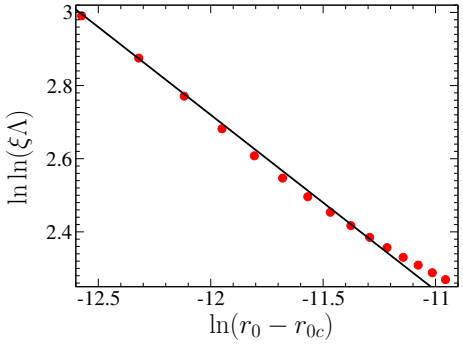

FIG. 17 (Color online) $\ln\ln(\Lambda\xi)$ vs $\ln(r_0 - r_{0c})$ in the high-temperature phase (Jakubczyk *et al.*, 2014). The solid line corresponds to a fit of the form (145) with $\gamma \simeq 0.48$.

Figure 16 shows $\rho_s(T)$ and $\eta(T)$ for $T \leq T_{\rm KT}$. The results are compatible with the temperature dependence

$$\rho_s(T) = \rho_s(r_{0c}^-)[1 + b\sqrt{r_{0c} - r_0}] \qquad (141)$$

of the stiffness in the vicinity of the transition (Chaikin and Lubensky, 1995) even though the square-root singularity is not perfectly captured (we find the exponent 0.579 instead of 0.5). Furthermore we obtain

$$\eta(T) \simeq \frac{0.155}{\rho_s(T)}. \qquad (142)$$

In the KT theory the long-distance physics is fully determined by noninteracting spinwaves with renormalized stiffness $\rho_s(T)$ since vortices are irrelevant in the low-temperature phase. This leads to $\eta(T) = 1/2\pi\rho_s(T) \simeq 0.159/\rho_s(T)$.[45] This exact relation is well approximated by the NPRG result (142).

3. High-temperature phase and essential scaling

In the high-temperature phase, the propagator takes the form

$$G_{k=0}(\mathbf{p}, \rho = 0) = [Z_{k=0}(0)\mathbf{p}^2 + U'_{k=0}(0)]^{-1} \qquad (143)$$

in the equilibrium field configuration $\rho = 0$. The correlation length is given by

$$\xi = \left(\frac{U'_{k=0}(0)}{Z_{k=0}(0)}\right)^{-1/2} \qquad (144)$$

[45] The long-distance behavior of the propagator can be obtained from the effective action $S[\theta] = (\rho_s(T)/2)\int d^2r\,(\boldsymbol{\nabla}\theta)^2$, where the phase variable θ is free of vortex singularities and represents the spinwave degrees of freedom. An elementary calculation of the propagator $G(\mathbf{r} - \mathbf{r}') \sim \langle e^{i\theta(\mathbf{r}) - i\theta(\mathbf{r}')}\rangle$ then yields an anomalous dimension $\eta(T) = 1/2\pi\rho_s(T)$.

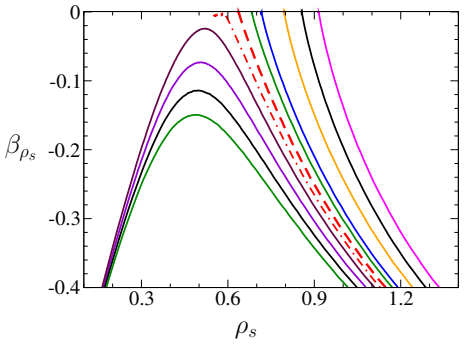

FIG. 18 (Color online) Beta function $\beta_{\rho_s} = -kd\rho_s/dk$ vs ρ_s obtained from the NPRG for various initial conditions (Jakubczyk *et al.*, 2014). The dashed line corresponds to the critical value $r_0 = -0.0015831$ deduced from the $k \to 0$ limit of $\rho_{s,k}$ (Sec. IV.A) while the dot-dashed line corresponds to the critical value $r_0 = -0.001577$ deduced from the essential scaling of the correlation length in the high-temperature phase (Sec. IV.B.3).

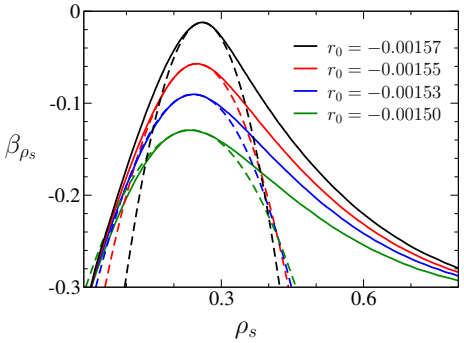

FIG. 19 (Color online) Beta function β_{ρ_s} in the high-temperature phase ($r_0 > r_{0c}$) obtained from the NPRG. The dashed lines correspond to parabolic fits.

and is shown in Fig. 17. The best fit of the form

$$\xi \sim \Lambda^{-1} \exp\left(\frac{c}{(r_0 - r_{0c})^\gamma}\right) \qquad (145)$$

gives $\gamma \simeq 0.48$ and $c \simeq 0.048$. This result is in good agreement with the essential singularity predicted by KT theory (which corresponds to $\gamma = 0.5$). Equation (145) allows us to obtain $r_{0c} \simeq -0.00157746$, to be compared with the previous estimate $r_{0c} \simeq -0.0015831$ (Sec. IV.A). KT theory predicts the product $bc = \pi/2$ to be universal (Chaikin and Lubensky, 1995). The NPRG results give $bc \simeq 0.34$ (see next section for an additional comment).

4. Comparison with standard KT flow

In the standard KT theory, the two variables of interest are the stiffness ρ_s and the vortex fugacity y. In the NPRG approach, we follow an infinite number of variables (through the functions $U_k(\rho)$, $Z_k(\rho)$ and $Y_k(\rho)$) but we do not have access to the vortex fugacity. To make a

comparison with the standard KT flow possible, we consider the beta function $\beta_{\rho_s} = -k d\rho_s/dk$. The KT theory predicts

$$\beta_{\rho_s} = -\pi(\rho_s - \rho_s^*)^2 - \frac{4}{\pi}C \tag{146}$$

in the vicinity of $\rho_s^* = 2/\pi$, where C is a constant which corresponds to different values of the initial vortex fugacity and is expected to vary linearly with $T - T_{\rm KT}$ (i.e. $r_0 - r_{0c}$). The NPRG result is shown in Figs. 18 and 19. We obtain a qualitative agreement with KT theory. In particular, in the high-temperature phase β_{ρ_s} vs ρ_s is given by parabolas whose distance to the axis $\beta_{\rho_s} = 0$ varies linearly with $r_0 - r_{0c}$ in agreement with (146) (Fig. 19). There are however two differences with the predictions of KT theory. First, the maxima of the parabolas are not located at ρ_s^* but are shifted to lower values as r_0 increases. This shift indicates that β_{ρ_s} contains a linear term in addition to the quadratic one. This linear term is however sufficiently small not to affect the essential scaling except maybe for extremely large values of the correlation length (Sec. IV.B.3). Second, the prefactor of the quadratic term varies with r_0 and differs from $-\pi$. For the high-temperature curves shown in Fig. 19, we find that it varies between -10.76 and -3.48 as we go away from $T_{\rm KT}$. The fact that we do not find the expected prefactor $-\pi$ for the quadratic term (in particular close to the KT transition temperature) explains the failure to obtain the correct universal value of the product bc (see preceding section). Very close to the transition point, the beta function β_{ρ_s} looses its parabolic shape and its maximum seems to turn into a singular point. This region however corresponds to a very large renormalization time $|t| = \ln(\Lambda/k)$ and therefore an extremely large correlation length, and we do not expect our results to be fully reliable.

V. THE VERTEX EXPANSION (NW, ND)

The derivative expansion discussed in Sec. III is a powerful method to (approximately) solve the exact flow equation satisfied by the scale-dependent effective action and obtain the critical exponents as well as the thermodynamic properties of the system. However, as already pointed out, the derivative expansion is justified only for small momenta ($|\mathbf{p}|$ smaller than k or the smallest mass in the problem) and therefore does not enable us to obtain the momentum dependence of correlation functions in the limit $k \to 0$.

The vertex expansion provides an alternative method to solve the flow equation. In Sec. II we noticed that the equation $\partial_t \Gamma_k$ implies an infinite hierarchy of equations for the 1PI vertices $\Gamma_k^{(n)}$. If we keep only a finite number of vertices, we then obtain a closed system of equations which can be solved. The accuracy of the vertex expansion strongly depends on the precise implementation of the truncation. For example, a truncation including only $\Gamma_k^{(2)}$ and $\Gamma_k^{(4)}$ at vanishing field $\boldsymbol{\phi} = 0$ would merely reproduce the one-loop perturbative RG approach.[46] The vertex expansion has been used to compute the momentum dependence of the correlation functions (Hasselmann *et al.*, 2007; Kopietz *et al.*, 2010; Ledowski *et al.*, 2004; Sinner *et al.*, 2008).

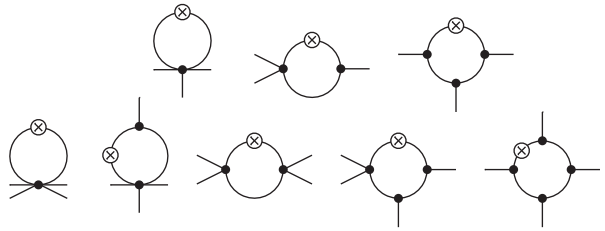

FIG. 20 Diagrammatic representation of the flow equations $\partial_t \Gamma_k^{(3)}$ (top) and $\partial_t \Gamma_k^{(4)}$ (bottom). Diagrams obtained by exchanging external legs are not shown.

In this section we discuss an approximation due to Blaizot, Méndez-Galain and Wschebor (BMW), which takes all vertices into account but preserves the full momentum dependence only for the low-order ones (Benitez *et al.*, 2009, 2012; Blaizot, 2011; Blaizot *et al.*, 2006a).[47,48] To leading order the BMW approximation reproduces the LPA, while the full momentum dependence of $\Gamma_k^{(2)}$ is preserved to next-to-leading order. Although it is not controlled by a small parameter, the accuracy of the BMW approximation can in principle be systematically improved.

A. The Blaizot–Méndez-Galain–Wschebor approximation

The infinite hierarchy of equations satisfied by the vertices follows from the dependence of $\partial_t \Gamma_k^{(n)}$ on $\Gamma_k^{(n+1)}$ and $\Gamma_k^{(n+2)}$. In the Blaizot–Méndez-Galain–Wschebor (BMW) approach, one approximates the flow equations of the vertices by neglecting the dependence of $\Gamma_k^{(s+1)}$ and $\Gamma_k^{(s+2)}$ on the internal (loop) momentum (for a certain s). For a constant field $\boldsymbol{\phi}$, this allows us to relate these vertices to the $\boldsymbol{\phi}$-derivative of $\Gamma_k^{(s)}$ and obtain a closed system of equations for $\Gamma_k^{(s)}(\boldsymbol{\phi})$, $\Gamma_k^{(s-1)}(\boldsymbol{\phi})$, etc.

The RG equation for $\Gamma_k^{(s)}$ has a one-loop structure which is inherited from the one-loop structure of the

[46] This truncation is often used in fermion systems where the Fermi-Dirac statistics and the presence of a Fermi surface makes more involved truncations difficult to implement (Metzner *et al.*, 2012).

[47] A similar approach was developed by Parola and Reatto in the context of liquid state theory (Parola and Reatto, 1984, 1995).

[48] For a related work, see (Hasselmann, 2012).

exact equation satisfied by the scale-dependent effective action. The equations $\partial_t\Gamma_k^{(2)}$, $\partial_t\Gamma_k^{(3)}$ and $\partial_t\Gamma_k^{(4)}$ are represented diagrammatically in Figs. 2 and 20. The two contributions to $\partial_t\Gamma_k^{(s)}(\mathbf{p}_1\cdots\mathbf{p}_s;\boldsymbol{\phi})$ involving $\Gamma_k^{(s+1)}$ and $\Gamma_k^{(s+2)}$ read

$$\sum_{\mathbf{q}} \dot{R}_k(\mathbf{q})G_k(\mathbf{q};\boldsymbol{\phi})^2\Gamma_k^{(s+2)}(\mathbf{p}_1\cdots\mathbf{p}_s,\mathbf{q},-\mathbf{q};\boldsymbol{\phi}) \quad (147)$$

and

$$\sum_{\mathbf{q}} \dot{R}_k(\mathbf{q})G_k(\mathbf{q};\boldsymbol{\phi})^2 G_k(\mathbf{p}_s-\mathbf{q};\boldsymbol{\phi})\Gamma_k^{(3)}(\mathbf{p}_s,-\mathbf{q},-\mathbf{p}_s+\mathbf{q}) \times \Gamma_k^{(s+1)}(\mathbf{p}_1\cdots\mathbf{p}_{s-1},\mathbf{p}_s-\mathbf{q},\mathbf{q};\boldsymbol{\phi}) \quad (148)$$

in a constant field $\boldsymbol{\phi}$ (for clarity we do not write the $O(N)$ index of the field and multiplicative factors). Let us now recall two crucial properties pointed out in Sec. III: i) Because of the $\dot{R}_k(\mathbf{q})$ term, the integral over the loop momentum $\mathbf{q}$ is dominated by $|\mathbf{q}| \lesssim k$. ii) The regulator term ΔS_k in the action ensures that the vertices $\Gamma_k^{(n)}(\mathbf{p}_1\cdots\mathbf{p}_n;\boldsymbol{\phi})$ are smooth functions of momenta and can be expanded in powers of $\mathbf{p}_i^2/k^2$ when $|\mathbf{p}_i| \ll k$, even in the critical case. The BMW approximation consists in setting $\mathbf{q}$ to zero in $\Gamma_k^{(s+1)}$ and $\Gamma_k^{(s+2)}$ while keeping the full dependence on the external momenta $\mathbf{p}_i$,[49] i.e.

$$\Gamma^{(s+1)}_{k,i_1\cdots i_{s+1}}(\mathbf{p}_1\cdots\mathbf{p}_{s-1},\mathbf{p}_s-\mathbf{q},\mathbf{q};\boldsymbol{\phi}) \to \Gamma^{(s+1)}_{k,i_1\cdots i_{s+1}}(\mathbf{p}_1\cdots\mathbf{p}_{s-1},\mathbf{p}_s,0;\boldsymbol{\phi}), \quad (149)$$

and

$$\Gamma^{(s+2)}_{k,i_1\cdots i_{s+2}}(\mathbf{p}_1\cdots\mathbf{p}_s,\mathbf{q},-\mathbf{q};\boldsymbol{\phi}) \to \Gamma^{(s+2)}_{k,i_1\cdots i_{s+2}}(\mathbf{p}_1\cdots\mathbf{p}_s,0,0;\boldsymbol{\phi}). \quad (150)$$

Noting that in a constant field

$$\Gamma^{(s+1)}_{k,\{i_j\}i_{s+1}}(\{\mathbf{p}_j\},0;\boldsymbol{\phi}) = \frac{1}{\sqrt{V}}\frac{\partial\Gamma^{(s)}_{k,\{i_j\}}(\{\mathbf{p}_j\};\boldsymbol{\phi})}{\partial\phi_{i_{s+1}}},$$
$$\Gamma^{(s+2)}_{\{i_j\}i_{s+1}i_{s+2}}(\{\mathbf{p}_j\},0,0;\boldsymbol{\phi}) = \frac{1}{V}\frac{\partial^2\Gamma^{(s)}_{k,\{i_j\}}(\{\mathbf{p}_j\};\boldsymbol{\phi})}{\partial\phi_{i_{s+1}}\partial\phi_{i_{s+2}}}, \quad (151)$$

we obtain an approximate equation for $\Gamma_k^{(s)}$ which involves only the vertices $\Gamma_k^{(s)}\cdots\Gamma_k^{(2)}$ and their derivatives wrt the constant field $\boldsymbol{\phi}$. We can proceed in a similar way to replace the vertex $\Gamma_k^{(s+1)}$ appearing in the flow equation of $\Gamma_k^{(s-1)}$ by a field-derivative of $\Gamma_k^{(s)}$. We thus end up with a closed system of equations for the vertices $\Gamma_k^{(s)}$, $\Gamma_k^{(s-1)}$, etc.

[49] If $s=2$, then one should set $\mathbf{q}=0$ in both $\Gamma_k^{(s+1)}$ and $\Gamma_k^{(3)}$ in Eq. (148).

1. $s=0$: LPA

To leading order, $s=0$, the BMW approximation reproduces the LPA. Let us consider the vertex $\Gamma_k^{(0)}(\boldsymbol{\phi}) = VU_k(\rho)$ in a constant field. Its flow equation is entirely determined by the two-point vertex $\Gamma^{(2)}_{k,ij}(\mathbf{p};\boldsymbol{\phi})$ [Eq. (46)]. The latter can be written as $\Gamma^{(2)}_{k,ij}(\mathbf{p};\boldsymbol{\phi}) = \mathbf{p}^2 + \Sigma_{k,ij}(\mathbf{p};\boldsymbol{\phi})$ with $\Sigma_{k,ij}$ the self-energy (we include r_0 in Σ). The BMW approximation consists in setting $\mathbf{p}$ to zero in the self-energy,

$$\Gamma^{(2)}_{k,ij}(\mathbf{p};\boldsymbol{\phi}) \to \mathbf{p}^2 + \Sigma_{k,ij}(0,\boldsymbol{\phi}) = \mathbf{p}^2 + \frac{\partial^2 U_k(\rho)}{\partial\phi_i\partial\phi_j}, \quad (152)$$

which yields the LPA equation (47) for the effective potential. Note that it would not make any sense to set $\mathbf{p}=0$ in $\Gamma_k^{(2)}(\mathbf{p};\boldsymbol{\phi})$ as this would suppress the momentum dependence of the bare two-point propagator. The LPA provides information on all $\Gamma_k^{(n)}$'s but only at vanishing momenta for $n \geq 3$ [Eq. (44)] while the momentum dependence of $\Gamma_k^{(2)}$ is not renormalized [Eq. (152)]. To obtain a non-trivial momentum dependence of the vertices, we must apply the BMW scheme to higher orders.

2. $s=2$: full momentum dependence of $\Gamma_k^{(2)}(\mathbf{p};\boldsymbol{\phi})$

Let us now consider the 2-point vertex and its flow equation (36). The BMW approximation with $s=2$ yields the closed equation

$$\partial_t\Gamma^{(2)}_{k,ij}(\mathbf{p};\boldsymbol{\phi}) = \frac{1}{2}\int_{\mathbf{q}}[\tilde{\partial}_t G_{k,i_1i_2}(\mathbf{q};\boldsymbol{\phi})]\frac{\partial^2\Gamma^{(2)}_{k,ij}(\mathbf{p};\boldsymbol{\phi})}{\partial\phi_{i_1}\partial\phi_{i_2}} - \int_{\mathbf{q}}[\tilde{\partial}_t G_{k,i_1i_2}(\mathbf{q};\boldsymbol{\phi})]\frac{\partial\Gamma^{(2)}_{k,ii_3}(\mathbf{p};\boldsymbol{\phi})}{\partial\phi_{i_2}} \times G_{k,i_3i_4}(\mathbf{p}+\mathbf{q};\boldsymbol{\phi})\frac{\partial\Gamma^{(2)}_{k,ji_4}(\mathbf{p};\boldsymbol{\phi})}{\partial\phi_{i_1}}. \quad (153)$$

In the approximation $s=2$ the n-point vertices depend on a single momentum and are obtained as derivatives of the two-point vertex,

$$\Gamma^{(n)}_{k,i_1\cdots i_n}(\mathbf{p},-\mathbf{p},0\cdots0;\boldsymbol{\phi}) = \partial_{\phi_{i_3}}\cdots\partial_{\phi_{i_n}}\Gamma_k^{(2)}(\mathbf{p};\boldsymbol{\phi}), \quad (154)$$

which may be viewed as an improvement of (44).

It is convenient to introduce the notation

$$\Gamma^{(2)}_{k,ij}(\mathbf{p};\boldsymbol{\phi}) = \Gamma_{A,k}(\mathbf{p};\rho)\delta_{i,j} + \phi_i\phi_j\Gamma_{B,k}(\mathbf{p};\rho), \quad (155)$$

where $\Gamma_{A,k}$ and $\Gamma_{B,k}$ are functions of the O(N) invariant ρ, and rewrite the longitudinal and transverse propagators as

$$G_{k,\mathrm{L}}(\mathbf{p};\rho) = [\Gamma_{A,k}(\mathbf{p};\rho) + 2\rho\Gamma_{B,k}(\mathbf{p};\rho) + R_k(\mathbf{p})]^{-1},$$
$$G_{k,\mathrm{T}}(\mathbf{p};\rho) = [\Gamma_{A,k}(\mathbf{p};\rho) + R_k(\mathbf{p})]^{-1}. \quad (156)$$

Equation (153) then yields,[50]

$$\partial_t \Gamma_{A,k} = -\frac{1}{2} I^{(2)}_{k,\mathrm{LL}} (\Gamma'_{A,k} + 2\rho \Gamma''_{A,k}) - \frac{1}{2} I^{(2)}_{k,\mathrm{TT}} [(N-1)\Gamma'_{A,k} + 2\Gamma_{B,k}] + 2\rho (J^{(3)}_{k,\mathrm{LT}} {\Gamma'_{A,k}}^2 + J^{(3)}_{k,\mathrm{TL}} {\Gamma_{B,k}}^2), \quad (157)$$

and

$$\partial_t \Gamma_{B,k} = \frac{1}{2\rho} (I^{(2)}_{k,\mathrm{TT}} - I^{(2)}_{k,\mathrm{LL}}) \Gamma_{B,k} - I^{(2)}_{k,\mathrm{LL}} \left(\frac{5}{2} \Gamma'_{B,k} + \rho \Gamma''_{B,k} \right) - \frac{1}{2} I^{(2)}_{k,\mathrm{TT}} (N-1) \Gamma'_{B,k} + J^{(3)}_{k,\mathrm{LL}} (\Gamma'_{A,k} + 2\Gamma_{B,k} + 2\rho \Gamma'_{B,k})^2 - J^{(3)}_{k,\mathrm{LT}} {\Gamma'_{A,k}}^2 - [J^{(3)}_{k,\mathrm{TL}} - (N-1) J^{(3)}_{k,\mathrm{TT}}] \Gamma^2_{B,k}, \quad (158)$$

where

$$\Gamma'_{A,k} = \frac{\partial}{\partial \rho} \Gamma_{A,k}, \quad \Gamma''_{A,k} = \frac{\partial^2}{\partial \rho^2} \Gamma_{A,k}, \quad \Gamma'_{B,k} = \frac{\partial}{\partial \rho} \Gamma_{B,k}, \quad (159)$$

and

$$J^{(n)}_{k,\alpha\beta}(\mathbf{p};\rho) = \int_{\mathbf{q}} \dot{R}_k(\mathbf{q}) G^{n-1}_{k,\alpha}(\mathbf{q};\rho) G_{k,\beta}(\mathbf{p}+\mathbf{q};\rho), \quad I^{(n)}_{k,\alpha\beta}(\rho) = J^{(n)}_{k,\alpha\beta}(\mathbf{p}=0;\rho), \quad (160)$$

with $\alpha, \beta = \mathrm{L}, \mathrm{T}$ (see Appendix F). For compactness, we have not written explicitly the $\mathbf{p}$ and ρ dependence in (157) and (158).

At this point, an important subtlety appears. The flow equation of the effective potential can be obtained either from (46) or from $\partial_t \Gamma_{A,k}(\mathbf{p};\rho)$ and $\partial_t \Gamma_{B,k}(\mathbf{p};\rho)$ using $\Gamma_{A,k}(\mathbf{p}=0;\rho) = U'_k(\rho)$ and $\Gamma_{B,k}(\mathbf{p}=0;\rho) = U''_k(\rho)$. Since Eq. (46) is exact while the flow equations (157) and (158) of the two-point vertex are not,[51] there is no guarantee that $\partial_t U_k(\rho)$ is consistent with $\partial_t \Gamma_{A,k}(\mathbf{p}=0;\rho)$ and $\partial_t \Gamma_{B,k}(\mathbf{p}=0;\rho)$. To circumvent this difficulty, one writes

$$\Gamma_{A,k}(\mathbf{p};\rho) = \mathbf{p}^2 + \Delta_{A,k}(\mathbf{p};\rho) + U'_k(\rho), \quad \Gamma_{B,k}(\mathbf{p};\rho) = \Delta_{B,k}(\mathbf{p};\rho) + U''_k(\rho), \quad (161)$$

where it is understood that the effective potential $U_k(\rho)$ is obtained from its exact flow equation (46). The "self-energies" $\Delta_{A,k}(\mathbf{p};\rho)$ and $\Delta_{B,k}(\mathbf{p};\rho)$ satisfy

$$\Delta_{A,k}(\mathbf{p}=0;\rho) = \Delta_{B,k}(\mathbf{p}=0;\rho) = 0. \quad (162)$$

By performing the BMW approximation on the equations

$$\partial_t \Delta_{A,k}(\mathbf{p};\rho) = \partial_t [\Gamma_{A,k}(\mathbf{p};\rho) - \Gamma_{A,k}(0;\rho)], \quad \partial_t \Delta_{B,k}(\mathbf{p};\rho) = \partial_t [\Gamma_{B,k}(\mathbf{p};\rho) - \Gamma_{B,k}(0;\rho)], \quad (163)$$

one ensures that the flow equation of the two-point vertex is consistent with that of the effective potential. The flow equations of the self-energies are given in Appendix F.

To accurately capture the fixed-point structure when the system is critical, we must introduce dimensionless variables and a field renormalization factor Z_k. In the derivative expansion (Sec. III), the latter describes the overall variation with k of the function $Z_k(\rho)$ [Eq. (40)]. Here we define Z_k by

$$Z_k = \frac{\partial}{\partial \mathbf{p}^2} \Gamma^{(2)}_{k,\mathrm{T}}(\mathbf{p};\rho)\Big|_{\mathbf{p}=\rho=0} \quad (164)$$

together with the running anomalous dimension $\eta_k = -\partial_t \ln Z_k$. In Eq. (164) we consider the renormalization point $\mathbf{p} = \rho = 0$ but a more general choice is possible as discussed in Appendix F (Benitez *et al.*, 2012). We can now define dimensionless variables,

$$\tilde{p} = \frac{|\mathbf{p}|}{k}, \quad \tilde{\rho} = Z_k k^{-d+2} \rho, \quad \tilde{U}_k(\tilde{\rho}) = k^{-d} U_k(\rho), \quad (165)$$

and dimensionless self-energies,

$$\tilde{\Delta}_{A,k}(\tilde{p};\tilde{\rho}) + \tilde{p}^2 = (Z_k k^2)^{-1} [\Delta_{A,k}(\mathbf{p};\rho) + \mathbf{p}^2], \quad \tilde{\Delta}_{B,k}(\tilde{p};\tilde{\rho}) = Z_k^{-2} k^{d-4} \Delta_{B,k}(\mathbf{p};\rho). \quad (166)$$

Here we take advantage of the isotropy of the system to write the self-energies $\tilde{\Delta}_{A,k}$ and $\tilde{\Delta}_{B,k}$ as functions of $\tilde{p}$. The corresponding flow equations are given in Appendix F. Together with (164) they imply

$$\eta_k = \frac{1}{2} \tilde{I}^{(2)}_{k,\mathrm{TT}}(\tilde{\rho}=0) \Big[N \frac{\partial}{\partial \tilde{p}^2} \tilde{\Delta}'_{A,k}(\tilde{p};\tilde{\rho}) + 2 \frac{\partial}{\partial \tilde{p}^2} \tilde{\Delta}_{B,k}(\tilde{p};\tilde{\rho}) \Big]_{\tilde{p}=\tilde{\rho}=0}, \quad (167)$$

where the dimensionless threshold function $\tilde{I}^{(2)}_{k,\mathrm{TT}}(\tilde{\rho})$ is defined in Appendix F.

The equations for the self-energies need to be completed by the flow equation of the dimensionless effective potential $\tilde{U}_k(\tilde{\rho})$ or, rather, its derivative $\tilde{W}_k(\tilde{\rho}) = \tilde{U}'_k(\tilde{\rho})$,

$$\partial_t \tilde{W}_k(\tilde{\rho}) = (\eta_k - 2)\tilde{W}_k(\tilde{\rho}) + (d - 2 + \eta_k)\tilde{\rho} \tilde{W}'_k(\tilde{\rho}) + \frac{1}{2} [\tilde{I}^{(1)}_{k,\mathrm{LL}}{}'(\tilde{\rho}) + (N-1) \tilde{I}^{(1)}_{k,\mathrm{TT}}{}'(\tilde{\rho})], \quad (168)$$

where $\tilde{I}^{(2)}_{k,\alpha\beta}{}'$ denotes a $\tilde{\rho}$ derivative.

The numerical resolution is performed on a fixed regular $(\tilde{p}, \tilde{\rho})$ grid with $0 \le \tilde{p} \le \tilde{p}_{\max}$ and $0 \le \tilde{\rho} \le \tilde{\rho}_{\max}$. With the exponential regulator (13), the contribution of the momentum interval $\tilde{q} \in [4, \infty[$ to the integrals $\tilde{I}_{k,\alpha}$ and $\tilde{J}^{(3)}_{k,\alpha\beta}$ is extremely small and can be neglected by restricting the integration domain to $[0, \tilde{p}_{\max}]$. When computing the double integral $\tilde{J}^{(3)}_{\alpha\beta}(\tilde{p}, \tilde{\rho})$, we need to evaluate $\tilde{\Delta}_A$ and $\tilde{\Delta}_B$ for momenta $\tilde{p} + \tilde{q}$ beyond $\tilde{p}_{\max}$. In such cases we set $\tilde{\Delta}_{A,B}(\tilde{p} > \tilde{p}_{\max}) = \tilde{\Delta}_{A,B}(\tilde{p}_{\max})$, an excellent

[50] Note that by using $G^2_{\mathrm{L}} - G^2_{\mathrm{T}} = 2\rho \Gamma_B (G_{\mathrm{L}} + G_{\mathrm{T}}) G_{\mathrm{L}} G_{\mathrm{T}}$, we can write $\frac{1}{2\rho}(I^{(2)}_{\mathrm{TT}} - I^{(2)}_{\mathrm{LL}})$ in (158) in a manifestly regular form at $\rho = 0$.

[51] Equation (46) is exact but the propagators in the rhs are approximated. Equations (157) and (158) as well as the vertices and propagators in their rhs are approximated.

TABLE III Critical exponent ν in the O(N) model obtained from the derivative expansion (DE) (Sec. III) and the BMW approximation (Sec. V) for $d = 3$. Also shown are the results obtained from field theory (FT) and Monte Carlo (MC) simulations.

N	DE $\mathcal{O}(\partial^2)$	DE $\mathcal{O}(\partial^4)$	DE $\mathcal{O}(\partial^6)$	BMW	FT	MC
1				0.632	0.6306(5) [a]	0.63002(10) [b]
2				0.674	0.6700(6) [a]	0.6717(1) [c]
3				0.715	0.7060(7) [a]	0.7112(5) [d]
4				0.754	0.741(6) [e]	0.749(2) [f]
10				0.889	0.859 [g]	–
100				0.990	0.989 [h]	–

[a](Pogorelov and Suslov, 2008), [b](Hasenbusch, 2010) , [c](Campostrini *et al.*, 2006), [d](Campostrini *et al.*, 2002), [e](Guida and Zinn-Justin, 1998), [f](Hasenbusch, 2001), [e](Antonenko and Sokolov, 1995)

TABLE IV Same as Table III but for the correction-to-scaling exponent ω.

N	DE $\mathcal{O}(\partial^2)$	DE $\mathcal{O}(\partial^4)$	DE $\mathcal{O}(\partial^6)$	BMW	FT	MC
1				0.78	0.788(3) [a]	0.832(6) [b]
2				0.75	0.780(10) [a]	0.785(20) [c]
3				0.73	0.780(20) [a]	0.773 [d]
4				0.72	0.774(20) [e]	0.765 [f]
10				0.80	–	–
100				1.00	–	–

TABLE V Same as Table III but for the anomalous dimension η.

N	DE $\mathcal{O}(\partial^2)$	DE $\mathcal{O}(\partial^4)$	DE $\mathcal{O}(\partial^6)$	BMW	FT	MC
1				0.039	0.0318(3) [a]	0.03627(10) [b]
2				0.041	0.0334(2) [a]	0.0381(2) [c]
3				0.040	0.0333(3) [a]	0.0375(5) [d]
4				0.038	0.0350(45) [e]	0.0365(10) [f]
10				0.022	0.024 [g]	–
100				0.0023	0.0027 [h]	–

approximation for $\tilde{p}_{\max} \geq 5$. To access the full momentum dependence, we also calculate $\Gamma_k^{(2)}(p;\tilde{\rho})$ at a set of fixed freely chosen external $p = |\mathbf{p}|$ values. For a given p, p/k is within the grid at the beginning of the flow. This is no longer so when $k < p/\tilde{p}_{\max}$; we then switch to the dimensionful flow equations (157) and (158), and set $J^{(3)}_{k,\alpha\beta}(\mathbf{p},\rho) = I^{(2)}_{k,\alpha\alpha}(\rho)G_{k,\beta}(\mathbf{p})$, an excellent approximation when $p > k\tilde{p}_{\max}$.

Even though the order $s = 2$ can be solved with a modest numerical cost, higher-order approximations turn out to be much more difficult to implement. For instance the $s = 4$ approximation requires to numerically solve the flow equation of the 4-point vertex $\Gamma_k^{(4)}(\mathbf{p}_1,\mathbf{p}_2,\mathbf{p}_3,\mathbf{p}_4;\boldsymbol{\phi})$ (which has 3 independent momentum variables), a very difficult task in practice.

B. Critical behavior

1. Critical exponents

(Ajuster cette section en fonction de la discussion dans Sec. III) Although the main goal of the BMW approximation is to obtain the full momentum dependence of low-order vertices, it can also be used to compute critical exponents and other zero-momentum quantities.

The method to study the system near criticality is similar to that used in the derivative expansion (Sec. III). We fine tune r_0 using a dichotomy procedure to reach the vicinity of the critical point $r_0 = r_{0c}$. From the behavior of the flow near criticality we then extract the correlation-length and correction-to-scaling exponents ν and ω. The anomalous dimension is directly estimated from the plateau observed in η_k.

The critical exponents exhibit a small dependence of the regular function $R_k(\mathbf{q})$ (i.e. the parameter α when

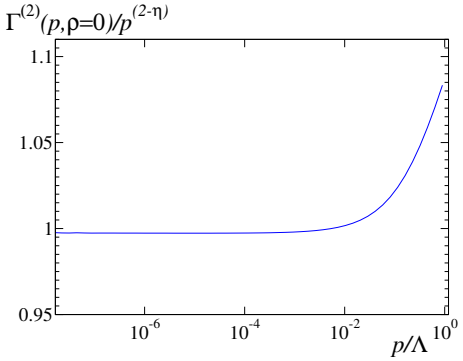

FIG. 21 (Color online) Ratio of the two-point vertex $\Gamma^{(2)}_{k=0}(\mathbf{p}, \phi = 0)$ and $|\mathbf{p}|^{2-\eta}$ at criticality for $d = 3$ and $N = 2$ ($\alpha = 2$ and $\tilde{p}_0 = \tilde{\rho}_0 = 0$). The ratio is normalized to be of order of unity at small $|p|$. The bare (initial) dimensionless coupling is $\tilde{u}_0 = 6.10^{-2}/N$.

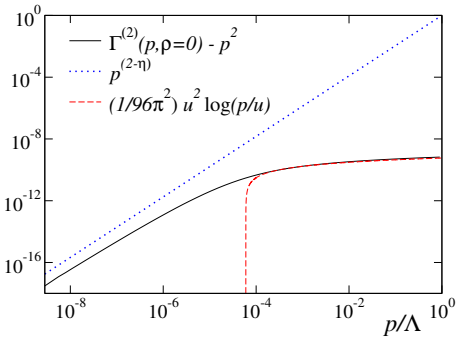

FIG. 22 (Color online) Two-point vertex $\Gamma^{(2)}_{k=0}(\mathbf{p}, \phi = 0)$ at criticality for $d = 3$ and $N = 2$ ($\alpha = 2$ and $\tilde{p}_0 = \tilde{\rho}_0 = 0$). The infrared behavior $|\mathbf{p}|^{2-\eta}$ with $\eta \simeq 0.041$ is also shown (the blue dotted line) as well as the ultraviolet behavior expected from the two-loop result (red dashed line).

the exponential regulator (13) is used) and the (*a priori* arbitrary) renormalization point $(\tilde{p}_0, \tilde{\rho}_0)$ where Z_k is computed [Eq. (F10)]. This dependence, which would not be present if the flow equation were solved exactly, can be used to optimize the choice of the parameters $\alpha, \tilde{p}_0, \tilde{\rho}_0$. One expects that the best estimates of the critical exponents are obtained when they show, locally, the weakest dependence on the parameters (principle of minimum sensitivity). The dependence on $\tilde{p}_0$ and $\tilde{\rho}_0$ turns out to be much weaker than that on α so that only the latter needs to be considered. As a function of α, critical exponents exhibit a single extremum located near $\alpha = 2$, which moreover points towards the best numerical estimates available in the literature. Following the principle of minimum sensitivity, we regard these extremum values, begin locally independent of α, as the best estimates of the critical exponents. The results for the O(N) model are summarized in Tables III-V and compared to those of the derivative expansion, resummed perturbation theory (referred to as field theory) and Monte Carlo simulations.

2. The 2-point vertex at and near criticality

We now study the momentum dependence of the 2-point vertex at criticality. In the infrared domain $|\mathbf{p}| \ll p_G$ (with $p_G \sim u_0^{1/(4-d)}$ the Ginzburg momentum scale), $\Gamma^{(2)}_{k=0}(\mathbf{p}, \phi = 0) \sim p_G^{\eta} |\mathbf{p}|^{2-\eta}$ (Fig. 21). The anomalous dimension η is in very good agreement with the result obtained from $-\lim_{k\to 0} \partial_t \ln Z_k$. (En dire plus ici: quelle sont les valeurs pour un cas particulier?) Thus the BMW approximation validates the determination of η used in the LPA' and the derivative expansion.

When $p_G \ll \Lambda$ (which requires u_0 to be small enough), one can clearly identify a perturbative regime $p_G \ll |\mathbf{p}| \ll \Lambda$ where the leading contribution to the 2-point vertex is given by the 2-loop self-energy correction (Fig. 22),

$$\Gamma^{(2)}_{k=0}(\mathbf{p}, 0) = \mathbf{p}^2 - \frac{N+2}{288\pi^2} u_0^2 \ln\left(\frac{|\mathbf{p}|}{u_0}\right). \qquad (169)$$

The BMW approximation reproduces (169) with a prefactor which is typically of order 0.9 (depending on the value of α).[52]

The intermediate momentum region between the infrared and the ultraviolet domains is also of interest. The quantity

$$c = -\frac{256}{u_0 N} \zeta(3/2)^{-4/3} \int d^3p \left[\frac{1}{\Gamma^{(2)}_{k=0}(\mathbf{p}, 0)} - \frac{1}{\mathbf{p}^2}\right] \qquad (170)$$

is very sensitive to the crossover region, since the integrand in (170) is peaked at $|\mathbf{p}| \sim p_G$ (Blaizot *et al.*, 2005), and has been used as a benchmark for nonperturbative approximations in the O(N) model. In the O(2) case and for $d = 3$, it determines the shift of the critical temperature due to interactions in the weakly interacting Bose gas (Sec. XIII). Table VI shows the value of c

TABLE VI Results for the quantity c defined by Eq. (170).

N	BMW	lattice	7 loops [a]
1	1.15	1.09(9) [b]	1.07(10)
2	1.37	1.32(2) [c]	1.27(10)
		1.29(5) [d]	
3	1.50		1.43(11)
4	1.63	1.60(10) [b]	1.54(11)
10	2.02		
100	2.36		

[a] (Kastening, 2004), [b] (Sun, 2003), [c] (Arnold and Moore, 2001), [d] (Kashurnikov *et al.*, 2001)

[52] Commenter "improved BMW" et (Parola and Reatto, 1984)???

for $d = 3$ and various values of N. The results obtained from the BMW approximation compare very well to those of lattice and/or seven-loop resummed calculations. In the large-N limit, where $c = 2.3$ ($c = 2.33$??? but $c = \mathcal{O}(1/N)$???) can be calculated analytically (Baym *et al.*, 2000), the BMW result differs from the exact value by less than 3%. Note that the large-N value of c is in fact of order $1/N$ and is not obtained exactly to the order $s = 2$ of the BMW approximation (Sec. VI).

The BMW scheme is not restricted to the critical point and can also be used to obtain the propagator in the critical domain where the correlation length is large but finite. For $N = 1$ and $|\mathbf{p}| \ll p_G$, one expects the scaling behavior

$$G(\mathbf{p}) = T\chi g_{\pm}(|\mathbf{p}|\xi), \tag{171}$$

where $\chi = G(\mathbf{p} = 0)/T$ is the uniform susceptibility and $g_{\pm}$ a universal scaling function ($\pm$ refers to the high- and low-temperature phases, respectively). The limiting forms of $g_{\pm}(x)$ for $x \to 0$ and $x \to \infty$ are well known but a complete determination of the function $g_{\pm}(x)$ is a very difficult problem. We refer to (Benitez *et al.*, 2012) for a detailed discussion of the BMW calculation. We shall see other examples where the BMW approximation is useful for computing universal scaling functions (Secs. XII and XIII). (Faut-il en dire plus sur le calcul de $g_{\pm}$?)

C. Simplified BMW schemes

Although the BMW equations can be solved with modest numerical effort in the O(N) model (in the simplest approximation, $s = 2$, going beyond the LPA), in more complicated cases the numerical solution may be out of reach. It is however possible to simplify the full equations and their numerical solution. For instance, one can supplement the BMW approximation with a truncation in field of the effective potential and the two-point vertex (Guerra *et al.*, 2007). While low-order truncations are not accurate (at least to compute the critical exponents), the procedure seems to converge rapidly with the order of the truncation in $d = 3$. Another possibility is to use approximate propagators to compute the threshold functions $\tilde{I}^{(2)}_{k,\alpha\beta}$ and $\tilde{J}^{(3)}_{k,\alpha\beta}$ (Benitez *et al.*, 2008; Blaizot *et al.*, 2007b). In the following, we shall see several examples where a simplified BMW scheme is used: KPZ equation (Sec. XI), interacting bosons (Sec. XIII), etc.

VI. THE O(N) MODEL IN THE LARGE-N LIMIT (NW)

A. Derivative expansion

B. BMW approximation

VII. LATTICE NPRG

In the preceding sections, we have discussed a NPRG approach for models defined in the continuum, where the short-distance physics is taken into account only *via* the introduction of a UV momentum cutoff Λ. This is sufficient to compute universal quantities such as critical exponents or scaling functions. The NPRG flow equation can also relate nonuniversal critical quantities (e.g. nonuniversal amplitudes of correlation functions) to microscopic details of a particular model if one is able to compute the effective action Γ_Λ at scale Λ starting from a microscopic description. Since Γ_Λ does not involve large length scales, in principle it can be computed by various methods such as perturbation theory. This type of approach has been followed to obtain the equation of state of carbon dioxide (Seide and Wetterich, 1999). In many cases however, it is desirable to implement the NPRG approach directly on the microscopic model. In lattice models for instance, the phase diagram depends on the lattice type, the range and strength of interactions as well as other details of the Hamiltonian. Deriving the effective action Γ_Λ of the system at a mesoscopic scale Λ (much smaller than the inverse lattice spacing) where a continuum model becomes reliable is in general a very difficult task.

The NPRG approach described in the preceding sections can be straightforwardly extended to lattice models (Dupuis and Sengupta, 2008). One still starts from the mean-field solution of the model but takes into account the discreteness of the lattice. In practice, this essentially amounts to replacing the $\mathbf{p}^2$ dispersion of the bare propagator by the actual lattice dispersion $\epsilon_0(\mathbf{p})$ and restricting the momentum to the first Brillouin zone. In some cases, however, the mean-field solution (used as the initial condition of the NPRG flow) is too far away from the actual state of the system to provide a reliable initial condition for the RG procedure.[53] In this section we discuss an alternative NPRG scheme for lattice models where the initial condition of the RG flow corresponds to the (local) limit of decoupled sites (Machado and Dupuis, 2010). The flow equation thus implements an expansion about the single-site limit and is reminiscent, to some extent, of Kadanoff's idea of block spins (Kadanoff, 1966) although the way intersite interactions are progressively

[53] This is the case in the Bose-Hubbard model where the superfluid–Mott-insulator transition is very difficult to study starting from the mean-field (Bogoliubov) theory (see Sec. XIII).

introduced when lowering the momentum scale k makes it significantly different from a real space RG. The lattice NPRG captures both local and critical fluctuations and therefore enables us to compute not only universal quantities (critical exponents) but also non-universal quantities such as transition temperatures and the amplitude of the order parameter. We consider both a lattice field theory (Sec. VII.A) and classical spin models (Sec. VII.B).

The possibility to start from an initial condition that already includes short-range fluctuations has been recognized before, and was used by Parola and Reatto in the Hierarchical Reference Theory of fluids (Parola and Reatto, 1995), an approach which bears many similarities with the lattice NPRG (see the discussion in Sec. VII.C). More recently, similar ideas have appeared in the RG approach to interacting fermions (Kinza and Honerkamp, 2013; Kinza *et al.*, 2013; Reuther and Thomale, 2014; Wentzell *et al.*, 2015).

A. Lattice field theory

Let us consider a lattice field theory defined on a d-dimensional hypercubic lattice,

$$S[\varphi] = \frac{1}{2}\sum_{\mathbf{q}} \varphi_{-\mathbf{q}}\epsilon_0(\mathbf{q})\varphi_{\mathbf{q}} + \sum_{\mathbf{r}} U_0(\varphi_{\mathbf{r}}), \tag{172}$$

where $\{\mathbf{r}\}$ denotes the N sites of the lattice. For simplicity, we consider a one-component real field $\varphi_{\mathbf{r}}$. The momentum $\mathbf{q}$ is restricted to the first Brillouin zone $]-\pi,\pi]^d$ of the reciprocal lattice. The potential U_0 is defined such that $\epsilon_0(\mathbf{q}=0) = 0$ but is otherwise arbitrary. $\epsilon_0(\mathbf{q}) \simeq \epsilon_0\mathbf{q}^2$ for $\mathbf{q}\to 0$ and $\max_{\mathbf{q}}\epsilon_0(\mathbf{q}) = \epsilon_0^{\max}$. The lattice spacing is taken as the unit length.

To implement the RG procedure, we follow the general recipe (Sec. II) and add to the action (172) the regulator term

$$\Delta S_k[\varphi] = \frac{1}{2}\sum_{\mathbf{q}} \varphi_{-\mathbf{q}} R_k(\mathbf{q})\varphi_{\mathbf{q}} \tag{173}$$

with the regulator function

$$R_k(\mathbf{q}) = \big(\epsilon_k - \epsilon_0(\mathbf{q})\big)\theta\big(\epsilon_k - \epsilon_0(\mathbf{q})\big). \tag{174}$$

$R_k(\mathbf{q})$ leaves the high-momentum modes ($\epsilon_0(\mathbf{q}) > \epsilon_k$) unaffected and gives a mass ϵ_k to the low-energy ones; their effective (bare) "dispersion" satisfies $\epsilon_0(\mathbf{q}) + R_k(\mathbf{q}) = \epsilon_k$. $R_k(\mathbf{q})$ is similar to the theta regulator (14) introduced in Sec. II for continuum models, but is parametrized by an energy scale ϵ_k rather than a momentum scale. In practice, it is convenient to write $\epsilon_k = \epsilon_0 k^2$ in terms of a momentum scale k.

In the presence of an external field, the partition function reads

$$\mathcal{Z}_k[h] = \int \mathcal{D}[\varphi]\, e^{-S[\varphi]-\Delta S_k[\varphi]+\sum_{\mathbf{r}} h_{\mathbf{r}}\varphi_{\mathbf{r}}} \tag{175}$$

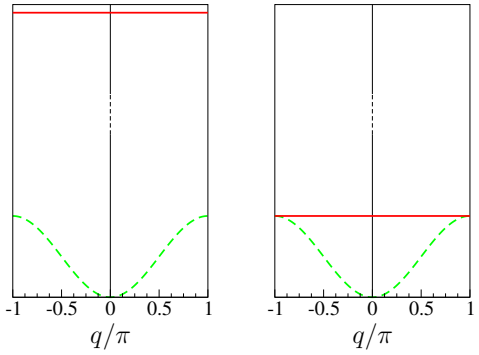

FIG. 23 (Color online) Initial effective dispersion $\epsilon_0(q) + R_k(q)$ in the standard (left panel) and lattice (right panel) NPRG schemes ($d = 1$ and $\epsilon_0(q) = 2\epsilon_0(1-\cos q)$). The green dashed line shows the bare dispersion $\epsilon_0(q)$.

and the order parameter is given by

$$\phi_{\mathbf{r}} = \langle\varphi_{\mathbf{r}}\rangle = \frac{\partial \ln \mathcal{Z}_k[h]}{\partial h_{\mathbf{r}}}. \tag{176}$$

The scale-dependent effective action

$$\Gamma_k[\phi] = -\ln \mathcal{Z}_k[h] + \sum_{\mathbf{r}} h_{\mathbf{r}}\phi_{\mathbf{r}} - \Delta S_k[\phi], \tag{177}$$

satisfies the exact flow equation

$$\partial_t\Gamma_k[\phi] = \frac{1}{2}\sum_{\mathbf{q}} \dot{R}_k(\mathbf{q})\big(\Gamma_k^{(2)}[\phi] + R_k\big)^{-1}_{\mathbf{q},-\mathbf{q}} \tag{178}$$

as the energy scale $\epsilon_k = \epsilon_0 k^2$ is varied. The sum over $\mathbf{q}$ in (178) is restricted to the first Brillouin zone. Since $R_{k=0}(\mathbf{q}) = 0$, $\Gamma_{k=0}[\phi]$ coincides with the effective action of the original model (172).

1. Standard NPRG scheme

The fact that the momentum $\mathbf{q}$ is restricted to the first Brillouin zone $]-\pi,\pi]^d$ and the dispersion $\epsilon_0(\mathbf{q})$ arbitrary does not prevent us to follow the NPRG procedure described in Sec. II (Dupuis and Sengupta, 2008). If the initial value Λ of the momentum scale k is chosen such that ϵ_Λ is much larger than all characteristic energy scales in the problem (in particular $\epsilon_0^{\max}$), all fluctuations are then frozen and the mean-field theory becomes exact: $\Gamma_\Lambda[\phi] = S[\phi]$ (see Fig. 23). The first part of the RG procedure, when ϵ_k varies between ϵ_Λ and $\epsilon_{k_{\rm in}} = \epsilon_0^{\max}$ is purely local, since the effective (bare) dispersion $\epsilon_0(\mathbf{q}) + R_k(\mathbf{q}) = \epsilon_k$ remains dispersionless for all modes. Only for $k < k_{\rm in}$ does the intersite coupling start to play a role. When $k \ll 1$, i.e. when $1/k$ is much larger than the lattice spacing, the lattice does not matter any more. This result is a direct consequence of the structure of the flow equation; the $\dot{R}_k$ term in (178) implies that only modes with $|\mathbf{q}| \lesssim k$ contributes to $\partial_t\Gamma_k$. When

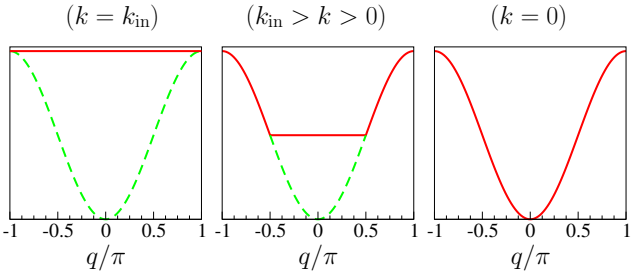

FIG. 24 (Color online) Effective (bare) dispersion $\epsilon_0(q) + R_k(q)$ for $k = k_{\rm in}$, $k_{\rm in} > k > 0$ and $k = 0$ with the regulator function (174) ($d = 1$ and $\epsilon_0(q) = 2\epsilon_0(1 - \cos q)$). The green dashed line shows the bare dispersion $\epsilon_0(q)$.

$k \ll 1$, one can therefore approximate $\epsilon_0(\mathbf{q}) \simeq \epsilon_0 \mathbf{q}^2$, and one recovers the flow equation of the continuum model obtained from (172) and (173) by replacing $\epsilon_0(\mathbf{q})$ by $\epsilon_0 \mathbf{q}^2$.

2. Lattice NPRG scheme

In the lattice NPRG (Machado and Dupuis, 2010), we start the RG procedure from $k = k_{\rm in}$, i.e. we bypass the initial stage of the flow $k_{\rm in} \leq k \leq \Lambda$ where the fluctuations are purely local (Fig. 23). The scale-dependent effective action $\Gamma_{k_{\rm in}}[\phi]$ is no longer given by the microscopic action $S[\phi]$ (since the mean-field solution is not exact for the action $S + \Delta S_{k_{\rm in}}$) but its computation reduces to a single-site problem which can be easily solved numerically (and even analytically in some models). In principle, the NPRG scheme can be defined with any regulator function provided that the latter satisfies the initial condition

$$R_{k_{\rm in}}(\mathbf{q}) = -\epsilon_0(\mathbf{q}) + C \tag{179}$$

ensuring that the sites are decoupled (the limit $C \to \infty$ corresponding to the standard scheme). The choice $C = \epsilon_{k_{\rm in}} = \epsilon_0^{\rm max}$ (rather than $C = 0$) made in (174) is however very natural, since it allows us to set up the RG procedure for $k < k_{\rm in}$ in the usual way, i.e. by modifying the (bare) dispersion of the low-energy modes $\epsilon_0(\mathbf{q}) < \epsilon_k$ without affecting the high-energy modes (Fig. 24). Note that for $k_{\rm in} > k > 0$, the effective coupling in real space (defined as the Fourier transform of $\epsilon_0(\mathbf{q}) + R_k(\mathbf{q})$) is long-range and oscillating. The oscillating part comes from the behavior of $R_k(\mathbf{q})$ for $\epsilon_0(\mathbf{q}) \sim \epsilon_k$.

The standard and lattice NPRG schemes thus differ only in the initial condition. Both schemes are equivalent for $k \leq k_{\rm in}$ when the flow equation (178) is solved exactly for $k > k_{\rm in}$ in the standard scheme. As shown below, this is the case for classical models even within simple approximations. In practice however, one often relies on an approximate solution of the flow equation. The NPRG lattice scheme is preferable whenever the (approximate) flow equation gives a poor description of $\Gamma_{k_{\rm in}}[\phi]$ starting from the mean-field result $\Gamma_\Lambda[\phi] = S[\phi]$. This is expected in quantum models (such as the (Bose-)Hubbard model) where on-site (quantum) fluctuations make the local limit non-trivial (Sec. XIII).

3. The Ising model in the LPA

As an application of the lattice NPRG, we consider the Ising model defined on a d-dimensional hypercubic lattice. We start from the action

$$S = -J\beta \sum_{\langle \mathbf{r},\mathbf{r}'\rangle} S_{\mathbf{r}} S_{\mathbf{r}'} \qquad (S_{\mathbf{r}} = \pm 1) \tag{180}$$

where $\langle \mathbf{r}, \mathbf{r}'\rangle$ denotes nearest-neighbor sites and $\beta = 1/T$. To apply the NPRG approach, one must first derive a field theory. To this end, one considers the action

$$S_\mu = -J\beta \sum_{\langle \mathbf{r},\mathbf{r}'\rangle} S_{\mathbf{r}} S_{\mathbf{r}'} - \mu\beta \sum_{\mathbf{r}} S_{\mathbf{r}}^2 \equiv -\frac{1}{2} \sum_{\mathbf{r},\mathbf{r}'} S_{\mathbf{r}} A^{(\mu)}_{\mathbf{r},\mathbf{r}'} S_{\mathbf{r}'}, \tag{181}$$

which differs from that of the Ising model only by the additive constant $-\mu\beta N$. The matrix $A^{(\mu)}$ is diagonal in Fourier space with eigenvalues

$$\lambda_\mu(\mathbf{q}) = 2\beta \Big(J \sum_{\nu=1}^{d} \cos q_\nu + \mu \Big). \tag{182}$$

For $\mu > Jd$ the matrix $A^{(\mu)}$ is positive ($\lambda_\mu(\mathbf{q}) > 0 \ \ \forall \mathbf{q}$) and can be inverted. We can then rewrite the partition function of the Ising model using a Hubbard-Stratonovich transformation,

$$\begin{aligned} Z_\mu &\propto \sum_{\{S_{\mathbf{r}}\}} \int_{-\infty}^{\infty} \prod_{\mathbf{r}} d\varphi_{\mathbf{r}}\, e^{-\frac{1}{2}\sum_{\mathbf{r},\mathbf{r}'} \varphi_{\mathbf{r}} A^{(\mu)-1}_{\mathbf{r},\mathbf{r}'} \varphi_{\mathbf{r}'} + \sum_{\mathbf{r}} \varphi_{\mathbf{r}} S_{\mathbf{r}}} \\ &\propto \int_{-\infty}^{\infty} \prod_{\mathbf{r}} d\varphi_{\mathbf{r}}\, e^{-\frac{1}{2}\sum_{\mathbf{r},\mathbf{r}'} \varphi_{\mathbf{r}} A^{(\mu)-1}_{\mathbf{r},\mathbf{r}'} \varphi_{\mathbf{r}'} + \sum_{\mathbf{r}} \ln\cosh \varphi_{\mathbf{r}}}. \end{aligned} \tag{183}$$

We thus obtain a lattice field theory with the action

$$\begin{aligned} S_\mu[\varphi] = \frac{1}{2} \sum_{\mathbf{q}} \varphi_{-\mathbf{q}} \left[\frac{1}{\lambda_\mu(\mathbf{q})} - \frac{1}{\lambda_\mu(0)} \right] \varphi_{\mathbf{q}} \\ + \sum_{\mathbf{r}} \left[\frac{\varphi_{\mathbf{r}}^2}{2\lambda_\mu(0)} - \ln\cosh \varphi_{\mathbf{r}} \right]. \end{aligned} \tag{184}$$

Rescaling the field, we can cast this action in the form (172) with

$$\begin{aligned} \epsilon_0(\mathbf{q}) &= 2d(Jd + \mu) \frac{1 - \gamma_{\mathbf{q}}}{Jd\gamma_{\mathbf{q}} + \mu}, \\ U_0(\varphi) &= \frac{Jd + \mu}{J} \varphi^2 - \ln\cosh\left(2\sqrt{\frac{\beta}{J}} (Jd + \mu) \varphi \right) \end{aligned} \tag{185}$$

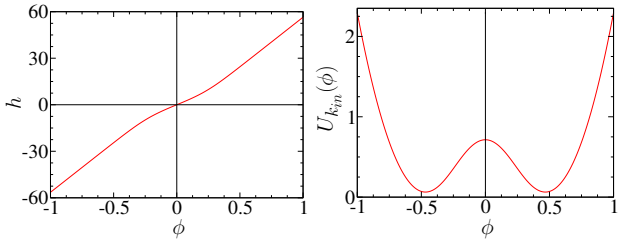

FIG. 25 (Color online) Left panel: function $h(\phi)$ obtained from the numerical solution of (188). Right panel: Effective potential $U_{k_{\rm in}}(\phi)$ [Eq. (190)]. $\mu = 5$, $T = 4.48J$ and $d = 3$.

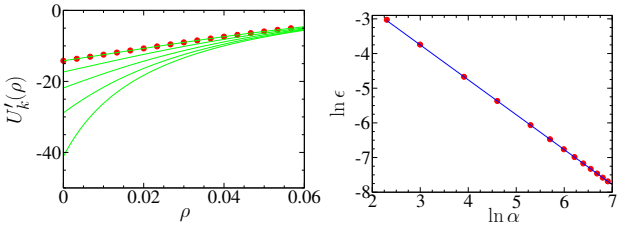

FIG. 26 (Color online) Left panel: Derivative $U'_k(\rho)$ of the effective potential for various values of k ranging from Λ to $k_{\rm in}$ ($\Lambda^2 = 10^3 k_{\rm in}^2$). The initial value $U_\Lambda(\rho) = U_0(\rho)$ is given by (185). The red points show the solution $U'_{k_{\rm in}}(\rho)$ directly obtained from a numerical solution of the single-site partition function $z_{k_{\rm in}}(h)$ [Eq. (187)]. Right panel: Relative error ϵ vs $\alpha = (\Lambda/k_{\rm in})^2$. $\mu = 5$, $T = 4.48J$ and $d = 3$.

($\gamma_{\mathbf{q}} = d^{-1}\sum_\nu \cos q_\nu$). The (bare) dispersion $\epsilon_0(\mathbf{q})$ includes long-range interactions, and $\epsilon_0(\pi,\pi,\cdots) = \epsilon_0^{\rm max}$ diverges for $\mu \to Jd$. In the limit $\mu \to \infty$ long-range interactions are suppressed and $\epsilon_0(\mathbf{q}) \to 2d(1-\gamma_{\mathbf{q}})$.

We are now in a position to apply the NPRG approach. In the standard scheme, the initial value $\Gamma_\Lambda[\phi] = S[\phi]$ of the effective action is defined by the action (172), with $\epsilon_0(\mathbf{q})$ and U_0 given by (185). In the lattice NPRG scheme, the initial value $U_{k_{\rm in}}$ of the effective potential has to be computed numerically. One has

$$Z_{k_{\rm in}}[h] = \prod_{\mathbf{r}} z_{k_{\rm in}}(h_{\mathbf{r}}), \tag{186}$$

where

$$z_{k_{\rm in}}(h) = \int_{-\infty}^{\infty} d\varphi\, e^{-\frac{1}{2}\epsilon_{k_{\rm in}}\varphi^2 - U_0(\varphi) + h\varphi}, \tag{187}$$

is the partition function of a single site in an external field h. The relation between $\phi_{\mathbf{r}}$ and $h_{\mathbf{r}}$ is obtained from the equation

$$\phi_{\mathbf{r}} = \frac{\partial}{\partial h_{\mathbf{r}}} \ln z_{k_{\rm in}}(h_{\mathbf{r}}), \tag{188}$$

which has to be computed and inverted numerically (Fig. 25). The initial value of the scale-dependent effective action then takes the form

$$\begin{aligned}\Gamma_{k_{\rm in}}[\phi] &= -\sum_{\mathbf{r}} \ln z_{k_{\rm in}}(h_{\mathbf{r}}) + \sum_{\mathbf{r}} h_{\mathbf{r}}\phi_{\mathbf{r}} - \Delta S_{k_{\rm in}}[\phi] \\ &= \sum_{\mathbf{r}} U_{k_{\rm in}}(\phi_{\mathbf{r}}) + \frac{1}{2}\sum_{\mathbf{q}} \phi_{-\mathbf{q}}\epsilon_0(\mathbf{q})\phi_{\mathbf{q}},\end{aligned} \tag{189}$$

where

$$U_{k_{\rm in}}(\phi) = \frac{1}{N}\Gamma_{k_{\rm in}}[\phi]\Big|_{\phi_{\mathbf{r}}=\phi} = -\ln z_{k_{\rm in}}(h) + h\phi - \frac{\epsilon_{k_{\rm in}}}{2}\phi^2 \tag{190}$$

is the effective potential (Fig. 25).

We solve the flow equation (178) in the LPA where the k-dependence of the dispersion is neglected,

$$\Gamma_k[\phi] = \sum_{\mathbf{r}} U_k(\rho_{\mathbf{r}}) + \frac{1}{2}\sum_{\mathbf{q}} \phi_{-\mathbf{q}}\epsilon_0(\mathbf{q})\phi_{\mathbf{q}}. \tag{191}$$

Here and in the following, we consider U_k as a function of $\rho_{\mathbf{r}} = \phi_{\mathbf{r}}^2/2$. From (178), one deduces

$$\partial_t U_k(\rho) = \frac{1}{2}\int_{\mathbf{q}} \frac{\dot R_k(\mathbf{q})}{\epsilon_0(\mathbf{q}) + R_k(\mathbf{q}) + U'_k(\rho) + 2\rho U''_k(\rho)}, \tag{192}$$

which is similar to (46) except for the momentum integration now limited to the first Brillouin zone. With the theta regulator function (174), Eq. (192) reduces to

$$\partial_t U_k(\rho) = \frac{\epsilon_k}{\epsilon_k + U'_k(\rho) + 2\rho U''_k(\rho)} \int_{\mathbf{q}} \theta\big(\epsilon_k - \epsilon_0(\mathbf{q})\big). \tag{193}$$

The integral over $\mathbf{q}$ can be rewritten as

$$\int_{\mathbf{q}} \theta\big(\epsilon_k - \epsilon_0(\mathbf{q})\big) = \int_0^{\epsilon_k} d\epsilon\, \mathcal{D}(\epsilon), \tag{194}$$

where

$$\mathcal{D}(\epsilon) = \int_{\mathbf{q}} \delta\big(\epsilon - \epsilon_0(\mathbf{q})\big). \tag{195}$$

When $k \ll 1$, we can use the low-energy approximations $\epsilon_0(\mathbf{q}) \simeq \epsilon_0 \mathbf{q}^2$ and $\mathcal{D}(\epsilon) \simeq 2v_d \epsilon^{d/2-1}/\epsilon_0^{d/2}$. Equation (192) then reduces to the LPA equation (47) derived in the continuum limit of the model (172) with the theta regulator (14) (see Sec. III.A). This implies that the critical exponents are the same as those obtained in the LPA of the continuum model.

In the local fluctuation regime $k_{\rm in} \le k \le \Lambda$, $S[\varphi] + \Delta S_k[\varphi]$ is a local action (no intersite coupling). It follows that both $-\ln \mathcal{Z}_k[h]$ and its Legendre transform reduce to a sum of single-site contributions. The LPA for the scale-dependent effective action $\Gamma_k[\phi]$ is then exact. Figure 26 shows the derivative U'_k of the effective potential for $\alpha = \epsilon_\Lambda/\epsilon_0^{\rm max} = (\Lambda/k_{\rm in})^2 = 10^3$. As k decreases from Λ to $k_{\rm in}$, the potential $U'_k(\rho)$ becomes nearly equal to the exact solution obtained from the numerical computation of the local partition function $z_{k_{\rm in}}(h)$ [Eqs. (187) and (190)]. The relative error as a function of α is shown in the right panel of Fig. 26. It decreases as $1/\alpha$, in agreement with

the fact that the validity of the mean-field (saddle-point) approximation to $Z_\Lambda[h]$ for large Λ is controlled by $R_\Lambda^{-1} \sim \epsilon_\Lambda^{-1} \sim \alpha^{-1}$. We therefore conclude that the standard and lattice NPRG schemes are equivalent in the LPA for classical lattice field theories.

The critical temperature is obtained from the divergence of the susceptibility $\chi = 1/U'_{k=0}(\rho = 0)$ or, equivalently, the divergence of the correlation length $\xi = \sqrt{\chi}$ (we omit a factor of T in the definition of the susceptibility). For $\alpha = 10^3$ and $d = 3$ one finds that $T_c \simeq 0.747\, T_c^{\rm MF}$ is independent of μ and in very good agreement with the "exact" result $T_c^{\rm exact} \simeq 0.752\, T_c^{\rm MF}$ obtained from Monte Carlo simulations (Wolff, 1989).

For further studies of the LPA flow equation, we refer to (Caillol, 2012a, 2013).

B. Classical spin models

In this section, we show that the lattice NPRG can be applied to classical spin models without first deriving a field theory. For simplicity, we consider the Ising model on a d-dimensional hypercubic lattice [Eq. (180)]. In the presence of an external field and a regulator term ΔS_k, the partition function reads

$$\begin{aligned} \mathcal{Z}_k[h] &= \sum_{\{S_\mathbf{r}\}} e^{\frac{J}{T}\sum_{\langle \mathbf{r},\mathbf{r}'\rangle} S_\mathbf{r} S_{\mathbf{r}'} - \frac{1}{2}\sum_{\mathbf{r},\mathbf{r}'} S_\mathbf{r} R_k(\mathbf{r},\mathbf{r}') S_{\mathbf{r}'} + \sum_\mathbf{r} h_\mathbf{r} S_\mathbf{r}} \\ &= \sum_{\{S_\mathbf{r}\}} e^{-\frac{1}{2}\sum_\mathbf{q} S_{-\mathbf{q}}[\epsilon_0(\mathbf{q}) - 2\epsilon_0 d + R_k(\mathbf{q})] S_\mathbf{q} + \sum_\mathbf{r} h_\mathbf{r} S_\mathbf{r}}, \end{aligned} \tag{196}$$

where

$$\epsilon_0(\mathbf{q}) = 2\epsilon_0 \sum_{\nu=1}^{d} (1 - \cos q_\nu), \tag{197}$$

with $\epsilon_0 = J/T$. Since $S_\mathbf{r}^2 = 1$, the term $2d\epsilon_0 \sum_\mathbf{q} S_{-\mathbf{q}} S_\mathbf{q}$ in (196) contributes a constant term to the action and can be omitted. The magnetization at site $\mathbf{r}$ is given by

$$m_\mathbf{r} = \langle S_\mathbf{r} \rangle = \frac{\partial \ln \mathcal{Z}_k[h]}{\partial h_\mathbf{r}} \tag{198}$$

and the scale-dependent effective action is defined by

$$\Gamma_k[m] = -\ln \mathcal{Z}_k[h] + \sum_\mathbf{r} h_\mathbf{r} m_\mathbf{r} - \Delta S_k[m]. \tag{199}$$

The standard NPRG scheme cannot be used, since the partition function is not expressed as a functional integral over a continuous variable. A "regulator" term $\epsilon_k \sum_\mathbf{q} S_{-\mathbf{q}} S_\mathbf{q} = \epsilon_k \sum_\mathbf{r} S_\mathbf{r}^2 = N\epsilon_k$ would only add a constant term to the action. On the contrary, there is no difficulty to apply the lattice NPRG scheme. With the regulator function (174), one has

$$Z_{k_{\rm in}}[h] = \sum_{\{S_\mathbf{r}\}} e^{-2d\epsilon_0 N + \sum_\mathbf{r} h_\mathbf{r} S_\mathbf{r}} = e^{-2d\epsilon_0 N} \prod_\mathbf{r} z(h_\mathbf{r}), \tag{200}$$

where

$$z(h) = \sum_{S=\pm 1} e^{hS} = 2\cosh(h) \tag{201}$$

is the partition function of a single site in an external field h. The magnetization at site $\mathbf{r}$,

$$m_\mathbf{r} = \frac{\partial}{\partial h_\mathbf{r}} \ln z(h_\mathbf{r}) = \tanh(h_\mathbf{r}), \tag{202}$$

varies between -1 and 1. Up to an additive constant, we obtain

$$\Gamma_{k_{\rm in}}[m] = \sum_\mathbf{r} U_{k_{\rm in}}(\rho_\mathbf{r}) + \frac{1}{2}\sum_\mathbf{q} m_{-\mathbf{q}} \epsilon_0(\mathbf{q}) m_\mathbf{q} \tag{203}$$

and the effective potential

$$\begin{aligned} U_{k_{\rm in}}(\rho) = &\frac{1}{2}(1+\sqrt{2\rho})\ln(1+\sqrt{2\rho}) \\ &+ \frac{1}{2}(1-\sqrt{2\rho})\ln(1-\sqrt{2\rho}) - 4d\epsilon_0\rho, \end{aligned} \tag{204}$$

where $\rho_\mathbf{r} = m_\mathbf{r}^2/2$ varies between 0 and 1/2. $U_{k_{\rm in}}(1/2) = \ln(2) - 2d\epsilon_0$ is finite but $U'_{k_{\rm in}}(\rho) \sim -\frac{1}{2}\ln(1-2\rho)$ diverges for $\rho \to 1/2$. This divergence suppresses the propagator

$$G_{k_{\rm in}}(\mathbf{q};\rho) = \frac{1}{\epsilon_{k_{\rm in}} + U'_{k_{\rm in}}(\rho) + 2\rho U''_{k_{\rm in}}(\rho)} \tag{205}$$

(in a constant field $\rho_\mathbf{r} = \rho$) and therefore the fluctuations corresponding to a magnetization $|m_\mathbf{r}| > 1$.

A comment is in order here. We have defined the scale-dependent effective action Γ_k as a modified Legendre transform which includes the explicit subtraction of $\Delta S_k[m]$ [Eq. (199)]. The definition of the scale-dependent effective action Γ_k is of course arbitrary provided that $\Gamma_{k=0}$ corresponds to the true Legendre transform of the original model. Since

$$U_{k_{\rm in}}(\rho) = \rho(1 - 4d\epsilon_0) + \mathcal{O}(\rho^2) \tag{206}$$

for $\rho \to 0$, we find that the initial transition temperature is determined by $1 = 4d\epsilon_0$, i.e. $T_c^{(k_{\rm in})} = 4dJ$, which differs from the mean-field transition temperature $T_c^{\rm MF} = 2dJ$ by a factor 2. $\Gamma_{k_{\rm in}}[m]$ assumes a mean-field treatment of the intersite coupling term $\frac{1}{2}\sum_\mathbf{q} S_{-\mathbf{q}}\epsilon_0(\mathbf{q}) S_\mathbf{q}$ as in the usual mean-field approach to the Ising model. The discrepancy between $T_c^{(k_{\rm in})}$ and $T_c^{\rm MF}$ comes from the fact that $\frac{1}{2}\sum_\mathbf{q} S_{-\mathbf{q}}\epsilon_0(\mathbf{q}) S_\mathbf{q}$ includes a local term $\frac{1}{2}\sum_\mathbf{r} 2d\epsilon_0 S_\mathbf{r}^2 = Nd\epsilon_0$. The latter contributes a mere constant to the action, but is considered at the mean-field level in the scale-dependent effective action where it gives a term $-d\epsilon_0 \sum_\mathbf{r} m_\mathbf{r}^2$. To make contact with the usual mean-field theory, we consider the scale-dependent effective action

$$\bar{\Gamma}_k[m] = \Gamma_k[m] + \frac{1}{2}\sum_\mathbf{r} R_k(\mathbf{r},\mathbf{r}) m_\mathbf{r}^2 \tag{207}$$

TABLE VII Critical temperature $T_c^{\rm NPRG}$ obtained in the LPA compared to the mean-field estimate $T_c^{\rm MF}$ and the Monte Carlo result $T_c^{\rm exact}$. All temperatures are in unit of J.

	$T_c^{\rm MF}$	$T_c^{\rm exact}$	$T_c^{\rm NPRG}$
Ising 3D	6	4.51 [a]	4.48
XY 3D	3	2.20 [b]	2.18
Heisenberg 3D	2	1.44 [c]	1.42

[a](Wolff, 1989) [b](Hasenbusch and Meyer, 1990) [c](Holm and Janke, 1993)

and the corresponding effective potential

$$\bar{U}_k(\rho) = U_k(\rho) + \rho R_k(\mathbf{r},\mathbf{r}). \tag{208}$$

$\bar{\Gamma}_k[m]$ differs from the true Legendre transform only by non-local terms. The initial value

$$\bar{U}_{k_{\rm in}}(\rho) = \rho(1-2d\epsilon_0) + \mathcal{O}(\rho^2) \tag{209}$$

reproduces the mean-field result $T_c^{(k_{\rm in})} = T_c^{\rm MF}$. Again we stress that Γ_k and $\bar{\Gamma}_k$ lead to the same $k=0$ results and in particular to the same critical temperature.

1. Local potential approximation

In the LPA, the flow equation of the effective potential is given by (192). The critical temperature is obtained from the criterion $U'_{k=0}(\rho=0)=0$. One finds $T_c \simeq 0.747\, T_c^{\rm MF}$ for the three-dimensional Ising model, in very good agreement with the results of Sec. VII.A and the "exact" result $T_c^{\rm exact} \simeq 0.752\, T_c^{\rm MF}$ obtained from Monte Carlo simulations (Wolff, 1989). A similar accuracy is obtained for the critical temperature of the XY and Heisenberg models in three dimensions (Table VII). Not surprisingly, the LPA is not as accurate in two dimensions (Machado and Dupuis, 2010). For the two-dimensional Ising model, $T_c \simeq 0.48\, T_c^{\rm MF}$, to be compared with the exact result $T_c^{\rm exact} = 2J/\ln(1+\sqrt{2}) \simeq 0.567\, T_c^{\rm MF}$ (Onsager, 1944).

Figure 27 shows the transition temperature $T_c^{(k)}$ of the three-dimensional Ising model deduced from the effective potentials U_k and $\bar{U}_k$ [Eq. (208)]. As k decreases, $T_c^{(k)}$ converges rapidly towards the actual transition temperature $T_c = T_c^{(k=0)}$. This result is due to the fact that all degrees of freedom contribute more or less equally to the thermodynamics. Once $k \ll k_{\rm in}$, thermodynamic quantities are therefore obtained with a reasonable accuracy. This also explains why the LPA, which does not correctly describe the long-distance limit of the propagator when $T \simeq T_c$, is remarkably successful in computing the transition temperature and other thermodynamic quantities.

Figure 28 shows the derivative $U'_k(\rho)$ of the effective potential for $k = k_{\rm in}$ and $k=0$ at criticality ($T = 0.747\, T_c^{\rm MF}$), as well as $U'_{k=0}(\rho)$ for $T=T_c$, $T>T_c$ and $T<T_c$. In the latter case, we find $U'_{k=0}(\rho)=0$ and therefore $U_{k=0}(\rho) = $ const for $\rho \le \rho_0$, in agreement with the convexity of the effective potential in the low-temperature (broken-symmetry) phase. $\rho_0 = m_0^2/2$ determines the actual magnetization m_0 of the system.

In Fig. 29, we show the uniform susceptibility $\chi = 1/U'_{k=0}(\rho=0)$ in the high-temperature phase, as well as the magnetization below T_c with the Essam-Fisher approximant (Essam and Fisher, 1963). We find the critical exponents $\nu = 2\beta = \gamma/2 \simeq 0.64-0.65$ (with $\eta=0$ in the LPA), in agreement with the result of the LPA with the regulator (174) (Sec. III.A).

2. Renormalization of the spectrum

A natural generalization of the LPA includes a renormalization of the amplitude of the dispersion. We therefore consider the Ansatz

$$\Gamma_k[m] = \sum_{\mathbf{r}} U_k(\rho_{\mathbf{r}}) + \frac{1}{2}\sum_{\mathbf{q}} A_k \epsilon_0(\mathbf{q}) m_{-\mathbf{q}} m_{\mathbf{q}}. \tag{210}$$

This approximation can be seen as the first step of a circular harmonic expansion of the renormalized dispersion

$$\epsilon(\mathbf{q}) = \sum_{n,m,l=0}^{\infty} \epsilon_{nml}[\cos(nq_x)\cos(mq_y)\cos(lq_z) - 1] \tag{211}$$

(written here for a three dimensional system). Since

$$\Gamma_k^{(2)}(\mathbf{q};\rho) = A_k\epsilon_0(\mathbf{q}) + U'_k(\rho) + 2\rho U''_k(\rho) \tag{212}$$

in a uniform field $\phi_{\mathbf{r}} = \sqrt{2\rho}$, we can define the renormalized dispersion amplitude by

$$A_k = \frac{1}{\epsilon_0}\Gamma_k^{(2)}(\mathbf{r}-\mathbf{r}';\rho_{0,k}), \tag{213}$$

where $\mathbf{r}$ and $\mathbf{r}'$ are nearest neighbors. The amplitude $A_k \equiv A_k(\rho_{0,k})$ should be understood as the first term in the expansion of the function

$$A_k(\rho) = A_k(\rho_{0,k}) + A_k^{(1)}(\rho_{0,k})(\rho-\rho_{0,k}) + \cdots \tag{214}$$

about the minimum $\rho_{0,k}$ of the effective potential $U_k(\rho)$. Another possible definition of the dispersion amplitude is $A_k \equiv A_k(\bar{\rho}_{0,k})$, where $\bar{\rho}_{0,k}$ is the minimum of $\bar{U}_k(\rho)$ [Eq. (208)]. The flow equation for A_k follows from (178) and (213),

$$\partial_t A_k = \frac{\gamma_3^2}{\epsilon_0}\int_{\mathbf{q}} \left(1 - \frac{\epsilon_0(\mathbf{q})}{2d\epsilon_0}\right) \dot{R}_k(\mathbf{q}) G(\mathbf{q})^2 \times \int_{\mathbf{p}} \left(1 - \frac{\epsilon_0(\mathbf{p})}{2d\epsilon_0}\right) G(\mathbf{p}), \tag{215}$$

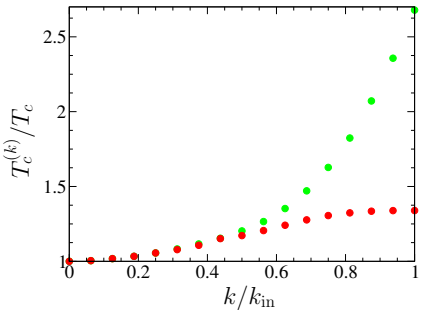

FIG. 27 (Color online) Transition temperature $T_c^{(k)}$ obtained from the effective potential U_k (green points) and $\bar{U}_k$ (red points).

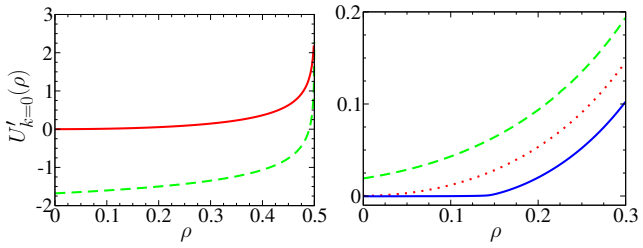

FIG. 28 (Color online) Left panel: Potentials $U'_{k=0}(\rho)$ (red solid line) and $U'_{k_{\rm in}}(\rho)$ (green dashed line) at criticality ($T = T_c$) in the LPA ($d = 3$). Right panel: Potential $U'_{k=0}(\rho)$ for $T = T_c$ (red dotted line), $T = 1.05\,T_c$ (green dashed line) and $T = 0.95\,T_c$ (blue solid line).

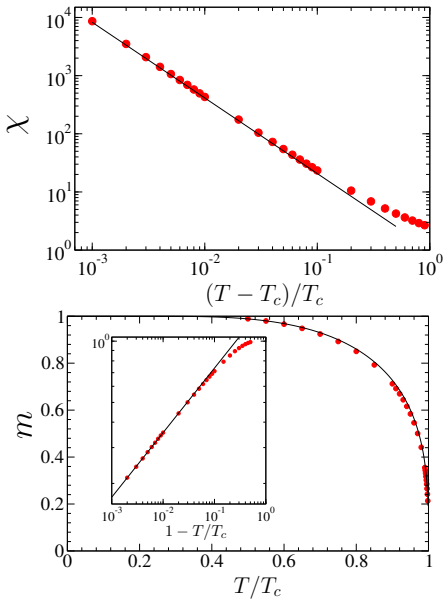

FIG. 29 (Color online) Top panel: Uniform susceptibility χ (red points) in the high-temperature phase and a fit $\chi \propto (T-T_c)^{-\gamma}$ with $\gamma = 2\nu \simeq 1.30$. Bottom panel: Magnetization m in the low-temperature phase (red points) and the Essam-Fisher approximant (Essam and Fisher, 1963) (solid line). The inset shows a fit to $m \propto (T_c - T)^{\beta}$ with $\beta = \nu/2 \simeq 0.32$.

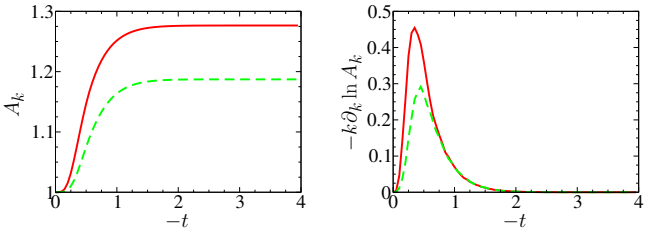

FIG. 30 (Color online) Left panel: $A_k(\rho_{0,k})$ (red solid line) and $A_k(\bar{\rho}_{0,k})$ (green dashed line) vs $-t = \ln(k_{\rm in}/k)$. Right panel: $-k\partial_k \ln A_k(\rho_{0,k})$ (red solid line) and $-k\partial_k \ln A_k(\bar{\rho}_{0,k})$ (green dashed line) vs $-t$. All curves are obtained at criticality ($T = T_c$) and for $d = 3$.

where $\gamma_3 = \sqrt{2\rho_{0,k}}[3U''_k(\rho_{0,k}) + 2\rho_{0,k}U'''_k(\rho_{0,k})]$. The flow equation for $U_k(\rho)$ is identical to (192) with $\epsilon_0(\mathbf{q})$ replaced by $A_k\epsilon_0(\mathbf{q})$.

Numerical results for $A_k(\rho_{0,k})$ and $A_k(\bar{\rho}_{0,k})$ are shown in Fig. 30. In both cases, A_k varies when $k \sim 1$, in agreement with the expectation that the amplitude of the harmonic $\cos(nq_\nu)$ should vary when $k \sim 1/n$ (Dupuis and Sengupta, 2008). The variation of A_k is moderate (from 1 to 1.27 for $A_k(\rho_{0,k})$ and from 1 to 1.19 for $A_k(\bar{\rho}_{0,k})$) and weakly affects the critical temperature which remains within a few percents of the exact result: $T_c = 0.74\,T_c^{\rm MF}$ with $A_k(\rho_{0,k})$ and $T_c = 0.72\,T_c^{\rm MF}$ with $A_k(\bar{\rho}_{0,k})$. We expect that including additional higher-order harmonics in the spectrum would improve the estimate of T_c.

3. LPA'

Including a finite number of harmonics is not sufficient to obtain a nonzero anomalous dimension. In this section we briefly discuss how a finite anomalous dimension can be obtained in the lattice NPRG. When $k \ll 1$, we can approximate $\epsilon_0(\mathbf{q})$ by $\epsilon_0\mathbf{q}^2$. In this regime, we can improve the LPA by including a field renormalization factor Z_k so that the renormalized dispersion $\epsilon(\mathbf{q})$ is given by $Z_k\epsilon_0(\mathbf{q}) \simeq Z_k\epsilon_0\mathbf{q}^2$. This improvement, referred to as LPA' in Sec. III.B, can be generalized to all values of k by writing the scale-dependent effective action as

$$\Gamma_k[m] = \sum_{\mathbf{r}} U_k(\rho_{\mathbf{r}}) + \frac{1}{2}\sum_{\mathbf{q}} m_{-\mathbf{q}} Z_k \epsilon_0(\mathbf{q}) m_{\mathbf{q}}. \qquad (216)$$

Although this Ansatz is formally similar to (210), Z_k should not be confused with the amplitude A_k introduced in the preceding section. Z_k is computed from the $\mathcal{O}(\mathbf{q}^2)$ part of the spectrum,

$$Z_k = \frac{1}{\epsilon_0}\lim_{\mathbf{q}\to 0}\frac{\partial}{\partial \mathbf{q}^2}\Gamma_k^{(2)}(\mathbf{q};\rho_{0,k}), \qquad (217)$$

and therefore receives contributions from all harmonics. The LPA' can be justified when $k \sim 1$ by noting that in this limit the renormalization of the spectrum is weak

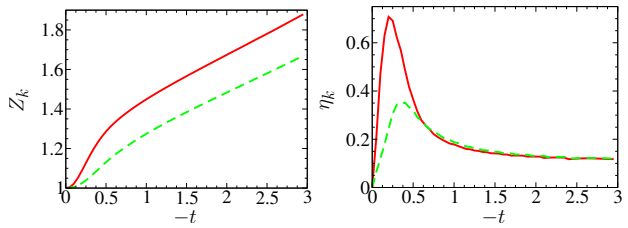

FIG. 31 (Color online) Left panel: Z_k vs $-t = \ln(k_{\rm in}/k)$ obtained with $\rho_{0,k}$ (red solid line) and $\bar\rho_{0,k}$ (green dashed line) ($d = 3$). Right panel: Anomalous dimension $\eta_k = -k\partial_k \ln Z_k$ obtained with $\rho_{0,k}$ (red solid line) and $\bar\rho_{0,k}$ (green dashed line).

($Z_k \sim 1$), so that the approximation $\epsilon(\mathbf{q}) \simeq Z_k \epsilon_0(\mathbf{q})$, valid for small $\mathbf{q}$, is expected to remain approximately valid in the whole Brillouin zone. Nevertheless, because short-range fluctuations are important for the thermodynamics, the LPA' might lead to a slight deterioration of the value of T_c obtained in the LPA. As in the preceding section, we can compute Z_k either from the minimum of $U_k(\rho)$ (as in Eq. (217)) or from the minimum $\bar\rho_{0,k}$ of $\bar U_k(\rho)$.

To obtain a fixed point when the system is critical, one should add the prefactor Z_k to the regulator function (174) and introduce the dimensionless variables $\tilde\rho = Z_k k^{-d}\epsilon_k \rho$ and $\tilde U_k(\tilde\rho) = k^{-d} U_k(\rho)$. This leads to the flow equations (Machado and Dupuis, 2010)

$$\partial_t \tilde U_k = -d\tilde U_k + (d-2+\eta_k)\tilde\rho \tilde U_k' + \frac{(2-\eta_k) I_1 + \eta_k I_2}{1 + \tilde U_k' + 2\tilde\rho \tilde U_k''},$$

$$\eta_k = 4\tilde\rho \big[3\tilde U_k'' + 2\tilde\rho \tilde U_k'''\big]^2 \frac{I_3 + \delta_{d,2}/(8\pi)}{\big(1 + \tilde U_k' + 2\tilde\rho \tilde U_k''\big)^4},$$

where

$$I_1 = \frac{k^{-d}}{2} \int_{\mathbf{q}} \theta\big(\epsilon_k - \epsilon_0(\mathbf{q})\big),$$

$$I_2 = \frac{k^{-d}}{2} \int_{\mathbf{q}} \frac{\epsilon_0(\mathbf{q})}{\epsilon_k} \theta\big(\epsilon_k - \epsilon_0(\mathbf{q})\big), \qquad (218)$$

$$I_3 = \frac{k^{2-d}}{4} \int_{\mathbf{q}} \frac{\epsilon_0(\mathbf{q}) \partial_{q_x}^2 \epsilon_0(\mathbf{q}) - [\partial_{q_x} \epsilon_0(\mathbf{q})]^2}{\epsilon_0(\mathbf{q})^2} \theta\big(\epsilon_k - \epsilon_0(\mathbf{q})\big).$$

In the expression of η_k, $\tilde U_k$ and its derivatives should be evaluated at $\tilde\rho_{0,k}$ or $\tilde{\bar\rho}_{0,k}$. For $d = 3$, we find $T_c = 0.8\, T_c^{\rm MF}$ when Z_k is defined with respect to the minimum $\rho_{0,k}$ of U_k, and $T_c = 0.74\, T_c^{\rm MF}$ if we use the minimum $\bar\rho_{0,k}$ of $\bar U_k$. The result is not as accurate as in the LPA (as anticipated above; see the discussion following Eq. (217)). Nevertheless, with $\bar\rho_{0,k}$ (the only case we discuss in the following), it remains within 2 percent of the exact result $T_c^{\rm exact} = 0.752\, T_c^{\rm MF}$. The flow of Z_k is shown in Fig. 31. For $-t < 1$, Z_k does not differ significantly from A_k (Fig. 30). In this regime, only the first harmonic (i.e. $\cos q_\nu$) is expected to vary and therefore contribute to Z_k. For $-t > 1$, the renormalization of higher-order harmonics makes Z_k deviate from A_k. While A_k saturates to ~ 1.19, $Z_k \sim k^{-\eta}$ diverges with an exponent given by the anomalous dimension $\eta = \lim_{k\to 0} \eta_k$. $\eta \simeq 0.1$ is a poor estimate of the exact result $\eta \simeq 0.036$ but agrees with previous estimates based on the LPA' (Dupuis and Sengupta, 2008). A ρ dependence of Z_k is expected to improve the value of η (Canet *et al.*, 2003).

C. Comparison with HRT

The lattice NPRG bears similarities with the Hierarchical Reference Theory (HRT) of fluids (Gianinetti and Parola, 2001; Ionescu *et al.*, 2007; Parola, 1986; Parola *et al.*, 2009; Parola and Reatto, 1984; Pini *et al.*, 1993) (for a review, see (Parola and Reatto, 1995)). The HRT is based on an exact treatment of short-distance (hard-core) interactions supplemented by a RG analysis of long-range interactions. The HRT also applies to classical spin models: as in the lattice NPRG, it starts from the local theory (decoupled sites) and takes into account the intersite coupling in a RG approach. Although the final results are very similar to those we have obtained in Secs. VII.B.1 and VII.B.2, the HRT nevertheless differs from the lattice NPRG in some technical aspects, e.g. the choice of the regulator function and the way degrees of freedom are progressively integrated out (Parola and Reatto, 1995; Pini *et al.*, 1993). Because it was first developed in the context of liquid state theory, the connection between HRT and the more standard formulation of the NPRG is not always obvious (for a discussion of the relation between HRT and RG, see (Caillol, 2006, 2009)). By contrast, the lattice NPRG is formulated in the usual language of statistical field theory. The various improvements over the LPA known for continuum models (Sec. III) can then be easily implemented in the lattice NPRG. In Sec. VII.B.3, we have discussed one of these improvements, the LPA', which allows to compute the anomalous dimension η.

VIII. MEMBRANES (DM)

IX. FRUSTRATED SPINS AND MATRIX MODELS (DM)

X. DISORDERED SYSTEMS (MT, GT, DM)

XI. OUT-OF-EQUIBRIUM SYSTEMS: KPZ, REACTION DIFFUSION... (LC, BD)

XII. QUANTUM O(N) MODEL

In this section we start with a brief reminder on quantum phase transitions before considering the NPRG approach to the quantum O(N) model. First we show that the NPRG flow, even with a simple truncation of the effective action, nicely illustrates the basic concepts of the theory of quantum critical points. Then we discuss the

(universal) thermodynamics and the "Higgs" amplitude mode in the vicinity of the quantum critical point (QCP).

A. Quantum phase transitions

In classical statistical mechanics, thermodynamics and dynamics decouple. The reason is that the particles' positions and momenta are independent variables in the partition function of a classical system. One can integrate out momenta (which yields a non-singular additive contribution to the free energy) and write the partition function in terms of the position variables only. To study the dynamics of the system, the knowledge of the partition function is therefore not sufficient, one needs an equation of motion (kinetic equation); see, e.g., Sec. XI. Near a second-order phase transition, in addition to the diverging length scale set by ξ, there is a diverging time scale $\tau_c \sim \xi^z$ whose divergence is controlled by the dynamical critical exponent z.

In quantum statistical mechanics, the situation is different. Coordinate and momentum variables are non-commuting operators so that statics and dynamics are not independent. The existence of $\hbar$ implies that any energy scale E that enters thermodynamics necessarily determines a time scale $\hbar/E$ (for clarity we momentarily restore $\hbar$ and k_B).[54]

Thus we expect quantum phase transitions, occurring at zero-temperature, to be qualitatively different from their classical counterparts (Sachdev, 2011; Sondhi *et al.*, 1997). Quantum phase transitions occur by changing a nonthermal control parameter of the system (such as pressure, magnetic field, chemical composition, etc.) and their critical fluctuations are driven by the Heisenberg uncertainty principle. In the following we focus on second-order (continuous) quantum phase transitions characterized by both a diverging length scale ξ and a vanishing energy scale Δ (or, equivalently, a diverging time scale $\xi_\tau \sim \hbar/\Delta$). In a gapped phase, Δ is typically the energy of the lowest excitation above the ground state and ξ the correlation length associated to order parameter fluctuations. In a gapless phase, Δ is the scale at which there is a qualitative change in the nature of the low-energy spectrum and ξ the associated length scale (e.g. the Josephson length ξ_J separating critical from noncritical behavior in broken-symmetry phases with Goldstone bosons). Let us call g the nonthermal control parameter and g_c its critical value at the QCP. In most cases

$$\xi \sim |g - g_c|^{-\nu}, \qquad \Delta \sim |g - g_c|^{z\nu}, \tag{219}$$

[54] One can also realize that the quantum partition function $Z = \mathrm{Tr}\, e^{-\beta \hat{H}}$ involves the trace of the evolution operator $\hat{U}(t) = e^{-\frac{i}{\hbar}\hat{H}t}$ for an imaginary time $t = -i\hbar\beta$ ($\beta = 1/k_B T$).

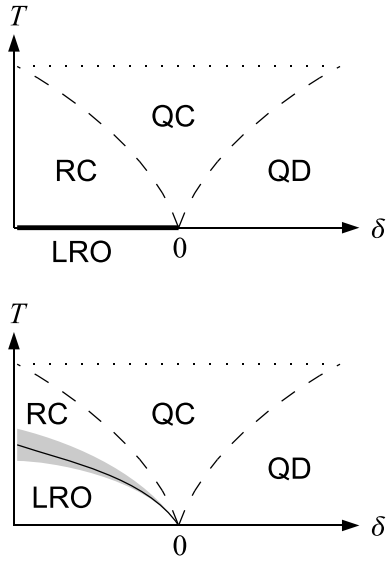

FIG. 32 Phase diagram in the vicinity of a QCP $\delta = T = 0$ ($\delta = g - g_c$). The dashed lines are crossover lines $T \sim |\delta|^{\nu z}$ obtained from the criterion $L_\tau = \hbar\beta \sim \xi_\tau$ (with ξ_τ the $T = 0$ correlation time). The dotted lines mark the onset of the high-T region where the physics is not controlled by the QCP anymore. RC: renormalized classical regime, QC: quantum critical regime, QD: quantum disordered regime. (Top) Long-range order (LRO) occurs only at $T = 0$. (Bottom) LRO occurs for $\delta < 0$ and $T \leq T_c(\delta)$. The shaded area shows the region of classical fluctuations in the vicinity of the transition line $T_c(\delta)$.

as g approaches g_c. We shall refer to ν as the correlation-length exponent and z as the dynamical critical exponent.

Strictly speaking, quantum phase transitions occur only at zero temperature. Since all experiments are necessarily at some nonzero, though possibly small, temperature, a central issue of the theory of quantum phase transitions is to describe the consequences of the $T = 0$ QCP on the physical properties at finite temperatures. Two situations can occur depending on whether long-range order can exist at finite temperatures. In the first one (Fig. 32, top panel), long-range order exists only at $T = 0$ for $g \leq g_c$ and all $T > 0$ properties are regular functions of g near $g = g_c$. In the second one, there is a line of finite-temperature second-order phase transitions which terminates at the $T = 0$ QCP. Since the typical frequency ω_c associated to critical fluctuations vanishes as we move closer to this phase transition line, it satisfies $\hbar\omega_c \ll k_B T$, so that critical fluctuations behave classically (even if quantum effects are important at short length scales). Any finite-temperature phase transition is therefore "classical" to the extent that the critical singularities can be described by a classical field theory (see the shaded area in Fig. 32).

Quite generally, we can distinguish three regions in the finite-temperature phase diagram separated by crossover

lines defined by $k_BT \sim \Delta \sim |g-g_c|^{z\nu}$ (Fig. 32). When $k_BT \gg \Delta$, the system is driven away from criticality by thermal fluctuations. The physics is then controlled primarily by the QCP and its thermal excitations (quantum critical regime). This usually results in unconventional power-law temperature dependencies of physical observables. When $g > g_c$ and $k_BT \ll \Delta$, temperature has little effect and the system is primarily disordered by quantum fluctuations (quantum disordered regime). When $g < g_c$ and $k_BT \ll \Delta$, the order is destroyed by thermal fluctuations. This regime, which can be described by an effective classical theory at low energies, is usually called the renormalized classical regime.

In the following, we consider the 2D quantum O(N) model, defined by the Euclidean action

$$S[\boldsymbol{\varphi}] = \int_0^{\beta\hbar} d\tau \int d^2r \Big\{ \frac{1}{2}(\boldsymbol{\nabla}\boldsymbol{\varphi})^2 + \frac{1}{2c_\Lambda^2}(\partial_\tau \boldsymbol{\varphi})^2 + \frac{r_0}{2}\boldsymbol{\varphi}^2 + \frac{u_0}{4!}(\boldsymbol{\varphi}^2)^2 \Big\}, \tag{220}$$

where $\boldsymbol{\varphi}$ is an N-component real field satisfying periodic boundary conditions $\boldsymbol{\varphi}(\mathbf{r},\tau) = \boldsymbol{\varphi}(\mathbf{r},\tau+\beta)$. It is a straightforward generalization to the quantum case of the classical O(N) model [Eq. (3)]. Contrary to the latter however, the coupling constants r_0 and u_0 are assumed to be temperature independent. c_Λ denotes the bare velocity of the $\boldsymbol{\varphi}$ field. The model is regularized by an ultraviolet cutoff Λ. In order to maintain the Lorentz invariance of the action (220), it is natural to impose the cutoff on both momenta and frequencies.

The phase diagram of the 2D quantum O($N \geq 3$) model is shown in Fig. 32 (top panel with $\delta = r_0 - r_{0c}$). At zero temperature ($\beta \to \infty$), the 2D quantum model is equivalent to the 3D classical model. There is a quantum phase transition between a disordered phase ($r_0 > r_{0c}$) and an ordered phase ($r_0 < r_{0c}$) where the O(N) symmetry of the action (220) is spontaneously broken (u_0 and c_Λ are considered as fixed parameters). The phase transition is governed by the three-dimensional Wilson-Fisher fixed point and the dynamical critical exponent $z = 1$ (this value follows from the (relativistic) Lorentz invariance of the action (220) at zero temperature). At finite temperatures, the system is always disordered for $N \geq 2$, in agreement with the Mermin-Wagner theorem. For $N = 2$ and $r_0 < r_{0c}$, there is a finite-temperature Kosterlitz-Thouless (KT) phase transition and the system exhibits algebraic order at low temperatures. The KT transition temperature line $T_{\rm KT}$ terminates at the QCP $r_0 = r_{0c}$.

B. RG flows

There is no difficulty to apply the NPRG approach to the 2D quantum O(N) since the only difference with the 3D classical model comes from the finite size β in the imaginary time direction (Rançon *et al.*, 2013; Reuter *et al.*, 1993; Tetradis and Wetterich, 1993). The scale-dependent effective action $\Gamma_k[\boldsymbol{\phi}]$ is a functional of a space- and time-dependent bosonic field $\boldsymbol{\phi}(\mathbf{r},\tau)$. Its variation with k is given by Wetterich's equation (30) where the trace should now be understood as a trace over space and time, as well as the O(N) index of the field. In practice, this amounts to replacing each momentum $\mathbf{q}$ by a frequency-momentum variable $q = (\mathbf{q}, i\omega_n)$, where $\omega_n = 2n\pi T$ (n integer) is a bosonic Matsubara frequency, and each momentum integration by

$$\int_q \equiv \int_{\mathbf{q}} T \sum_{\omega_n}. \tag{221}$$

We shall use an exponential regulator function which acts both on momenta and frequencies,

$$R_k(q) = Z_{A,k}\left(\mathbf{q}^2 + \frac{\omega_n^2}{c_k^2}\right) r\left(\frac{\mathbf{q}^2 + \omega_n^2/c_k^2}{k^2}\right), \tag{222}$$

where $r(Y) = 1/(e^Y - 1)$. c_k denotes the running velocity at scale k and the k-dependent constant $Z_{A,k}$ is defined below [Eq. (223)]. This regulator function respects the Lorentz invariance of the quantum O(N) model at zero temperature. In the following, we restrict ourselves to $N \geq 2$.

We use a derivative expansion where the scale-dependent effective action is approximated by (Rançon *et al.*, 2013)

$$\Gamma_k[\boldsymbol{\phi}] = \int_0^\beta d\tau \int_{\mathbf{r}} \Big\{ \frac{Z_{A,k}}{2}(\boldsymbol{\nabla}\boldsymbol{\phi})^2 + \frac{V_{A,k}}{2}(\partial_\tau \boldsymbol{\phi})^2 + U_k(\rho) \Big\}, \tag{223}$$

which corresponds to the LPA' (Sec. III.B). It differs from the LPA by the introduction of two field renormalization constants $Z_{A,k}$ and $V_{A,k}$ ($Z_{A,\Lambda} = 1$ and $V_{A,\Lambda} = c_\Lambda^{-2}$). It is the minimal ansatz beyond the LPA which includes a nonzero anomalous dimension at the QCP. The LPA is exact in the large-N limit (Sec. VI), and studies of the three-dimensional quantum Ising model ($N = 1$) suggest that it remains fairly accurate for all values of N (Blaizot *et al.*, 2007a, 2011a). To further simplify the analysis, we expand the effective potential $U_k(\rho)$ about the position $\rho_{0,k}$ of its minimum as in Eq. (95). There are strong indications that the LPA' is a good approximation even when it is supplemented by a truncation of the effective potential (Canet *et al.*, 2003). We shall see explicitly below that the truncated LPA' is accurate – and nearly exact in the renormalized classical regime – in the limit $N \to \infty$.

The propagator $G_k = (\Gamma_k^{(2)} + R_k)^{-1}$ in a constant field $\boldsymbol{\phi}$ is defined by its transverse and longitudinal parts,

$$\begin{aligned} G_{k,\rm T}^{-1}(q;\rho) &= Z_{A,k}\mathbf{q}^2 + V_{A,k}\omega_n^2 + U_k'(\rho) + R_k(q) \\ G_{k,\rm L}^{-1}(q;\rho) &= Z_{A,k}\mathbf{q}^2 + V_{A,k}\omega_n^2 + U_k'(\rho) \end{aligned} \tag{224}$$

$$+ 2\rho U_k''(\rho) + R_k(q),$$

In the disordered phase ($\rho_{0,k} = 0$), all modes exhibit a gap $m_k = (U_k'(0)/V_{A,k})^{1/2}$ (for $R_k(q) \to 0$) corresponding to a finite correlation length $\xi_k = c_k/m_k$ where $c_k = (Z_{A,k}/V_{A,k})^{1/2}$ is the renormalized velocity. In the ordered phase ($\rho_{0,k} > 0$), $U_k'(\rho_{0,k})$ vanishes and the transverse modes are gapless for $R_k(q) \to 0$ (Goldstone modes). The stiffness is defined by $\rho_{s,k} = 2Z_{A,k}\rho_{0,k}$ (see Sec. IV for a precise definition of $\rho_{s,k}$).

The derivation of the flow equations follows the method described in Sec. III. The effective potential satisfies the equation

$$\partial_t U_k(\rho) = \frac{1}{2}\int_q \partial_t R_k(q)[G_{k,\mathrm{L}}(q;\rho) + (N-1)G_{k,\mathrm{T}}(q;\rho)], \tag{225}$$

from which we can deduce the RG equations for $\rho_{0,k}$, δ_k and λ_k. The flow equations for $Z_{A,k}$ and $V_{A,k}$ are obtained by noting that

$$\begin{aligned} Z_{A,k} &= \lim_{q\to 0}\frac{\partial}{\partial \mathbf{q}^2}\Gamma^{(2)}_{k,\mathrm{T}}(q;\rho_{0,k}),\\ V_{A,k} &= \lim_{q\to 0}\frac{\partial}{\partial \omega_n^2}\Gamma^{(2)}_{k,\mathrm{T}}(q;\rho_{0,k}). \end{aligned} \tag{226}$$

The RG equations take the final form

$$\begin{aligned} \partial_t\rho_{0,k} &= -\frac{3}{2}I_{k,\mathrm{L}} - \frac{N-1}{2}I_{k,\mathrm{T}} \quad \text{if} \quad \rho_{0,k} > 0,\\ \partial_t\delta_k &= \frac{\lambda_k}{2}(N+2)I_{k,\mathrm{L}} \quad \text{if} \quad \rho_{0,k} = 0,\\ \partial_t\lambda_k &= -\lambda_k^2[9J_{k,\mathrm{LL}}(0) + (N-1)J_{k,\mathrm{TT}}(0)],\\ \partial_t Z_{A,k} &= -2\lambda_k^2\rho_{0,k}\frac{\partial}{\partial \mathbf{p}^2}[J_{k,\mathrm{TL}}(p) + J_{k,\mathrm{LT}}(p)]\big|_{p=0},\\ \partial_t V_{A,k} &= -2\lambda_k^2\rho_{0,k}\frac{\partial}{\partial \omega_n^2}[J_{k,\mathrm{TL}}(p) + J_{k,\mathrm{LT}}(p)]\big|_{p=0}, \end{aligned} \tag{227}$$

while the equation for the thermodynamic potential (per unit volume) $U_k(\rho_{0,k})$ is directly obtained from (225). We have introduced the threshold functions

$$\begin{aligned} I_{k,\alpha} &= \int_q \tilde{\partial}_t G_{k,\alpha}(q;\rho_{0,k}),\\ J_{k,\alpha\beta}(p) &= \int_q [\tilde{\partial}_t G_{k,\alpha}(q;\rho_{0,k})]G_{k,\beta}(p+q;\rho_{0,k}), \end{aligned} \tag{228}$$

with $\alpha,\beta = \mathrm{L},\mathrm{T}$. The operator $\tilde{\partial}_t = (\partial_t R_k)\partial_{R_k}$ acts only on the t dependence of the cutoff function R_k. The propagators $G_{k,\mathrm{L}}(q;\rho_{0,k})$ and $G_{k,\mathrm{T}}(q;\rho_{0,k})$ are given by (224) with $U_k'(\rho_{0,k}) = \delta_k$ and $U_k''(\rho_{0,k}) = \lambda_k$.

To make the fixed point manifest when the system is critical, we introduce the dimensionless variables

$$\begin{aligned} &\tilde{\rho}_{0,k} = k^{1-d}(Z_{A,k}V_{A,k})^{1/2}\rho_{0,k}, \quad \tilde{\delta}_k = (Z_{A,k}k^2)^{-1}\delta_k,\\ &\tilde{\lambda}_k = k^{d-3}Z_{A,k}^{-3/2}V_{A,k}^{-1/2}\lambda_k, \quad \tilde{T}_k = T/c_k k \end{aligned} \tag{229}$$

as well as the running anomalous dimensions

$$\eta_k = -\partial_t \ln Z_{A,k}, \quad \tilde{\eta}_k = -\partial_t \ln V_{A,k}. \tag{230}$$

For the sake of generality, we consider here an arbitrary space dimension d. The dimensionless flow equations are given in (Rançon *et al.*, 2013). We can define a running dynamical critical exponent $z_k = [\tilde{T}_k]$ from $[Z_{A,k}] = \eta_k$, $[V_{A,k}] = \tilde{\eta}_k$ and $[T] = 0$:

$$z_k = 1 - \frac{\eta_k - \tilde{\eta}_k}{2}. \tag{231}$$

The (true) dynamical critical exponent is defined by $z = \lim_{k\to 0} z_k$.[55]

In the zero-temperature limit, we recover the flow equations of the $(d+1)$-dimensional classical O(N) model in the LPA' (Sec. III.B). Lorentz invariance ensures that $\eta_k = \tilde{\eta}_k$ for all values of k. z_k remains equal to unity and there is no renormalization of the velocity: $c_k = c_\Lambda$ (which we denote merely by c in the following). The QCP is reached by fine tuning r_0 to a critical value r_{0c} (with u_0 and c fixed). Critical fluctuations show up in the RG flow below the Ginzburg momentum scale $k_G \sim cu_0N$. In the vicinity of the QCP, we can define an energy scale $\Delta \equiv \Delta(r_0)$ which vanishes as $r_0 \to r_{0c}$. When $r_0 > r_{0c}$, the ground state is disordered and we choose Δ to be equal to the $T = 0$ excitation gap $m_{k=0}$ of the $\boldsymbol{\varphi}$ field. $\xi = c/\Delta$ is then the correlation length. When $r_0 < r_{0c}$ it is convenient to take Δ negative such that $-\Delta$ is the excitation gap in the disordered phase at the point located symmetrically with respect to the QCP, i.e. $|\Delta(r_0)| = m_{k=0}(2r_{0c} - r_0)$. $|\Delta|$ is then proportional to the stiffness ρ_s, the ratio $|\Delta|/\rho_s$ being universal (Rançon *et al.*, 2013). The length $c/|\Delta|$ is of the order of the Josephson length $\xi_J = c/\rho_s$. The latter separates the critical regime $k_J \ll k \ll k_G$ from the Goldstone regime $k \ll k_J = \xi_J^{-1}$ dominated by the Goldstone modes. With these definitions, Δ varies from negative to positive values as we go across the QCP coming from the ordered phase.

At finite temperatures, in addition to the characteristic momentum scale $k_\Delta = |\Delta|/c$, one must also consider the thermal length $k_T = 2\pi T/c$ associated to the crossover between the quantum ($k \gg k_T$) and classical ($k \ll k_T$) regimes. In the latter, only classical (thermal) fluctuations ($\omega_n = 0$) contribute to the RG flow. The three regimes of the phase diagram in Fig. 32 (top panel) are defined by $k_T \gg k_\Delta$ (quantum critical), $k_T \ll k_\Delta$ and $r_0 > r_{0c}$ (quantum disordered), and $k_T \ll k_\Delta$ and $r_0 < r_{0c}$ (renormalized classical).

In the following, we discuss only the universal part of the flow $k \ll k_G$.

---

[55] At criticality, where $Z_{A,k} \sim k^{-\eta}$ and $V_{A,k} \sim k^{-\tilde{\eta}}$, $Z_{A,k}\mathbf{p}^2 + V_{A,k}\omega^2 \sim k^{-\eta}\mathbf{p}^2 + k^{-\tilde{\eta}}\omega^2$. If we identify k with $|\mathbf{p}|$, we find that ω scales like $|\mathbf{p}|^z$ with $z = 1 - (\eta - \tilde{\eta})/2$.

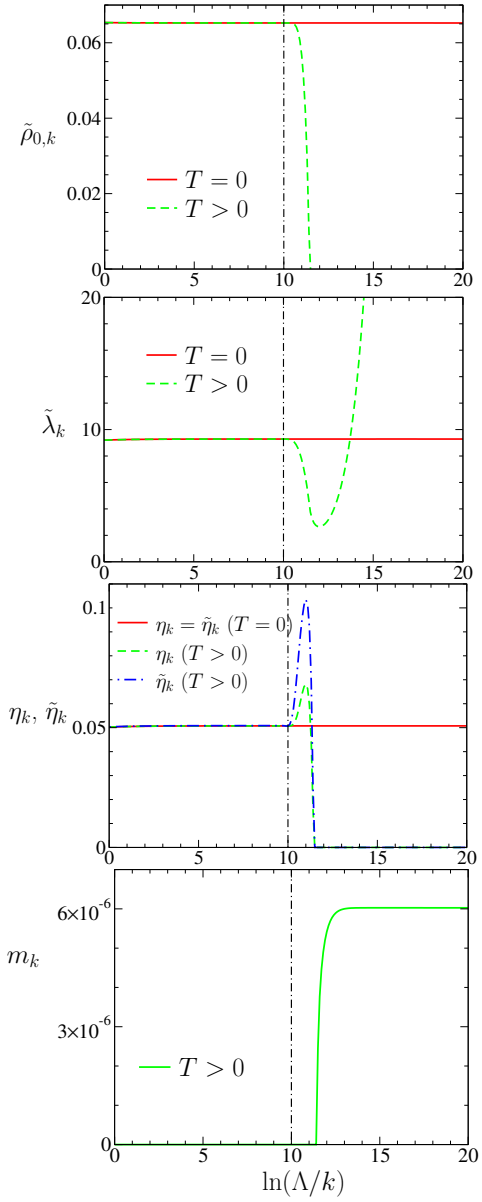

FIG. 33 (Color online) RG flows in the quantum critical regime ($d = 2$ and $N = 3$) (Rançon *et al.*, 2013). The vertical dash-dotted line shows the thermal momentum scale $k_T = \Lambda e^{-10}$. [$\Lambda = c_\Lambda = 1$, $u_0 = 27.6$, $r_{0c} \simeq 0.065355$.]

1. Quantum critical regime

The RG flow in the quantum critical regime is shown in Fig. 33 for $N = 3$. The parameters of the microscopic action (220) are chosen such that the initial value Λ of the momentum cutoff is of the order of the Ginzburg scale k_G. At the QCP ($r_0 = r_{0c}$) and for $T = 0$, we observe plateaus characteristic of critical behavior: $\tilde{\rho}_{0,k} \sim \tilde{\rho}^*_{\rm crit}$, $\tilde{\lambda}_k \sim \tilde{\lambda}^*_{\rm crit}$, and $\eta_k = \tilde{\eta}_k = \eta$ (with η the anomalous dimension at the three-dimensional Wilson-Fisher fixed point). The LPA' gives $\nu \simeq 0.699$ and $\eta = 0.0507$, to be compared with the best estimates for the three-dimensional O(3) model obtained from resummed perturbative calculations ($\nu \simeq 0.7060$, $\eta = 0.0333$), Monte Carlo simulations ($\nu \simeq 0.7112$, $\eta = 0.0375$), or the NPRG in the BMW approximation ($\nu \simeq 0.715$, $\eta = 0.040$) (see tables III and V).

At finite temperatures, the flow is modified when k becomes smaller than the thermal scale k_T: $\tilde{\rho}_{0,k}$ and $\eta_k, \tilde{\eta}_k$ rapidly vanish while $\tilde{\lambda}_k$ diverges; the (dimensionful) order parameter $\rho_{0,k}$ vanishes and $m_k = \sqrt{\delta_k / V_{A,k}}$ takes a finite value (indicating that the system is in a disordered phase). Near k_T, η_k and $\tilde{\eta}_k$ differ, implying a breakdown of Lorentz invariance, but the velocity is only weakly renormalized (Rançon *et al.*, 2013).

2. Quantum disordered regime

Figure 34 shows the flow in the quantum disordered regime. At $T = 0$, the critical flow terminates at $k \sim k_\Delta$. For $k \lesssim k_\Delta$, $\tilde{\rho}_{0,k}$ and $\eta_k = \tilde{\eta}_k$ vanish while $\tilde{\lambda}_k$ diverges; the (dimensionful) order parameter $\rho_{0,k}$ vanishes and $m_k = \sqrt{\delta_k / V_{A,k}}$ takes a finite value. As expected, a finite temperature has hardly any effect on the flow when $k_T \ll k_\Delta$. Only for $k_T \sim k_\Delta$ (i.e. near the crossover to the quantum critical regime) do we observe a modification of the $T = 0$ flow.

3. Renormalized classical regime

The flow in the renormalized classical regime is shown in Fig. 35. The plateaus observed for $k \gg k_J \sim \Lambda e^{-10}$ in $\tilde{\rho}_{0,k}$, $\tilde{\lambda}_k$ and $\eta_k, \tilde{\eta}_k$ show that the behavior of the system at sufficiently high energies (or short distances) is critical. This critical regime terminates at the Josephson scale k_J. For $k \ll k_J$, longitudinal fluctuations are suppressed (the (dimensionless) mass $2\tilde{\lambda}_k \tilde{\rho}_{0,k}$ of the longitudinal mode is much larger than unity) and the flow is dominated by the Goldstone modes. The anomalous dimensions η_k and $\tilde{\eta}_k$ then nearly vanish and the dimensionless interaction $\tilde{\lambda}_k$ exhibits a second plateau whose physical meaning is discussed below. At finite temperatures, this plateau terminates at the thermal scale k_T with $\tilde{\lambda}_k$ vanishing for $k \ll k_T$.

In the Goldstone regime, the flow equations simplify into

$$\begin{aligned} \partial_t \tilde{\rho}_{0,k} &= \left(1 - d - \frac{\eta_k + \tilde{\eta}_k}{2}\right) \tilde{\rho}_{0,k} - \frac{N-1}{2} \tilde{I}_{k,\mathrm{T}}, \\ \partial_t \tilde{\lambda}_k &= (d-3)\tilde{\lambda}_k - \tilde{\lambda}_k^2 (N-1) \tilde{J}_{k,\mathrm{TT}}(0), \end{aligned} \tag{232}$$

where $\tilde{I}_{k,\mathrm{T}}$ and $\tilde{J}_{k,\mathrm{TT}}$ are dimensionless threshold functions.[56] $\tilde{\rho}_{0,k}$ becomes very large in the renormalized clas-

[56] We refer to (Rançon *et al.*, 2013) for a detailed discussion of the dimensionless threshold functions.

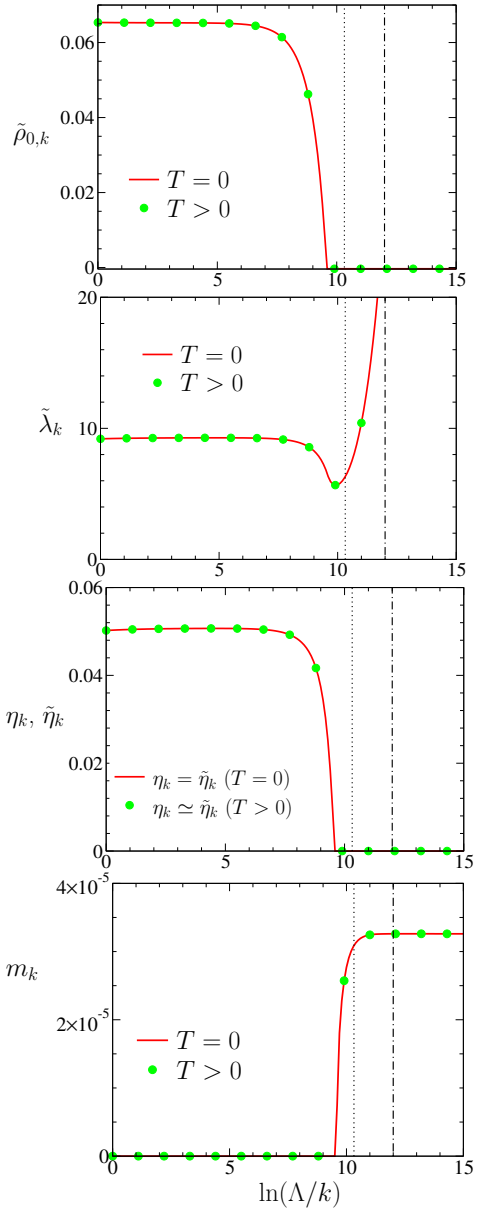

FIG. 34 (Color online) Same as Fig. 33 but in the quantum disordered regime ($r_0 = r_{0c}(1 - 10^{-6})$) (Rançon *et al.*, 2013). The dotted and dash-dotted vertical lines show the momentum scales k_Δ and $k_T = \Lambda e^{-12}$, respectively.

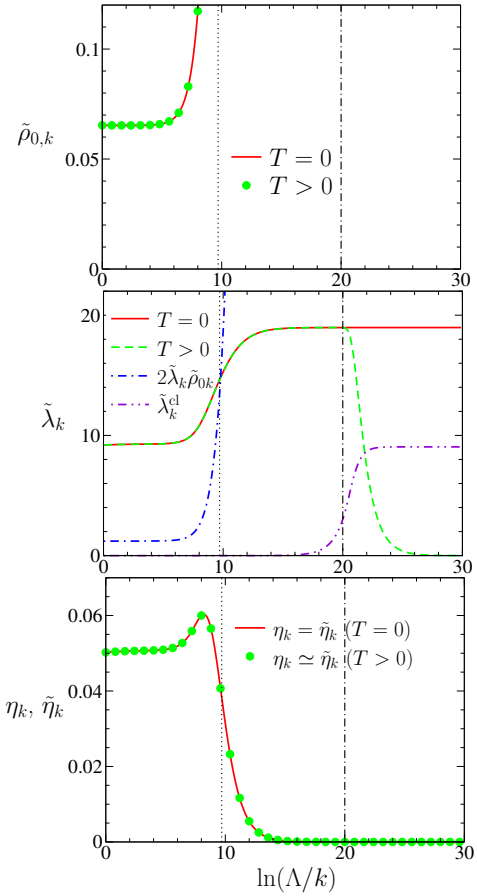

FIG. 35 (Color online) Same as Fig. 33 but in the renormalized classical regime ($r_0 = r_{0c}(1 + 10^{-5})$) (Rançon *et al.*, 2013). The dotted and dash-dotted vertical lines show the momentum scales k_J and $k_T = \Lambda e^{-20}$, respectively.

sical regime. Although η_k and $\tilde{\eta}_k$ are very small in the Goldstone regime, the term $(\eta_k + \tilde{\eta}_k)\tilde{\rho}_{0,k}$ is of order 1 and must be kept. For k smaller than the inverse correlation length ξ^{-1}, $\tilde{\rho}_{0,k}$ will ultimately vanish, but ξ being exponentially large this is not seen in Fig. 35.

For $k_T \ll k \ll k_J$ (quantum Goldstone regime), we find the fixed-point value

$$\tilde{\lambda}^* = \frac{d-3}{(N-1)\tilde{J}_{k,\mathrm{TT}}(0)} = \frac{4\pi^{3/2}}{(N-1)(2-\sqrt{2})}, \qquad (233)$$

where the last value is obtained for $d = 2$. This fixed-point value shows up as a plateau $\tilde{\lambda}_k \simeq \tilde{\lambda}^*$ for $k_T \ll k \ll k_J$, which should not be confused with the plateau $\tilde{\lambda}_k \simeq \tilde{\lambda}^*_{\rm crit}$ corresponding to the critical regime $k_J \ll k \ll k_G$ (Fig. 35). As discussed in Sec. III.B.4, the constant value $\tilde{\lambda}_k \simeq \tilde{\lambda}^*$ and the diverging $\tilde{\rho}_{0,k} \sim k^{1-d}$ (corresponding to a constant value of the order parameter $\rho_{0,k}$) imply a divergence of the longitudinal propagator in the infrared limit: $G_{\rm L}(p) \sim 1/(\omega_n^2 + c^2\mathbf{p}^2)^{(3-d)/2}$ for $k_T \ll |\mathbf{p}|, |\omega_n|/c \ll k_J$ and $d < 3$ (the vanishing is logarithmic for $d = 3$) (Sachdev, 1999; Zwerger, 2004).[57,58]

In the classical Goldstone regime $\xi^{-1} \ll k \ll k_T$, the flow is dominated by classical ($\omega_n = 0$) transverse fluctuations and $\tilde{\lambda}_k$ vanishes linearly with k. Since only the classical component $\boldsymbol{\phi}(\mathbf{r}) \equiv \boldsymbol{\phi}(\mathbf{r}, i\omega_n = 0)/\sqrt{\beta}$ of the field

[57] The divergence of the longitudinal propagator $G_{\rm L}(p)$ can be deduced from (124) with the replacement $d \to d + 1$ and $\mathbf{p}^2 \to \mathbf{p}^2 + \omega_n^2/c^2$.

[58] This implies that the (retarded) longitudinal propagator $G^R_{\rm L}(\mathbf{p}, \omega) \sim 1/(\omega^2 - c^2\mathbf{p}^2)^{(3-d)/2}$ has no pole-like structure but a branch cut, and the dynamical structure factor exhibits a critical continuum above the usual delta peak $\delta(\omega - c|\mathbf{p}|)$ due to the Goldstone modes.

matters, the effective action (223) becomes

$$\Gamma_k^{\rm cl}[\boldsymbol{\phi}] = \beta \int d^d r \left\{ \frac{Z_{A,k}}{2} (\boldsymbol{\nabla}\boldsymbol{\phi})^2 + \frac{\lambda_k}{2} (\rho - \rho_{0,k})^2 \right\} \quad (234)$$

for $\rho_{0,k} > 0$. Rescaling the field $\boldsymbol{\phi} \to \sqrt{T}\boldsymbol{\phi}$, we obtain the usual form

$$\Gamma_k^{\rm cl}[\boldsymbol{\phi}] = \int d^d r \left\{ \frac{Z_{A,k}}{2} (\boldsymbol{\nabla}\boldsymbol{\phi})^2 + \frac{\lambda_k^{\rm cl}}{2} (\rho - \rho_{0,k})^2 \right\} \quad (235)$$

of the effective action for a classical model in the LPA', with the coupling constant $\lambda_k^{\rm cl} = T\lambda_k$. The appropriate dimensionless variable

$$\tilde{\lambda}_k^{\rm cl} = \lambda_k^{\rm cl} Z_{A,k}^{-2} k^{d-4} \quad (236)$$

satisfies the RG equation

$$\partial_t \tilde{\lambda}_k^{\rm cl} = (d-4)\tilde{\lambda}_k^{\rm cl} - (N-1)\tilde{J}_{k,\rm TT}^{\rm cl}(0)(\tilde{\lambda}_k^{\rm cl})^2 \quad (237)$$

with the threshold function $\tilde{J}_{k,\rm TT}^{\rm cl} = \tilde{T}_k^{-1}\tilde{J}_{k,\rm TT}$.[56] This equation admits the fixed-point value

$$\tilde{\lambda}^{\rm cl*} = \frac{d-4}{(N-1)\tilde{J}_{k,\rm TT}^{\rm cl}(0)} = \frac{4\pi}{(N-1)\ln 2}, \quad (238)$$

where the last value is obtained for $d = 2$ (see Fig. 35). We deduce that, for $\xi^{-1} \ll |\mathbf{p}| \ll k_T$ and $d < 4$, the longitudinal propagator $G_{k=0,\rm L}(\mathbf{p}, i\omega_n = 0)$ diverges as $1/|\mathbf{p}|^{4-d}$ (see Sec. III.B.4).

Goldstone regime and NLσM. In the Goldstone regime $\xi^{-1} \ll k \ll k_J$, be it quantum ($k \gg k_T$) or classical ($k \ll k_T$), we expect an effective NLσM description to hold. In Sec. III.B.3.b, we have shown that the coupling constant of the NLσM is simply $\tilde{g}_k = 1/2\tilde{\rho}_{0,k}$. It therefore satisfies the RG equation

$$\partial_t \tilde{g}_k = -\left(1 - d - \frac{\eta_k + \tilde{\eta}_k}{2}\right)\tilde{g}_k + (N-1)\tilde{I}_{k,\rm T}\tilde{g}_k^2. \quad (239)$$

This equation should be considered together with the RG equation of the dimensionless temperature $\tilde{T}_k = T/c_k k$,

$$\partial_t \tilde{T}_k = -\left(1 - \frac{\eta_k - \tilde{\eta}_k}{2}\right)\tilde{T}_k. \quad (240)$$

Following Chakravarty *et al.* (Chakravarty *et al.*, 1989), we consider the coupling constants $\tilde{g}_k$ and $\tilde{t}_k = \tilde{g}_k\tilde{T}_k$ (rather than $\tilde{g}_k$ and $\tilde{T}_k$), with

$$\partial_t \tilde{t}_k = -(2 - d - \eta_k)\tilde{t}_k + (N-1)\tilde{I}_{k,\rm T}\tilde{g}_k\tilde{t}_k. \quad (241)$$

In the quantum Goldstone regime $k \gg k_T$, the system is effectively in the zero-temperature limit since $\tilde{T}_k \ll 1$. In this limit, Eq. (239) becomes[59]

$$\partial_t \tilde{g}_k = -(1-d)\tilde{g}_k - 2\frac{K_{d+1}}{d+1}(N-2)\tilde{g}_k^2 \quad (242)$$

($K_d(2\pi)^d = 4v_d(2\pi)^d$ is the surface of the d-dimensional unit sphere), which is nothing but the RG equation of the $(d+1)$-dimensional classical NLσM. In particular, we find that the $\mathcal{O}(\tilde{g}_k^2)$ term vanishes for the O(2) model ($N = 2$) as expected. However the coefficient of $(N-2)\tilde{g}_k^2$ depends on the RG scheme (i.e. the regular function R_k) and in general differs from the result of (Chakravarty *et al.*, 1989) obtained with a sharp momentum cutoff. Only in one dimension do we recover the result of (Chakravarty *et al.*, 1989), in agreement with the fact that the beta function of the classical two-dimensional NLσM is universal (i.e. independent of the RG scheme) to one- and two-loop orders (Friedan, 1985).

There is a quantum classical crossover when $k \sim k_T$, and for $k \ll k_T$ the system is governed by an effective classical NLσM with coupling constant $\tilde{t}_k$ (Chakravarty *et al.*, 1989). The latter satisfies the RG equation[59]

$$\partial_t \tilde{t}_k = -(2-d)\tilde{t}_k - 2\frac{K_d}{d}(N-2)\tilde{t}_k^2 \quad (243)$$

of the d-dimensional classical NLσM. Again, for $d = 2$, we find a perfect agreement with the results of (Chakravarty *et al.*, 1989), including the coefficient of the $(N-2)\tilde{t}_k^2$ term, due to the universality of the one-loop beta function in that case.

C. Universal thermodynamics

In the critical regime $|\Delta|, T \ll ck_G$ near the QCP, the pressure of the two-dimensional quantum O(N) model writes

$$P(T) = P(0) + N\frac{T^3}{c^2}\mathcal{F}_N\left(\frac{\Delta}{T}\right), \quad (244)$$

where $\mathcal{F}_N$ is a universal scaling function, c the velocity of the critical fluctuations at the QCP and $|\Delta| \equiv |\Delta(r_0)|$ the characteristic zero temperature energy scale defined in Sec. XII.B. In addition to $\mathcal{F}_N$, one can compute the universal scaling function which determines the excitation gap

$$m(T) = TF_N\left(\frac{\Delta}{T}\right) \quad (245)$$

[59] Eqs. (242) and (243) are obtained using a regulator function $R_k(\mathbf{q})$ acting only on momenta. We refer to (Rançon *et al.*, 2013) for a detailed discussion of the conditions under which Eqs. (242,243) hold.

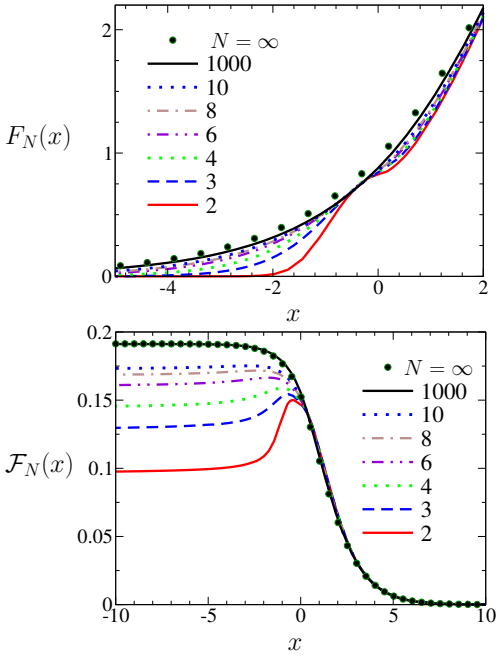

FIG. 36 (Color online) Universal scaling functions F_N and $\mathcal{F}_N$ for various values of N obtained from the NPRG (Rançon *et al.*, 2013). The black points show the analytic results (246) in the limit $N \to \infty$.

at finite temperatures. In the limit $N \to \infty$ (taken with $u_0 N$ fixed), the scaling functions can be computed exactly (Rançon *et al.*, 2013),

$$F_\infty(x) = 2\,\mathrm{asinh}\left(\frac{1}{2}e^{x/2}\right),$$
$$\mathcal{F}_\infty(x) = \frac{1}{2\pi}\left[\frac{x^3}{12}\Theta(x) - \frac{x}{4}F_\infty(x)^2 + \frac{1}{6}F_\infty(x)^3 \right. \quad (246)$$
$$\left. + F_\infty(x)\mathrm{Li}_2\left(e^{-F_\infty(x)}\right) + \mathrm{Li}_3\left(e^{-F_\infty(x)}\right)\right].$$

$\mathrm{Li}_s(z)$ is a polylogarithm,

$$\mathrm{Li}_s(z) = \sum_{k=1}^{\infty}\frac{z^k}{k^s}, \quad (z \in \mathbb{C},\ |z| < 1), \qquad (247)$$

and $\Theta(x)$ denotes the step function. It should be noted that the scaling function $F_\infty(x)$ as well as $\mathcal{F}_\infty(0)$ agree with results obtained from the NLσM in the large-N limit (Chubukov *et al.*, 1994; Sachdev, 1993, 2011).

Once the QCP is located and the energy scale Δ determined as a function of $r_0 - r_{0c}$, one can compute the gap $m(T)$ and the pressure $P(T)$, and deduce the universal scaling functions $F_N(x)$ and $\mathcal{F}_N(x)$ [Eqs. (245,244)]. Figure 36 shows the universal scaling functions F_N and $\mathcal{F}_N$ for various values of N. In the limit $N \to \infty$, the truncated LPA' slightly differs from the exact result for the excitation gap $m(T)$ but turns out to be extremely accurate for the computation of the pressure $P(T)$ (the LPA' would be exact without the truncation of $U_k(\rho)$).

TABLE VIII $\tilde{\mathcal{C}}_N/N$ as obtained from the NPRG and the large-N approach [Eq. (250)].

N	1000	10	8	6	4	3	2
$\tilde{\mathcal{C}}_N/N$ to $\mathcal{O}(1/N)$	0.800	0.767	0.758	0.744	0.716	0.689	0.633
$\tilde{\mathcal{C}}_N/N$ (NPRG)	0.812	0.796	0.793	0.788	0.781	0.775	0.767

For smaller values of N, F_N and $\mathcal{F}_N$ differ significantly from the $N \to \infty$ limit. While the large-N result remains a good approximation in the quantum disordered regime, it becomes inaccurate in the quantum critical and renormalized classical regimes. In particular, it misses the nonmonotonic behavior of $\mathcal{F}_N(x)$ in the quantum critical regime ($|x|$ *lesssim*1) for $N \lesssim 10$. The possibility of such a nonmonotonic behavior is discussed in (Neto and Fradkin, 1993).

In the renormalized classical regime, it is possible to reinterpret the large-N result so that it becomes consistent with the NPRG approach even for small values of N. Since the correlation length ξ is exponentially large, we expect the thermodynamics to be dominated by the $N-1$ modes corresponding to transverse fluctuations to the local order. In the NPRG approach, these modes show up as Goldstone modes as long as $\rho_{0,k} > 0$ (i.e. $k \gtrsim \xi^{-1}$) and dominate the RG flow as in the large-N approach. Since $N-1$ is identified with N in the large-N approach, the latter overestimates the pressure, and therefore the scaling function $\mathcal{F}_N$, by a factor $N/(N-1)$. The large-N result, when rescaled by a factor $(N-1)/N$, is indeed consistent with the NPRG approach (Rançon *et al.*, 2013). This shows that in the renormalized classical regime

$$P(T) \simeq (N-1)\frac{\zeta(3)}{2\pi}\frac{T^3}{c^2}, \qquad (248)$$

which is nothing but the pressure of $N-1$ free bosonic modes with dispersion $\omega = c|\mathbf{q}|$. The very small excitation gap of the transverse fluctuations ($m \ll T$) does not influence the thermodynamics. For $N = 2$ and $N = 3$, Eq. (248) agrees with a RG analysis of the non-linear sigma model (NLσM) (Hofmann, 2010, 2014).

Of particular interest is the temperature variation of the pressure at the QCP ($\Delta = 0$). Following (Sachdev, 1993), we express the pressure as

$$P(T) = P(0) + \frac{\zeta(3)}{2\pi}\tilde{\mathcal{C}}_N\frac{T^3}{c^2} \qquad (249)$$

for $\Delta = 0$, where $\tilde{\mathcal{C}}_N = N 2\pi \mathcal{F}_N(0)/\zeta(3)$. In the large-$N$ limit (Chubukov *et al.*, 1994),

$$\frac{\tilde{\mathcal{C}}_N}{N} \simeq \frac{4}{5} - \frac{0.3344}{N} + \mathcal{O}\left(N^{-2}\right). \qquad (250)$$

The agreement between the $\mathcal{O}(1/N)$ result and the NPRG one rapidly deteriorates for $N \lesssim 10$ (Table VIII).

D. "Higgs" amplitude mode

In the broken-symmetry phase we expect, in additional to the $N-1$ Goldstone modes, a gapped amplitude "Higgs" mode. In the preceding sections, we have seen that this mode does not show up in the longitudinal propagator when $d < 3$. Because of the inevitable coupling between longitudinal and transverse fluctuations, the longitudinal propagator is dominated by Goldstone modes and singular at small $\mathbf{p}, \omega_n$ when $1 < d < 3$. This infrared divergence is likely to mask any resonance due to the amplitude mode. As pointed out by (Podolsky *et al.*, 2011), this does not necessarily imply that a Higgs resonance cannot be observed. The O(N)-invariant scalar susceptibility

$$\chi_s(p) = \int_0^\beta d\tau \int d^d r\, e^{-i(\mathbf{p}\cdot\mathbf{r}-\omega_n\tau)} \times \left[\langle \boldsymbol{\varphi}(\mathbf{r},\tau)^2 \boldsymbol{\varphi}(0,0)^2\rangle - \langle \boldsymbol{\varphi}(0,0)^2\rangle^2\right] \quad (251)$$

has a spectral function which vanishes as ω^{d+1} for $\mathbf{p} = 0$ and is therefore a good candidate for the observation of the Higgs resonance. Nevertheless, since the Higgs mode can decay into two Goldstone modes, there is no guarantee that it is a well-defined (long-lived) excitation in particular near the QCP.

In three dimensions, where the effective field theory is four-dimensional and noninteracting at the QCP, the Higgs resonance becomes sharper and sharper as the QCP is approached. This has been beautifully confirmed in the quantum antiferromagnet $TlCuCl_3$ (Rüegg *et al.*, 2008) and in cold atoms (Bissbort *et al.*, 2011). In two dimensions, the field theory is strongly coupled at the QCP and the existence of a Higgs resonance is not guaranteed. Nevertheless, a signature of the Higgs mode has recently been observed in a two-dimensional Bose gas in an optical lattice in the vicinity of the superfluid–Mott-insulator transition (Endres *et al.*, 2012).

The Higgs mode near a two-dimensional relativistic QCP has been studied with various techniques: large-N expansion (Podolsky and Sachdev, 2012), quantum Monte Carlo simulations (Chen *et al.*, 2013; Gazit *et al.*, 2013a,b; Pollet and Prokof'ev, 2012), NPRG (Rançon and Dupuis, 2014; Rose *et al.*, 2015) and $\epsilon = 4-(d+1)$ expansion about $d = 3$ (Katan and Podolsky, 2015). For $N = 2$ and $N = 3$, these studies have conclusively shown that the Higgs resonance shows up in the scalar susceptibility and remains a well-defined excitation arbitrary close to the QCP. Here we discuss the NPRG approach of (Rose *et al.*, 2015) based on the BMW approximation and restrict ourselves to the zero temperature limit where the 2D quantum model is equivalent to the 3D classical model. The spectral function $\chi_s''(\omega) = \Im[\chi_s(\mathbf{p}=0, i\omega_n \to \omega + i0^+)]$ of the quantum model can be simply obtained from the scalar susceptibility $\chi_s(\mathbf{p})$ of the classical model by an analytical continuation: $\chi_s''(\omega) = \chi_s(|\mathbf{p}| \to -i\omega + 0^+)$.[60] In the following, we therefore discuss the 3D classical O(N) model but, having in mind the 2D quantum model, we shall refer to the critical point of the classical model as the QCP.

Since the composite field $\boldsymbol{\varphi}^2(\mathbf{r})$ has scaling dimension $3 - 1/\nu$ at the QCP, standard scaling arguments imply that the $T = 0$ spectral function can be written in the form (Podolsky and Sachdev, 2012)

$$\chi_s''(\omega) = \mathcal{A}_\pm \Delta^{3-2/\nu} \Phi_{s,\pm}\left(\frac{\omega}{\Delta}\right), \quad (252)$$

where the index $+/-$ refers to the disordered and ordered phases, respectively. Δ is chosen as in the preceding sections except for the sign: we now take Δ to be positive in both the ordered and disordered $T = 0$ phases. $\mathcal{A}_\pm$ is a nonuniversal cutoff-dependent constant while $\Phi_{s,\pm}(x)$ is a universal scaling function. Since $\chi_s''(\omega)$ must become independent of Δ when $\Delta \to 0$, we must have $\Phi_{s,\pm}(x) \sim x^{3-2/\nu}$ for $x \gg 1$. In the ordered phase, the low-energy behavior $\omega \ll \Delta$ is entirely determined by the Goldstone modes and $\chi_s''(\omega) \sim \omega^3$ (Podolsky and Sachdev, 2012), i.e. $\Phi_{s,-}(x) \sim x^3$. In the disordered phase, the system is gapped and we expect $\chi_s''(\omega)$ to vanish for $\omega < 2\Delta$, i.e. $\Phi_{s,+}(x) \propto \Theta(x-2)$. (Since $\chi_s''(\omega) = -\chi_s''(-\omega)$ is odd, we discuss only the positive frequency part.)

The spectral function can be computed exactly in the large-N limit ($N \to \infty$ with $u_0 N$ fixed) (Podolsky *et al.*, 2011). In the scaling limit $|\omega| \ll ck_G$ ($k_G \sim cu_0 N$ is the Ginzburg momentum scale introduced in Sec. XII.B), one finds that

$$\chi_s''(\omega) = \frac{1}{N}\left(\frac{12}{cu_0}\right)^2 \frac{4\omega^3}{\omega^2 + \left(\frac{4\Delta}{\pi}\right)^2} \quad (253)$$

crosses over from a ω^3 dependence at small ω to a linear behavior at large ω with no sign of a Higgs resonance. $1/N$ corrections seem to indicate a peak in $\chi_s''(\omega)$ at finite frequency in the scaling limit (Podolsky and Sachdev, 2012).

To compute the scalar susceptibility, we introduce a source term $-\int d^3r\, h\boldsymbol{\varphi}^2$ in the action of the 3D classical O(N) model, so that

$$\chi_s(\mathbf{p}) = \left.\frac{\delta^2 \ln Z[h]}{\delta h(-\mathbf{p})\delta h(\mathbf{p})}\right|_{h=0}, \quad (254)$$

where $Z[h]$ is the source-dependent partition function of the system. The effective action $\Gamma[\boldsymbol{\phi}, h]$ becomes a

[60] The analytical continuation is performed using a Padé approximant method (Vidberg and Serene, 1977).

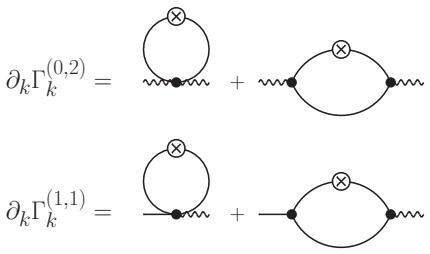

FIG. 37 Diagrammatic representation of the flow equations satisfied by the vertices $\Gamma_k^{(0,2)}$ and $\Gamma_k^{(1,1)}$ (signs and symmetry factors are not shown). The vertex $\Gamma_k^{(n,m)}$ is represented by a black dot with n solid lines and m wavy lines, and the cross stands for $\partial_k R_k$.

functional of both the order parameter $\boldsymbol{\phi} = \langle \boldsymbol{\varphi} \rangle$ and the source h. The scalar susceptibility can be expressed as (Rançon and Dupuis, 2014; Rose *et al.*, 2015)

$$\chi_s(\mathbf{p}) = -\Gamma^{(0,2)}(\mathbf{p}, \bar{\boldsymbol{\phi}}) + \sum_{i,j} \Gamma_i^{(1,1)}(\mathbf{p}, \bar{\phi}) \times \Gamma_{ij}^{(2,0)-1}(\mathbf{p}, \bar{\boldsymbol{\phi}}) \Gamma_j^{(1,1)}(\mathbf{p}, \bar{\phi}), \tag{255}$$

where $|\bar{\boldsymbol{\phi}}| = \sqrt{2\rho_0}$ is the order parameter for $h = 0$ and we have introduced the vertices

$$\Gamma^{(0,2)}(\mathbf{p}, \phi) = \left. \frac{\delta^2 \Gamma[\boldsymbol{\phi}, h]}{\delta h(-\mathbf{p}) \delta h(\mathbf{p})} \right|_{\boldsymbol{\phi}=\text{const}, h=0},$$
$$\Gamma_i^{(1,1)}(\mathbf{p}, \phi) = \left. \frac{\delta^2 \Gamma[\boldsymbol{\phi}, h]}{\delta \phi_i(-\mathbf{p}) \delta h(\mathbf{p})} \right|_{\boldsymbol{\phi}=\text{const}, h=0}. \tag{256}$$

Since $\boldsymbol{\phi}$ transforms like a vector under O(N) rotations while h is a scalar,

$$\Gamma_i^{(1,1)}(\mathbf{p}, \boldsymbol{\phi}) = \phi_i f(\mathbf{p}, \rho),$$
$$\Gamma^{(0,2)}(\mathbf{p}, \boldsymbol{\phi}) = \gamma(\mathbf{p}, \rho), \tag{257}$$

where f and γ are functions of the O(N) invariant ρ. To determine the scalar susceptibility in the NPRG approach, we must therefore consider the k-dependent vertices $\Gamma_k^{(0,2)}$ and $\Gamma_k^{(1,1)}$ or, equivalently, the k-dependent functions $f_k(\mathbf{p}, \rho)$ and $\gamma_k(\mathbf{p}, \rho)$.

$\Gamma_k^{(0,2)}$ and $\Gamma_k^{(1,1)}$ satisfy the RG equations shown diagrammatically in Fig. 37. More generally, denoting by $\Gamma_k^{(n,m)}$ the vertex obtained by taking n (m) functional derivatives wrt $\boldsymbol{\phi}$ (h) of the scale-dependent effective action $\Gamma_k[\boldsymbol{\phi}]$, we find that $\partial_k \Gamma_k^{(n,m)}$ involves $\Gamma_k^{(n+1,m)}$ and $\Gamma_k^{(n+2,m)}$. This infinite hierarchy of equations can be closed using the BMW approximation, which amounts to neglecting the momentum in the 3- and 4-point vertices appearing in the RG equations $\partial_k \Gamma_k^{(0,2)}$ and $\partial_k \Gamma_k^{(1,1)}$ shown in Fig. 37 (see Sec. V for a detailed discussion of the BMW approximation) (Rose *et al.*, 2015). This yields two coupled equations for the functions f_k and γ_k [Eq. (257)], which must be solved together with the BMW equations for the 2-point vertex $\Gamma_k^{(2,0)}$ (see Sec. V). These equations are exact in the large-N limit and reproduce (253) in the scaling limit.

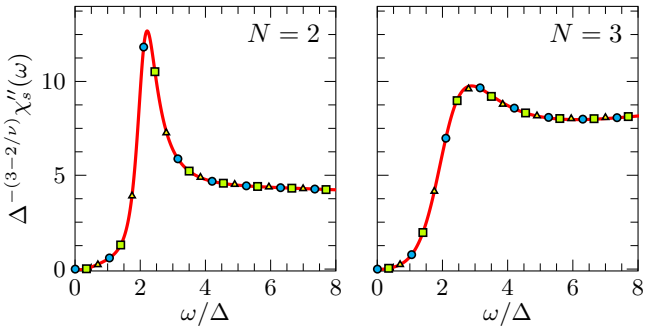

FIG. 38 (Color online) Spectral function $\chi_s''(\omega)$ of the scalar susceptibility in the ordered phase for $N = 2$ and $N = 3$ (Rose *et al.*, 2015). The solid line and the symbols corresponds to different values of $r_0 - r_{0c}$.

TABLE IX Universal ratio m_H/Δ obtained from NPRG, (Q)MC and ϵ expansion.

N	3	2
NPRG (Rose *et al.*, 2015)	2.7	2.2
MC (Gazit *et al.*, 2013a)	2.2(3)	2.1(3)
QMC (Chen *et al.*, 2013)		3.3(8)
ϵ expansion (Katan and Podolsky, 2015)	1.64	1.67

Figure 38 shows the universal scaling function $\Phi_{s,-}''(x)$ in the ordered phase for $N = 2$ and $N = 3$. The various curves, obtained for different values of $r_0 - r_{0c}$, show data collapse in agreement with the scaling form (252) expected in the critical regime. For $N = 2$, we find a well-defined Higgs resonance whose position $\omega = m_H$ and full width at half maximum vanishes as the QCP is approached. For $m_H \ll \omega$, we find $\chi_s''(\omega) \sim \omega^{3-2/\nu}$ with $\nu \simeq 0.673$ the critical exponent of the 3D classical O(2) model. Up to a multiplicative factor (which depends on the nonuniversal factor $\mathcal{A}_-$ in (252)), the shape of the resonance, given by the universal scaling function $\Phi_{s,-}$, is in very good agreement with the MC results of (Gazit *et al.*, 2013a,b). The Higgs resonance is still visible, although less pronounced, for $N = 3$. The universal ratio m_H/Δ, shown in Table IX, is compatible with MC estimates of (Gazit *et al.*, 2013a,b). No Higgs resonance is found for $N \geq 4$.

In the disordered phase, the spectral function $\chi_s''(\omega)$ vanishes for $|\omega| < 2\Delta$, where Δ is the excitation gap of the $\boldsymbol{\varphi}$ field (Fig. 39). Contrary to a suggestion that a Higgs-like resonance may also exist in the disordered phase (Chen *et al.*, 2013; Pollet and Prokof'ev, 2012), we find that $\chi_s''(\omega)$ rises smoothly above the threshold at $\omega = 2\Delta$ with no sign of a local maximum for $\omega \gtrsim 2\Delta$. Similar conclusions were reached from MC

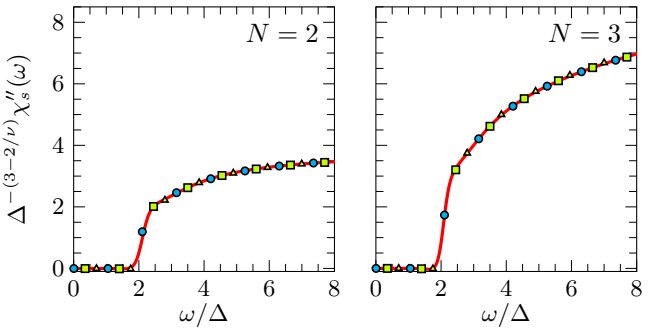

FIG. 39 (Color online) Same as Fig. 38 but in the disordered phase (Rose *et al.*, 2015).

simulations (Gazit *et al.*, 2013b) and $4-(d+1)$ expansion (Katan and Podolsky, 2015).

XIII. INTERACTING BOSONS

The (Euclidean) action of interacting bosons writes

$$S = \int_0^\beta d\tau \int d^d r \left[\psi^* \left(\partial_\tau - \mu - \frac{\boldsymbol{\nabla}^2}{2m} \right) \psi + \frac{g}{2} (\psi^* \psi)^2 \right], \tag{258}$$

where ψ is a complex field, m the boson mass and μ the chemical potential. The repulsive interaction $g > 0$ is assumed to be local in space and the model is regularized by a momentum cutoff Λ.

In Sec. XIII.A, we discuss the zero-temperature superfluid phase. First we briefly comment on the necessity to go beyond the Bogoliubov theory to understand the infrared behavior of the one-particle propagator and then show that the NPRG allows one to determine the exact infrared behavior of the one-particle propagator. Finally, we show how the BMW approximation can be used to compute the shift of the transition temperature T_c in a dilute Bose gas wrt to the Bose-Einstein-condensation temperature T_c^0. The superfluid–Mott-insulator transition in lattice boson systems (Bose-Hubbard model) is discussed in Sec. XIII.B.

A. Superfluidity in a dilute Bose gas

1. Breakdown of Bogoliubov's theory

The action (258) differs from the (relativistic) quantum O(2) model studied in Sec. XII by the presence of a first-order time-derivative term reflecting Galilean invariance. This makes the quantum phase transition between the vacuum state ($\mu < 0$) and the superfluid state ($\mu > 0$) markedly different from the $T = 0$ phase transition in the quantum O(2) model. The vacuum-superfluid transition has a dynamical exponent $z = 2$ and its upper critical dimension is $d_c^+ = 2$ (Sachdev, 2011).

In spite of these important differences, there are remarkable similarities between the relativistic and Galilean-invariant O(2) models in the broken-symmetry phase. In the quantum O($N \geq 2$) model, the longitudinal propagator $G_{\rm L}(\mathbf{p}, i\omega) \sim 1/(\omega^2 + c^2\mathbf{p}^2)^{(3-d)/2}$ exhibits an infrared divergence in the ordered phase when $d \leq 3$ (the vanishing is logarithmic for $d = 3$); see Sec. XII.B.3. We shall see that the same behavior is observed in the superfluid phase of interacting boson systems.

Historically, the divergence of the longitudinal susceptibility was encountered (although not recognized as such) early on in the study of superfluid bosons. The first attempts to improve the Bogoliubov theory of superfluidity (Bogoliubov, 1947) were made difficult by a singular perturbation theory plagued by infrared divergences (Beliaev, 1958a,b; Gavoret and Nozières, 1964; Hugenholtz and Pines, 1959). Although these divergences cancel out in local gauge invariant physical quantities (pressure, sound velocity, etc.), they have a definite physical origin since they reflect the divergence of the longitudinal susceptibility. Using field-theoretical diagrammatic methods to handle the infrared divergences of the perturbation theory, Nepomnyashchii and Nepomnyashchii showed that one of the fundamental quantities of a Bose superfluid, the anomalous self-energy $\Sigma_{\rm an}(p)$, vanishes in the limit $p = (\mathbf{p}, i\omega_n) \to 0$ in dimension $d \leq 3$,

$$\Sigma_{\rm an}(p = 0) = 0, \tag{259}$$

even though the low-energy mode remains phonon-like with a linear spectrum (Nepomnyashchii and Nepomnyashchii, 1975; Nepomnyashchii, 1983; Nepomnyashchii and Nepomnyashchii, 1978). This exact result shows that the Bogoliubov approximation, where the linear spectrum and the superfluidity rely on a finite value of the anomalous self-energy (namely $\Sigma_{\rm an}(p) = \mu$), breaks down at low energy. In three dimensions, the Bogoliubov theory remains nevertheless valid down to an exponentially small energy scale. An alternative approach to superfluidity, based on a phase-amplitude representation of the boson field, has been proposed by Popov (Popov, 1972, 1983; Popov and Seredniakov, 1979). This approach is free of infrared singularities and agrees with the asymptotic low-energy behavior of $\Sigma_{\rm an}(p)$ obtained by Nepomnyashchii and Nepomnyashchii (Popov and Seredniakov, 1979) but is restricted to the (low-momentum) hydrodynamic regime.

2. NPRG approach

The instability of the Bogoliubov fixed point in dimension $d \leq 3$ toward a different fixed point characterized by the divergence of the longitudinal susceptibility has been confirmed by Castellani *et al.* (Castellani *et al.*, 1997; Pistolesi *et al.*, 2004). Using a field-theoretical

RG approach supplemented by the Ward identities associated to the local gauge symmetry, these authors obtained the exact infrared behavior of a Bose superfluid at zero temperature. Related results, both at zero (Benfatto, 1994; Bijlsma and Stoof, 1996; Cenatiempo and Giuliani, 2014; Dupuis, 2009a,b, 2011; Dupuis and Sengupta, 2007; Sinner *et al.*, 2009, 2010; Wetterich, 2008) and finite (Andersen and Strickland, 1999; Eichler *et al.*, 2009; Floerchinger and Wetterich, 2008, 2009a,b; Rançon and Dupuis, 2012c) temperatures, have been obtained by several authors within the framework of the (nonperturbative) RG.

In this section, we show that the NPRG approach provides us with a natural framework to study the superfluid phase. We first show that the infrared behavior of the one-particle propagator can be obtained from the scale-dependent effective action Γ_k without actually solving the RG equations. This analysis is then corroborated by the numerical solution of the flow equations.

The implementation of the NPRG to interacting bosons follows the approach of Sec. XII. We add to the action (258) the infrared regulator term

$$\Delta S_k[\psi^*,\psi] = \sum_p \psi^*(p) R_k(p) \psi(p) \tag{260}$$

and consider the k-dependent effective action

$$\begin{aligned}\Gamma_k[\phi^*,\phi] = & -\ln Z_k[J^*,J] + \int_0^\beta d\tau \int d^d r (J^*\phi + \text{c.c.}) \\ & - \Delta S_k[\phi^*,\phi],\end{aligned} \tag{261}$$

where $\phi(x) = \langle \psi(x) \rangle$ is the superfluid order parameter. In general one chooses a regulator function $R_k(\mathbf{p}) = Z_{A,k} \epsilon_{\mathbf{p}} r(\mathbf{p}^2/k^2)$ acting only on momenta (the k-dependent variable $Z_{A,k}$ is defined below).[61] J denotes a complex external source that couples linearly to the boson field ψ. Γ_k satisfies the RG equation (30) with initial condition $\Gamma_\Lambda = S$.[62]

[61] Choosing a frequency-independent regulator function ensures that the causality of the propagator (i.e. $G(\mathbf{p},\tau) \propto \Theta(\tau)$) in vacuum ($\mu \leq 0$ and $T = 0$) is satisfied. This property is likely to be important when studying the thermodynamics of the dilute Bose gas whose universality follows from the existence of a quantum critical point between the vacuum ($\mu \leq 0$) and the superfluid phase ($\mu \geq 0$). On the other hand, the infrared behavior of the propagator in the superfluid phase is best understood using a "relativistic" regulator function acting both on frequencies and momenta (Dupuis, 2009a).

[62] If $R_\Lambda < \infty$ (which is often the case in practice) the initial condition of the RG flow is not given by the mean-field solution $\Gamma_\Lambda = S$. In the end, however, all physical properties will be expressed in terms of "infrared" quantities (boson density, superfluid density, scattering length, etc.) with no reference to the microscopic action.

a. Derivative expansion. We consider the LPA' ansatz

$$\begin{aligned}\Gamma_k[\phi^*,\phi] = & \int_0^\beta d\tau \int d^d r \Big[U_k(n) \\ & + \phi^* \Big(Z_{C,k} \partial_\tau - V_{A,k} \partial_\tau^2 - \frac{Z_{A,k}}{2m} \boldsymbol{\nabla}^2 \Big) \phi \Big],\end{aligned} \tag{262}$$

where $n = |\phi|^2$ denotes the condensate density. Note that neither the regulator function $R_k(\mathbf{p})$ nor the ansatz (262) satisfy Galilean invariance at zero temperature. Nevertheless the Ward identity associated to Galilean invariance (first of Eqs. (270) below) remains very well satisfied.[63]

Because of the U(1) symmetry of the microscopic action (258), the effective potential $U_k(n)$ is a function of the condensate density n. Its minimum determines the condensate density $n_{0,k}$ and the thermodynamics potential per unit volume $U(n_{0,k})$ in the equilibrium state. The effective action (262) contains a second-order time-derivative term which is not present in the initial condition. We shall see that this term plays a crucial role when $d \leq 3$ (Dupuis and Sengupta, 2007; Wetterich, 2008). The initial condition at scale $k = \Lambda$ is given by

$$\begin{aligned} U_\Lambda(n) &= -\mu n + \frac{g}{2} n^2, \\ Z_{A,\Lambda} = Z_{C,\Lambda} &= 1, \quad V_{A,\Lambda} = 0. \end{aligned} \tag{263}$$

It is convenient to write the boson field $\phi = (\phi_1 + i\phi_2)/\sqrt{2}$ in terms of two real fields ϕ_1 and ϕ_2. Because of the U(1) symmetry, the two-point vertex in a constant (i.e. uniform and time-independent) field takes the form

$$\begin{aligned}\Gamma^{(2)}_{k,ij}(p;\phi) = & \, \delta_{i,j} \Gamma_{A,k}(p;n) + \phi_i \phi_j \Gamma_{B,k}(p;n) \\ & + \epsilon_{i,j} \Gamma_{C,k}(p;n),\end{aligned} \tag{264}$$

where $\epsilon_{i,j}$ is the antisymmetric tensor and $i,j \in \{1,2\}$. $\Gamma_{A,k}$, $\Gamma_{B,k}$ and $\Gamma_{C,k}$ are functions of the condensate density n. Due to parity and time-reversal invariance, they are even functions of $\mathbf{p}$ and ω, except $\Gamma_{C,k}$ which is odd in ω. With the ansatz (262),

$$\begin{aligned} \Gamma_{A,k}(p;n) &= Z_{A,k} \epsilon_{\mathbf{p}} + V_{A,k} \omega^2 + U_k'(n), \\ \Gamma_{B,k}(p;n) &= U_k''(n), \qquad \Gamma_{C,k}(p;n) = Z_{C,k} \omega. \end{aligned} \tag{265}$$

The functions Γ_A, Γ_B and Γ_C can be related to the normal and anomalous self-energies. For a constant and real field $\phi(x) = \sqrt{n}$, i.e. $\phi_i(x) = \delta_{i,1}\sqrt{2n}$,

$$\begin{aligned}\Sigma_{k,\mathrm{n}}(p;n) - G_0^{-1}(p) &= \Gamma_{A,k}(p;n) + n\Gamma_{B,k}(p;n) - i\Gamma_C(p;n) \\ &= U_k'(n) + nU_k''(n) + Z_{A,k}\epsilon_{\mathbf{p}} \\ &\quad - Z_{C,k} i\omega + V_{A,k}\omega^2,\end{aligned} \tag{266}$$

[63] See Appendix A in (Floerchinger and Wetterich, 2008) for a detailed discussion of symmetries.

and the anomalous self-energy

$$\Sigma_{k,\mathrm{an}}(p;n) = n\Gamma_B(p;n) = nU_k''(n) \tag{267}$$

is real.

From the effective action (262), we can extract the main physical properties of the superfluid phase. The condensate density $n_{0,k}$ is defined by $U_k'(n_{0,k}) = 0$. Using equations (266) and (267), we then deduce that the self-energy satisfies the Hugenholtz-Pines theorem (Hugenholtz and Pines, 1959)

$$\Sigma_{k,\mathrm{n}}(p=0;n_{0,k}) - \Sigma_{k,\mathrm{an}}(p=0;n_{0,k}) = \mu. \tag{268}$$

The excitation spectrum is obtained from the zeros of the determinant of the 2×2 matrix $\Gamma_k^{(2)}(p;n_{0,k})$ (after analytic continuation $i\omega \to \omega + i0^+$). For $\mathbf{p},\omega \to 0$, we find a Goldstone mode (the Bogoliubov sound mode) with velocity

$$c_k = \left(\frac{Z_{A,k}/2m}{V_{A,k} + Z_{C,k}^2/2\lambda_k n_{0,k}}\right)^{1/2}, \tag{269}$$

where $\lambda_k = U_k''(n_{0,k})$. By considering a static twist of the phase of the order parameter, we obtain the superfluid density $n_{s,k} = Z_{A,k}n_{0,k}$ (Dupuis, 2009a).

At zero temperature, Galilean invariance and gauge invariance imply the following Ward identities (Dupuis, 2009a; Pistolesi *et al.*, 2004; Wetterich, 2008),

$$\begin{aligned} \bar{n}_k &= Z_{A,k}n_{0,k} = n_{s,k}, \\ V_{A,k} &= -\frac{1}{2n_{0,k}}\frac{\partial^2 U_k}{\partial\mu^2}\bigg|_{n_{0,k}}, \\ Z_{C,k} &= -\frac{\partial^2 U_k}{\partial\mu\partial n}\bigg|_{n_{0,k}} = \lambda_k\frac{dn_{0,k}}{d\mu}, \end{aligned} \tag{270}$$

where we consider the effective potential $U_k(\mu,n)$ as a function of the two independent variables μ and n. The condensate density $n_{0,k}(\mu)$ is then defined by $\partial U/\partial n|_{n_{0,k}} = 0$ while the mean boson density is obtained from $\bar{n}_k = -dU_k(\mu,n_{0,k})/d\mu$. Equations (270) imply in turn that the compressibility $\kappa_k = \bar{n}_k^{-2}d\bar{n}_k/d\mu$ and the velocity c_k are given by

$$\begin{aligned} \bar{n}_k^2\kappa_k &= 2n_{0,k}V_{A,k} + \frac{Z_{C,k}^2}{\lambda_k}, \\ c_k &= \left(\frac{n_{s,k}}{m\kappa_k\bar{n}_k^2}\right)^{1/2}. \end{aligned} \tag{271}$$

Since $n_{s,k} = \bar{n}_k$ at zero temperature, the Bogoliubov sound mode velocity coincides with the the macroscopic sound velocity $1/(m\kappa_k\bar{n}_k)^{1/2}$ (Gavoret and Nozières, 1964).

b. Infrared limit of the one-particle propagator. Let us consider the anomalous self-energy $\Sigma_{k,\mathrm{an}}(p;n_{0,k}) = \lambda_k n_{0,k}$ in the equilibrium state. Since $\Sigma_{k=0,\mathrm{an}}(p=0;n_{0,k=0})$ vanishes for $d \le 3$ [Eq. (259)] while $n_{0,k=0} > 0$, λ_k must vanish for $k=0$. Let us assume that

$$\lambda_k \sim \begin{cases} k^{3-d} & \text{for } d<3, \\ |\ln k|^{-1} & \text{for } d=3, \end{cases} \tag{272}$$

when $k\to 0$. If we replace k by $\sim \sqrt{\mathbf{p}^2 + \omega^2/c^2}$, we then reproduce the small-p dependence of the anomalous self-energy obtained by (Nepomnyashchii and Nepomnyashchii, 1978). Furthermore, as we shall see, the hypothesis (272) is internally consistent. It is sufficient, when combined with the thermodynamic relations (270), to obtain the exact infrared behavior of the one-particle propagator.

Since thermodynamic quantities, including the condensate "compressibility" $dn_{0,k}/d\mu$ must remain finite in the limit $k\to 0$, we deduce from (270) that $Z_{C,k} \sim \lambda_k \sim k^{3-d}$ vanishes in the infrared limit. It follows that $c_k \to (Z_{A,k}/2mV_{A,k})^{1/2}$ for $k\to 0$. Both $Z_{A,k} = \bar{n}_k/n_{0,k}$ and the macroscopic sound velocity c_k being finite at $k=0$, $V_{A,k}$ (which vanishes in the Bogoliubov approximation) must be nonzero when $k\to 0$. The suppression of $Z_{C,k}$, together with a finite value of $V_{A,k}$, shows that Γ_k exhibits a "relativistic" (Lorentz) invariance in the infrared limit and therefore becomes similar to the effective action of the classical O(2) model in dimension $d+1$ (Dupuis and Sengupta, 2007; Wetterich, 2008). In the ordered phase, the coupling constant of this model vanishes as $\lambda_k \sim k^{4-(d+1)}$ for $d+1 \le 4$ (Sec. III.B.4), which is nothing but our starting assumption (272). Thus we find that for $k\to 0$, the existence of a linear spectrum is due to the relativistic form of the effective action rather than a nonzero value of λ_k as in the Bogoliubov theory.

From the 2-point vertex $\Gamma_k^{(2)}$, we deduce the one-particle propagator $G_k = -\Gamma_k^{(2)-1}$.[64] In the domain of validity of the derivative expansion, $|\mathbf{p}|^2, |\omega|^2/c_k^2 \ll k \ll k^{3-d}$ for $k\to 0$ (and $d\le 3$), one obtains

$$\begin{aligned} G_{k,\mathrm{LL}}(p;n_{0,k}) &= -\frac{1}{2\lambda_k n_{0,k}}, \\ G_{k,\mathrm{TT}}(p;n_{0,k}) &= -\frac{2mc_k^2 n_{0,k}}{\bar{n}_k}\frac{1}{\omega^2 + c_k^2\mathbf{p}^2}, \\ G_{k,\mathrm{LT}}(p;n_{0,k}) &= \frac{dn_{0,k}}{d\mu}\frac{mc_k^2}{\bar{n}_k}\frac{\omega}{\omega^2 + c_k^2\mathbf{p}^2}, \end{aligned} \tag{273}$$

with the identification $G_{\mathrm{LL}} \equiv G_{11}$, $G_{\mathrm{TT}} \equiv G_{22}$ and $G_{\mathrm{LT}} \equiv G_{12}$ for a real field $\phi = \sqrt{n}$. One way to obtain the limit $k=0$ of the propagators (at fixed p) from

[64] As discussed in Sec. II.A.2, we define here the physical propagator as $-\Gamma_k^{(2)-1}$ rather than $-(\Gamma_k^{(2)} + R_k)^{-1}$. Note also that we define the propagator $G_{ij} = -\langle\psi_i\psi_j\rangle$ with a minus sign.

the derivative expansive is to stop the RG flow when $k \sim (\mathbf{p}^2+\omega^2/c^2)^{1/2}$. Since thermodynamic quantities are not expected to flow in the infrared limit, they can be approximated by their $k=0$ values. As for the longitudinal propagator $G_{k=0,\mathrm{LL}}$, its value is obtained from the replacement $\lambda_k \to C(\omega^2+c^2\mathbf{p}^2)^{(3-d)/2}$ (with C a constant). Equations (273) yield the exact expression of the normal and anomalous (connected) propagators in the low-energy limit, $G_{\rm n}(p)=-\langle\psi(p)\psi^*(p)\rangle_c$ and $G_{\rm an}(p)=-\langle\psi(p)\psi(-p)\rangle_c$, respectively (Castellani *et al.*, 1997; Dupuis, 2009a,b; Pistolesi *et al.*, 2004):

$$\begin{aligned} G_{\rm n}(p) =& -\frac{n_0 mc^2}{\bar{n}}\frac{1}{\omega^2+c^2\mathbf{p}^2}-\frac{dn_0}{d\mu}\frac{mc^2}{\bar{n}}\frac{i\omega}{\omega^2+c^2\mathbf{p}^2} \\ &+\frac{1}{2}G_{\rm LL}(p), \\ G_{\rm an}(p) =& \frac{n_0 mc^2}{\bar{n}}\frac{1}{\omega^2+c^2\mathbf{p}^2}+\frac{1}{2}G_{\rm LL}(p), \end{aligned} \tag{274}$$

where

$$G_{\rm LL}(p) \simeq -\frac{1}{2\Sigma_{\rm an}(p)} \tag{275}$$

is deduced from (273) with $\lambda_k \to C(\omega^2+c^2\mathbf{p}^2)^{(3-d)/2}$.

c. RG flows. The preceding conclusions can be confirmed by the numerical solution of the flow equations. For simplification, we consider the following truncation of the effective potential,

$$U_k(n)=U_{0,k}+\frac{\lambda_k}{2}(n-n_{0,k})^2. \tag{276}$$

We then obtain

$$\begin{aligned} \partial_t n_{0,k} &= \frac{3}{2}I_{k,\mathrm{LL}}+\frac{1}{2}I_{k,\mathrm{TT}} \\ \partial_t \lambda_k &= -\lambda_k^2\left[9J_{k;\mathrm{LL},\mathrm{LL}}(0)-6J_{k;\mathrm{LT},\mathrm{LT}}(0)+J_{k;\mathrm{TT},\mathrm{TT}}(0)\right], \end{aligned} \tag{277}$$

and

$$\begin{aligned} \partial_t Z_{A,k} =& -2\lambda_k^2 n_{0,k}\frac{\partial}{\partial\epsilon_{\mathbf{p}}}\left[J_{k;\mathrm{LL},\mathrm{TT}}(p)+J_{k;\mathrm{TT},\mathrm{LL}}(p)\right. \\ &\left.+2J_{k;\mathrm{LT},\mathrm{LT}}(p)\right]\Big|_{p=0}, \\ \partial_t Z_{C,k} =& 2\lambda_k^2 n_{0,k}\frac{\partial}{\partial\omega}\left[J_{k;\mathrm{TT},\mathrm{LT}}(p)-J_{k;\mathrm{LT},\mathrm{TT}}(p)\right. \\ &\left.-3J_{k;\mathrm{LL},\mathrm{LT}}(p)+3J_{k;\mathrm{LT},\mathrm{LL}}(p)\right]\Big|_{p=0}, \\ \partial_t V_{A,k} =& -2\lambda_k^2 n_{0,k}\frac{\partial}{\partial\omega^2}\left[J_{k;\mathrm{LL},\mathrm{TT}}(p)+J_{k;\mathrm{TT},\mathrm{LL}}(p)\right. \\ &\left.+2J_{k;\mathrm{LT},\mathrm{LT}}(p)\right]\Big|_{p=0}, \end{aligned} \tag{278}$$

where the threshold functions I_α and $J_{\alpha\beta}(p)$ are defined by (228).

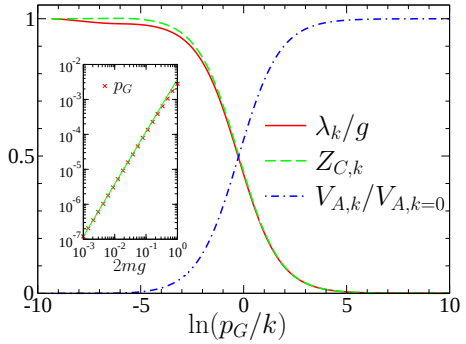

FIG. 40 (Color online) λ_k, $Z_{C,k}$ and $V_{A,k}$ vs $\ln(p_G/k)$, where $p_G=\sqrt{(gm)^3\bar{n}}/4\pi$, for $\bar{n}=0.01$, $2mg=0.1$ and $d=2$ [$\ln(p_G/p_h)\simeq -5.87$]. The inset shows p_G vs $2mg$ obtained from the criterion $V_{A,p_G}=V_{A,k=0}/2$ [the Green solid line is a fit to $p_G\sim(2mg)^{3/2}$] (Dupuis, 2009a).

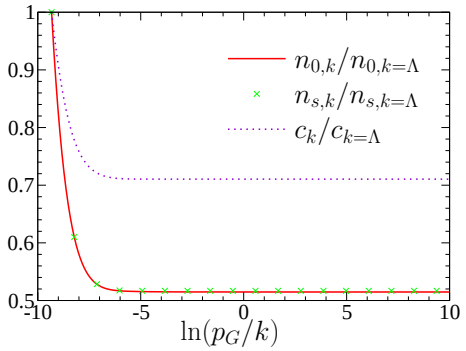

FIG. 41 (Color online) Condensate density $n_{0,k}$, superfluid density $n_{s,k}$ and Goldstone mode velocity c_k vs $\ln(p_G/k)$. The parameters are the same as in Fig. 40 (Dupuis, 2009a).

The flow of λ_k, $Z_{C,k}$ and $V_{A,k}$ is shown in Fig. 40 for a two-dimensional system in the weak-coupling limit.[65] We can clearly distinguish two regimes separated by the Ginzburg momentum scale $p_G\sim\sqrt{(gm)^3\bar{n}}$ (see the inset in the figure). In the (perturbative) Bogoliubov regime $k\gg p_G$, $Z_{A,k}\simeq Z_{C,k}\simeq 1$ and $V_{A,k}\simeq 0$, while λ_k remains nearly equal to its initial value $\lambda_\Lambda=g$. In the (non-perturbative) Goldstone regime $k\ll p_G$, we find that both λ_k and $Z_{C,k}$ vanish linearly with k in agreement with the previous conclusions, while $V_{A,k}$ takes a finite value. This regime is dominated by phase fluctuations and characterized by the vanishing of the anomalous self-energy $\Sigma_{k,\mathrm{an}}(p=0)=\lambda_k n_{0,k}\sim k$ and the divergence of the longitudinal propagator $G_{k,\mathrm{LL}}$.

The condensate density $n_{0,k}$, the superfluid density $n_{s,k}$ and the Goldstone mode velocity c_k are not sensitive to the Ginzburg scale (Fig. 41). This result is particularly striking for the velocity c_k, whose expression involves the parameters λ_k, $Z_{C,k}$ and $V_{A,k}$ which all strongly vary

[65] For a three-dimensional system in the weak-coupling limit, the Ginzburg scale p_G is exponentially small so that deviations from Bogoliubov theory appear only at extremely small energies.

when $k \sim p_G$. More generally, all physical quantities related to correlation functions obtained as averages of local gauge-invariant operators (like the density-density correlation function) are expected to be free of infrared divergences (Pistolesi *et al.*, 2004) and insensitive to the Ginzburg scale.

In the Goldstone regime $k \ll p_G$, it is possible to neglect longitudinal fluctuations (Dupuis, 2009a, 2011; Wetterich, 2008). Using $n_{0,k} \simeq n_{0,k=0}$, $Z_{A,k} \simeq Z_{A,k=0}$ and $V_{A,k} \simeq V_{A,k=0}$, one then finds

$$\partial_t \tilde{\lambda}_k = (1-\epsilon)\tilde{\lambda}_k,$$
$$\eta_{C,k} = -8\frac{v_{d+1}}{d+1}\frac{\tilde{\lambda}_k}{\tilde{V}_{A,k}^{1/2}}, \quad \partial_t \eta_{C,k} = -\epsilon\eta_{C,k} - \eta_{C,k}^2, \quad (279)$$
$$\partial_t \tilde{V}_{A,k} = 2(1+\eta_{C,k})\tilde{V}_{A,k},$$

where $\epsilon = 3-d$, $\tilde{\lambda}_k = k^{d-2} Z_{A,k}^{-1} Z_{C,k}^{-1} \lambda_k$, $\tilde{V}_{A,k} = k^2 Z_{A,k} Z_{C,k}^{-2} V_{A,k}$ and $\eta_{C,k} = -\partial_t \ln Z_{C,k}$. Equations (279) are obtained with a relativistic regulator function acting both on momenta and frequencies.[61] Thus $\eta_{C,k} \to -\epsilon$, $\tilde{\lambda}_k \sim k^{1-\epsilon}$ and $\lambda_k, Z_{C,k} \sim k^\epsilon$ for $k \to 0$, in agreement with previous conclusions (for $d=3$, $\lambda_k, Z_{C,k} \sim |\ln k|^{-1}$ vanish logarithmically).

The anisotropy between time and space in the Goldstone regime $k \ll p_G$ (where the average effective action takes a relativistic form) can be eliminated by an appropriate rescaling of frequencies and fields. This leads to an isotropic relativistic model with dimensionless condensate density and coupling constant defined by (Dupuis, 2009a)

$$\tilde{n}'_{0,k} = \tilde{V}_{A,k}^{1/2} \tilde{n}_{0,k}, \qquad \tilde{\lambda}'_k = \tilde{V}_{A,k}^{-1/2} \tilde{\lambda}_k. \quad (280)$$

$\tilde{\lambda}'_k$ satisfies the RG equation

$$\partial_t \tilde{\lambda}'_k = -\epsilon \tilde{\lambda}'_k + 8\frac{v_{d+1}}{d+1} \tilde{\lambda}'^2_k, \quad (281)$$

which is nothing but the RG equation of the coupling constant of the $(d+1)$-dimensional classical O(2) model in the broken-symmetry phase [see Eq. (128)]. $\tilde{\lambda}'_k$ reaches a fixed-point value λ'^*_k when $d+1<4$. In the infrared limit, we find

$$\lambda_k = k^{3-d} Z_{A,k}^{3/2} V_{A,k}^{1/2} \tilde{\lambda}'_k \sim k^\epsilon \tilde{\lambda}'^*_k \quad (282)$$

if we approximate $Z_{A,k} \simeq Z_{A,k=0}$ and $V_{A,k} \simeq V_{A,k=0}$. The vanishing of $\lambda_k \sim k^\epsilon$ and the divergence of the longitudinal susceptibility is therefore the consequence of the existence of a fixed point $\tilde{\lambda}'^*_k$ for the coupling constant of the effective $(d+1)$-dimensional O(2) model which describes the Goldstone regime $k \ll p_G$. To describe the entire hydrodynamic regime $k \ll p_h$, we should in principle relax the assumption $V_{A,k} \simeq V_{A,k=0}$, since $V_{A,k}$ strongly varies for $k \sim p_G$, which makes the analytical solution of the RG equations much more difficult. In Ref. (Sinner *et al.*, 2010), it was shown that Eq. (281) is nevertheless in good agreement with the numerical solution of the flow equations in the entire hydrodynamic regime, which allows us to estimate the Ginzburg momentum scale using (132),

$$p_G \simeq \left[\frac{8 v_{d+1} g}{(d+1)\epsilon}\right]^{1/\epsilon}. \quad (283)$$

It is possible to compute the full momentum and frequency dependence of the self-energies $\Sigma_{\rm n}(p)$ and $\Sigma_{\rm an}(p)$ using BMW-like approximations. Dupuis (Dupuis, 2009a,b) has shown that the low-energy singularity of the anomalous self-energy in two dimensions, $\Sigma_{\rm an}(p) \sim (\omega^2 + c^2\mathbf{p}^2)^{1/2}$, is reproduced form the NPRG approach. Sinner *et al.* (Sinner *et al.*, 2009, 2010) have computed the entire spectral line shape in three and two dimensions, including the damping (inverse life time) $\gamma_{\mathbf{p}}$ of the sound mode. Their findings $\gamma_{\mathbf{p}} \sim |\mathbf{p}|^{2d-1}$ agree with Beliaev's result in three dimensions (Beliaev, 1958a,b) and with known results in two dimensions (Chung and Bhattacherjee, 2009; Kreisel *et al.*, 2008).

d. Thermodynamics. The NPRG approach can also be used to compute the thermodynamics of the Bose gas. In the low-temperature dilute regime ($ma^2\mu, ma^2 T \ll 1$), for $d \geq 2$ the pressure takes the form

$$P(\mu,T) = \left(\frac{m}{2\pi}\right)^{d/2} T^{d/2+1} \mathcal{F}^{(d)}_{\rm DBG}\left(\frac{\mu}{T}, \tilde{g}(T)\right), \quad (284)$$

where $\mathcal{F}^{(d)}_{\rm DBG}$ is a universal scaling function characteristics of the d-dimensional dilute Bose gas universality class. This expression follows from the existence of a QCP at $\mu = T = 0$ between the vacuum and the superfluid phase (Rançon and Dupuis, 2012c). Above the upper critical dimension $d_c^+ = 2$ of the quantum phase transition, the interaction is a dangerously irrelevant variable (in the RG sense) and enters the scaling function $\mathcal{F}^{(d)}_{\rm DBG}$. In dimensionless form it is defined by

$$\tilde{g}(\epsilon) = \begin{cases} 8\pi\sqrt{2ma_3^2\epsilon} & \text{if } d=3, \\ -\frac{4\pi}{\ln\left(\frac{1}{2}\sqrt{2ma_2^2\epsilon}+C\right)} & \text{if } d=2, \end{cases} \quad (285)$$

where a_d is the d-dimensional scattering length and C the Euler constant. In three dimensions, the universal scaling function $\mathcal{F}^{(3)}_{\rm DBG}$ can be computed perturbatively in some regimes (but not near the superfluid transition temperature; see Sec. XIII.A.3). The two-dimensional scaling function $\mathcal{F}^{(2)}_{\rm DBG}$ has been determined using the NPRG (Rançon and Dupuis, 2012c), in good agreement with QMC simulations (Prokof'ev *et al.*, 2001; Prokof'ev and Svistunov, 2002) and experiments in cold atom systems (Hung *et al.*, 2011; Yefsah *et al.*, 2011; Zhang *et al.*, 2012). In Sec. XIII.B.2 we shall discuss in more detail the calculation of the pressure in a Bose gas near the Mott-insulator–superfluid transition.

3. Superfluid transition of a dilute Bose gas

In a three-dimensional dilute Bose gas, the pressure is determined by a universal scaling function $\mathcal{F}_{\rm DBG}(\mu/T, \tilde{g}(T))$ depending on μ/T and $ma^2\mu$ [Eqs. (284,285)]. The superfluid transition corresponds to a singularity of $\mathcal{F}_{\rm DBG}(\mu/T, \tilde{g}(T))$ as a function of T. It follows that the ratio T_c/μ between the superfluid transition temperature and the chemical potential must be a universal function of $ma^2\mu$ (a denotes the three-dimensional s-wave scattering length). If the density n, rather than the chemical potential, is fixed, then T_c in unit of $n^{2/3}/2m$ must be a universal function of na^3.

In the absence of interactions ($a = 0$), the bosons undergo a Bose-Einstein condensation at the temperature

$$T_c^0 = \frac{2\pi}{m}\left(\frac{n}{\zeta(3/2)}\right)^{2/3}, \tag{286}$$

where $\zeta(z)$ the Riemann Zeta function. For weak interactions, the shift $\Delta T_c/T_c^0 = (T_c - T_c^0)/T_c^0$ in the transition temperature is a universal function of na^3. The dependence of $\Delta T_c/T_c^0$ on a has remained a controversial issue for a long time and even the sign of the effect has been debated (Huang, 1999; Lee and Yang, 1958; Toyoda, 1982). It is now understood that

$$\frac{\Delta T_c}{T_c^0} = c(an^{1/3}) \tag{287}$$

increases linearly with a (Baym *et al.*, 1999; Baym, G. *et al.*, 2001; Grüter *et al.*, 1997; Holzmann and Krauth, 1999; Holzmann, M. *et al.*, 1999) and the proportionality coefficient c has been estimated from various approaches. As we shall see, the difficulty in getting a precise estimate of c comes from the fact that it requires the knowledge of the one-particle propagator at T_c in a large momentum range including the crossover region $|\mathbf{p}| \sim p_G$ between the critical and noncritical regimes (p_G denotes the Ginzburg momentum scale, see below). The determination of c is therefore a nonperturbative problem which can be dealt with the NPRG (Benitez *et al.*, 2009, 2012; Blaizot, 2008; Blaizot *et al.*, 2005). However, since the full knowledge of the momentum dependence of the propagator is required, the derivative expansion used in the preceding sections is not sufficient and one has to resort to the BMW approximation (Sec. V).

It turns out to be easier to compute the shift $\Delta n_c = n_c - n_c^0$ in the critical density at fixed temperature rather than the shift ΔT_c at fixed density. Since $T_c^0 \propto (n_c^0)^{2/3}$, one has

$$\frac{\Delta T_c}{T_c^0} = -\frac{2}{3}\frac{\Delta n_c}{n_c^0}. \tag{288}$$

In the normal phase $T \geq T_c$, the density

$$n = -T\sum_{\omega_n}\int_{\mathbf{p}} G(\mathbf{p}, i\omega_n)e^{i\omega_n 0^+} \tag{289}$$

can be computed from the one-particle propagator

$$G(\mathbf{p}, i\omega_n) = [i\omega_n + \mu - \epsilon_{\mathbf{p}} - \Sigma(\mathbf{p}, i\omega_n)]^{-1}, \tag{290}$$

with $\Sigma(\mathbf{p}, i\omega_n)$ the self-energy. The transition occurs when $G(0,0)^{-1} = 0$, i.e. $\mu = \Sigma(0,0)$. Thus the shift Δn_c in the critical density is given by

$$\Delta n_c = -T\sum_{\omega_n}\int_{\mathbf{p}}\left[\frac{1}{i\omega_n - \epsilon_{\mathbf{p}} - \Sigma(\mathbf{p}, i\omega_n) - \Sigma(0,0)} - \frac{1}{i\omega_n - \epsilon_{\mathbf{p}}}\right]e^{i\omega_n 0^+}. \tag{291}$$

Let us first consider the Hartree-Fock (mean-field) correction to the self-energy,

$$\Sigma_{\rm HF} = -2gT\sum_{\omega_n}\int_{\mathbf{p}} G(\mathbf{p}, i\omega_n)e^{i\omega_n 0^+} = 2gn. \tag{292}$$

This self-energy correction merely shifts the chemical potential and does not change the critical temperature and the critical density (as obvious from (291)). At the transition, $\Sigma_{\rm HF} = \mu$ and Eq. (292) reproduces the noninteracting result (286).

Thus the relevant self-energy corrections for the shift Δn_c start at order g^2. In the dilute Bose gas, in order to organize perturbation theory in terms of the small parameter na^3 (with a the s-wave scattering length), one has to replace the bare interaction g by the T-matrix in vacuum, which amounts to identifying g with $4\pi a/m$. One could therefore naively conclude that Δn_c is at least of order a^2 whereas, as we shall see, Δn_c is linear in a. This linear dependence comes from critical modes, with momenta of the order of or smaller than the Ginzburg momentum scale p_G, which introduce nonanalyticity in a. Since a finite Matsubara frequency acts as an infrared cutoff, if $p_G \ll p_T = \sqrt{2mT} \sim \lambda^{-1}$ (with $\lambda = \sqrt{2\pi/mT}$ the thermal de Broglie wavelength), then critical fluctuations are entirely due to classical modes $\omega_n = 0$ and the formula (291) for Δn_c now includes only the $\omega_n = 0$ contribution. In this classical approximation, which is always justified when $a \to 0$ (see below), the expression for the density becomes ultraviolet divergent but the shift Δn_c [Eq. (291)] remains well defined.

Since we need only consider the classical field $\psi_{\rm cl}(\mathbf{p}) = \psi(\mathbf{p}, i\omega_n = 0)/\sqrt{\beta}$ in the limit $a \to 0$, it is convenient to consider the effective action $S[\psi_{\rm cl}]$,

$$e^{-S[\psi_{\rm cl}]} = \int \mathcal{D}[\psi(i\omega_n \neq 0)]\, e^{-S[\psi]}, \tag{293}$$

obtained by integrating out nonclassical modes. The latter renormalize the bare classical-field action which can be read off from (258). Renormalization of the quadratic term is unimportant as it does not change the critical density. To leading order in a, the coupling constant (i.e. the coefficient of the quartic term) becomes $4\pi a/m$. In

addition, higher-order terms (e.g. $|\psi_{\rm cl}|^6$) are generated but these terms are of higher order in a. Thus we are left with an effective action of the form

$$S[\psi_{\rm cl}] = \beta \int d^3r \left\{ \frac{1}{2m}|\nabla\psi_{\rm cl}|^2 - \mu|\psi_{\rm cl}|^2 + \frac{2\pi a}{m}|\psi_{\rm cl}|^4 \right\}. \tag{294}$$

Parametrizing the complex field $\psi_{\rm cl} = \sqrt{mT}(\varphi_1 + i\varphi_2)$ by a 2-component real field $\boldsymbol{\varphi} = (\varphi_1, \varphi_2)$, we finally obtain the action of the classical O(2) model,

$$S[\boldsymbol{\varphi}] = \int d^3r \left\{ \frac{1}{2}(\boldsymbol{\nabla}\boldsymbol{\varphi})^2 + \frac{r_0}{2}\boldsymbol{\varphi}^2 + \frac{u_0}{4!}(\boldsymbol{\varphi}^2)^2 \right\}, \tag{295}$$

where $r_0 = -2\mu m$ and $u_0 = 96\pi^2 a/\lambda^2$. The action (295) should be supplemented with a ultraviolet cutoff Λ of the order of $p_T \sim \lambda^{-1}$, whose origin is the neglect of the nonzero Matsubara frequencies. The Ginzburg momentum scale p_G is of order u_0 and the condition $p_G \ll p_T$ for nonclassical modes to be noncritical translates into $a \ll \lambda$.

Let us point out that the classical action $S[\boldsymbol{\varphi}]$ can also be understood from the RG point of view. Suppose we integrate the RG flow down to the momentum scale $p_T = \sqrt{2mT}$. Since $p_T \gg p_\mu = \sqrt{2m\mu}$ near the transition,[66] the RG flow at momentum scales larger than p_T is effectively in vacuum ($T = 0$ and $n = 0$). In three dimensions, the flow in vacuum is controlled by a Gaussian fixed point and the interactions are irrelevant (Sachdev, 2011). The 2-body interaction is however dangerously irrelevant (the upper critical dimension for the vacuum-superfluid transition is $d_c^+ = 2$) and cannot be ignored. For momentum scales smaller than $1/a$, it becomes momentum independent and equal to $4\pi a/m$. Higher-order (irrelevant) interactions can be ignored. At momentum scales smaller than p_T, nonclassical modes do not contribute to the flow anymore. Thus, the renormalized action at the thermal scale p_T corresponds to a classical field theory with coupling constant $4\pi a/m$ [Eq. (294)].

Noting that

$$G(\mathbf{p}, i\omega_n = 0) = -\beta\langle\psi_{\rm cl}(\mathbf{p})\psi_{\rm cl}^*(\mathbf{p})\rangle = -\frac{2m}{\Gamma^{(2)}(\mathbf{p})}, \tag{296}$$

where $\Gamma^{(2)}(\mathbf{p})$ is the 2-point vertex of the classical field theory (295), we finally obtain

$$\begin{aligned}\Delta n_c &= 2mT \int_{\mathbf{p}} \left(\frac{1}{\Gamma^{(2)}(\mathbf{p})} - \frac{1}{\mathbf{p}^2} \right) \\ &= -\frac{2}{\pi\lambda^2} \int_0^\infty d|\mathbf{p}| \frac{U(\mathbf{p})}{U(\mathbf{p}) + \mathbf{p}^2},\end{aligned} \tag{297}$$

[66] This follows from $ma^2\mu, ma^2T \ll 1$ and $ma^2\mu \sim (ma^2T)^{3/2}$ for $T \sim T_c$.

TABLE X Coefficient c vs N [Eq. (300)] obtained from the NPRG in the BMW approximation (Benitez *et al.*, 2012). Also shown are the results from lattice and seven-loop resummed calculations.

N	NPRG	Lattice	Seven loops[a]
1	1.15	1.09(9) [b]	1.07(10)
2	1.37	1.32(2) [c]	1.27(10)
		1.29(5) [d]	
3	1.50		1.43(11)
4	1.63	1.60(10) [b]	1.54(11)
10	2.02		
100	2.36		

[a] (Kastening, 2004), [b] (Sun, 2003), [c] (Arnold and Moore, 2001), [d] (Kashurnikov *et al.*, 2001).

where $U(\mathbf{p}) = \Gamma^{(2)}(\mathbf{p}) - \mathbf{p}^2$. From scaling arguments,[67]

$$U(|\mathbf{p}| = x u_0) = u_0^2 \sigma\left(x, \frac{u_0}{\Lambda}\right) \equiv u_0^2 \sigma(x) \tag{298}$$

in the limit $u_0/\Lambda \sim a/\lambda \to 0$, so that

$$\Delta n_c = -\frac{2}{\pi\lambda^2} u_0 \int_0^\infty dx \frac{\sigma(x)}{\sigma(x) + x^2} \tag{299}$$

is proportional to a.

From Eqs. (297,299), we conclude that the proportionality coefficient c in (287) reads

$$c = -\frac{256\pi^3}{\zeta(3/2)^{4/3}} \frac{\Delta\langle\boldsymbol{\varphi}^2\rangle}{N u_0}, \tag{300}$$

where $N = 2$ and

$$\begin{aligned}\frac{\Delta\langle\boldsymbol{\varphi}^2\rangle}{N u_0} &= \frac{\langle\boldsymbol{\varphi}^2\rangle - \langle\boldsymbol{\varphi}^2\rangle_{u_0=0}}{N u_0} \\ &= -\frac{1}{2\pi^2} \int_0^\infty dx \frac{\sigma(x)}{\sigma(x) + x^2}\end{aligned} \tag{301}$$

depends on the 2-point vertex $\Gamma^{(2)}(\mathbf{p})$ of the classical theory at criticality. At this point, one can generalize the coefficient c to arbitrary N such that $\boldsymbol{\varphi}$ becomes a N-component real field and $\Gamma^{(2)}$ the 2-point vertex of the O(N) model at criticality. In the large-N limit, $c = 8\pi/3\zeta(3/2)^{4/3} \simeq 2.33$ can be computed exactly (Arnold and Tomášik, 2001; Baym *et al.*, 2000). The integrand in (297) is peaked at $|\mathbf{p}| \sim p_G$ (Blaizot *et al.*, 2005) so that Δn_c is highly sensitive to the crossover between the critical and noncritical regimes. For this reason, the calculation of c has been used as a benchmark for nonperturbative approximations in the O(N) model. The NPRG

[67] Eq. (298) can be written in the more standard form $U(\mathbf{p}) = p_G^2 \sigma(|\mathbf{p}|/p_G, p_G/\Lambda)$.

results (Benitez *et al.*, 2009, 2012; Blaizot *et al.*, 2005), compared to the best ones available in the literature, are presented in Table X.[68] For all values of N where lattice and/or seven-loop resummed calculations exist, the NPRG results are within the error bars of those calculations, except for $N = 2$, where very precise lattice results are available. In the large N limit, the NPRG result differs from the exact value $c \simeq 2.33$ by less than 3%.[69]

B. Superfluid–Mott-insulator transition

In this section we discuss the superfluid–Mott-insulator transition in lattice boson systems. After a brief introduction to the Bose-Hubbard model, we describe the NPRG approach.

1. The Bose-Hubbard model

The Bose-Hubbard model is defined by the Hamiltonian

$$\hat{H} = -t \sum_{\langle \mathbf{r},\mathbf{r}' \rangle} \left(\hat{\psi}^\dagger_{\mathbf{r}} \hat{\psi}_{\mathbf{r}'} + \text{h.c.} \right) - \mu \sum_{\mathbf{r}} \hat{\psi}^\dagger_{\mathbf{r}} \hat{\psi}_{\mathbf{r}} + \frac{U}{2} \sum_{\mathbf{r}} \hat{\psi}^\dagger_{\mathbf{r}} \hat{\psi}^\dagger_{\mathbf{r}} \hat{\psi}_{\mathbf{r}} \hat{\psi}_{\mathbf{r}}, \tag{302}$$

where $\{\mathbf{r}\}$ denotes the N sites of a lattice and $\langle \mathbf{r}, \mathbf{r}' \rangle$ nearest-neighbor sites. t is the hopping amplitude, U the on-site interaction and μ the chemical potential. We consider a d-dimensional hypercubic lattice ($d \geq 2$) and take the lattice spacing as the unit length.

The existence of a (zero-temperature) quantum phase transition in the Bose-Hubbard model can be understood from simple arguments (Fisher *et al.*, 1989). Let us first assume that there is one boson per site on average ($\bar{n} = 1$). In the limit $t/U \to 0$, in the ground state there must be one boson localized at each lattice site. Moving a particle would create an empty and a doubly-occupied site, which requires a very large energy (U) wrt the gain in kinetic energy (t). In the opposite limit $U/t \to 0$, bosons can move in the lattice and form a Bose-Einstein condensate. Thus, as the ratio t/U increases, we expect a quantum phase transition between an insulating ground state (known as a Mott insulator) and a superfluid ground state. Suppose now that we add a few particles to the system so that the density $\bar{n}$ (i.e. the average number of bosons per site) becomes slightly larger than unity. The bosons can then move without changing the number of singly- and doubly-occupied sites, so that we expect the system to be superfluid even in the limit $t/U \to 0$. More generally, we expect a Mott-insulator–superfluid transition for commensurate densities and a superfluid ground state for any incommensurate density (provided $t > 0$). For an incommensurate density $\bar{n} = \bar{n}_c + \delta\bar{n}$, we can view the excess particles (or holes if $\delta\bar{n} < 0$) wrt the commensurate density $\bar{n}_c$ as a dilute gas of delocalized particles responsible for the superfluidity of the system. We shall see that this simple picture can actually be justified and made quantitative by renormalization-group arguments.

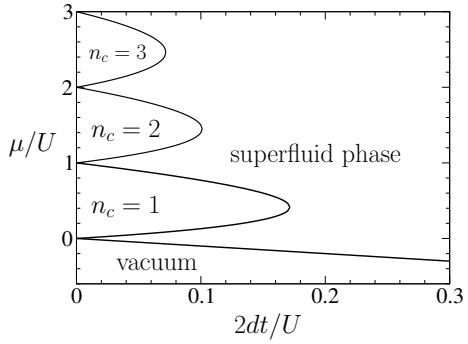

FIG. 42 Mean-field phase diagram of the d-dimensional Bose-Hubbard model showing the first three Mott lobes, the vacuum ($n_c = 0$) and the superfluid phase.

Since the Bogoliubov theory assumes small fluctuations of the boson operator $\hat{\psi}_{\mathbf{r}}$ about its mean value (Sec. XIII.A.1), it does not apply to the Mott transition or the strongly correlated superfluid phase where the condensate density n_0 is much smaller than the density $\bar{n}$ (regardless of the limitations at low energy discussed in Sec. XIII.A.1). Nevertheless, at an elementary level the superfluid–Mott-insulator transition can be captured by a mean-field decoupling of the intersite hopping term, $\hat{\psi}^\dagger_{\mathbf{r}} \hat{\psi}_{\mathbf{r}'} \to \hat{\psi}^\dagger_{\mathbf{r}} \langle \hat{\psi}_{\mathbf{r}'} \rangle + \langle \hat{\psi}^\dagger_{\mathbf{r}} \rangle \hat{\psi}_{\mathbf{r}'} - \langle \hat{\psi}^\dagger_{\mathbf{r}} \rangle \langle \hat{\psi}_{\mathbf{r}'} \rangle$, while the local part is treated exactly. For a uniform order parameter $\psi = \langle \hat{\psi}_{\mathbf{r}} \rangle$, this yields an effective single-site Hamiltonian which can be solved (at least numerically) exactly. The mean-field phase diagram consists of a series of Mott lobes labeled by an integer n_c corresponding to the density in the insulator (Fig. 42). n_c vanishes if μ is negative and is defined by $n_c - 1 \leq \mu/U \leq n_c$ if $\mu > 0$. When the density of bosons $\bar{n}$ is incommensurate, the ground state is always superfluid for any nonzero value of t (Fisher *et al.*, 1989; Sachdev, 2011; Stoof *et al.*, 2009).

In the Mott insulator, the mean density of bosons $\bar{n} = n_c$ is independent of μ and the compressibility vanishes: $\kappa = \bar{n}^{-2} d\bar{n}/d\mu^2 = 0$. The tip of the Mott lobe corresponds to a transition at constant density. Such a transition is driven by a change in the interaction strength t/U. The corresponding quantum critical point is a quantum multicritical point (QMCP) as two parameters (t

[68] Let us also mention the result $c = 1.23$ obtained, for $N = 2$, in (Hasselmann *et al.*, 2004; Ledowski *et al.*, 2004); however, as discussed in (Blaizot *et al.*, 2006b), it is difficult to gauge the quality of the approximations made in this work.

[69] Note that the large-N behavior of c is, in fact, of order $1/N$ (Baym *et al.*, 2000), which is not calculated exactly in the BMW approximation.

and μ) have to be fine tuned. The transition is in the universality class of the O(2) (or XY) model in dimensions $d+1$ with a dynamical critical exponent $z=1$ (Fisher *et al.*, 1989). The lower and upper critical dimensions are $d_c^- = 1$ and $d_c^+ = 3$, respectively. Away from the Mott lobe tip, the transition is accompanied by a density change. This (generic) transition, which can occur at fixed t/U by varying the chemical potential, is the universality of the vacuum-superfluid transition of the dilute Bose gas (Fisher *et al.*, 1989).

2. NPRG approach

The NPRG approach to the Bose-Hubbard model (Rançon and Dupuis, 2011a,b) is based on the lattice NPRG discussed in Sec. VII for classical field theories and spin systems. The lattice NPRG assumes as initial condition the local limit of decoupled sites. The standard NPRG approach would start from the mean-field (Bogoliubov) theory, which is not a suitable starting point to describe the Mott transition. We shall see that the lattice NPRG allows us not only to study the critical properties of the Mott transition but also to accurately determine the phase diagram and compute nonuniversal quantities such as the velocity of the critical fluctuations at a QMCP.

The function $R_k(\mathbf{q})$ in the "regulator" term ΔS_k [Eq. (260)] modifies the bare dispersion $t_\mathbf{q}$ of the bosons. In the lattice NPRG, it is chosen such that $t_\mathbf{q} + R_\Lambda(\mathbf{q})$ vanishes. The action $S+\Delta S_\Lambda$ then corresponds to the local limit of decoupled sites. In practice, we choose

$$R_k(\mathbf{q}) = -Z_{A,k}\epsilon_k \mathrm{sgn}(t_\mathbf{q})(1-y_\mathbf{q})\Theta(1-y_\mathbf{q}), \tag{303}$$

with $\Lambda = \sqrt{2d}$, $\epsilon_k = tk^2$, $y_\mathbf{q} = (2dt - |t_\mathbf{q}|)/tk^2$. We denote by $l = \ln(k/\Lambda)$ the (negative) RG "time". The k-dependent constant $Z_{A,k}$ is defined below. For small k, the function $R_k(\mathbf{q})$ gives a mass $\sim k^2$ to the low-energy modes $|\mathbf{q}| \lesssim k$ and acts as an infrared regulator term as in the standard NPRG scheme.

Apart from the choice of the regulator function, the lattice NPRG is similar to the one used to study interacting bosons in the continuum (Sec. XIII.A.2). The initial condition is defined by

$$\Gamma_\Lambda[\phi^*,\phi] = \Gamma_\mathrm{loc}[\phi^*,\phi] + \int_0^\beta d\tau \sum_\mathbf{q} \phi^*(\mathbf{q}) t_\mathbf{q} \phi(\mathbf{q}), \tag{304}$$

where $\Gamma_\mathrm{loc}[\phi^*,\phi]$ is the effective action in the local limit. Γ_Λ reproduces the results of the strong-coupling RPA, an improvement over the mean-field theory (Sec. XIII.B.1) which includes Gaussian fluctuations of the boson field (Menotti and Trivedi, 2008; Ohashi *et al.*, 2006; van Oosten *et al.*, 2001; Sengupta and Dupuis, 2005; Sheshadri *et al.*, 1993; Stoof *et al.*, 2009).

It is not possible to compute the functional Γ_Λ for arbitrary time-dependent fields. One can however easily obtain the effective potential $V_\mathrm{loc}(n)$ and the 2-point vertex $\Gamma^{(2)}_\mathrm{loc}$ in a time-independent field, starting from the single-site Hamiltonian

$$\hat{H}_\mathrm{loc} = -\mu\hat{n} + \frac{U}{2}\hat{n}(\hat{n}-1) - J^*\hat{\psi} - J\hat{\psi}^\dagger, \tag{305}$$

where $\hat{n} = \hat{\psi}^\dagger\hat{\psi}$ and J is a time-independent complex source. In Fock space, this Hamiltonian can be represented by a tridiagonal matrix which can be numerically diagonalized if we truncate the Hilbert space by retaining only low-energy states. At zero temperature, the effective potential is defined by $V_\mathrm{loc}(n) = E_0 + J^*\phi + J\phi^*$ where E_0 is the ground state energy and $\phi \equiv \phi(J^*,J)$, $\phi^* \equiv \phi^*(J^*,J)$ are obtained by numerically inverting $\phi = -\partial E_0/\partial J^*$ and $\phi^* = -\partial E_0/\partial J$. To obtain the 2-point vertex $\Gamma^{(2)}_\mathrm{loc} = -G^{-1}_\mathrm{loc}$, we calculate the normal and anomalous Green functions,

$$\begin{aligned} G_{\mathrm{loc,n}}(\tau) &= -\langle T_\tau \hat{\psi}(\tau)\hat{\psi}^\dagger(0)\rangle + |\langle\hat{\psi}\rangle|^2, \\ G_{\mathrm{loc,an}}(\tau) &= -\langle T_\tau \hat{\psi}(\tau)\hat{\psi}(0)\rangle + \langle\hat{\psi}\rangle^2 \end{aligned} \tag{306}$$

($\hat{\psi}^{(\dagger)}(\tau) = e^{\tau\hat{H}}\hat{\psi}^{(\dagger)}e^{-\tau\hat{H}}$ and T_τ is a time-ordering operator) using the numerically known eigenstates of $\hat{H}_\mathrm{loc}$.

To simplify the flow equations, we use a derivative expansion where

$$\begin{aligned} &\Gamma_{A,k}(q;n) = Z_{A,k}(n)\epsilon_\mathbf{q} + V_{A,k}(n)\omega^2 + V'_k(n), \\ &\Gamma_{B,k}(q;n) = V''_k(n), \\ &\Gamma_{C,k}(q;n) = Z_{C,k}(n)\omega. \end{aligned} \tag{307}$$

Since it is crucial to retain the full lattice structure at the beginning of the flow, in (307) we use the free boson dispersion $\epsilon_\mathbf{q} = t_\mathbf{q} + 2dt$ and define $Z_{A,k}$ as

$$Z_{A,k}(n) = \frac{1}{t}\lim_{q\to 0}\frac{\partial}{\partial\mathbf{q}^2}\Gamma_{A,k}(q;n), \tag{308}$$

so that $Z_{A,k}(n)$ has the meaning of a field renormalization factor (and should not be confused with a renormalization of the hopping amplitude between nearest-neighbor sites). Note that we include in the 2-point vertex an ω^2 term. Not only is this term crucial in the superfluid phase (Sec. XIII.A.2), but it also distinguishes between the two universality classes of the transition. At the QMCP, $Z_{C,k}$ vanishes for $k\to 0$ and the effective action exhibits Lorentz invariance (or particle-hole symmetry).

In the lattice NPRG, the local physics is taken into account by the initial condition at scale $k=\Lambda$. Solving the flow equations for $k<\Lambda$ amounts to implementing a t/U expansion. For $k \ll \Lambda$, Eqs. (307,308) become equivalent to the LPA'. Although we rely on a derivative expansion of the vertices to solve the flow equations, the latter cannot be derived directly from a simple ansatz

of the effective action Γ_k. The reason is that it is difficult to propose an approximation of the initial effective action Γ_Λ based on a derivative expansion since we do not know its expression for arbitrary time-dependent fields. To circumvent this difficulty we start from the BMW approximation where we deal only with quantities computed in a constant field which, for $k = \Lambda$, can be obtained from the local Hamiltonian (305). Using the ansatz (307) in addition to the BMW approximation, we obtain flow equations for $V_k(n)$, $Z_{A,k}(n)$, $Z_{C,k}(n)$ and $V_{A,k}(n)$.

The numerical solution of the flow equations can be further simplified by approximating $V_{A,k}(n)$ and $Z_{A,k}(n)$ by $V_{A,k} \equiv V_{A,k}(n_{0,k})$ and $Z_{A,k} \equiv Z_{A,k}(n_{0,k})$. To determine accurately the phase diagram, it is nevertheless necessary to keep the full n-dependence of $Z_{C,k}(n)$ and $V_k(n)$. When accuracy is not the primary goal, it is possible to approximate $Z_{C,k}(n)$ by $Z_{C,k}(n_{0,k})$ and expand the effective potential to quadratic order about its minimum,

$$V_k(n) = \begin{cases} V_{0,k} + \frac{\lambda_k}{2}(n - n_{0,k})^2 & \text{if } n_{0,k} > 0, \\ V_{0,k} + \delta_k n + \frac{\lambda_k}{2} n^2 & \text{if } n_{0,k} = 0. \end{cases} \tag{309}$$

With these approximations, the RG equations become similar to those of the continuum model, the only difference coming from the choice of the regulator function $R_k(\mathbf{q})$ and the use of the full lattice dispersion $\epsilon_\mathbf{q}$ in (307).

a. $T = 0$ phase diagram and critical behavior. For given values of t, U and μ, the ground state can be deduced from the values of the condensate density n_0 ($n_0 > 0$ in the superfluid phase). (To alleviate the notations, we drop the subscript k whenever we refer to a $k = 0$ quantity, e.g. $n_0 \equiv n_{0,k=0}$.) The most accurate results, obtained by keeping the full n dependence of $V_k(n)$ and $Z_{C,k}(n)$ are shown in Fig. 43. Both in three and two dimensions, the transition line between the superfluid phase and the Mott insulator is very close to the quantum Monte Carlo (QMC) result (Capogrosso-Sansone *et al.*, 2007, 2008): the tip of the Mott lobe ($t/U = 0.0339$, $\mu/U = 0.3992$) differs from the QMC data only by (0.001%, 3%) in three dimensions, while in two dimensions the tip is located at ($t/U = 0.060, \mu/U = 0.387$), which corresponds to a relative error of order (1.5%, 4%). For comparison, in Fig. 43 we also show the mean-field (or strong-coupling RPA) phase diagram as well as the one obtained from Dynamical Mean-Field Theory (Anders *et al.*, 2010, 2011).

To make the fixed point manifest when the system is critical, we use the dimensionless variables defined in table XI. At a QMCP the anomalous dimensions are defined by

$$\eta_{A,k} = -\partial_l \ln Z_{A,k}, \qquad \eta_{V,k} = -\partial_l \ln V_{A,k}. \tag{310}$$

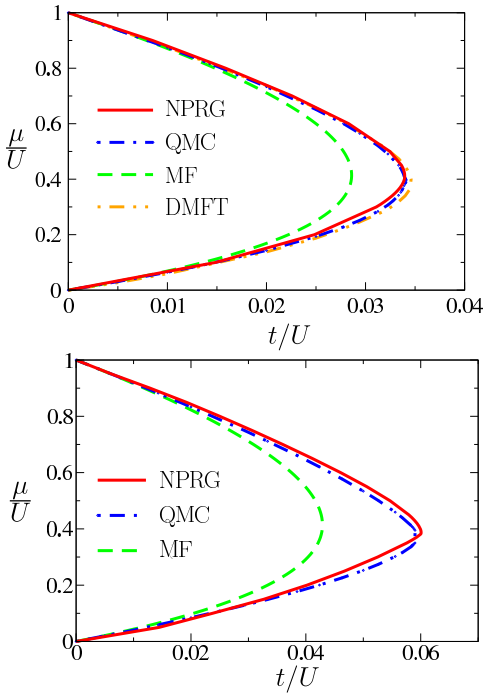

FIG. 43 (Color online) (Top) Phase diagram of the three-dimensional Bose-Hubbard model (Rançon and Dupuis, 2011b). Only the first Mott lobe ($\bar{n} = 1$) is shown. The (green) dashed line shows the mean-field (or strong-coupling RPA) phase diagram. The QMC data are obtained from (Capogrosso-Sansone *et al.*, 2007) and the Dynamical Mean-Field Theory (DMFT) data from (Anders *et al.*, 2011). (Bottom) Phase diagram of the two-dimensional Bose-Hubbard model (Rançon and Dupuis, 2011b). The QMC data are obtained from (Capogrosso-Sansone *et al.*, 2008).

TABLE XI Dimensionless variables ($Z_{C,k} \equiv Z_{C,k}(n_{0,k})$).

	QMCP	generic transition
$\tilde{\mathbf{q}}$	$\mathbf{q}/k$	$\mathbf{q}/k$
$\tilde{\omega}$	$\left(\frac{V_{A,k}}{Z_{A,k}\epsilon_k}\right)^{1/2}\omega$	$\left(\frac{Z_{C,k}}{Z_{A,k}\epsilon_k}\right)\omega$
$\tilde{n}$	$k^{-d}(V_{A,k}Z_{A,k}\epsilon_k)^{1/2}n$	$k^{-d}Z_{C,k}n$
$\tilde{V}_k(\tilde{n})$	$k^{-d}\left(\frac{V_{A,k}}{Z_{A,k}\epsilon_k}\right)^{1/2}V_k(n)$	$k^{-d}\left(\frac{Z_{C,k}}{Z_{A,k}\epsilon_k}\right)V_k(n)$
$\tilde{\delta}_k$	$(Z_{A,k}\epsilon_k)^{-1}\delta_k$	$(Z_{A,k}\epsilon_k)^{-1}\delta_k$
$\tilde{\lambda}_k$	$k^d V_{A,k}^{-1/2}(Z_{A,k}\epsilon_k)^{-3/2}\lambda_k$	$k^d(Z_{C,k}Z_{A,k}\epsilon_k)^{-1}\lambda_k$
$\tilde{Z}_{C,k}(\tilde{n})$	$(V_{A,k}Z_{A,k}\epsilon_k)^{-1/2}Z_{C,k}(n)$	
$\tilde{V}_{A,k}$		$Z_{A,k}\epsilon_k Z_{C,k}^{-2}V_{A,k}$

It is useful to introduce the k-dependent exponent

$$z_k = 1 - \frac{\eta_{A,k} - \eta_{V,k}}{2}, \tag{311}$$

whose $k = 0$ value gives the dynamical critical exponent z. At a QMCP, we expect $\eta_A = \eta_V \equiv \eta$ (for $k = 0$) and $z = 1$ (with $\eta \equiv \eta_{O(2)}^{(d+1)}$ the anomalous dimension at the $(d+1)$-dimensional O(2) critical point). It is however

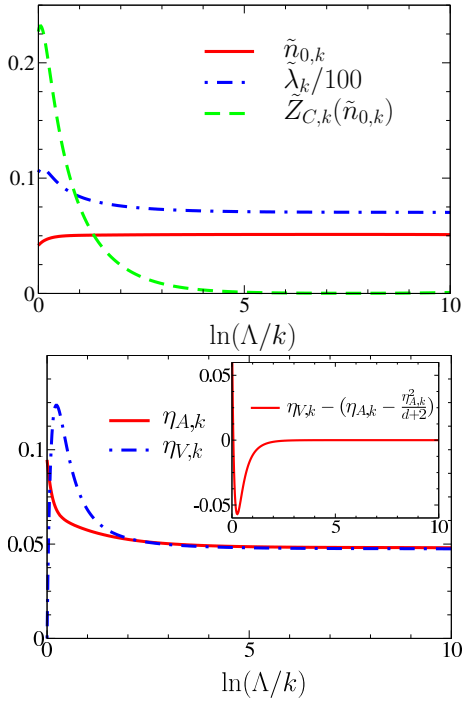

FIG. 44 (Color online) (Top) Dimensionless condensate density $\tilde{n}_{0,k}$, coupling constant $\tilde{\lambda}_k$ and $\tilde{Z}_{C,k}(\tilde{n}_{0,k})$ vs $\ln(\Lambda/k)$ at the QMCP $\bar{n} = 1$ for $d = 2$. (Bottom) Anomalous dimensions $\eta_{A,k}$ and $\eta_{V,k}$ vs $\ln(\Lambda/k)$ (Rançon and Dupuis, 2011a).

possible that the regulator function $R_k(\mathbf{q})$, which does not satisfy the Lorentz invariance at the QMCP, modifies the expected critical behavior. Setting $Z_{C,k}(n) = 0$ in the flow equations, we find $\eta_{V,k} = \eta_{A,k} - \eta_{A,k}^2/(d+2)$. Given the small value of the anomalous dimension in the $(d+1)$-dimensional O(2) model ($d = 2, 3$), the identities $\eta_A = \eta_V$ and $z = 1$ turn out to be satisfied to a very good accuracy (see below).

Figure 44 shows results obtained at the two-dimensional QMCP corresponding to the superfluid–Mott-insulator transition with density $\bar{n} = 1$. The plateaus observed for the dimensionless condensate density $\tilde{n}_{0,k}$ and coupling constant $\tilde{\lambda}_k$, as well as for the (running) anomalous dimensions $\eta_{A,k}$ and $\eta_{V,k}$, are characteristic of critical behavior. We clearly see the emergence of Lorentz invariance as k decreases: $\tilde{Z}_{C,k}(\tilde{n}_{0,k}) \sim k$ is suppressed while $\eta_{A,k}$ and $\eta_{V,k}$ become nearly equal (implying $z_k \simeq 1$). We find the critical exponents $\nu = 0.699$, $\eta_A = 0.049$, $\eta_V = \eta_A(1 - \eta_A/4) = 0.049$ and $z = 1.000$, in agreement with the expected results of the LPA' in the three-dimensional O(2) model. Near the QMCP, $|\tilde{Z}_{C,k}(\tilde{n}_{0,k})|$ first decreases towards zero before increasing, $|\tilde{Z}_{C,k}(\tilde{n}_{0,k})| \sim 1/k \sim e^{-l}$, as the flow runs away from the critical surface so that the critical exponent associated with the scaling field $\tilde{Z}_{C,k}(\tilde{n}_{0,k})$ is equal to one (Fisher *et al.*, 1989; Rançon and Dupuis, 2011a).

At the generic transition, $Z_{C,k}(n_{0,k})$ remains nonzero and $V_{A,k}\omega^2$ is subleading wrt $Z_{C,k}(n_{0,k})\omega$. The dynamical critical exponent is $z = 2$ and the upper critical dimension $d_c^+ = 2$. The transition for $d \geq 2$ is governed by the Gaussian fixed point (with logarithmic corrections for $d = 2$) defined by $\tilde{n}_0^* = \tilde{\lambda}^* = \tilde{V}_A^* = 0$ and $\eta_A = \eta_C = 0$ ($\eta_{C,k} = -k\partial_k \ln Z_{C,k}(n_{0,k})$). The dimensionless variables used to study the generic transition are given in table XI. The (running) dynamical exponent z_k is given by

$$z_k = 2 - \eta_{A,k} + \eta_{C,k} \tag{312}$$

and satisfies $\lim_{k\to 0} z_k = 2$.

b. Universal thermodynamics near the generic transition. Near the Mott transition, the scale-dependent effective action can be approximated by

$$\Gamma_k[\phi^*,\phi] = \int_0^\beta d\tau \int d^3r \big[\phi^*(Z_{C,k}\partial_\tau - V_{A,k}\partial_\tau^2 - Z_{A,k}t\boldsymbol{\nabla}^2 + \delta_k)\phi + \frac{\lambda_k}{2}(n - n_{0,k})^2 + V_{0,k}\big], \tag{313}$$

where we now consider the three-dimensional case[70] and neglect the field dependence of $Z_{C,k}(n)$. Since we are interested in the low-energy limit, we consider the continuum limit where $\mathbf{r}$ becomes a continuous variable. Higher-order (in derivative or field) terms neglected in (313) give subleading contributions to the infrared behavior. Most physical quantities of interest can be directly deduced from Eq. (313). The pressure is given by $P(\mu,T) = -V_{0,k=0}$. In the superfluid phase, the superfluid stiffness can be expressed as $\rho_s(\mu,T) = 2tZ_{A,k=0}n_{0,k=0}$ and the sound velocity reads $c(\mu,T) = [\rho_s(\mu,T)/\bar{n}^2\kappa(\mu,T)]^{1/2}$ where $\kappa = \partial^2 P/\partial\mu^2$.

$Z_C \equiv Z_{C,k=0}$ and $\delta \equiv \delta_{k=0}$ are related by the Ward identity $Z_C = -\partial\delta/\partial\mu$ (Rançon and Dupuis, 2011a; Sachdev, 2011). At a generic QCP ($\mu = \mu_c, T = 0$) where $Z_C \neq 0$, the effective action $\Gamma \equiv \Gamma_{k=0}$ [Eq. (313)] takes the form

$$\Gamma[\phi^*,\phi] = \int_0^\beta d\tau \int d^3r \Big[\phi^*\big(Z_C\partial_\tau - Z_A t\boldsymbol{\nabla}^2\big)\phi + \frac{\lambda}{2}|\phi|^4\Big] \tag{314}$$

up to a constant term $\beta N V_0$. From Eq. (314), we can identify the elementary excitations at the QCP. On the lower part of the transition line (for a given Mott lobe), Z_C is negative and it is convenient to perform a particle-hole transformation $\phi \leftrightarrow \phi^*$ (which changes the sign of the ∂_τ term in (314)). We can then define a quasi-particle field

$$\bar{\phi}(\mathbf{r},\tau) = \sqrt{|Z_C|}\phi(\mathbf{r},\tau), \tag{315}$$

[70] A similar analysis can be made for the two-dimensional Bose-Hubbard model (Rançon and Dupuis, 2012c).

and rewrite the effective action as

$$\Gamma[\bar{\phi}^*,\bar{\phi}] = \int_0^\beta d\tau \int d^3r \left[\bar{\phi}^*\left(\partial_\tau - \frac{\boldsymbol{\nabla}^2}{2m^*}\right)\bar{\phi} + \frac{1}{2}\frac{4\pi a^*}{m^*}|\bar{\phi}|^4\right], \tag{316}$$

where

$$m^* = \frac{|Z_C|}{2tZ_A} = m\frac{|Z_C|}{Z_A}, \qquad a^* = \frac{m^*\lambda}{4\pi Z_C^2}, \tag{317}$$

with $m = 1/2t$ the effective mass of the free bosons moving in the lattice. We deduce from Eqs. (315,316) that elementary excitations are quasi-particles with mass m^* and spectral weight $Z_{\rm qp} = |Z_C|^{-1}$. They are particle-like if $Z_C > 0$ and hole-like if $Z_C < 0$. The effective interaction between two quasi-particles is determined by the effective "scattering length" a^*.

The quantum phase transition at $\mu = -6t$ between the superfluid phase and the vacuum (which can be seen as a Mott insulator with vanishing density) differs from the superfluid-vacuum transition in a continuum model only by the presence of the lattice. In this case, $Z_A = Z_C = 1$ (the one-particle propagator is not renormalized), so that $Z_{\rm qp} = 1$ and $m^* = m = 1/2t$. Furthermore, the interaction constant can be calculated analytically (by solving the two-body problem) and related to the scattering length a of the bosons moving in the lattice: $\lambda = 4\pi a/m = 8\pi t a$, which gives $a^* = a = 1/[8\pi(t/U + A)]$ with $A \simeq 0.1264$.

For a generic QCP between the superfluid phase and a Mott insulating phase with nonzero density ($\bar{n} = 1, 2, 3, \cdots$), the values of $Z_{\rm qp}$, m^* and a^* can be obtained from the numerical solution of the NPRG equations. Figure 45 shows $Z_{\rm qp}, m^*, a^*$ as a function of t/U for the transition between the superfluid phase and the Mott insulator with density $\bar{n} = 1$. The vanishing of Z_C at the QMCP implies that m^* vanishes while $Z_{\rm qp}$ and a^* diverge as we approach the tip of the Mott lobe. In addition to the NPRG results, in Fig. 45 we show m^* obtained from QMC simulations (Capogrosso-Sansone *et al.*, 2007) as well as m^* and $Z_{\rm qp}$ obtained from the strong-coupling RPA (Rançon and Dupuis, 2012b). The RPA value for the hopping amplitude at the tip of the Mott lobe, $t_c/U \simeq 0.0286$, is far away from the QMC ($t_c/U = 0.034083$) or NPRG ($t_c/U = 0.0339$) results. Nevertheless the RPA predictions for the quasi-particle weight $Z_{\rm qp}$ and the effective mass m^*, when plotted as a function of t/t_c, are in good agreement with the NPRG and QMC results.

Once the values of the non universal parameters $Z_{\rm qp}$, m^* and a^* are known, we can write the pressure in the scaling form (Rançon and Dupuis, 2012a,b)

$$P(\mu,T) = P_c + \bar{n}_c\delta\mu + \left(\frac{m^*}{2\pi}\right)^{3/2} T^{5/2}\mathcal{F}_{\rm DBG}\left(\pm\frac{\delta\mu}{T}, \tilde{g}(T)\right), \tag{318}$$

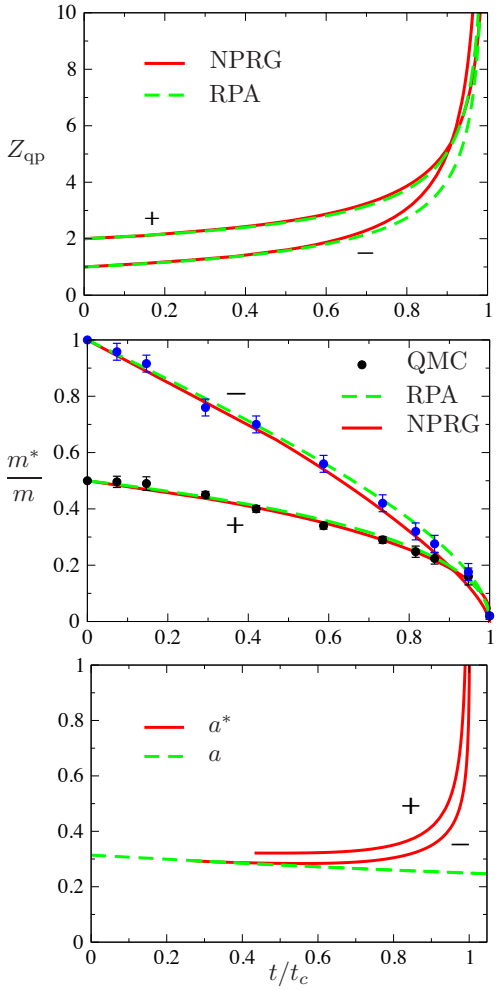

FIG. 45 (Color online) Quasi-particle weight $Z_{\rm qp}$, effective mass m^* and scattering length a^* vs t/t_c at the QCP between the superfluid phase and the Mott insulator $\bar{n} = 1$ (t_c is the value of t at the tip of the Mott lobe) (Rançon and Dupuis, 2012b). The QMC data are taken from (Capogrosso-Sansone *et al.*, 2007). In the bottom figure, a denotes the scattering length of the free bosons in the lattice. The + and − signs refer to the upper and lower parts of the transition line.

where $\delta\mu = \mu - \mu_c$. $P_c + \bar{n}_c\delta\mu$ denotes the regular part of the pressure at the transition; P_c and $\bar{n}_c$ are the pressure and the density at the QCP, respectively. The + (−) sign in (318) corresponds to particle (hole) doping (i.e. the upper (lower) part of the transition line for a given Mott lobe). $\mathcal{F}_{\rm DBG}$ is a universal scaling function characteristic of the dilute-Bose-gas universality class. The energy-dependent (dimensionless) interaction constant $\tilde{g}(T)$ is defined by $\tilde{g}(\epsilon) = 8\pi\sqrt{2m^*a^{*2}|\epsilon|}$ and is entirely determined by m^* and a^*. It is a dangerously irrelevant variable (in the RG sense) and cannot be neglected. The fact that the quasi-particle weight $Z_{\rm qp}$ does not appear in (318) is a consequence of the gauge invariance of the

microscopic action (Rançon and Dupuis, 2012b).[71]

The scaling function $\mathcal{F}_{\rm DBG}$ of the three-dimensional Bose gas can be computed perturbatively in some limits. For instance, when $\mathrm{sgn}(Z_C)\delta\mu < 0$ and $|\delta\mu| \gg T$, the pressure is given by

$$P(\mu,T) = P_c + \bar{n}_c\delta\mu + \left(\frac{m^*}{2\pi}\right)^{3/2} T^{5/2} e^{-|\delta\mu|/T} \tag{319}$$

and corresponds to a dilute classical gas. For $\delta\mu = 0$ (quantum critical regime),

$$P(\mu_c,T) = P_c + \zeta(5/2)\left(\frac{m^*}{2\pi}\right)^{3/2} T^{5/2}, \tag{320}$$

while in the zero-temperature superfluid phase,

$$P(\mu,0) = P_c + \bar{n}_c\delta\mu + \frac{m^*\delta\mu^2}{8\pi a^*}\left(1 - \frac{64}{15\pi}\sqrt{m^*a^{*2}|\delta\mu|}\right), \tag{321}$$

where the last two terms correspond to the "mean-field" result and the "Lee-Huang-Yang" correction, respectively. Differentiating (321) wrt μ, we obtain

$$\bar{n}(\mu,0) = \bar{n}_c + \frac{m^*\delta\mu}{4\pi a^*}\left(1 - \frac{16}{3\pi}\sqrt{m^*a^{*2}|\delta\mu|}\right), \tag{322}$$

which allows us to rewrite $P(\mu,0)$ as a function of $\bar{n}(\mu,0) - \bar{n}_c$: we recover the standard expression of the $T = 0$ pressure in a dilute Bose gas but with $\bar{n} - n_c$ instead of the full density $\bar{n}$ of the fluid. Thus, in the vicinity of a generic QCP, the excess density of particles (or holes) $\bar{n} - \bar{n}_c$ wrt the commensurate density of the Mott insulator behaves as a dilute gas of quasi-particles. Equations (319-322) are very well satisfied by the NPRG results (Rançon and Dupuis, 2012a,b).

One can obtain similar scaling forms for other thermodynamic quantities: density, compressibility, superfluid density, etc. Of particular interest is the condensate density n_0. Since only the coherent part of the excitations (i.e. the quasi-particles $\bar{\phi}$) condenses, one has

$$n_0(\mu,T) = Z_{\rm qp}\left(\frac{m^*|\delta\mu|}{2\pi}\right)^{3/2} \mathcal{I}\left(\frac{T}{|\delta\mu|}, \tilde{g}(\delta\mu)\right) \tag{323}$$

near the superfluid–Mott-insulator transition. The fact that $n_0(\mu,T)$, contrary to other thermodynamic quantities, depends on the quasi-particle weight can be understood by noting that it is not a gauge invariant quantity.

[71] This result bears some analogy with Fermi liquid theory where gauge invariance ensures that the coupling of the electromagnetic scalar and vector potentials to the elementary excitations (Landau's quasi-particles) is not renormalized. See, *e.g.*, (Nozières, 1964).

From standard results on the dilute Bose gas, we also obtain the transition temperature

$$T_c = \frac{2\pi}{m^*}\left(\frac{m^*|\delta\mu|}{8\pi\zeta(3/2)a^*}\right)^{2/3} \tag{324}$$

near the QCP. Equations (323) and (324) are confirmed by the NPRG results (Rançon and Dupuis, 2012b).

At the QCP ($\delta\mu = 0$), one can clearly distinguish two regimes in the RG flow: i) a high-energy (or short-distance) regime $k \gtrsim k_x$ where lattice effects are important and the dimensionless coupling constant $\tilde{\lambda}_k$ is large, ii) a weak-coupling regime $k \lesssim k_x$ where $\tilde{\lambda}_k \ll 1$ and the flow is governed by the Gaussian fixed point $\tilde{\lambda} = 0$: λ_k, $Z_{C,k}$ and $Z_{A,k}$ are then nearly equal to their fixed-point values while $\tilde{\lambda}_k \propto k$ vanishes in agreement with its scaling dimension $[\tilde{\lambda}_k] = 4 - d - z = -1$ at the Gaussian fixed point ($d = 3$ and $z = 2$). In the momentum regime $|\mathbf{q}| \lesssim k_x$, the quasi-particles with mass m^* and scattering length a^* are well defined and the physics becomes universal (insofar as all physical quantities depend only on m^* and a^* besides μ and T). The crossover scale k_x between the two regimes is typically of the order of Λ (k_x^{-1} is equal to a few lattice spacings).

Away from the QCP, chemical potential and temperature introduce two new momentum scales: the "healing" scale[72] $k_h = \sqrt{2m^*|\delta\mu|}$ and the thermal scale $k_T = \sqrt{2m^*T}$. Universality requires $k_h, k_T \ll k_x$. Since $k_x \sim a^{*-1} \sim 1$ (except close to the tip of the Mott lobe) these conditions can be rewritten as

$$\sqrt{2m^*a^{*2}|\delta\mu|} \ll 1, \qquad \sqrt{2m^*a^{*2}T} \ll 1. \tag{325}$$

In the low-energy limit the system behaves as a gas of weakly-interacting quasi-particles if the dimensionless coupling constants $\tilde{\lambda}_{k_h} \simeq 8\pi k_h a^*$ and $\tilde{\lambda}_{k_T} \simeq 8\pi k_T a^*$ are small. Since $k_x \sim 1$, universality ($k_h, k_T \ll k_x$) implies weak coupling ($k_h a^*, k_T a^* \ll 1$). Thus, when conditions (325) are satisfied, the excess density of particles (or holes) wrt the Mott insulator behaves as a dilute Bose gas. In the zero-temperature superfluid phase, using Eq. (322) the weak-coupling/universality condition $k_h a^* \ll 1$ can be rewritten as

$$\sqrt{|\bar{n} - \bar{n}_c|a^{*3}} \ll 1. \tag{326}$$

This is the usual condition for a boson gas to be dilute except that it involves the excess density of particles (or holes) $|\bar{n} - \bar{n}_c|$ (with respect to the commensurate density of the Mott insulator) rather than the full density $\bar{n}$ of the fluid. For $k \lesssim k_h$, λ_k and $Z_{C,k}$ depart from their fixed-point values at $\delta\mu = 0$ and vanish logarithmically

[72] On the Mott insulator side $\mathrm{sgn}(Z_C)\delta\mu \le 0$, k_h corresponds to the correlation length.

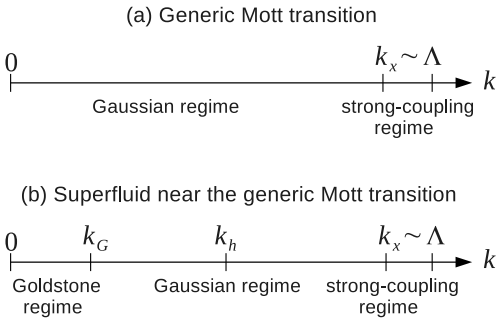

FIG. 46 Characteristic momentum scales at the generic Mott transition and in the nearby superfluid phase.

below a "Ginzburg" momentum scale p_G which is exponentially small at weak coupling ($\tilde{\lambda}_{k_h} \ll 1$). For $k \lesssim p_G$, the flow is dominated by the Goldstone (phase) mode and characterized by the divergence of the longitudinal propagator. We thus recover the infrared behavior in the superfluid phase discussed in Sec. XIII.A. The various regimes of the RG flow are summarized in Fig. 46.

Since m^*/m is typically of order 1 for $\bar{n}_c$ not too large (except near the tip of the Mott lobe), the condition $k_T a^* = \sqrt{2m^* a^{*2} T} \ll 1$ can be rewritten as $T \ll t$. The crossover temperature scale below which the thermodynamics becomes universal is set by the hopping amplitude t.

c. Universal thermodynamic near a QMCP. At a QMCP $Z_C = -\partial\delta/\partial\mu$ vanishes and $z = 1$. The QMCP is similar to the critical point of the $(d+1)$-dimensional O(2) model. When Z_C vanishes, the $T = 0$ phase transition is controlled by the Wilson-Fisher fixed point of the O(2) model in dimensions $d+1$ (for d smaller than the upper critical dimension $d_c^+ = 3$). There is one relevant variable (that we denote by r) with scaling dimension $1/\nu$ given by the correlation-length exponent $\nu \equiv \nu_{\mathrm{O(2)}}^{(d+1)}$. If we move away from the Mott-lobe tip in an arbitrary direction in the plane $(t/U, \mu/U)$, Z_C will in general not vanish. In that case, in addition to r one must consider a second relevant variable: Z_C. It can be shown, using the fact that the scaling dimension $y = 1$ of Z_C satisfies $1 - y\nu_{\mathrm{O(2)}}^{(d+1)} > 0$, that Z_C drops out of the scaling relations and the QMCP looks like an ordinary $(d+1)$-dimensional O(2) critical point (Fisher *et al.*, 1989).

This implies that the universal (critical) behavior in the vicinity of a QMCP can be obtained from the quantum O(2) model studied in Sec. XII. Critical fluctuations have a linear dispersion $\omega = c|\mathbf{p}|$ with velocity c. At $T = 0$, deviations from criticality are measured by a characteristic energy scale $|\Delta|$. In the Mott phase, Δ is equal to the single-particle excitation gap. In the superfluid phase, we take Δ negative such that $|\Delta| = -\Delta$ is the gap in the Mott phase at the point located symmetrically wrt the QMCP (see Sec. XII). $\Delta = \alpha U[(t_c - t)/U]^{\nu z}$ can be related to the distance $t_c - t$ to the QMCP. Both c and α depend on the QMCP considered.[73]

TABLE XII Velocity c and parameter α at the QMCP's (t_c, μ_c) corresponding to the first three Mott lobes of the two-dimensional Bose-Hubbard model (Rançon and Dupuis, 2013). The QMC data is taken from (Capogrosso-Sansone *et al.*, 2008).

Mott lobe	$\bar{n}_c = 1$	$\bar{n}_c = 2$	$\bar{n}_c = 3$
c/t_c NPRG	4.88	8.53	12.14
c/t_c QMC	4.8 ± 0.2		
c/t_c RPA	5.74	9.85	13.89
α	2.238	3.374	4.222

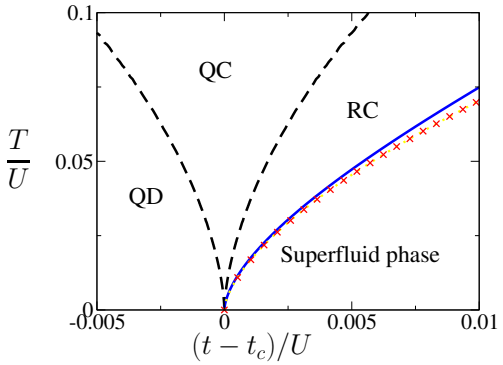

FIG. 47 (Color online) Phase diagram near the QMCP (t_c, μ_c) of the first Mott lobe for a constant chemical potential $\mu = \mu_c$ (QD: quantum disordered, QC: quantum critical, RC: renormalized classical). The (blue) solid line shows the BKT transition temperature obtained from $T_{\mathrm{KT}} = 1.59\,\rho_s(T = 0)$; the (red) crosses correspond to $T/U = 1.28[(t - t_c)/U]^{\nu}$ (with $\nu = 0.63$). The dashed crossover lines are obtained from the criterion $|\Delta| = T$ (Rançon and Dupuis, 2013).

We now focus on the two-dimensional case. In table XII we show the values of α and c together with the RPA and QMC results. The phase diagram near the QMCP (t_c, μ_c) of the first Mott lobe is shown in Fig. 47 with the three characteristic regimes (QD, QC and RC) discussed in Sec. XII. In the renormalized classical regime, there is a BKT phase transition between a high-temperature normal phase and a low-temperature superfluid phase with algebraic order. To estimate T_{KT}, one can use $T_{\mathrm{KT}} = \mathcal{C}\rho_s$ where $\rho_s = \rho_s(T = 0)$ is the zero-temperature superfluid stiffness (obtained in the NPRG approach) and $\mathcal{C}$ a universal number close to $\pi/2$. T_{KT} in Fig. 47 is obtained with $\mathcal{C} = 1.59$ (Rançon *et al.*,

[73] α depends also on the path followed to approach the QMCP. The values reported in table XII correspond to a path at constant chemical potential μ_c.

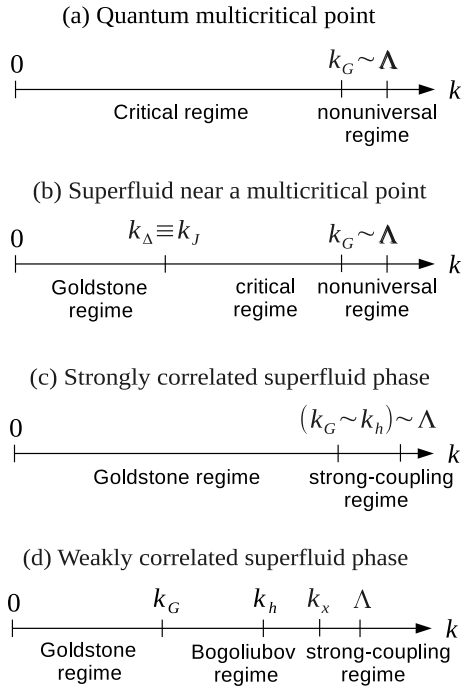

FIG. 48 Characteristic momentum scales at a QMCP and in the nearby superfluid phase. (k_J^{-1} denotes the Josephson length.)

2013).[74] Near the QMCP the transition temperature is well approximated by $T_{\rm KT}/U \simeq 1.28[(t-t_c)/U]^\nu$, in very good agreement with the QMC result $T_{\rm KT}/U \simeq 1.29[(t-t_c)/U]^\nu$ (Capogrosso-Sansone *et al.*, 2008).

As in the case of the generic transition we can study the approach to universality. At a QMCP, we can distinguish two regimes: i) a (high-energy) nonuniversal regime $k \gtrsim p_G$ where lattice effects are important and the dimensionless coupling constant $\tilde\lambda_k$ varies strongly with k, ii) a universal (critical) regime $k \ll p_G$ where $\tilde\lambda_k$ is close to its fixed-point value $\tilde\lambda^*$. The crossover (Ginzburg) scale is of the order of the inverse lattice spacing (the Ginzburg length p_G^{-1} is typically equal to a few lattice spacings).

Away from the QMCP, the energy scale $|\Delta|$ and the temperature define two new momentum scales, $k_\Delta = |\Delta|/c$ and $k_T = T/c$, where c is the velocity of the critical fluctuations. k_Δ^{-1} is the correlation length in the zero-temperature Mott insulator and corresponds to the Josephson length in the superfluid phase. Universality requires $k_\Delta, k_T \ll p_G$, i.e. $|\Delta|, T \ll c p_G$. If we approximate $c \simeq \sqrt{t_c U}(\bar n_c^2 + \bar n_c)^{1/4}$ by its value in the strong-coupling RPA, we obtain the conditions $|\Delta|, T \ll p_G \sqrt{t_c U}(\bar n_c^2 + \bar n_c)^{1/4}$ for the system to be in the universal regime. This should be compared with the crossover scale $\sim t$ which controls the universal behavior in the vicinity of a generic QCP. As we move away from the QMCP in the superfluid phase, the Josephson momentum scale k_Δ increases and becomes of the order of $p_G \sim \Lambda$. The system is then not in the critical regime anymore and $k_\Delta \equiv k_h$ should rather be interpreted as a healing scale. Moving deeper into the superfluid phase both p_G and k_h decrease, and we finally reach a weakly correlated phase, where $p_G \ll k_h$ (Sec. XIII.A), which is similar to the superfluid phase near a generic QCP (Fig. 46). The various regimes of the renormalization-group flow are summarized in Fig. 48.

[74] The BKT transition temperature is related to the jump of the stiffness by $T_{\rm BKT} = (\pi/2)\rho_s(T_{\rm BKT}^-)$ (Nelson and Kosterlitz, 1977). The fact fact $\mathcal{C} = T_{\rm BKT}/\rho_s \simeq \pi/2$ (with $\rho_s \equiv \rho_s(T=0)$) is due to $\rho_s(T_{\rm BKT}^-)$ differing only slightly from ρ_s (Rançon *et al.*, 2013).

XIV. INTERACTING FERMIONS

In the previous sections, we have focused on classical or bosonic quantum systems. The NPRG approach can also be used for fermionic systems. However, the Fermi-Dirac statistics and the existence of a Fermi surface at nonzero density lead to complications which, contrary to the case of bosons, prevents us to straightforwardly apply the approximation schemes (such as the derivative expansion or the BMW approximation) designed for classical systems. In this section, we give a brief overview of the Wilsonian fermionic RG (Sec. XIV.A). We show how the latter can be formulated in the 1PI framework but emphasize the difficulties due to the Fermi-Dirac statistics and the Grassmannian nature of the fermion field (Sec. XIV.B). Finally we describe improvements of the fermionic RG, mainly based on a partial "bosonization" of the action (Sec. XIV.C).

A. Wilsonian fermionic RG

In condensed-matter physics, one of the first application of RG ideas goes back to the work of Bychkov *et al.* on the one-dimensional electron gas (Bychkov *et al.*, 1966). In one dimension, interacting fermions are characterized by competing fluctuations (singlet/triplet superconductivity and charge/spin density waves) which lead to a breakdown of Landau's Fermi liquid theory even when the system is metallic (Giamarchi, 2004). Bychkov *et al.* showed that the summation of the so-called Parquet diagrams allows one to treat the various fluctuations on an equal footing. Later on, taking advantage of the logarithmic structure of the perturbation theory, Menyhard and Solyom set up a multiplicative RG approach to the one-dimensional electron gas where the vertices renormalize multiplicatively upon a change $E_0 \to E_0(l) = E_0 e^{-l}$ of the bandwidth (Menyhard and Solyom, 1973; Sólyom, 1979). The multiplicative RG bears similarities with the Gell-Mann–Low RG (Gell-Mann and Low, 1954) in quantum electrodynamics and, to lowest

(one-loop) order, is equivalent to the Parquet approach. The modern Kadanoff-Wilson approach, based on the functional integral formalism and the progressive integration of fermionic degrees of freedom, was introduced by Bourbonnais and Caron in the 1980s (Bourbonnais, 1985; Bourbonnais and Caron, 1991). While the multiplicative RG was limited to a small number of marginal variables, the Wilsonian fermionic RG can deal with relevant, marginal or irrelevant variables and is perfectly suited to study higher-dimensional systems (Bourbonnais and Caron, 1991; Shankar, 1994).

The partition function of a d-dimensional fermion system can be written as a functional integral over a Grassmannian field. To some extent, the (Euclidean) action $S[\psi^*,\psi]$ is similar to that of the φ^4 field theory used in the theory of critical phenomena. This suggests to follow a Kadanoff-Wilson RG procedure by successively integrating out the fermionic degrees of freedom (Bourbonnais, 1985; Bourbonnais and Caron, 1991; Shankar, 1994). Since the low-temperature properties of metals are dominated by electronic states near the Fermi level, it is natural to use the electronic energy $\xi_{\mathbf{p}}=\epsilon_{\mathbf{p}}-\mu$ measured from the Fermi level as an energy scaling parameter. The RG procedure then consists of successive partial integrations of the fermion field degrees of freedom in the band energy shell $[E_0(l+dl),E_0(l)]\cup[-E_0(l),-E_0(l+dl)]$ with $E_0(l)=E_0e^{-l}$.

However, in dimensions $d\geq 2$, the existence of a Fermi surface introduces some complications.[75] Since low-energy fermion states lie near the Fermi surface, it is not possible to neglect the momentum dependence of the renormalized (scale-dependent) constants $g_i(p_1\cdots p_4)$. Writing $\mathbf{p}=(\xi_{\mathbf{p}},\mathbf{\Omega}_{\mathbf{p}})$ with $\mathbf{\Omega}_{\mathbf{p}}$ an angular variable, we can set $\xi_{\mathbf{p}_i}=\omega_i=0$ $(i=1,\cdots,4)$ in $g_i(p_1\cdots p_4)$ since the dependence in these variables is irrelevant. The interaction constant $g_i(\mathbf{\Omega}_{\mathbf{p}_1}\cdots\mathbf{\Omega}_{\mathbf{p}_4})$ is then reduced to a functional of four (or three if we use momentum conservation) angular variables. This makes the fermionic RG necessary functional (Shankar, 1994) and considerably increases the complexity of the method, even to one-loop order (Metzner *et al.*, 2012; Zanchi and Schulz, 2000).

B. 1PI formalism

To make contact with the NPRG approach to classical and bosonic quantum systems, let us first show how the fermionic RG can be formulated in the 1PI formalism (Berges *et al.*, 2002; Honerkamp *et al.*, 2001; Kopietz *et al.*, 2010; Metzner *et al.*, 2012). The partition function

$$Z_k[J]=\int\mathcal{D}[\psi]e^{-S_0[\psi]-S_{\rm int}[\psi]-\Delta S_k[\psi]+\sum_\alpha J_\alpha\psi_\alpha} \tag{327}$$

is written as a functional integral over a Grassmannian field ψ_α where the collective index $\alpha=(\mathbf{r},\tau,\sigma,c)$ stands for position variable, imaginary time, spin projection along a given axis and charge index. The latter, $c=\pm$, is such that $\psi_\alpha=\psi_\sigma(\mathbf{r},\tau)$ if $c=-$ and $\psi_\alpha=\psi^*_\sigma(\mathbf{r},\tau)$ if $c=+$. The "regulator" takes the usual form $\Delta S_k=\frac{1}{2}\sum_{\alpha,\alpha'}\psi_\alpha R_{k,\alpha\alpha'}\psi_{\alpha'}$. The function R_k is chosen such that only high-energy states, that is states away from the Fermi level, contribute to the partition function. A common choice is

$$G_0^{-1}(p)+R_k(p)=\frac{\Theta(|\xi_{\mathbf{p}}|-k)}{i\omega_n-\xi_{\mathbf{p}}}, \tag{328}$$

where $G_0(p)=(i\omega_n-\xi_{\mathbf{p}})^{-1}$ is the noninteracting propagator and k denotes an energy scale. The scale-dependent effective action

$$\Gamma_k[\phi]=-\ln Z[J]+\sum_\alpha J_\alpha\phi_\alpha-\Delta S_k[\phi] \tag{329}$$

is a functional of the Grassmann variable $\phi_\alpha=\delta\ln Z[J]/\delta J_\alpha$ and satisfies Wetterich's equation (30).

Thus in quantum systems the scale-dependent effective action satisfies the same equation regardless of the statistics of the particles. Nevertheless, there are important differences between bosonic and fermionic systems. In the latter, ϕ being a Grassmann variable, the functional $\Gamma_k[\phi]$ is defined only *via* its Taylor expansion about $\phi=0$. Only the vertices $\Gamma_k^{(n)}$ computed in a vanishing field $\phi=0$ bear a physical meaning. As a consequence, neither the derivative expansion nor the BMW approximation, which both require to consider the effective potential and/or the vertices for a nonzero value of the field, make sense in fermionic systems. The only possible approximation scheme is to truncate the expansion of the effective action,

$$\Gamma_k[\phi]=\Gamma_k[0]+\frac{1}{2}\sum_{\alpha_1,\alpha_2}\Gamma^{(2)}_{k,\alpha_1\alpha_2}\phi_{\alpha_1}\phi_{\alpha_2}+\frac{1}{4!}\sum_{\alpha_1\cdots\alpha_4}\Gamma^{(4)}_{k,\alpha_1\cdots\alpha_4}\phi_{\alpha_1}\phi_{\alpha_2}\phi_{\alpha_3}\phi_{\alpha_4}+\cdots \tag{330}$$

and consider the corresponding flow equations for the n-point vertices $\Gamma_k^{(n)}$ (with typically $n\leq 4$ or $n\leq 6$). Such a truncation amounts to performing a loop expansion and therefore remains fundamentally a weak-coupling approximation though a nontrivial one due to the momentum dependence of the interaction vertices (see the discussion in Sec. XIV.A).[76,77]

[75] One-dimensional systems are special since the Fermi surface reduces to two Fermi points $\pm p_F$.

[76] The 1PI approach presents two main advantages wrt to the Wilson-Polchinski one. It yields flow equations which are local in k, i.e. $\partial_k\Gamma_k^{(n)}$ is a function of $\Gamma_k^{(n)}$ and $\Gamma_k^{(n+1)}$ at the same scale k (Chitov and Bourbonnais, 2003; Zanchi and Schulz, 2000), and no one-particle-reducible terms appear.

[77] Note that in bosonic (or classical) systems, low-order truncations

A related difficulty comes from the fact that $\phi_\alpha = \langle\psi_\alpha\rangle$ is not an order parameter in a fermionic system. Order parameters are defined by composite fields: $\psi^*_\sigma\psi_{\sigma'}$ for a charge- or spin-density wave, $\psi_\sigma\psi_{\sigma'}$ for a superconductor. Phase transitions are signaled by a divergence of the order-parameter susceptibility and a concomitant divergence of some interaction vertices which prevents to continue the RG flow into the broken-symmetry phase unless one introduces explicitly a symmetry-breaking field (Gersch *et al.*, 2005; Maier and Honerkamp, 2012; Salmhofer *et al.*, 2004). Moreover, fluctuations due to bosonic composite fields are not properly taken care of. Thus even in the absence of a phase transition, the fermionic RG becomes uncontrolled when strong collective fluctuations with a large correlation length set in.

Notwithstanding these limitations, the fermionic RG has proven to be a powerful and unbiased method to study interacting fermion systems. In contrast to standard (RPA-like) diagrammatic resummations, it treats various types of instabilities on an equal footing and does not require any *a priori* knowledge of the ground state of the system. The RG has been particularly useful to understand one- and quasi-one-dimensional systems (Bourbonnais and Caron, 1991; Sólyom, 1979) in connection with the physics of strongly anisotropic organic conductors (Bourbonnais and Caron, 1988, 1991; Bourbonnais and Sedeki, 2009; Nickel *et al.*, 2005, 2006; Sedeki *et al.*, 2012). It has also been used to study the two-dimensional Hubbard model (Giering and Salmhofer, 2012; Halboth and Metzner, 2000; Honerkamp *et al.*, 2001; Husemann *et al.*, 2012; Husemann and Salmhofer, 2009; Katanin, 2004; Zanchi and Schulz, 2000) as well as other models of strongly correlated fermions; for recent reviews see (Metzner *et al.*, 2012; Platt *et al.*, 2013).

C. Beyond perturbative RG

One possibility to circumvent some of the difficulties of the fermionic RG is to "bosonize" the fermionic degrees of freedom *via* a Hubbard-Stratonovich transformation of the interaction term in the microscopic action $S[\psi]$ (Baier *et al.*, 2005, 2000, 2004; Gies and Wetterich, 2002; Schütz *et al.*, 2005). This transforms the original interacting fermion system into a system of free fermions interacting with a bosonic field. One of the difficulties of this approach is to consider various types of instabilities on an equal footing; for recent works in this direction see (Friederich *et al.*, 2011; Krahl *et al.*, 2009; Krahl and Wetterich, 2007). On the other hand it is possible to treat the bosonic degrees of freedom with the standard methods of the NPRG. In particular, there are no difficulties to study phases with spontaneously broken symmetries since the bosonic Hubbard-Stratonovich field plays the role of an order parameter. Furthermore the approach is not restricted to the weak-coupling limit, as it partially relies on the NPRG, and critical fluctuations of (collective) bosonic fluctuations are taken care of.

A first option is to fully integrate out the fermion field in order to obtain an action for the auxiliary field of the Hubbard-Stratonovich transformation as originally discussed by Hertz (Hertz, 1976; Millis, 1993). The effective bosonic theory can then be studied with the standard methods of the NPRG described in the preceding sections of this review (Bauer *et al.*, 2011; Jakubczyk *et al.*, 2010, 2008). The main limitation of this approach is that integrating out gapless fermionic degrees of freedom may lead to nonlocal terms in the bosonic action (Belitz *et al.*, 2005) and makes a RG analysis difficult.

Alternatively, one may keep both fermionic and (auxiliary) bosonic degrees of freedom in the action. Although the Hubbard-Stratonovich transformation yields an action with no interaction between fermions, the later is unavoidably generated by the renormalization procedure. It can however be eliminated along the RG flow by means of a "dynamical" bosonization at each scale k (Gies and Wetterich, 2002). The nontrivial part of the effective action then comes from the boson-boson interaction whereas the fermions are coupled to the bosons but do not interact with each other. Again the bosonic degrees of freedom can be treated with the NPRG method, making the analysis nonperturbative. Both the Hubbard model (Baier *et al.*, 2005, 2000, 2004; Friederich *et al.*, 2011; Krahl *et al.*, 2009; Krahl and Wetterich, 2007) and the BCS-BEC crossover (Bartosch *et al.*, 2009; Birse *et al.*, 2005; Diehl *et al.*, 2007a,b; Eberlein and Metzner, 2013; Floerchinger *et al.*, 2008; Scherer *et al.*, 2011; Strack *et al.*, 2008) have been studied along these lines.

A two-particle-irreducible (2PI) NPRG approach has also been proposed. Although the 2PI formalism in the framework of the NPRG has been considered in various contexts (Blaizot *et al.*, 2011b; Nagy and Sailer, 2011; Pawlowski, 2007; Polonyi and Sailer, 2005), few works have focused on interacting fermions (Dupuis, 2005, 2014; Rentrop *et al.*, 2015; Rentrop *et al.*, 2016; Wetterich, 2007; **?**). In the 2PI NPRG, the scale-dependent effective action $\Gamma_k[G]$ is a functional of the one-particle propagator. The "classical" variable is thus bosonic in nature; it is itself an order parameter and there are no difficulties to describe phases with spontaneously broken symmetries. It is even possible to start the RG flow in a broken-symmetry phase (with the Hartree-Fock-RPA theory as the initial condition) (Dupuis, 2014). Furthermore, we expect 2PI vertices to be much less singular than their 1PI counterparts, so that they can be parameterized by means of a small number of coupling constants.

---

of the effective action remain nonperturbative (in the sense that beta functions include terms of infinite order in the coupling constants) if one expands about a nonzero value of the field.

The (full, i.e., 1PI) momentum-frequency-dependent vertex is computed from the 2PI vertex by solving a Bethe-Salpeter equation. Thus, contrary to the fermionic 1PI RG approach, there is no need to discretize the momentum space into patches to keep track of the momentum dependence of the two-particle 1PI vertex when solving numerically the flow equations. Whether or not the 2PI NPRG could provide us with a viable alternative to the 1PI NPRG requires further works.

Finally, let us mention recent attempts to implement the fermionic RG using an exactly solvable interacting reference problem (rather than the noninteracting limit) as starting point for the RG flow (Katanin, 2015, 2016; Taranto *et al.*, 2014; Wentzell *et al.*, 2015).[78] As a specific example, the Dynamical Mean-Field Theory (DMFT) solution (Georges and Kotliar, 1992; Metzner and Vollhardt, 1989) has been chosen as initial condition in the Hubbard model (Taranto *et al.*, 2014). DMFT, which allows for an accurate treatment of local correlations, has played an essential role in our understanding of the Mott metal-insulator transition (Georges *et al.*, 1996). By choosing DMFT as the starting point of the RG flow, a significant part of correlation effects is included nonperturbatively already from the very beginning. Nonlocal spatial correlations are then taken into account by the RG flow. One thus hopes to overcome the main restrictions of the two methods: the lack of nonlocal correlations in DMFT and the restriction to weak coupling in the practical implementation of the fermionic RG.

ACKNOWLEDGMENTS

We are grateful for fruitful collaborations and/or discussions with...

Appendix A: Fourier transforms

The Fourier transformed of the field $\varphi_i(\mathbf{r})$ is defined by

$$\begin{aligned}\varphi_i(\mathbf{p}) &= \frac{1}{\sqrt{V}}\int_{\mathbf{r}} e^{-i\mathbf{p}\cdot\mathbf{r}}\varphi_i(\mathbf{r}),\\ \varphi_i(\mathbf{r}) &= \frac{1}{\sqrt{V}}\sum_{\mathbf{p}} e^{i\mathbf{p}\cdot\mathbf{r}}\varphi_i(\mathbf{p}),\end{aligned} \tag{A1}$$

where $V = L^d$ is the volume of the system, and we use the notation

$$\int_{\mathbf{r}} \equiv \int d^d r. \tag{A2}$$

For periodic boundary conditions, $\varphi_i(\mathbf{r}+L) = \varphi_i(\mathbf{r})$, the momentum $\mathbf{p}$ is quantized: $p_j = n_j(2\pi/L)$ $(1 \le j \le d$ and $n_j \in Z)$. In the thermodynamic limit, $\mathbf{p}$ becomes a continuous variable and

$$\frac{1}{V}\sum_{\mathbf{p}} \to \int \frac{d^d p}{(2\pi)^d} \equiv \int_{\mathbf{p}} \qquad (V\to\infty). \tag{A3}$$

Similarly, we define the Fourier transformed of the n-point correlation function (B2) and the n-point vertex (B11) by

$$\begin{aligned}G^{(n)}_{\{i_j\}}[\{\mathbf{p}_j\};\mathbf{h}] &= \frac{1}{V^{n/2}}\int_{\{\mathbf{r}_j\}} e^{-i\sum_j \mathbf{p}_j\cdot\mathbf{r}_j} G^{(n)}_{\{i_j\}}[\{\mathbf{r}_j\};\mathbf{h}]\\ &= \langle\varphi_{i_1}(\mathbf{p}_1)\cdots\varphi_{i_n}(\mathbf{p}_n)\rangle.\end{aligned} \tag{A4}$$

and

$$\Gamma^{(n)}_{\{i_j\}}[\{\mathbf{p}_j\};\boldsymbol{\phi}] = \frac{1}{V^{n/2}}\int_{\{\mathbf{r}_j\}} e^{-i\sum_j \mathbf{p}_j\cdot\mathbf{r}_j}\Gamma^{(n)}_{\{i_j\}}[\{\mathbf{r}_j\};\boldsymbol{\phi}]. \tag{A5}$$

Using

$$\frac{\delta}{\delta\phi_i(\mathbf{r})} = \sum_{\mathbf{p}}\frac{\delta\phi_i(\mathbf{p})}{\delta\phi_i(\mathbf{r})}\frac{\delta}{\delta\phi_i(\mathbf{p})} = \frac{1}{\sqrt{V}}\sum_{\mathbf{p}} e^{i\mathbf{p}\cdot\mathbf{r}}\frac{\delta}{\delta\phi_i(-\mathbf{p})}, \tag{A6}$$

we obtain

$$\Gamma^{(n)}_{\{i_j\}}[\{\mathbf{p}_j\};\boldsymbol{\phi}] = \frac{\delta^n\Gamma[\boldsymbol{\phi}]}{\delta\phi_{i_1}(-\mathbf{p}_1)\cdots\delta\phi_{i_n}(-\mathbf{p}_n)}. \tag{A7}$$

For a quantum system in the Euclidean formalism, a bosonic field $\varphi_i(x)$ is a function of the space-time variable $x = (\mathbf{r},\tau)$ and is periodic in imaginary time, $\varphi_i(\mathbf{r},\tau+\beta) = \varphi_i(\mathbf{r},\tau)$, with $\beta = 1/T$ the inverse temperature. Its Fourier transform $\varphi_i(p)$ is a function of $p = (\mathbf{p}, i\omega_n)$ with $\omega_n = n2\pi T$ (n integer) a Matsubara frequency. All previous definitions apply if we replace V by βV and $\mathbf{p}\cdot\mathbf{r}$ by $px = \mathbf{p}\cdot\mathbf{r} - \omega_n\tau$. In the zero-temperature limit, Matsubara sums become integrals,

$$\frac{1}{\beta}\sum_{\omega_n} \to \int_{-\infty}^{\infty}\frac{d\omega}{2\pi} \qquad (\beta\to\infty). \tag{A8}$$

A fermionic field is an anticommuting Grassmann variable and is antiperiodic in imaginary time: $\varphi_i(\mathbf{r},\tau+\beta) = -\varphi_i(\mathbf{r},\tau)$. Accordingly, fermionic Matsubara frequencies are defined as $\omega_n = (2n+1)\pi T$ (n integer).

Appendix B: The effective action formalism

In this Appendix we briefly review the effective action formalism (Le Bellac, 1991; Zinn-Justin, 1996). In statistical physics, the effective action is nothing but the Gibbs free energy and therefore contains all information about the thermodynamics of the system. It is also the generating functional of 1PI vertices, which are closely related to the correlation functions. We consider the O(N) model defined by the action (3).

[78] See Secs. VII and XIII.B for similar ideas in classical and bosonic quantum systems.

1. Effective action

In the presence of an external source $\mathbf{h}(\mathbf{r})$ which couples linearly to the field $\boldsymbol{\varphi}$, the partition function is defined by

$$Z[\mathbf{h}] = \int \mathcal{D}[\boldsymbol{\varphi}]\, e^{-S[\boldsymbol{\varphi}]+\int_{\mathbf{r}} \mathbf{h}\cdot\boldsymbol{\varphi}} \tag{B1}$$

By taking functional derivatives we obtain the n-point correlation functions (or Green functions)

$$\begin{aligned} G^{(n)}_{\{i_j\}}[\{\mathbf{r}_j\};\mathbf{h}] &= \langle \varphi_{i_1}(\mathbf{r}_1)\cdots\varphi_{i_n}(\mathbf{r}_n)\rangle \\ &= \frac{1}{Z[\mathbf{h}]}\frac{\delta^n Z[\mathbf{h}]}{\delta h_{i_1}(\mathbf{r}_1)\cdots\delta h_{i_n}(\mathbf{r}_n)}, \end{aligned} \tag{B2}$$

where $\langle\cdots\rangle = Z[\mathbf{h}]^{-1}\int\mathcal{D}[\boldsymbol{\varphi}]\cdots e^{-S[\boldsymbol{\varphi}]+\int_{\mathbf{r}}\mathbf{h}\cdot\boldsymbol{\varphi}}$. Note that $G^{(n)}[\mathbf{h}]$ is a functional of the external source $\mathbf{h}$. It is often convenient to consider the connected correlation functions

$$\begin{aligned} G^{(n)}_{c,\{i_j\}}[\{\mathbf{r}_j\};\mathbf{h}] &= \langle \varphi_{i_1}(\mathbf{r}_1)\cdots\varphi_{i_n}(\mathbf{r}_n)\rangle_c \\ &= \frac{\delta^n W[\mathbf{h}]}{\delta h_{i_1}(\mathbf{r}_1)\cdots\delta h_{i_n}(\mathbf{r}_n)} \end{aligned} \tag{B3}$$

obtained from the generating functional $W[\mathbf{h}] = \ln Z[\mathbf{h}]$. For the lowest orders, one easily finds

$$G^{(1)}_{c,i}[\mathbf{r};\mathbf{h}] = G^{(1)}_{i}[\mathbf{r};\mathbf{h}] = \phi_i(\mathbf{r}), \tag{B4}$$

and

$$G^{(2)}_{c,i_1i_2}[\mathbf{r}_1,\mathbf{r}_2;\mathbf{h}] = G^{(2)}_{i_1i_2}[\mathbf{r}_1,\mathbf{r}_2;\mathbf{h}] - \phi_{i_1}(\mathbf{r}_1)\phi_{i_2}(\mathbf{r}_2), \tag{B5}$$

where $\phi_i(\mathbf{r}) \equiv \phi_i[\mathbf{r};\mathbf{h}] = \langle\varphi_i(\mathbf{r})\rangle$ is the order parameter. A nonzero value of $\boldsymbol{\phi}(\mathbf{r})$ in the limit $\mathbf{h}\to 0$ implies that the O(N) symmetry of the action is spontaneously broken.

The effective action is defined as the Legendre transform of $W[\mathbf{h}]$:

$$\Gamma[\boldsymbol{\phi}] = -W[\mathbf{h}] + \int_{\mathbf{r}} \mathbf{h}\cdot\boldsymbol{\phi}. \tag{B6}$$

In Eq. (B6), $\mathbf{h}\equiv\mathbf{h}[\boldsymbol{\phi}]$ is a functional of $\boldsymbol{\phi}$ obtained by inverting the equation of state $\boldsymbol{\phi} = \boldsymbol{\phi}[\mathbf{h}]$ [Eq. (B4)]. The latter can be equivalently written as

$$\frac{\delta\Gamma[\boldsymbol{\phi}]}{\delta\phi_i(\mathbf{r})} = h_i(\mathbf{r}). \tag{B7}$$

The equilibrium state $\boldsymbol{\phi}_{\rm eq}$ for vanishing external source is thus obtained from the minima of $\Gamma[\boldsymbol{\phi}]$. The free energy of the system $F = -T\ln Z[\mathbf{h}=0] = T\Gamma[\boldsymbol{\phi}_{\rm eq}]$ is simply obtained by evaluating $\Gamma[\boldsymbol{\phi}]$ in the equilibrium configuration $\boldsymbol{\phi}_{\rm eq}$.

We can use (B1) and (B7) to obtain a functional integral representation of the effective action,

$$e^{-\Gamma[\boldsymbol{\phi}]} = \int \mathcal{D}[\boldsymbol{\varphi}]\, e^{-S[\boldsymbol{\varphi}]+\int_{\mathbf{r}}\frac{\delta\Gamma[\boldsymbol{\phi}]}{\delta\boldsymbol{\phi}(\mathbf{r})}\cdot(\boldsymbol{\varphi}(\mathbf{r})-\boldsymbol{\phi}(\mathbf{r}))}. \tag{B8}$$

For the scale-dependent effective action (8), Eq. (B8) becomes

$$\begin{aligned} e^{-\Gamma_k[\boldsymbol{\phi}]} = \int \mathcal{D}[\boldsymbol{\varphi}]\, e^{-S[\boldsymbol{\varphi}]+\int_{\mathbf{r}}(\varphi_i(\mathbf{r})-\phi_i(\mathbf{r}))\frac{\delta\Gamma_k[\boldsymbol{\phi}]}{\delta\phi_i(\mathbf{r})}} \\ \times e^{-\frac{1}{2}\int_{\mathbf{r},\mathbf{r}'}(\varphi_i(\mathbf{r})-\phi_i(\mathbf{r}))R_k(\mathbf{r}-\mathbf{r}')(\varphi_i(\mathbf{r}')-\phi_i(\mathbf{r}'))} \end{aligned} \tag{B9}$$

(this equation follows from (5) and (9)). Since $R_\Lambda(\mathbf{q})$ diverges,

$$e^{-\frac{1}{2}\int_{\mathbf{r},\mathbf{r}'}(\varphi_i(\mathbf{r})-\phi_i(\mathbf{r}))R_k(\mathbf{r}-\mathbf{r}')(\varphi_i(\mathbf{r}')-\phi_i(\mathbf{r}'))} \sim \delta(\boldsymbol{\varphi}(\mathbf{r})-\boldsymbol{\phi}(\mathbf{r})) \tag{B10}$$

behaves as a functional Dirac delta for $k\to\Lambda$, which leads to (10).

2. 1PI vertices

The effective action if the generating functional of the one-particle-irreducible (1PI) vertices (the reason for this terminology will become clear below)

$$\Gamma^{(n)}_{\{i_j\}}[\{\mathbf{r}_j\};\boldsymbol{\phi}] = \frac{\delta^n\Gamma[\boldsymbol{\phi}]}{\delta\phi_{i_1}(\mathbf{r}_1)\cdots\delta\phi_{i_n}(\mathbf{r}_n)}. \tag{B11}$$

The correlation functions $G^{(n)}_c$ can be expressed in terms of the $\Gamma^{(n)}$'s. Taking the functional derivative of Eq. (B7) wrt the field, we obtain

$$\begin{aligned} \delta(x_1-x_2) &= \frac{\delta}{\delta h(x_2)}\frac{\delta\Gamma[\boldsymbol{\phi}]}{\delta\phi(x_1)} \\ &= \int dx_3 \frac{\delta^2\Gamma[\boldsymbol{\phi}]}{\delta\phi(x_1)\delta\phi(x_3)}\frac{\delta\phi(x_3)}{\delta h(x_2)} \\ &= \int dx_3 \frac{\delta^2\Gamma[\boldsymbol{\phi}]}{\delta\phi(x_1)\delta\phi(x_3)}\frac{\delta^2 W[\mathbf{h}]}{\delta h(x_3)\delta h(x_2)} \end{aligned} \tag{B12}$$

(we use the notations $x\equiv(i,\mathbf{r})$, $\int dx = \int_{\mathbf{r}}\sum_i$) or, in matrix form,

$$\Gamma^{(2)}[\boldsymbol{\phi}] = G^{(2)}_c[\mathbf{h}]^{-1}. \tag{B13}$$

$\Gamma^{(2)} = G_0^{-1} + \Sigma$ is often expressed in terms of the self-energy Σ, where $G_0(\mathbf{p}) = (\mathbf{p}^2 + r_0)^{-1}$ is the bare 2-point propagator. Eq. (B13) then becomes Dyson's equation $G_c = G_0 - G_0\Sigma G_c$.

By taking an additional functional derivative in (B12), we obtain a relation between the 3-point Green function and the 3-point vertex,

$$\begin{aligned} G^{(3)}_c(x_1,x_2,x_3) = -\int du_1du_2du_3 G_c(x_1,u_1)G_c(x_2,u_2) \\ \times G_c(x_3,u_3)\Gamma^{(3)}(u_1,u_2,u_3), \end{aligned} \tag{B14}$$

as shown diagrammatically in Fig. 49. To alleviate the notations, we do not write the functional dependence of the correlation functions on $\mathbf{h}$ and use $G_c\equiv G^{(2)}_c$. Similarly, we can relate the 4-point correlation function to the 1PI vertices as shown in Fig. 49. Thus, if we know the (low-order) 1PI vertices, we can deduce the (low-order) correlation functions.

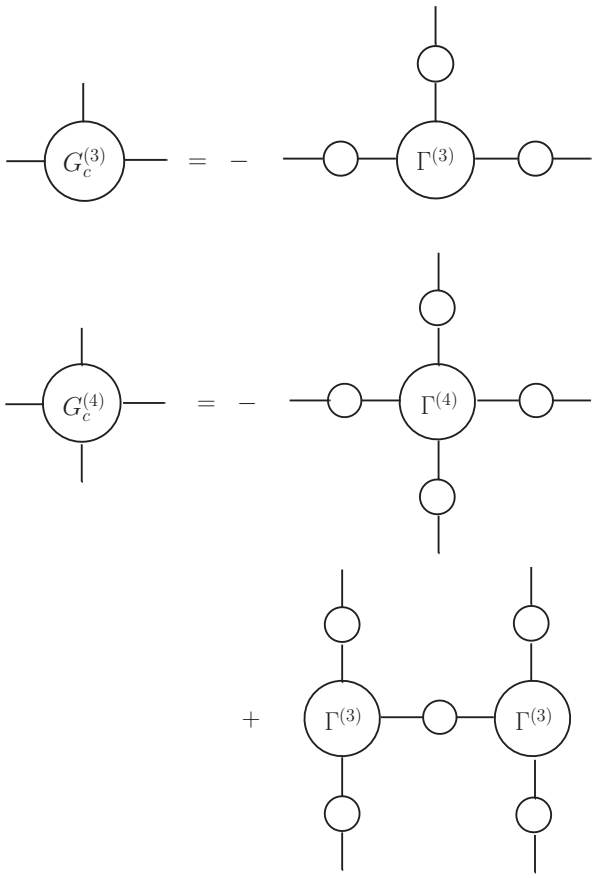

FIG. 49 Diagrammatic representation of the relation between the connected Green functions $G_c^{(3)}$,$G_c^{(4)}$ and the 1PI vertices $\Gamma^{(3)}$,$\Gamma^{(4)}$. (Diagrams obtained by exchanging external lines are not shown.)

3. Loop expansion

A systematic expansion of the effective action can be set up by defining the partition function

$$Z[\mathbf{h}] = \int \mathcal{D}[\boldsymbol{\varphi}]\, e^{-l(S[\boldsymbol{\varphi}]-\int_{\mathbf{r}}\mathbf{h}\cdot\boldsymbol{\varphi})} \tag{B15}$$

and the effective action

$$\Gamma[\boldsymbol{\phi}] = -\frac{1}{l}\ln[\mathbf{h}] + \int_{\mathbf{r}} \mathbf{h}\cdot\boldsymbol{\phi}. \tag{B16}$$

with a real parameter l (which will eventually be set to unity).

In the limit $l\to\infty$, the saddle-point approximation becomes exact,

$$\lim_{l\to\infty} \ln Z[h] = -S[\boldsymbol{\varphi}_{\rm cl}] + \int_{\mathbf{r}} \mathbf{h}\cdot\boldsymbol{\varphi}_{\rm cl}, \tag{B17}$$

where the classical field is defined by

$$\left.\frac{\delta S[\boldsymbol{\varphi}]}{\delta\boldsymbol{\varphi}(\mathbf{r})}\right|_{\boldsymbol{\varphi}_{\rm cl}} - \mathbf{h}(\mathbf{r}) = 0. \tag{B18}$$

This gives

$$\lim_{l\to\infty}\Gamma[\boldsymbol{\phi}] \equiv \Gamma_{\rm cl}[\boldsymbol{\phi}] = S[\boldsymbol{\phi}], \tag{B19}$$

where $\Gamma_{\rm cl}$ is referred to as the classical effective action. From (B19), we deduce

$$\begin{aligned}
\Gamma^{(1)}_{{\rm cl},i}[\mathbf{r}_1;\boldsymbol{\phi}] &= (-\boldsymbol{\nabla}^2_{\mathbf{r}_1} + r_0)\phi_i(\mathbf{r}_1) + \frac{u_0}{6}\boldsymbol{\phi}^2(\mathbf{r}_1)\phi_i(\mathbf{r}_1),\\
\Gamma^{(2)}_{{\rm cl},ij}[\mathbf{r}_1,\mathbf{r}_2;\boldsymbol{\phi}] &= \Big\{\frac{u_0}{6}[\boldsymbol{\phi}(\mathbf{r}_1)^2 + 2\phi_i(\mathbf{r}_1)\phi_j(\mathbf{r}_1)]\\
&\quad + \delta_{i,j}(-\boldsymbol{\nabla}^2_{\mathbf{r}_1} + r_0)\Big\}\delta(\mathbf{r}_1-\mathbf{r}_2),\\
\Gamma^{(3)}_{{\rm cl},ijk}[\{\mathbf{r}_j\};\boldsymbol{\phi}] &= \frac{u_0}{3}\delta(\mathbf{r}_1,\mathbf{r}_2,\mathbf{r}_3)[\delta_{i,j}\phi_k(\mathbf{r}) + {\rm perm}],\\
\Gamma^{(4)}_{{\rm cl},ijkl}[\{\mathbf{r}_j\};\boldsymbol{\phi}] &= \frac{u_0}{3}\delta(\mathbf{r}_1,\mathbf{r}_2,\mathbf{r}_3,\mathbf{r}_4)[\delta_{i,j}\delta_{k,l} + {\rm perm}],
\end{aligned} \tag{B20}$$

where "perm" denotes all possible permutations of the indices (ijk) or $(ijkl)$, and we use the notation $\delta(\mathbf{r}_1,\mathbf{r}_2,\mathbf{r}_3) = \delta(\mathbf{r}_1-\mathbf{r}_2)\delta(\mathbf{r}_2-\mathbf{r}_3)$, etc. $\Gamma_{\rm cl}$ reproduces the mean-field (or Landau) theory. From the equation of state (B7) with $\mathbf{h}=0$, we find

$$\rho_0 = \frac{1}{2}\boldsymbol{\phi}^2 = \begin{cases} 0 & \text{if } r_0 \geq 0,\\ -3\frac{r_0}{u_0} & \text{if } r_0 \leq 0,\end{cases} \tag{B21}$$

assuming a uniform field $\boldsymbol{\phi}$. In the broken-symmetry phase, the 2-point vertex is defined by its longitudinal and transverse parts,

$$\Gamma^{(2)}_{\rm cl,L}(\mathbf{p};\boldsymbol{\phi}) = \mathbf{p}^2 + 2|r_0|, \quad \Gamma^{(2)}_{\rm cl,T}(\mathbf{p};\boldsymbol{\phi}) = \mathbf{p}^2, \tag{B22}$$

while $\Gamma^{(2)}_{{\rm cl},ij}(\mathbf{p};\boldsymbol{\phi}) = \delta_{i,j}(\mathbf{p}^2 + r_0)$ in the symmetric phase. The classical propagator $G_{\rm cl} = \Gamma^{(2)-1}_{\rm cl}$ in the uniform field $\boldsymbol{\phi}$ can also be obtained directly from the functional integral (B1) by taking into account Gaussian fluctuations of the $\boldsymbol{\varphi}$ field about its the mean-field value $\boldsymbol{\phi}$ (Ma, 2000).

It is possible to compute the correction to $\Gamma_{\rm cl}$ in a systematic expansion in $1/l$. To leading order,

$$\Gamma[\boldsymbol{\phi}] = S[\boldsymbol{\phi}] - \frac{1}{2l}{\rm Tr}\ln(G_{\rm cl}[\boldsymbol{\phi}]) + \mathcal{O}(l^{-2}). \tag{B23}$$

Taking the first- and second-order functional derivatives of (B23), we obtain the 1-point vertex

$$\Gamma^{(1)}_i[\mathbf{r}_1;\boldsymbol{\phi}] = \Gamma^{(1)}_{{\rm cl},i}[\mathbf{r}_1;\boldsymbol{\phi}] + \frac{1}{2l}{\rm Tr}\big\{G_{\rm cl}[\boldsymbol{\phi}]\Gamma^{(3)}_{{\rm cl},i}[\mathbf{r}_1;\boldsymbol{\phi}]\big\} \tag{B24}$$

and the 2-point vertex

$$\begin{aligned}
\Gamma^{(2)}_{ij}[\mathbf{r}_1,\mathbf{r}_2;\boldsymbol{\phi}] &= \Gamma^{(2)}_{{\rm cl},ij}[\mathbf{r}_1,\mathbf{r}_2;\boldsymbol{\phi}]\\
&\quad + \frac{1}{2l}{\rm Tr}\big\{G_{\rm cl}[\boldsymbol{\phi}]\Gamma^{(4)}_{{\rm cl},ij}[\mathbf{r}_1,\mathbf{r}_2;\boldsymbol{\phi}]\\
&\quad - G_{\rm cl}[\boldsymbol{\phi}]\Gamma^{(3)}_{{\rm cl},j}[\mathbf{r}_2;\boldsymbol{\phi}]G_{\rm cl}[\boldsymbol{\phi}]\Gamma^{(3)}_{{\rm cl},i}[\mathbf{r}_1;\boldsymbol{\phi}]\big\}
\end{aligned} \tag{B25}$$

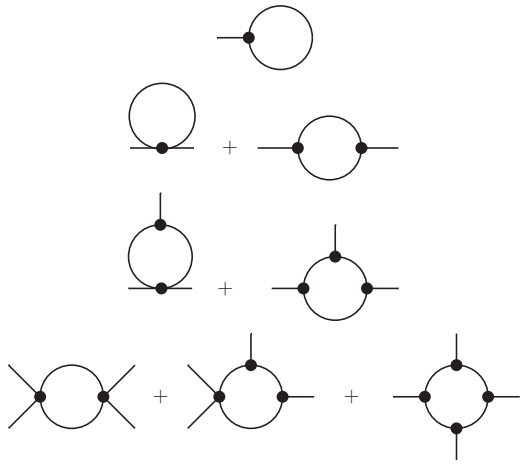

FIG. 50 Diagrammatic representation of the one-loop correction to the classical n-point vertex $\Gamma_{\rm cl}^{(n)}$ ($n=1,2,3,4$). The solid line stands for the classical propagator $G_{\rm cl}$ and the dot with n legs for the classical vertices $\Gamma_{\rm cl}^{(n)}$. (Diagrams obtained by exchanging external lines are not shown and symmetry factors are not indicated.)

(the trace Tr is defined after Eq. (30)). The $\mathcal{O}(1/l)$ correction to the two-point vertex (or, equivalently, to the classical self-energy $\Sigma_{\rm cl}=\Gamma_{\rm cl}^{(2)}-G_0^{-1}$) is given by the one-loop diagrams constructed with the classical propagator and vertices [Eqs. (B20)] (Fig. 50). By taking additional functional derivatives we obtain the $\mathcal{O}(1/l)$ correction to the classical 3- and 4-point vertices as shown in Fig. 50. This correction includes all one-loop diagrams that are 1PI (i.e. that cannot be separated into two disconnected pieces by by cutting a single line).

The expansion can be pushed to higher orders. To $\mathcal{O}(l^{-n})$, the contribution to $\Gamma[\phi]$ is given by all 1PI diagrams with n loops.

Appendix C: Threshold functions for the classical O(N) model

In this Appendix, we review the main properties of the threshold functions $l_n^d(w,\eta)$ and $m_{22}^d(w,\eta)$ involved in the LPA and LPA'.[79] Additional threshold functions must be defined for the second order of the derivative expansion (see Appendix E).

[79] In the literature, one often finds a more general threshold function $m_{n_1,n_2}^d(w,\eta)$ which we do not consider here since it is not needed for our discussion. Nevertheless, we keep the standard notation for $m_{22}^d(w,\eta)$.

1. Definitions

The threshold function l_n^d is defined by

$$l_n^d(w,\eta)=-\frac{n+\delta_{n,0}}{2}\int_0^\infty dy\, y^{d/2}\frac{\eta r+2yr'}{[y(1+r)+w]^{n+1}}$$
$$=-\frac{1}{2}\tilde\partial_t\int_0^\infty dy\, y^{d/2-1}\frac{1}{[y(1+r)+w]^n}\quad (n\neq 0), \tag{C1}$$

where the second line is obtained using $\tilde\partial_t=(\dot R_k)\partial_{R_k}$ and

$$\dot R_k(\mathbf{q})=-Z_k\mathbf{q}^2(\eta r(y)+2yr'(y)),$$
$$\tilde\partial_t r(y)=\tilde\partial_t\frac{R_k(\mathbf{q})}{Z_k\mathbf{q}^2}=\frac{\dot R_k(\mathbf{q})}{Z_k\mathbf{q}^2}. \tag{C2}$$

In the LPA, where $Z_k=1$ and $\eta=0$, we use the notation $l_n^d(w)\equiv l_n^d(w,0)$.

The function $m_{22}^d(w,\eta)$ is defined by

$$m_{22}^d(w,\eta)=-\frac{1}{2}\tilde\partial_t\int_0^\infty dy\, y^{d/2}\frac{(1+r+yr')^2}{P(w)^2P(0)^2} \tag{C3}$$

where $P(w)=y(1+r)+w$ (see Eq. (92)). In Eq. (C3), the operator $\tilde\partial_t$ acts on both R_k and R_k', and should be understood as

$$\tilde\partial_t=(\partial_t R_k)\frac{\partial}{\partial R_k}+(\partial_t R_k')\frac{\partial}{\partial R_k'}, \tag{C4}$$

where

$$R_k'(\mathbf{q})=Z_k(r+yr'),$$
$$\partial_t R_k'(\mathbf{q})=-Z_k[\eta_k r+(\eta_k+4)yr'+2y^2r'']. \tag{C5}$$

We therefore obtain

$$\tilde\partial_t=-(\eta r+2yr')\frac{\partial}{\partial r}\bigg|_{R'}$$
$$-[\eta r+(\eta+4)yr'+2y^2r'']y^{-1}\frac{\partial}{\partial r'}\bigg|_R. \tag{C6}$$

Using

$$\tilde G_{k,ii}'=-(1+r+yr')\tilde G_{k,ii}^2, \tag{C7}$$

and

$$\frac{\partial}{\partial r}\tilde G_{k,ii}'\bigg|_{R_k'}=2y(1+r+yr')\tilde G_{k,ii}^3,$$
$$\frac{\partial}{\partial r'}\tilde G_{k,ii}'\bigg|_{R_k}=-y\tilde G_{k,ii}^2, \tag{C8}$$

we finally obtain

$$m_{22}^d(w,\eta)=-\int_0^\infty dy\, y^{d/2}\frac{1+r+yr'}{P(w)^2P(0)^2}\bigg\{y(\eta r+2yr')$$
$$\times(1+r+yr')\left[\frac{1}{P(w)}+\frac{1}{P(0)}\right]$$
$$-\eta r-(\eta+4)yr'-2y^2r''\bigg\}. \tag{C9}$$

2. Large-w behavior

For $w \gg 1$, $l_n^d(w,\eta)$ and $m_{22}^d(w,\eta)$ decrease as power laws:

$$l_n^d(w,\eta) \sim \frac{1}{w^{n+1}}, \quad m_{22}^d(w,\eta) \sim \frac{1}{w^2}. \tag{C10}$$

3. Universal values

From the above definitions, one easily obtains

$$l_2^4(0,0) = -2\int_0^\infty dy \frac{r'}{(1+r)^3} = \frac{1}{1+r^2}\Big|_0^\infty = 1 \tag{C11}$$

and

$$l_1^2(0,0) = -\int_0^\infty dy \frac{r'}{(1+r)^2} = \frac{1}{1+r}\Big|_0^\infty = 1 \tag{C12}$$

using

$$\lim_{y\to\infty} r(y) = 0 \quad \text{and} \quad \lim_{y\to 0} yr(y) = 1. \tag{C13}$$

These two conditions follow from $R_k(\mathbf{q}) \simeq 0$ for $|\mathbf{q}| \gg k$ and $\lim_{\mathbf{q}\to 0} R_k(\mathbf{q}) = Z_k k^2$. We also find

$$\begin{aligned}\lim_{w\to\infty} w^2 m_{22}^{d=2}(w,0) &= 2\int_0^\infty dy \frac{1+r+yr'}{(1+r)^3} \\ &\quad \times [(1+r)(r'+y'') - yr'^2] \\ &= \frac{1+r+yr'}{1+r}\Big|_0^\infty = 1,\end{aligned} \tag{C14}$$

using again (C13). Equations (C11,C12,C14) hold for any regulator function r.

4. Theta regulator

With the theta regulator (14),

$$\begin{aligned} r(y) &= \frac{1-y}{y}\Theta(1-y), \\ r'(y) &= -\frac{1}{y^2}\Theta(1-y) - \frac{1-y}{y}\delta(1-y), \\ r''(y) &= \frac{2}{y^3}\Theta(1-y) + \frac{2}{y^2}\delta(1-y) + \frac{1-y}{y}\delta'(1-y), \end{aligned} \tag{C15}$$

the function r satisfies $y(1+r) = 1$ for $0 \le y \le 1$. This leads to

$$\begin{aligned} l_n^d(w,\eta) = &-\frac{n+\delta_{n,0}}{2}\frac{1}{(1+w)^{n+1}} \\ &\times \int_0^1 dy\, y^{d/2}\left(\eta\frac{1-y}{y} - \frac{2}{y}\right) \\ = &(n+\delta_{n,0})\frac{2}{d}\left(1 - \frac{\eta}{d+2}\right)\frac{1}{(1+w)^{n+1}}. \end{aligned} \tag{C16}$$

Noting that $1 + r + yr' = \Theta(y-1)$, we deduce that $(1+r+yr')r = (1+r+yr')r' = 0$ and

$$m_{22}^d(w,\eta) = 2\int_0^\infty dy\, y^{d/2}\frac{(1+r+yr')y^2 r''}{P(w)^2 P(0)^2}. \tag{C17}$$

The product $(1+r+yr')r''$ is ill-defined with the theta regulator because of the derivative δ' of the Dirac function in r''. To circumvent this difficulty, we integrate by parts,

$$\begin{aligned} m_{22}^d(w,\eta) = &-2\int_0^\infty dy\, r' \frac{\partial}{\partial y}\frac{y^{d/2+2}(1+r)}{P(w)^2P(0)^2} \\ &-\int_0^\infty dy\, r'^2 \frac{\partial}{\partial y}\frac{y^{d/2+3}}{P(w)^2P(0)^2}. \end{aligned} \tag{C18}$$

The integral is now limited to the interval $[0,1]$, where $P(w) = 1+w$, and we obtain

$$\begin{aligned} m_{22}^d(w,\eta) &= \frac{1}{(1+w)^2}\left(\frac{d}{2} - 1\right)\int_0^1 dy\, y^{d/2-2} \\ &= \frac{1}{(1+w)^2}, \end{aligned} \tag{C19}$$

which is independent of η.

Appendix D: Anomalous dimension in the LPA'

The flow equation of the field renormalization factor is obtained from

$$\partial_t Z_k = \lim_{\mathbf{p}\to 0} \frac{\partial}{\partial \mathbf{p}^2} \partial_t \Gamma_{k,\mathrm{T}}^{(2)}(\mathbf{p}; \rho_{0,k}). \tag{D1}$$

In the following, we assume that the uniform field $\boldsymbol{\phi} = (\sqrt{2\rho_{0,k}}, 0, \cdots, 0)$ points along the first direction. We can then identify $\Gamma_{k,11}^{(2)}$ with $\Gamma_{k,\mathrm{L}}^{(2)}$, and $\Gamma_{k,ii}^{(2)}$ $(i \neq 1)$ with $\Gamma_{k,\mathrm{T}}^{(2)}$. The k dependence of $\Gamma_{k,\mathrm{T}}^{(2)}(\mathbf{p};\rho_{0,k})$ is due to the k dependence of the vertex $\Gamma_{k,\mathrm{T}}^{(2)}(\mathbf{p};\rho)$ as well as that of $\rho_{0,k}$. Thus we have

$$\begin{aligned} &\partial_t \Gamma_{k,\mathrm{T}}^{(2)}(\mathbf{p};\rho_{0,k}) \\ &\quad = \partial_t \Gamma_{k,\mathrm{T}}^{(2)}(\mathbf{p};\rho)\big|_{\rho_{0,k}} + \sum_{i,\mathbf{q}} \frac{\delta \Gamma_{k,\mathrm{T}}^{(2)}(\mathbf{p};\rho_{0,k})}{\delta\phi_i(\mathbf{q})}\partial_t\phi_i(\mathbf{q}) \\ &\quad = \partial_t \Gamma_{k,\mathrm{T}}^{(2)}(\mathbf{p};\rho)\big|_{\rho_{0,k}} + \sqrt{V}\Gamma_{k,221}^{(3)}(\mathbf{p},-\mathbf{p},0)\partial_t\sqrt{2\rho_{0,k}}, \end{aligned} \tag{D2}$$

where

$$\partial_t \phi_i(\mathbf{q}) = \delta_{i,1}\delta_{\mathbf{q},0}\sqrt{V}\partial_t\sqrt{2\rho_{0,k}} \tag{D3}$$

is the variation of $\phi_i(\mathbf{q})$ due to a change $\partial_t\sqrt{2\rho_{0,k}}$ of the first component ϕ_1 of the uniform field. From the effective action (80) in the LPA', one easily finds

$$\Gamma^{(3)}_{k,ijl}(\mathbf{p}_1,\mathbf{p}_2,\mathbf{p}_3;\rho_{0,k}) = \delta_{\sum_i \mathbf{p}_i,0}\frac{1}{\sqrt{V}}\big[\sqrt{2\rho_{0,k}}U''_{0,k}(\delta_{i,j}\delta_{l,1}+\delta_{i,l}\delta_{j,1}+\delta_{j,l}\delta_{i,1}) + (2\rho_{0,k})^{3/2}U'''_{0,k}\delta_{i,1}\delta_{j,1}\delta_{l,1}\big] \quad \text{(D4)}$$

and

$$\Gamma^{(4)}_{k,ijlm}(\mathbf{p}_1,\mathbf{p}_2,\mathbf{p}_3,\mathbf{p}_4;\rho_{0,k}) = \delta_{\sum_i \mathbf{p}_i,0}\frac{1}{V}\big\{U''_{0,k}(\delta_{i,j}\delta_{l,m}+\delta_{i,l}\delta_{j,m}+\delta_{i,m}\delta_{j,l}) + 2\rho_{0,k}U'''_{0,k}[\delta_{i,j}\delta_{l,m}(\delta_{i,1}+\delta_{m,1})+\delta_{i,l}\delta_{j,m}(\delta_{i,1}+\delta_{m,1}) + \delta_{i,m}\delta_{j,l}(\delta_{j,1}+\delta_{m,1})] + 4\rho^2_{0,k}U^{(4)}_{0,k}\delta_{i,1}\delta_{j,1}\delta_{l,1}\delta_{m,1}\big\}, \quad \text{(D5)}$$

where $U^{(n)}_{0,k} = U^{(n)}_k(\rho_{0,k})$. Since $\Gamma^{(3)}_k$ is momentum independent, the last term in the rhs of (D2) does not depend on $\mathbf{p}$ so that

$$\partial_t Z_k = \lim_{\mathbf{p}\to 0}\frac{\partial}{\partial \mathbf{p}^2}\partial_t \Gamma^{(2)}_{k,\mathrm{T}}(\mathbf{p};\rho)\big|_{\rho_{0,k}}. \quad \text{(D6)}$$

From equations (36) and (D5), we deduce that $\Gamma^{(2)}_k(\mathbf{p};\rho)$ satisfies the equation

$$\partial_t \Gamma^{(2)}_{k,\mathrm{T}}(\mathbf{p};\rho) = \frac{1}{2}\tilde{\partial}_t\int_{\mathbf{q}}\big\{\big[U''_k(\rho)+10\rho U'''_k(\rho)\big]G_{k,\mathrm{L}}(\mathbf{q};\rho) + (N+1)U''_k(\rho)G_{k,\mathrm{T}}(\mathbf{q};\rho) - 2\rho U''_k(\rho)^2\tilde{\partial}_t\int_{\mathbf{q}}G_{k,\mathrm{L}}(\mathbf{q};\rho)G_{k,\mathrm{T}}(\mathbf{p}+\mathbf{q};\rho), \quad \text{(D7)}$$

which leads to

$$\partial_t Z_k = -2\rho_{0,k}{U''_{0,k}}^2\lim_{\mathbf{p}\to 0}\frac{\partial}{\partial \mathbf{p}^2}\tilde{\partial}_t\int_{\mathbf{q}}G_{k,\mathrm{L}}(\mathbf{q};\rho_{0,k}) \times G_{k,\mathrm{T}}(\mathbf{p}+\mathbf{q};\rho_{0,k}). \quad \text{(D8)}$$

To alleviate the notations, from now on we drop the dependence of the propagators on $\rho_{0,k}$. We use

$$G_{k,ii}(\mathbf{p}+\mathbf{q}) = G_{k,ii}(\mathbf{q}) + (2\mathbf{p}\cdot\mathbf{q}+\mathbf{p}^2)G'_{k,ii}(\mathbf{q}) + 2(\mathbf{p}\cdot\mathbf{q})^2 G''_{k,ii}(\mathbf{q}) + \mathcal{O}(|\mathbf{p}|^3), \quad \text{(D9)}$$

where

$$G'_{k,ii}(\mathbf{q}) = \partial_{\mathbf{q}^2}G_{k,ii}(\mathbf{q}) \quad \text{(D10)}$$

is defined as a derivative wrt $\mathbf{q}^2$. This leads to

$$\int_{\mathbf{q}}G_{k,\mathrm{L}}(\mathbf{q})G_{k,\mathrm{T}}(\mathbf{p}+\mathbf{q}) = \int_{\mathbf{q}}G_{k,\mathrm{L}}(\mathbf{q})\Big[G_{k,\mathrm{T}}(\mathbf{q}) + \mathbf{p}^2 G'_{k,\mathrm{T}}(\mathbf{q}) + \frac{2}{d}\mathbf{p}^2\mathbf{q}^2 G''_{k,\mathrm{T}}(\mathbf{q})\Big] \quad \text{(D11)}$$

to order $\mathbf{p}^2$, and

$$\frac{\partial}{\partial \mathbf{p}^2}\int_{\mathbf{q}}G_{k,\mathrm{L}}(\mathbf{q})G_{k,\mathrm{T}}(\mathbf{p}+\mathbf{q}) = \int_{\mathbf{q}}G_{k,\mathrm{L}}(\mathbf{q})\Big[G'_{k,\mathrm{T}}(\mathbf{q})+\frac{2}{d}\mathbf{q}^2G''_{k,\mathrm{T}}(\mathbf{q})\Big] = 4v_d\int_0^\infty d|\mathbf{q}|\,|\mathbf{q}|^{d-1}G_{k,\mathrm{L}}(\mathbf{q})\Big[G'_{k,\mathrm{T}}(\mathbf{q})+\frac{2}{d}\mathbf{q}^2G''_{k,\mathrm{T}}(\mathbf{q})\Big] \quad \text{(D12)}$$

for $\mathbf{p}\to 0$. Using the variable $x=\mathbf{q}^2$ and integrating by part (noting that $G'_{k,ii} = \partial_x G_{k,ii}$), we obtain

$$\lim_{\mathbf{p}\to 0}\frac{\partial}{\partial \mathbf{p}^2}\int_{\mathbf{q}}G_{k,\mathrm{L}}(\mathbf{q})G_{k,\mathrm{T}}(\mathbf{p}+\mathbf{q}) = -4\frac{v_d}{d}\int_0^\infty dx\,x^{d/2}G'_{k,\mathrm{L}}(\mathbf{q})G'_{k,\mathrm{T}}(\mathbf{q}) = -8\frac{v_d}{d}\int_0^\infty d|\mathbf{q}|\,|\mathbf{q}|^{d+1}G'_{k,\mathrm{L}}(\mathbf{q})G'_{k,\mathrm{T}}(\mathbf{q}) \quad \text{(D13)}$$

and in turn (86).

Introducing the dimensionless propagators $\tilde{G}_{k,ii} = Z_k k^2 G_{k,ii}$, i.e.

$$\tilde{G}_{k,\mathrm{L}}(y,\tilde{\rho}) = [y(1+r)+\tilde{U}'_k(\tilde{\rho})+2\tilde{\rho}U''_k(\tilde{\rho})]^{-1} \qquad \tilde{G}_{k,\mathrm{T}}(y,\tilde{\rho}) = [y(1+r)+\tilde{U}'_k(\tilde{\rho})]^{-1} \quad \text{(D14)}$$

($y=\mathbf{p}^2/k^2$) and using

$$G'_{k,ii} = \frac{1}{Z_k k^4}\partial_y\tilde{G}_{k,ii} \equiv \frac{1}{Z_k k^4}\tilde{G}'_{k,ii}, \quad \text{(D15)}$$

we obtain Eq. (91) where the threshold function m^d_{22} is defined by

$$m^d_{22}(2\tilde{\rho}_{0,k}\tilde{U}''_{0,k},\eta_k) = -\frac{1}{2}\tilde{\partial}_t\int_0^\infty dy\,y^{d/2}\tilde{G}'_{k,11}\tilde{G}'_{k,22}, \quad \text{(D16)}$$

with the propagators $\tilde{G}'_{k,ii}$ evaluated at the minimum $\tilde{\rho}_{0,k}$ of the effective potential. Finally we use the fact that in the LPA' η_k is nonzero only if $\rho_{0,k}>0$, which allows us to set $\tilde{U}'_k(\tilde{\rho}_{0,k})=0$ in (D16) and rewrite $m^d_{22}(w,\eta)$ as in (92).

Appendix E: Derivative expansion to second order

To second order of the derivative expansion, the flow equations for the dimensionless variables read

$$\partial_t\tilde{U}'_k = (\eta_k-2)\tilde{U}'_k+\eta_k\tilde{\rho}\tilde{U}''_k - 2(N-1)L(1,0,d)\tilde{U}''_k - 2(N-1)L(1,0,d+2)\tilde{Z}'_k + L(0,1,d)\left(-4\tilde{\rho}\tilde{U}_k{}^{(3)} - 6\tilde{U}''_k\right)$$

$$- 2L(0,1,d+2)\left(\tilde{\rho}\tilde{Y}_k' + \tilde{Y}_k + \tilde{Z}_k'\right), \tag{E1}$$

$$\begin{aligned}\partial_t \tilde{Z}_k = {}& \eta\tilde{Z}_k - (-d-\eta+2)\tilde{\rho}\tilde{Z}_k' - 2L(1,0,d)\left((N-1)\tilde{Z}_k' + \tilde{Y}_k\right) + 16\tilde{\rho}L(1,1,d)\tilde{U}_k''\tilde{Z}_k' + \frac{8\tilde{\rho}L(1,1,d+2)\tilde{Z}_k'\left(d\tilde{Y}_k + \tilde{Z}_k'\right)}{d} \\ & - 2L(0,1,d)\left(2\tilde{\rho}\tilde{Z}_k'' + \tilde{Z}_k'\right) - \frac{16\tilde{\rho}\left(\tilde{U}_k''\right)^2 M_{\rm LT}(2,2,d)}{d} - \frac{16\tilde{\rho}\tilde{Y}_k\tilde{U}_k'' M_{\rm LT}(2,2,d+2)}{d} - \frac{4\tilde{\rho}\tilde{Y}_k^2 M_{\rm LT}(2,2,d+4)}{d} \\ & + \frac{16\tilde{\rho}K(2,1,d)\tilde{U}_k''\left(\tilde{Y}_k - 2\tilde{Z}_k'\right)}{d} + \frac{8\tilde{\rho}\tilde{Y}_k K(2,1,d+2)\left(\tilde{Y}_k - 2\tilde{Z}_k'\right)}{d},\end{aligned} \tag{E2}$$

and

$$\begin{aligned}\partial_t \tilde{Y}_k = {}& (d-2+2\eta)\tilde{Y}_k - (-d-\eta+2)\tilde{\rho}\tilde{Y}_k' - \frac{8\tilde{Y}_k K(2,1,d+2)\left(\tilde{Y}_k - 2\tilde{Z}_k'\right)}{d} - \frac{16K(2,1,d)\tilde{U}_k''\left(\tilde{Y}_k - 2\tilde{Z}_k'\right)}{d} \\ & + 4(N-1)\tilde{Y}_k L(2,0,d)\tilde{U}_k'' + 2L(1,0,d)\left(\frac{\tilde{Y}_k}{\tilde{\rho}} - (N-1)\tilde{Y}_k'\right) + \frac{4(N-1)L(2,0,d+2)\tilde{Z}_k'\left(d\tilde{Y}_k + \tilde{Z}_k'\right)}{d} \\ & + 8L(0,2,d)\left(2\tilde{\rho}\tilde{U}_k{}^{(3)} + 3\tilde{U}_k''\right)\left(\tilde{\rho}\tilde{Y}_k' + \tilde{Y}_k + \tilde{Z}_k'\right) - 16L(1,1,d)\tilde{U}_k''\tilde{Z}_k' - \frac{2L(0,1,d)\left(5\tilde{\rho}\tilde{Y}_k' + 2\tilde{\rho}^2\tilde{Y}_k'' + \tilde{Y}_k\right)}{\tilde{\rho}} \\ & + \frac{4(2d+1)L(0,2,d+2)\left(\tilde{\rho}\tilde{Y}_k' + \tilde{Y}_k + \tilde{Z}_k'\right)^2}{d} - \frac{8L(1,1,d+2)\tilde{Z}_k'\left(d\tilde{Y}_k + \tilde{Z}_k'\right)}{d} - \frac{8M_{\rm L}(0,4,d)\left(2\tilde{\rho}\tilde{U}_k{}^{(3)} + 3\tilde{U}_k''\right)^2}{d} \\ & - \frac{16M_{\rm L}(0,4,d+2)\left(2\tilde{\rho}\tilde{U}_k{}^{(3)} + 3\tilde{U}_k''\right)\left(\tilde{\rho}\tilde{Y}_k' + \tilde{Y}_k + \tilde{Z}_k'\right)}{d} - \frac{8M_{\rm L}(0,4,d+4)\left(\tilde{\rho}\tilde{Y}_k' + \tilde{Y}_k + \tilde{Z}_k'\right)^2}{d} \\ & + \frac{16\tilde{Y}_k M_{\rm LT}(2,2,d+2)\tilde{U}_k''}{d} + \frac{16M_{\rm LT}(2,2,d)\left(\tilde{U}_k''\right)^2}{d} + \frac{4\tilde{Y}_k^2 M_{\rm LT}(2,2,d+4)}{d} - \frac{16(N-1)M_{\rm T}(4,0,d+2)\tilde{U}_k''\tilde{Z}_k'}{d} \\ & - \frac{8(N-1)M_{\rm T}(4,0,d)\left(\tilde{U}_k''\right)^2}{d} - \frac{8(N-1)M_{\rm T}(4,0,d+4)\left(\tilde{Z}_k'\right)^2}{d}.\end{aligned} \tag{E3}$$

Note that with the choice of normalization in Eqs. (136), the angular factor v_d does not appear in the flow equations. Equations (E1-E3) must be solved with the initial conditions $\tilde{U}_\Lambda(\tilde{\rho}) = \tilde{r}_0\tilde{\rho} + (\tilde{u}_0/6)\tilde{\rho}^2$, $\tilde{Z}_\Lambda(\tilde{\rho}) = 1$ and $\tilde{Y}_\Lambda(\tilde{\rho}) = 0$, where $\tilde{r}_0 = r_0\Lambda^{-2}$ and $\tilde{u}_0 = u_0 v_d \Lambda^{d-4}$.

The equation for η_k is obtained from the renormalization condition $\partial_t \tilde{Z}_k(\tilde{\rho}_{\rm r}) = 0$. We have introduced the threshold functions

$$\begin{aligned}L(n_1,n_2,d) &= -\frac{1}{2}\tilde{\partial}_t \int_0^\infty dy\, y^{d/2-1}\tilde{G}_{\rm T}^{n_1}\tilde{G}_{\rm L}^{n_2}, \\ M_{\rm T}(n_1,n_2,d) &= -\frac{1}{2}\tilde{\partial}_t \int_0^\infty dy\, y^{d/2}\tilde{G}_{\rm T}'\tilde{G}_{\rm T}^{n_1-4}\tilde{G}_{\rm L}^{n_2}, \\ M_{\rm L}(n_1,n_2,d) &= -\frac{1}{2}\tilde{\partial}_t \int_0^\infty dy\, y^{d/2}\tilde{G}_{\rm L}'\tilde{G}_{\rm T}^{n_1}\tilde{G}_{\rm L}^{n_2-4}, \\ M_{\rm LT}(n_1,n_2,d) &= -\frac{1}{2}\tilde{\partial}_t \int_0^\infty dy\, y^{d/2}\tilde{G}_{\rm L}'\tilde{G}_{\rm T}'\tilde{G}_{\rm T}^{n_1-2}\tilde{G}_{\rm L}^{n_2-2}, \\ K(n_1,n_2,d) &= \frac{1}{2}\tilde{\partial}_t \int_0^\infty dy\, y^{d/2}\tilde{G}_{\rm T}'\tilde{G}_{\rm T}^{n_1-2}\tilde{G}_{\rm L}^{n_2},\end{aligned} \tag{E4}$$

and the dimensionless transverse and longitudinal propagators [see Eqs. (134)]

$$\begin{aligned}\tilde{G}_{\rm L}^{-1}(y) &= y[\tilde{Z}_k + \tilde{\rho}\tilde{Y}_k + r(y)] + \tilde{U}_k' + 2\tilde{\rho}\tilde{U}_k'', \\ \tilde{G}_{\rm T}^{-1}(y) &= y[\tilde{Z}_k + r(y)] + \tilde{U}_k'.\end{aligned} \tag{E5}$$

To alleviate the notations, we do not write explicitly the k and $\tilde{\rho}$ dependence of the threshold functions and the propagators, and use $\tilde{G}' = \partial_y \tilde{G}$. The operator $\tilde{\partial}_t$ is defined by (C4) and (C5).

The threshold functions are used here to present the flow equations in a concise way. In practice however, we write the rhs of the flow equations as a single integral which is computed using an equally-spaced grid in the variable $\sqrt{y}$.

Appendix F: Flow equations in the BMW approximation

In this Appendix we derive the flow equations satisfied by the self-energies $\Delta_{A,k}$ and $\Delta_{B,k}$ in the BMW approximation (Sec. V). From (155), we can compute the first-

and second-order derivatives of $\Gamma^{(2)}_{k,ij}(\mathbf{p};\boldsymbol{\phi})$ wrt the field $\boldsymbol{\phi}$. Choosing $\boldsymbol{\phi} = (\sqrt{2\rho}, 0 \cdots 0)$, we can then identify $\Gamma_{k,11}$ with $\Gamma_{A,k} + 2\rho\Gamma_{B,k}$ and $\Gamma_{k,ii}$ $(i \neq 1)$ with $\Gamma_{A,k}$. This gives

$$\frac{\partial}{\partial\phi_l}\Gamma^{(2)}_{k,ij} = \sqrt{2\rho}\big[\delta_{i,j}\delta_{l,1}(\Gamma'_{A,k} + \delta_{i,1}2\rho\Gamma'_{B,k}) + (\delta_{i,l}\delta_{j,1} + \delta_{j,l}\delta_{i,1})\Gamma_{B,k}\big] \tag{F1}$$

and

$$\frac{\partial^2}{\partial\phi_l\partial\phi_m}\Gamma^{(2)}_{k,ij} = \delta_{i,j}\delta_{l,m}(\Gamma'_{A,k} + \delta_{l,1}2\rho\Gamma''_{A,k}) + (\delta_{i,l}\delta_{j,m} + \delta_{j,l}\delta_{i,m})\Gamma_{B,k} + \big[\delta_{i,1}(\delta_{j,m}\delta_{l,1} + \delta_{l,m}\delta_{j,1}) + \delta_{m,1}(\delta_{i,l}\delta_{j,1} + \delta_{j,l}\delta_{i,1}) + \delta_{i,m}\delta_{j,1}\delta_{l,1}\big]2\rho\Gamma'_{B,k} + \delta_{i,1}\delta_{j,1}\delta_{l,1}\delta_{m,1}4n^2\Gamma''_{B,k}. \tag{F2}$$

The flow equations (157) of $\Gamma_{A,k}$ and $\Gamma_{B,k}$ follow from (153), (F1) and (F2). Then using (163) we find that the self-energies $\Delta_{A,k}$ and $\Delta_{B,k}$ satisfy

$$\partial_t\Delta_{A,k} = -\frac{1}{2}I^{(2)}_{k,\mathrm{LL}}(\Delta'_{A,k} + 2\rho\Delta''_{A,k}) - \frac{1}{2}I^{(2)}_{k,\mathrm{TT}}[(N-1)\Delta'_{A,k} + 2\Delta_{B,k}] + 2\rho\big[J^{(3)}_{k,\mathrm{LT}}(\Delta'_{A,k} + U''_k)^2 + J^{(3)}_{k,\mathrm{TL}}(\Delta_{B,k} + U''_k)^2 - (I^{(3)}_{k,\mathrm{LT}} + I^{(3)}_{k,\mathrm{TL}})U''^2_k\big] \tag{F3}$$

and

$$\partial_t\Delta_{B,k} = \frac{1}{2\rho}(I^{(2)}_{k,\mathrm{TT}} - I^{(2)}_{k,\mathrm{LL}})\Delta_{B,k} - I^{(2)}_{k,\mathrm{LL}}\left(\frac{5}{2}\Delta'_{B,k} + \rho\Delta''_{B,k}\right) - \frac{1}{2}I^{(2)}_{k,\mathrm{TT}}(N-1)\Delta'_{B,k} + J^{(3)}_{k,\mathrm{LL}}(\Delta'_{A,k} + 2\Delta_{B,k} + 2\rho\Delta'_{B,k} + 3U''_k + 2\rho U'''_k)^2 - J^{(3)}_{k,\mathrm{LT}}(\Delta'_{A,k} + U''_k)^2 - [J^{(3)}_{k,\mathrm{TL}} - (N-1)J^{(3)}_{k,\mathrm{TT}}](\Delta_{B,k} + U''_k)^2 - I^{(3)}_{k,\mathrm{LL}}(3U''_k + 2\rho U'''_k)^2 + [I^{(3)}_{k,\mathrm{LT}} + I^{(3)}_{k,\mathrm{TL}} - (N-1)I^{(3)}_{k,\mathrm{TT}}]U''^2_k, \tag{F4}$$

where $I^{(n)}_{\alpha\beta}(\rho)$ and $J^{(n)}_{\alpha\beta}(\mathbf{p};\rho)$ are defined in (160). For compactness, we have not written explicitly the $\mathbf{p}$ and ρ dependence in (F1-F4).

In dimensionless form [Eqs. (166)], we obtain

$$\partial_t\tilde{\Delta}_{A,k} = (\eta_k - 2)(\tilde{\Delta}_{A,k} + \tilde{p}^2) + (d - 2 + \eta_k)\tilde{\rho}\tilde{\Delta}'_{A,k} + \tilde{p}(\partial_{\tilde{p}}\tilde{\Delta}_{A,k} + 2\tilde{p}) - \frac{1}{2}\tilde{I}^{(2)}_{k,\mathrm{LL}}(\tilde{\Delta}'_{A,k} + 2\tilde{\rho}\tilde{\Delta}''_{A,k}) - \frac{1}{2}\tilde{I}^{(2)}_{k,\mathrm{TT}}[(N-1)\tilde{\Delta}'_{A,k} + 2\tilde{\Delta}_{B,k}] + 2\tilde{\rho}\big[\tilde{J}^{(3)}_{k,\mathrm{LT}}(\tilde{\Delta}'_{A,k} + \tilde{U}''_k)^2 + \tilde{J}^{(3)}_{k,\mathrm{TL}}(\tilde{\Delta}_{B,k} + \tilde{U}''_k)^2 - (\tilde{I}^{(3)}_{k,\mathrm{LT}} + \tilde{I}^{(3)}_{k,\mathrm{TL}})\tilde{U}''^2_k\big], \tag{F5}$$

and

$$\partial_t\tilde{\Delta}_{B,k} = (d - 4 + 2\eta_k)\tilde{\Delta}_{B,k} + (d - 2 + \eta_k)\tilde{\rho}\tilde{\Delta}'_{B,k} + \tilde{p}\partial_{\tilde{p}}\tilde{\Delta}_{B,k} + \frac{1}{2\tilde{\rho}}(\tilde{I}^{(2)}_{k,\mathrm{TT}} - \tilde{I}^{(2)}_{k,\mathrm{LL}})\tilde{\Delta}_{B,k} - \tilde{I}^{(2)}_{k,\mathrm{LL}}\left(\frac{5}{2}\tilde{\Delta}'_{B,k} + \tilde{\rho}\tilde{\Delta}''_{B,k}\right) - \frac{1}{2}\tilde{I}^{(2)}_{k,\mathrm{TT}}(N-1)\tilde{\Delta}'_{B,k} + \tilde{J}^{(3)}_{k,\mathrm{LL}}(\tilde{\Delta}'_{A,k} + 2\tilde{\Delta}_{B,k} + 2\tilde{\rho}\tilde{\Delta}'_{B,k} + 3\tilde{U}''_k + 2\tilde{\rho}U'''_k)^2 - \tilde{J}^{(3)}_{k,\mathrm{LT}}(\tilde{\Delta}'_{A,k} + \tilde{U}''_k)^2 - [\tilde{J}^{(3)}_{k,\mathrm{TL}} - (N-1)\tilde{J}^{(3)}_{k,\mathrm{TT}}] \times (\tilde{\Delta}_{B,k} + \tilde{U}''_k)^2 - \tilde{I}^{(3)}_{k,\mathrm{LL}}(3\tilde{U}''_k + 2\tilde{\rho}\tilde{U}'''_k)^2 + [\tilde{I}^{(3)}_{k,\mathrm{LT}} + \tilde{I}^{(3)}_{k,\mathrm{TL}} - (N-1)\tilde{I}^{(3)}_{k,\mathrm{TT}}]\tilde{U}''^2_k, \tag{F6}$$

where

$$\begin{aligned}\tilde{I}^{(2)}_{k,\alpha\beta}(\tilde{\rho}) &= Z_k k^{-d+2} I^{(2)}_{\alpha\beta}(\rho) \\ &= -4v_d\int_0^\infty d\tilde{q}\,\tilde{q}^{d+1}(\eta_k r + 2\tilde{q}^2 r')\tilde{G}_\alpha(\tilde{q};\tilde{\rho})^2, \\ \tilde{J}^{(3)}_{k,\alpha\beta}(\tilde{p};\tilde{\rho}) &= Z_k^2 k^{-d+4} J^{(3)}_{\alpha\beta}(\mathbf{p};\rho) \\ &= -4v_d\int_0^\infty d\tilde{q}\,\tilde{q}^{d+1}(\eta_k r + 2\tilde{q}^2 r') \\ &\quad\times \tilde{G}_\alpha(\tilde{q};\tilde{\rho})^2\tilde{G}_\beta(\tilde{p}+\tilde{q};\tilde{\rho}).\end{aligned} \tag{F7}$$

The dimensionless propagator in (F7) is defined by

$$\begin{aligned}\tilde{G}_{k,\mathrm{L}}(\tilde{p};\tilde{\rho}) &= \big[\tilde{p}^2(1+r) + \tilde{\Delta}_{A,k}(\tilde{p};\tilde{\rho}) + 2\tilde{\rho}\tilde{\Delta}_{B,k}(\tilde{p};\tilde{\rho}) \\ &\quad + \tilde{U}'_k(\tilde{\rho}) + 2\tilde{\rho}\tilde{U}''_k(\tilde{\rho})\big]^{-1}, \\ \tilde{G}_{k,\mathrm{T}}(\tilde{p};\tilde{\rho}) &= \big[\tilde{p}^2(1+r) + \tilde{\Delta}_{A,k}(\tilde{p};\tilde{\rho}) + \tilde{U}'_k(\tilde{\rho})\big]^{-1},\end{aligned} \tag{F8}$$

using $R_k(\mathbf{p}) = Z_k k^2 y r$ and $r \equiv r(\tilde{p}^2)$.

The anomalous dimension η_k can be obtained from equation (164),

$$Z_k = \frac{\partial}{\partial\mathbf{p}^2}[\mathbf{p}^2 + \tilde{\Delta}_{A,k}(\tilde{p},\tilde{\rho})]\Big|_{\mathbf{p}=\rho=0}. \tag{F9}$$

Using (166), this gives

$$\frac{\partial}{\partial\tilde{p}^2}\tilde{\Delta}_{A,k}(\tilde{p};\tilde{\rho})\Big|_{\tilde{p}_0,\tilde{\rho}_0} = 0, \tag{F10}$$

where we now consider an arbitrary renormalization point $(\tilde{p}_0, \tilde{\rho}_0)$. Taking the derivative ∂_t in equation (F10) and making use of (F5), we deduce an equation for η_k. Noting that $\tilde{I}_{\mathrm{L}}(\tilde{\rho}=0) = \tilde{I}_{\mathrm{T}}(\tilde{\rho}=0)$, we finally obtain Eq. (167) for the particular choice $\tilde{p}_0 = \tilde{\rho}_0 = 0$.

For numerical reasons, it is convenient to consider the quantities (Pourquoi?)

$$\tilde{Y}_A(\tilde{p};\tilde{\rho}) = \frac{\tilde{\Delta}_A(\tilde{p};\tilde{\rho})}{\tilde{p}^2}, \quad \tilde{Y}_B(\tilde{p};\tilde{\rho}) = \frac{\tilde{\Delta}_B(\tilde{p};\tilde{\rho})}{\tilde{p}^2}. \tag{F11}$$

The corresponding flow equations are easily deduced from (F5) and (F6) (Benitez *et al.*, 2012), while Eq. (167) becomes

$$\eta_k = \frac{1}{2}\tilde{I}^{(2)}_{k,\mathrm{TT}}(\tilde{\rho}=0)[N\tilde{Y}'_A(0,0) + 2\tilde{Y}_B(0,0)]. \tag{F12}$$

From (46), we easily deduce the flow equation

$$\partial_t \tilde{U}_k = -d\tilde{U}_k + (d-2+\eta_k)\tilde{\rho}\tilde{U}'_k + 2v_d \int_0^\infty d\tilde{q}\, \tilde{q}^{d+1} \times (\eta_k r + 2\tilde{q}^2 r')[\tilde{G}_{k,\mathrm{L}} + (N-1)\tilde{G}_{k,\mathrm{T}}] \quad \text{(F13)}$$

of the dimensionless effective potential $\tilde{U}_k(\tilde{\rho})$. Equation (F13) leads to (168).

Appendix G: Numerical methods (BD, NW)

Appendix H: Symmetries (BD, NW)

Appendix I: Connection with perturbation theory (NW)

REFERENCES

Adams, J., N. Tetradis, J. Berges, F. Freire, C. Wetterich, and S. Bornholdt (1995), Mod. Phys. Lett. A **10**, 2367, arXiv:hep-th/9507093.

Ambegaokar, V., B. I. Halperin, D. R. Nelson, and E. D. Siggia (1980), Phys. Rev. B **21**, 1806.

Anders, P., E. Gull, L. Pollet, M. Troyer, and P. Werner (2010), Phys. Rev. Lett. **105**, 096402.

Anders, P., E. Gull, L. Pollet, M. Troyer, and P. Werner (2011), New J. Phys. **13** (7), 075013.

Andersen, J. O., and M. Strickland (1999), Phys. Rev. A **60** (2), 1442.

Antonenko, S. A., and A. I. Sokolov (1995), Phys. Rev. E **51**, 1894.

Aoki, K.-I., K. Morikawa, W. Souma, J.-I. Sumi, and H. Terao (1998), Prog. Theor. Phys. **3**, 451.

Arnold, P., and G. Moore (2001), Phys. Rev. Lett. **87**, 120401.

Arnold, P., and B. Tomáusik (2001), Phys. Rev. A **64**, 053609.

Bacsó, V., N. Defenu, A. Trombettoni, and I. Nndori (2015), Nucl. Phys. B **901**, 444 .

Bagnuls, C., and C. Bervillier (2001), Phys. Rep. **348**, 91.

Baier, B., E. Bick, and C. Wetterich (2005), Phys. Lett. B **605**, 144.

Baier, T., E. Bick, and C. Wetterich (2000), Phys. Rev. B **62**, 15471.

Baier, T., E. Bick, and C. Wetterich (2004), Phys. Rev. B **70**, 125111.

Ball, R. D., P. E. Haagensen, J. I. Latorre, and E. Moreno (1995), Phys. Lett. B **347**, 80.

Bartosch, L., P. Kopietz, and A. Ferraz (2009), Phys. Rev. B **80**, 104514.

Bauer, J., P. Jakubczyk, and W. Metzner (2011), Phys. Rev. B **84**, 075122.

Baym, G., J.-P. Blaizot, M. Holzmann, F. Laloë, and D. Vautherin (1999), Phys. Rev. Lett. **83**, 1703.

Baym, G., J.-P. Blaizot, and J. Zinn-Justin (2000), Europhys. Lett. **49** (2), 150.

Baym, G.,, Blaizot, J.-P., Holzmann, M., Lalo, F., and Vautherin, D. (2001), Eur. Phys. J. B **24** (1), 107.

Beliaev, S. T. (1958a), Sov. Phys. JETP **7**, 289, zh. Eksp. Teor. Fiz. 34, 417 (1958).

Beliaev, S. T. (1958b), Sov. Phys. JETP **7**, 299, zh. Eksp. Teor. Fiz. 34, 433 (1958).

Belitz, D., T. R. Kirkpatrick, and T. Vojta (2005), Rev. Mod. Phys. **77** (2), 579.

Benfatto, G. (1994), in *Constructive results in field theory, statistical mechanics, and condensed matter physics*, edited by V. Rivasseau (Springer Verlag, New York) p. 219.

Benitez, F., J.-P. Blaizot, H. Chaté, B. Delamotte, R. Méndez-Galain, and N. Wschebor (2009), Phys. Rev. E **80**, 030103(R).

Benitez, F., J.-P. Blaizot, H. Chaté, B. Delamotte, R. Méndez-Galain, and N. Wschebor (2012), Phys. Rev. E **85**, 026707.

Benitez, F., R. Méndez-Galain, and N. Wschebor (2008), Phys. Rev. B **77**, 024431.

Berezinskii, V. L. (1971), Sov. Phys. JETP **34**, 610.

Berges, J., N. Tetradis, and C. Wetterich (2002), Phys. Rep. **363**, 223.

Bijlsma, M., and H. T. C. Stoof (1996), Phys. Rev. A **54** (6), 5085.

Birse, M. C., B. Krippa, J. A. McGovern, and N. R. Walet (2005), Phys. Lett. B **605**, 287.

Bissbort, U., S. Götze, Y. Li, J. Heinze, J. S. Krauser, M. Weinberg, C. Becker, K. Sengstock, and W. Hofstetter (2011), Phys. Rev. Lett. **106**, 205303.

Blaizot, J. P. (2008), lectures given at the 2006 ECT* School "Renormalization Group and Effective Field Theory Approaches to Many-Body Systems", Trento, Italy., arXiv:0801.0009.

Blaizot, J.-P. (2011), Phil. Trans. R. Soc. A **369**, 2735.

Blaizot, J.-P., R. M. Galain, and N. Wschebor (2005), Europhys. Lett. **72** (5), 705.

Blaizot, J.-P., A. Ipp, R. Mndez-Galain, and N. Wschebor (2007a), Nucl. Phys. A **784** (14), 376 .

Blaizot, J.-P., A. Ipp, and N. Wschebor (2011a), Nucl. Phys. A **849** (1), 165 .

Blaizot, J.-P., R. Méndez-Galain, and N. Wschebor (2006a), Phys. Lett. B **632**, 571.

Blaizot, J.-P., R. Méndez-Galain, and N. Wschebor (2006b), Phys. Rev. E **74**, 051117.

Blaizot, J.-P., R. Méndez-Galain, and N. Wschebor (2007b), Eur. Phys. J. B **58**, 297.

Blaizot, J.-P., J. M. Pawlowski, and U. Reinosa (2011b), Phys. Lett. B **696** (5), 523 .

Bogoliubov, N. N. (1947), J. Phys. (USSR) **11**, 23.

Bourbonnais, C. (1985), "Fluctuations quantiques dans les systèmes à basse dimensionalité: théorie et applications aux conducteurs organiques," Ph.D thesis, Université de Sherbrooke.

Bourbonnais, C., and L. G. Caron (1988), Europhys. Lett. **5**, 209.

Bourbonnais, C., and L. G. Caron (1991), Int. J. Mod. Phys. B **5**, 1033.

Bourbonnais, C., and A. Sedeki (2009), Phys. Rev. B **80**, 085105.

Bychkov, Y. A., L. P. Gorkov, and I. Dzyaloshinskii (1966), Sov. Phys. JETP **23**, 489.

Caillol, J. M. (2006), Mol. Phys. **104**, 1931.

Caillol, J. M. (2009), J. Phys. A **42**, 225004.

Caillol, J.-M. (2012a), Nucl. Phys. B **865** (2), 291 .

Caillol, J.-M. (2012b), Nucl. Phys. B **855** (3), 854 .

Caillol, J.-M. (2013), Condens. Matter Phys. **16**, 43005.

Campostrini, M., M. Hasenbusch, A. Pelissetto, P. Rossi, and E. Vicari (2002), Phys. Rev. B **65**, 144520.

Campostrini, M., M. Hasenbusch, A. Pelissetto, and E. Vicari (2006), Phys. Rev. B **74**, 144506.

Canet, L., H. Chaté, and B. Delamotte (2015), Unpublished.
Canet, L., B. Delamotte, D. Mouhanna, and J. Vidal (2003), Phys. Rev. D **67**, 065004.
Capogrosso-Sansone, B., N. V. Prokof'ev, and B. V. Svistunov (2007), Phys. Rev. B **75** (13), 134302.
Capogrosso-Sansone, B., S. G. Söyler, N. Prokof'ev, and B. Svistunov (2008), Phys. Rev. A **77** (1), 015602.
Castellani, C., C. Di Castro, F. Pistolesi, and G. C. Strinati (1997), Phys. Rev. Lett. **78** (9), 1612.
Cenatiempo, S., and A. Giuliani (2014), J. of Stat. Phys. , 1.
Chaikin, P. M., and T. C. Lubensky (1995), *Principles of Condensed Matter Physics* (Cambridge University Press).
Chakravarty, S., B. I. Halperin, and D. R. Nelson (1989), Phys. Rev. B **39** (4), 2344.
Chen, K., L. Liu, Y. Deng, L. Pollet, and N. Prokof'ev (2013), Phys. Rev. Lett. **110**, 170403.
Chitov, G. Y., and C. Bourbonnais (2003), Nucl. Phys. B **663** (3), 568 .
Chubukov, A. V., S. Sachdev, and J. Ye (1994), Phys. Rev. B **49**, 11919.
Chung, M. C., and A. B. Bhattacherjee (2009), New J. Phys. **11**, 123012, arXiv:0809.3632.
Comellas, J. (1998), Nucl. Phys. B **509** (3), 662 .
Delamotte, B. (2012), in *Renormalization Group and Effective Field Theory Approaches to Many-Body Systems*, Lecture Notes in Physics, Vol. 852, edited by A. Schwenk and J. Polonyi (Springer Berlin Heidelberg) pp. 49–132.
Delamotte, B., D. Mouhanna, and M. Tissier (2004), Phys. Rev. B **69** (13), 134413.
Diehl, S., H. Gies, J. M. Pawlowski, and C. Wetterich (2007a), Phys. Rev. A **76**, 021602.
Diehl, S., H. Gies, J. M. Pawlowski, and C. Wetterich (2007b), Phys. Rev. A **76**, 053627.
Dupuis, N. (2005), Eur. Phys. J. B **48**, 319.
Dupuis, N. (2009a), Phys. Rev. A **80** (4), 043627.
Dupuis, N. (2009b), Phys. Rev. Lett. **102** (19), 190401.
Dupuis, N. (2011), Phys. Rev. E **83**, 031120.
Dupuis, N. (2014), Phys. Rev. B **89**, 035113.
Dupuis, N., and K. Sengupta (2007), Europhys. Lett. **80**, 50007.
Dupuis, N., and K. Sengupta (2008), Eur. Phys. J. B **66**, 271.
Eberlein, A., and W. Metzner (2013), Phys. Rev. B **87**, 174523.
Eichler, C., N. Hasselmann, and P. Kopietz (2009), Phys. Rev. E **80** (5), 051129.
Endres, M., T. Fukuhara, D. Pekker, M. Cheneau, P. Schau, C. Gross, E. Demler, S. Kuhr, and I. Bloch (2012), Nature **487**, 454.
Essam, J. W., and M. E. Fisher (1963), J. Chem. Phys. **38**, 802.
Fisher, M. (1998), Rev. Mod. Phys. **70**, 653.
Fisher, M. P. A., P. B. Weichman, G. Grinstein, and D. S. Fisher (1989), Phys. Rev. B **40** (1), 546.
Floerchinger, S., M. Scherer, S. Diehl, and C. Wetterich (2008), Phys. Rev. B **78**, 174528.
Floerchinger, S., and C. Wetterich (2008), Phys. Rev. A **77**, 053603.
Floerchinger, S., and C. Wetterich (2009a), Phys. Rev. A **79**, 063602.
Floerchinger, S., and C. Wetterich (2009b), Phys. Rev. A **79** (1), 013601.
Friedan, D. H. (1985), Ann. Phys. (N.Y.) **163**, 318.
Friederich, S., H. C. Krahl, and C. Wetterich (2011), Phys. Rev. B **83**, 155125.
Gavoret, J., and P. Nozières (1964), Ann. Phys. (N.Y.) **28**, 349.
Gazit, S., D. Podolsky, and A. Auerbach (2013a), Phys. Rev. Lett. **110**, 140401.
Gazit, S., D. Podolsky, A. Auerbach, and D. P. Arovas (2013b), Phys. Rev. B **88**, 235108.
Gell-Mann, M., and F. E. Low (1954), Phys. Rev. **95**, 1300.
Georges, A., and G. Kotliar (1992), Phys. Rev. B **45**, 6479.
Georges, A., G. Kotliar, W. Krauth, and M. J. Rozenberg (1996), Rev. Mod. Phys. **68** (1), 13.
Gersch, R., C. Honerkamp, D. Rohe, and W. Metzner (2005), Eur. Phys. J. B **48** (3), 349.
Gersdorff, G. v., and C. Wetterich (2001), Phys. Rev. B **64** (5), 054513.
Giamarchi, T. (2004), *Quantum physics in one dimension* (Oxford University Press, Oxford).
Gianinetti, P., and A. Parola (2001), Phys. Rev. B **63**, 104414.
Giering, K.-U., and M. Salmhofer (2012), Phys. Rev. B **86**, 245122.
Gies, H., and C. Wetterich (2002), Phys. Rev. D **65**, 065001.
Gräter, M., and C. Wetterich (1995), Phys. Rev. Lett. **75** (3), 378.
Grüter, P., D. Ceperley, and F. Laloë (1997), Phys. Rev. Lett. **79**, 3549.
Guerra, D., R. Méndez-Galain, and N. Wschebor (2007), Eur. Phys. J. B **59**, 357.
Guida, R., and J. Zinn-Justin (1998), Journal of Physics A: Mathematical and General **31** (40), 8103.
Halboth, C. J., and W. Metzner (2000), Phys. Rev. B **61**, 7364.
Hasenbusch, M. (2001), J. Phys. A **34** (40), 8221.
Hasenbusch, M. (2010), Phys. Rev. B **82**, 174433.
Hasenbusch, M., and S. Meyer (1990), Phys. Lett. B **241** (2), 238 .
Hasselmann, N. (2012), Phys. Rev. E **86**, 041118.
Hasselmann, N., S. Ledowski, and P. Kopietz (2004), Phys. Rev. A **70**, 063621.
Hasselmann, N., A. Sinner, and P. Kopietz (2007), Phys. Rev. E **76**, 10.1103/PhysRevE.76.040101.
Hertz, J. A. (1976), Phys. Rev. B **14** (3), 1165.
Hofmann, C. P. (2010), Phys. Rev. B **81**, 014416.
Hofmann, C. P. (2014), Journal of Statistical Mechanics: Theory and Experiment **2014** (2), P02006.
Holm, C., and W. Janke (1993), Phys. Rev. B **48**, 936.
Holzmann, M., and W. Krauth (1999), Phys. Rev. Lett. **83**, 2687.
Holzmann, M.,, Grter, P., and Lalo, F. (1999), Eur. Phys. J. B **10** (4), 739.
Honerkamp, C., M. Salmhofer, N. Furukawa, and T. M. Rice (2001), Phys. Rev. B **63**, 035109.
Huang, K. (1999), Phys. Rev. Lett. **83**, 3770.
Hugenholtz, N. M., and D. Pines (1959), Phys. Rev. **116** (3), 489.
Hung, C.-L., X. Zhang, N. Gemelke, and C. Chin (2011), Nature **470**, 236.
Husemann, C., K.-U. Giering, and M. Salmhofer (2012), Phys. Rev. B **85**, 075121.
Husemann, C., and M. Salmhofer (2009), Phys. Rev. B **79**, 195125.
Ionescu, C. D., A. Parola, D. Pini, and L. Reatto (2007), Phys. Rev. E **76**, 031113.
Jakubczyk, P., J. Bauer, and W. Metzner (2010), Phys. Rev.

B **82**, 045103.
Jakubczyk, P., N. Dupuis, and B. Delamotte (2014), Phys. Rev. E **90**, 062105.
Jakubczyk, P., P. Strack, A. A. Katanin, and W. Metzner (2008), Phys. Rev. B **77**, 195120.
José, J. V., L. P. Kadanoff, S. Kirkpatrick, and D. R. Nelson (1977), Phys. Rev. B **16**, 1217.
Kadanoff, L. P. (1966), Physics **2**, 263.
Kashurnikov, V. A., N. V. Prokof'ev, and B. V. Svistunov (2001), Phys. Rev. Lett. **87**, 120402.
Kastening, B. (2004), Phys. Rev. A **69**, 043613.
Katan, Y. T., and D. Podolsky (2015), Phys. Rev. B **91**, 075132.
Katanin, A. A. (2004), Phys. Rev. B **70**, 115109.
Katanin, A. A. (2015), Sov. Phys. JETP **120**, 6, arXiv:1412.7266 [cond-mat.str-el].
Katanin, A. A. (2016), "Using the (extended) dynamical mean field theory as a starting point for the two-particle irreducible functional renormalization-group approach for strongly-correlated systems," arXiv:1604.01702.
Kinza, M., and C. Honerkamp (2013), Phys. Rev. B **88**, 195136.
Kinza, M., J. Ortloff, J. Bauer, and C. Honerkamp (2013), Phys. Rev. B **87**, 035111.
Kopietz, P., L. Bartosch, and F. Schütz (2010), *Introduction to the Functional Renormalization Group* (Springer, Berlin).
Kosterlitz, J. M., and D. J. Thouless (1973), J. of Phys. C **6**, 1181.
Kosterlitz, J. M., and D. J. Thouless (1974), J. Phys. C **7**, 1046.
Krahl, H. C., J. A. Müller, and C. Wetterich (2009), Phys. Rev. B **79**, 094526.
Krahl, H. C., and C. Wetterich (2007), Phys. Lett. A **367**, 263.
Kreisel, A., F. Sauli, N. Hasselmann, and P. Kopietz (2008), Phys. Rev. B **78**, 035127.
Le Bellac, M. (1991), *Quantum and Statistical Field Theory*, Oxford Science Publ (Oxford University Press).
Ledowski, S., N. Hasselmann, and P. Kopietz (2004), Phys. Rev. A **69** (6), 061601.
Lee, T. D., and C. N. Yang (1958), Phys. Rev. **112**, 1419.
Litim, D. F. (2001), Phys. Rev. D **64**, 105007.
Ma, S. K. (New edition, 2000), *Modern Theory of Critical Phenomena* (Advanced Books Classics).
Machado, T., and N. Dupuis (2010), Phys. Rev. E **82** (4), 041128.
Maier, S. A., and C. Honerkamp (2012), Phys. Rev. B **86**, 134404.
Menotti, C., and N. Trivedi (2008), Phys. Rev. B **77** (23), 235120.
Menyhard, N., and J. Solyom (1973), J. Low Temp. Phys. **12**, 529.
Mermin, N. D., and H. Wagner (1966), Phys. Rev. Lett. **17** (22), 1133.
Metzner, W., M. Salmhofer, C. Honerkamp, V. Meden, and K. Schönhammer (2012), Rev. Mod. Phys. **84**, 299.
Metzner, W., and D. Vollhardt (1989), Phys. Rev. Lett. **62**, 324.
Millis, A. J. (1993), Phys. Rev. B **48** (10), 7183.
Minnhagen, P. (1987), Rev. Mod. Phys. **59**, 1001.
Minnhagen, P., and G. G. Warren (1981), Phys. Rev. B **24**, 2526.
Morris, T. R. (1994a), Phys. Lett. B **329** (23), 241 .
Morris, T. R. (1994b), Phys. Lett. B **334** (34), 355 .
Morris, T. R. (2005), JHEP **2005** (07), 027.
Morris, T. R., and M. D. Turner (1998), Nucl. Phys. B **509** (3), 637 .
Nagy, S., I. Nándori, J. Polonyi, and K. Sailer (2009), Phys. Rev. Lett. **102**, 241603.
Nagy, S., and K. Sailer (2011), Annals of Physics **326** (8), 1839 .
Nandori, I. (2011), "Coulomb gas and sine-gordon model in arbitrary dimension," arXiv:1108.4643.
Nelson, D. R., and J. M. Kosterlitz (1977), Phys. Rev. Lett. **39**, 1201.
Nelson, D. R., and R. A. Pelcovits (1977), Phys. Rev. B **16** (5), 2191.
Nepomnyashchii, A. A., and Y. A. Nepomnyashchii (1975), JETP Lett. **21**, 1, pis'ma Zh. Eksp. Teor. Fiz. 21, 3 (1975).
Nepomnyashchii, Y. A. (1983), Sov. Phys. JETP **58**, 722, zh. Eksp. Teor. Fiz. 85, 1244 (1983).
Nepomnyashchii, Y. A., and A. A. Nepomnyashchii (1978), Sov. Phys. JETP **48**, 493, zh. Eksp. Teor. Fiz. 75, 976 (1978).
Neto, A. C., and E. Fradkin (1993), Nucl. Phys. B **400** (13), 525 .
Nickel, J. C., R. Duprat, C. Bourbonnais, and N. Dupuis (2005), Phys. Rev. Lett. **95** (24), 247001.
Nickel, J. C., R. Duprat, C. Bourbonnais, and N. Dupuis (2006), Phys. Rev. B **73** (16), 165126.
Nozières, P. (1964), *Interacting Fermi Systems* (Benjamin, New-York).
Ohashi, Y., M. Kitaura, and H. Matsumoto (2006), Phys. Rev. A **73** (3), 033617.
Onsager, L. (1944), Phys. Rev. **65** (3-4), 117.
van Oosten, D., P. van der Straten, and H. T. C. Stoof (2001), Phys. Rev. A **63** (5), 053601.
Pangon, V. (2012), Int. J. Mod. Phys. A **27**, 1250014.
Parola, A. (1986), J. Phys. C: Solid State Phys. **19**, 5071.
Parola, A., D. Pini, and L. Reatto (2009), "The smooth cut-off hierarchical reference theory of fluids," arXiv:0901.2064.
Parola, A., and L. Reatto (1984), Phys. Rev. Lett. **53**, 2417.
Parola, A., and L. Reatto (1995), Adv. Phys. **44**, 211.
Patasinskij, A. Z., and V. L. Pokrovskij (1973), Sov. Phys. JETP **37**, 733, zh. Eksp. Teor. Fiz. 64, 1445 (1973).
Pawlowski, J. M. (2007), Annals of Physics **322** (12), 2831 .
Peláez, M., and N. Wschebor (2015), "The ordered phase of $o(n)$ model within the non-perturbative renormalization group," arXiv:1510.05709.
Pini, D., A. Parola, and L. Reatto (1993), J. Stat. Phys. **72**, 1179.
Pistolesi, F., C. Castellani, C. Di Castro, and G. C. Strinati (2004), Phys. Rev. B **69** (2), 024513.
Platt, C., W. Hanke, and R. Thomale (2013), Adv. in Phys. **62**, 453, arXiv:1310.6191 [cond-mat.supr-con].
Podolsky, D., A. Auerbach, and D. P. Arovas (2011), Phys. Rev. B **84**, 174522.
Podolsky, D., and S. Sachdev (2012), Phys. Rev. B **86**, 054508.
Pogorelov, A. A., and I. M. Suslov (2008), Sov. Phys. JETP **106**, 1118.
Polchinski, J. (1984), Nucl. Phys. B **231**, 269.
Pollet, L., and N. Prokof'ev (2012), Phys. Rev. Lett. **109**, 010401.
Polonyi, J., and K. Sailer (2005), Phys. Rev. D **71**, 025010.
Polyakov, A. M. (1975), Phys. Lett. B **59**, 79.
Popov, V. (1972), Theor. and Math. Phys. (Sov.) **11** (2), 478.

Popov, V. N. (1983), *Functional Integrals in Quantum Field Theory and Statistical Physics* (Reidel, Dordrecht, Holland).

Popov, V. N., and A. V. Seredniakov (1979), Sov. Phys. JETP **50**, 193, zh. Eksp. Teor. Fiz. 77, 377 (1979).

Prokof'ev, N., O. Ruebenacker, and B. Svistunov (2001), Phys. Rev. Lett. **87** (27), 270402.

Prokof'ev, N., and B. Svistunov (2002), Phys. Rev. A **66** (4), 043608.

Rançon, A., and N. Dupuis (2011a), Phys. Rev. B **84**, 174513.

Rançon, A., and N. Dupuis (2011b), Phys. Rev. B **83** (17), 172501.

Rançon, A., and N. Dupuis (2012a), Phys. Rev. A **85**, 011602(R).

Rançon, A., and N. Dupuis (2012b), Phys. Rev. A **86**, 043624.

Rançon, A., and N. Dupuis (2012c), Phys. Rev. A **85**, 063607.

Rançon, A., and N. Dupuis (2013), Europhys. Lett. **104** (1), 16002.

Rançon, A., and N. Dupuis (2014), Phys. Rev. B **89**, 180501.

Rançon, A., O. Kodio, N. Dupuis, and P. Lecheminant (2013), Phys. Rev. E **88**, 012113.

Rentrop, J. F., S. G. Jakobs, and V. Meden (2015), J. Phys. A **48** (14), 145002.

Rentrop, J. F., V. Meden, and S. G. Jakobs (2016), "Renormalization group flow of the luttinger-ward functional: conserving approximations and application to the anderson impurity model," arXiv:1602.06120.

Reuter, M., N. Tetradis, and C. Wetterich (1993), Nucl. Phys. B **401** (3), 567 .

Reuther, J., and R. Thomale (2014), Phys. Rev. B **89**, 024412.

Rose, F., F. Léonard, and N. Dupuis (2015), Phys. Rev. B **91**, 224501.

Rüegg, C., B. Normand, M. Matsumoto, A. Furrer, D. F. McMorrow, K. W. Krämer, H. U. Güdel, S. N. Gvasaliya, H. Mutka, and M. Boehm (2008), Phys. Rev. Lett. **100**, 205701.

Sachdev, S. (1993), Phys. Lett. B **309** (34), 285 .

Sachdev, S. (1999), Phys. Rev. B **59** (21), 14054.

Sachdev, S. (2011), *Quantum Phase Transitions*, 2nd ed. (Cambridge University Press, Cambridge, England).

Salmhofer, M., C. Honerkamp, W. Metzner, and O. Lauscher (2004), Prog. Theor. Phys. **112** (6), 943.

Scherer, M. M., S. Floerchinger, and H. Gies (2011), Phil. Trans. R. Soc. A **369** (1946), 2779.

Schütz, F., L. Bartosch, and P. Kopietz (2005), Phys. Rev. B **72**, 035107.

Sedeki, A., D. Bergeron, and C. Bourbonnais (2012), Phys. Rev. B **85**, 165129.

Seide, S., and C. Wetterich (1999), Nucl. Phys. B **562** (3), 524 .

Sengupta, K., and N. Dupuis (2005), Phys. Rev. A **71** (3), 033629.

Shankar, R. (1994), Rev. Mod. Phys. **66** (1), 129.

Sheshadri, K., H. R. Krishnamurthy, R. Pandit, and T. V. Ramakrishnan (1993), Europhys. Lett. **22**, 257.

Sinner, A., N. Hasselmann, and P. Kopietz (2008), J. Phys.: Condens. Matter **20**, 075208.

Sinner, A., N. Hasselmann, and P. Kopietz (2009), Phys. Rev. Lett. **102** (12), 120601.

Sinner, A., N. Hasselmann, and P. Kopietz (2010), Phys. Rev. A **82** (6), 063632.

Sólyom, J. (1979), Adv. Phys. **28**, 201.

Sondhi, S. L., S. M. Girvin, J. P. Carini, and D. Shahar (1997), Rev. Mod. Phys. **69** (1), 315.

Stoof, H. T. C., K. B. Gubbels, and D. B. M. Dickerscheid (2009), *Ultracold Quantum Fields* (Springer).

Strack, P., R. Gersch, and W. Metzner (2008), Phys. Rev. B **78**, 014522.

Sun, X. (2003), Phys. Rev. E **67**, 066702.

Taranto, C., S. Andergassen, J. Bauer, K. Held, A. Katanin, W. Metzner, G. Rohringer, and A. Toschi (2014), Phys. Rev. Lett. **112**, 196402.

Tetradis, N., and D. Litim (1996), Nucl. Phys. B **464** (3), 492 .

Tetradis, N., and C. Wetterich (1992), Nucl. Phys. B **383**, 197.

Tetradis, N., and C. Wetterich (1993), Nucl. Phys. B **398** (3), 659 .

Tetradis, N., and C. Wetterich (1994), Nucl. Phys. B **422**, 541.

Toyoda, T. (1982), Annals of Physics **141** (1), 154 .

Vidberg, H., and J. Serene (1977), J. Low Temp. Phys. **29** (3-4), 179192.

Wegner, F. J., and A. Houghton (1973), Phys. Rev. A **8**, 401.

Wentzell, N., C. Taranto, A. Katanin, A. Toschi, and S. Andergassen (2015), Phys. Rev. B **91**, 045120.

Wetterich, C. (1993a), Z. Phys. C **57** (3), 451.

Wetterich, C. (1993b), Phys. Lett. B **301**, 90.

Wetterich, C. (1993c), Z. Phy. C **60** (3), 461469.

Wetterich, C. (2007), Phys. Rev. B **75**, 085102.

Wetterich, C. (2008), Phys. Rev. B **77** (6), 064504.

Wilson, K. G. (1971a), Phys. Rev. B **4** (9), 3174.

Wilson, K. G. (1971b), Phys. Rev. B **4** (9), 3184.

Wilson, K. G. (1972), Phys. Rev. Lett. **28** (9), 548.

Wilson, K. G. (1975), Rev. Mod. Phys. **47**, 773.

Wilson, K. G. (1983), Rev. Mod. Phys. **55**, 583.

Wilson, K. G., and M. E. Fisher (1972), Phys. Rev. Lett. **28** (4), 240.

Wilson, K. G., and J. B. Kogut (1974), Phys. Rep. **12**, 75.

Wolff, U. (1989), Physics Letters B **228** (3), 379 .

Yefsah, T., R. Desbuquois, L. Chomaz, K. J. Günter, and J. Dalibard (2011), Phys. Rev. Lett. **107**, 130401.

Zanchi, D., and H. J. Schulz (2000), Phys. Rev. B **61**, 13609.

Zhang, X., C.-L. Hung, S.-K. Tung, and C. Chin (2012), Science **335**, 1070.

Zinn-Justin, J. (1996), *Quantum Field Theory and Critical Phenomena* (Third Edition, Clarendon Press, Oxford).

Zumbach, G. (1994), Nucl. Phys. B **413** (3), 754 .

Zwerger, W. (2004), Phys. Rev. Lett. **92** (2), 027203.